Supporting Information

Table of Contents

Abbreviations and Symbols

A	absorbance; absolute response of luminometer
Ac_2O	acetic anhydride
Alloc	allyloxy carbonyl
aq	aqueous
AU	absorbance units
AUC	area under curve
Boc	*tert*-butyloxycarbonyl
BODIPY	dipyrrometheneboron difluoride
BINAP	2,2'-bis(diphenylphosphino)-1,1'-binaphthyl
br	broad
BRET	bioluminescence resonance energy transfer
BSA	bovine serum albumin
c	concentration
COSY	correlation spectroscopy
CTZ	coelenterazine
CTZ-400a	coelenterazine 400a
d	duplet
DCM	dichloromethane
DDQ	2,3-dichloro-5,6-dicyano-1,4-benzoquinone
DEA	diethylamine
DEE	diethyl ether
DIC	*N,N'*-diisopropylcarbodiimide
DMA	dimethylanthracene
DMEM	Dulbecco's modified eagle's medium
DMF	*N,N*-dimethylformamide
DMSO	dimethyl sulfoxide
DPBF	1,3-diphenylisobenzofuran
DPBS	Dulbecco's phosphate-buffered saline
dppf	1,1'-bis(diphenylphosphino)ferrocene
E	FRET efficiency
E. coli	*Escherichia coli*
EDTA	ethylenediaminetetraacetic acid
EI	electron ionization
ESI	electrospray ionization
et al.	and others
EtOAc	ethyl acetate
EtOH	ethanol
FBS	fetal bovine serum
FRET	Förster resonance energy transfer
Grad	gradient
H6	hexa histidine-tag
HiBiT	11 amino acid peptide that binds with high affinity to LgBiT, forming active NLuc
HOAc	acetic acid
HMBC	heteronuclear multiple bond correlation spectroscopy
HPLC	high-performance liquid chromatography
HSQC	heteronuclear single quantum coherence
HRMS	high-resolution mass spectrometry
Hz	hertz
IPTG	Isopropyl β-D-1-thiogalactopyranoside
IR	infrared spectroscopy

J	coupling constant (in NMR spectrometry)
k	first-order rate constant
K_m	Michaelis Menten constant
LB	lysogeny broth
LED	light-emitting diode
LgBiT	large BiT, subunit of NLuc
m	multiplet (NMR); medium (IR)
m/z	mass-to-charge ratio
MeCN	acetonitrile
MeOH	methanol
Mtt	4-methyltrityl
NLuc	nano luciferase
NaOH	sodium hydroxide
NHS	*N*-hydroxysuccinimide
NIS	*N*-iodosuccinimide
NMM	N-methylmorpholine
NMR	nuclear magnetic resonance
ns	nanoseconds
OD_{600}	optical density at 600 nm
PPh_3	triphenyl phosphine
ppm	part per million
*p*TsOH	*p*-toluenesulfonic acid
q	quartet
qi	quintet
RAM	rink amide resin
RFU	relative fluorescence units
RLU	relative light units
rt	room temperature
s	singlet (NMR); strong (IR)
SD	standard deviation
SPPS	solid phase peptide synthesis
t	triplet (spectra)
TEA	triethylamine
TEBA	benzyltriethylammonium chloride
TBS	Tris-buffered saline
TFA	trifluoracetic acid
TFE	trifluoroethanol
THF	tetrahydrofuran
TIPS	triisopropylsilane
TLC	thin-layer chromatography
TMG	tetramethyl guanidine
TMS	tetramethyl silane
Tris	tris(hydroxymethyl)aminomethane
UV-vis	ultraviolet-visible
w	weak (IR)
Φ_Δ	singlet oxygen quantum yield
Φ_{BL}	luminescence quantum yield
Φ_F	fluorescence quantum yield
δ	chemical shift in parts per million downfield from tetramethyl silane
ε	molar extinction coefficient
η	solvent refractive index
τ	fluorescence lifetime

τ_D	fluorescence lifetime of FRET-donor
τ_{DA}	fluorescence lifetime of FRET-donor in the presence of the acceptor
λ	wavelength

General Information and Experimental Procedures

Materials

All commercial reagents were purchased from the following companies and used without further purification: benzyl bromide, bis(triphenylphosphine)palladium chloride, trifluoroacetic acid (TFA), triisopropyl silane (TIPS), caesium carbonate, 2,6-lutidine, phenylsilane, sodium chloride from Acros organics; sodium borohydride, 1,3-diphenylisobenzofuran (DPBF), boron trifluoride diethyl etherate and palladium on carbon (10 wt % loading), formic aicd, resazurin sodium salt, phenyl phosphonic dichloride, iodic acid, rose bengal, sodium azide, sulphur, thionyl chloride and 4-methyltrityl chloride from Alfa Aesar; 2,4-dimethylpyrrole, palladium(II) acetate and Fmoc-amino acids for SPPS from from BLDpharm; oxyma, 6-bromohexanoic acid, *N*-iodosuccinimide (NIS) and *N,N'*-diisopropylcarbodiimide (DIC) from Carbolution; piperidine from Carlo Erba; D_2O from Deutero GmbH; $CDCl_3$ and DMSO-d_6 from Eurisotop; 2,2'-bis(diphenylphosphino)-1,1'-binaphthyl (BINAP) and di-*tert*-butyl dicarbonate from fluorochem; dimethylformamide (DMF) peptide grade from Iris Biotech (Germany); *N*-hydroxysuccinimide (NHS) from Novabiochem; Dulbeccos modified eagle medium (DMEM) and Dulbecco's phosphate buffered saline (DPBS) from Gibco (Thermo Fisher Scientific); benzyltriethylammonium chloride (TEBA), benzyl 2-bromoacetate and sodium hydroxide from Thermo Fisher Scientific; fetal bovine serum (FBS) from PAN Biotech; dimethyl sulfoxide (DMSO), pyridine, *tert*-butanol and absolute ethanol (EtOH) from Merck; iodine, phenyboronic acid, triphenylphosphine, *p*-toluenesulfonyl azide solution 11-15 % (w/w) in toluene, tetramethylguanidine (TMG), *N*-methylmorpholine (NMM), rhodium(II) acetate, allyl chloroformate, IGEPAL® CA-630, absolute EtOH, trypan blue, trypsin-EDTA, 1,2-dibromethane, chlorobenzene, 2,3-dichloro-5,6-dicyano-1,4-benzoquinone (DDQ), penicillin-streptomycin, ammonia (25%, aq), isopropyl beta-*D*-thiogalactoside (IPTG), 1,4-dioxane, acetic anhydride, propan-1,2-diol, potassium carbonate, sodium carbonate, sodium thiosulfate, Si-dimethylanthracene (Si-DMA), tergitol and bovine serum albumin (BSA) from Sigma Aldrich ; tris(hydroxymethyl)aminomethane (Tris) ultrapure from AppliChem; 4-hydroxybenzaldehyde, ethyl 2-(diethoxyphosphoryl)acetate, benzaldehyde, 1,2-dichlorbenzene, benzyl alcohol, luminol, nitromethane, potassium *tert*-butoxide carbon tetrabromide, succinic anhydride, trifluoro ethanol (TFE), tetrakis(triphenylphosphine) palladium(0) and erythrosine B from TCI; ethylene diamine, imidazole, kanamycin, *L*-phenylalanine, *L*-tyrosine, potassium iodine, tween, zinc dust and diethylamine from Roth; 2-amino-3,5-dibromopyrazine and [1,1'-bis(diphenylphosphino)ferrocene]-palladium(II) dichloride from chemPUR; HPLC-grade methanol (MeOH), HPLC-grade acetonitril (MeCN), glycerol, triethylamine (TEA), Tris-buffered saline (TBS), concentrated hydrochlorid acid and acetic acid from VWR. Organic solvents were dried using standard procedures.[1] Water was purified with an ultrapure water purification system (Stakpure).

Unless otherwise stated, all reactions were performed under atmospheric conditions. All purchased chemicals were used without further purification unless otherwise indicated, all solvents used for synthesis were purified via distillation except for water and HPLC-grade solvents. If dried solvents were used, it is mentioned in the synthesis procedures. Silica gel 60 (Merck, 0.063-0.200 mm) was used for flash column chromatography. Analytical thin-layer chromatography (TLC) was carried out using pre-coated 60 F254 silica gel slides (Merck). The TLC-plates were developed with the following stains or visualized via UV irradiation:

1. UV light (254 nm)
2. ninhydrin developer (100 mg ninhydrin, 0.5 mL AcOH, 100 mL *n*-BuOH)
3. permanganate developer (3 g $KMnO_4$, 20 g K_2CO_3, 5 mL NaOH (aq), 5% (w/v), 300 mL H_2O)
4. cerium molybdate developer (12 g of $(NH_4)_2MoO_4$, 0.5 g of $Ce(NH_4)_2(MoO_4)_3$, 15 mL of H_2SO_4, 235 mL H_2O)

All chemical structures were created using ChemDraw 20.0 software.

Nuclear Magnetic Resonance (NMR) Spectroscopy

NMR spectra were recorded at 300 K using the following instruments: A Bruker AV II HD 300 MHz spectrometer at frequencies of 300 MHz (^{1}H) or 75 MHz (^{13}C); a Bruker AV III HD 250 MHz at a frequency of 282 MHz (^{19}F); and a Bruker AV III HD 500 MHz spectrometer at frequencies of 500 MHz (^{1}H) or 125 MHz (^{13}C). 2D-NMR spectra were recorded with a Bruker AV III HD 500 MHz spectrometer. The ^{1}H and ^{13}C NMR spectra were referenced to solvent residue peaks. As internal standards, deuterated chloroform ($CDCl_3$) or deuterated dimethyl sulfoxide (DMSO-d_6) with tetramethylsilane (TMS) or deuterated water (D_2O) were used. Solvent shifts in ppm: $CDCl_3$, δ = 7.26 ppm (^{1}H) and 77.2 ppm (^{13}C); DMSO-d_6, δ = 2.50 ppm (^{1}H) and 39.5 ppm (^{13}C); D_2O, δ = 4.79 ppm (^{1}H).[2] Automatically measured ^{1}H-NMR spectra were recorded from -0.5 to 14.0 ppm, manually measured spectra were recorded from -0.5 to 10.0 ppm, unless otherwise noted. All ^{13}C-NMR spectra were recorded from -5 to 215 ppm. The assignment of the signals was based on 2D NMR, i.e. HSQC, HMBC and COSY. The coupling constants (*J*) are noted in Hz and the multiplicity is specified as follows: s = singlet, d = duplet, t = triplet, q = quartet, qi = quintet, m = multiplet and br = broad. The evaluation of the obtained spectra was carried out using Bruker TopSpin 4.1.3 software.

High-Resolution Mass Spectrometry (HRMS)

High resolution electrospray ionization (ESI) mass spectra were acquired with an LTQ-FT Ultra mass spectrometer (Thermo Fischer Scientific), high resolution electron ionization (EI) mass spectra were recorded using an AccuTOF GCv mass spectrometer (JEOL). HPLC-MS analysis performed with a LTQ-FT Ultra coupled to an Agilent 1260 Infinity II HPLC (Agilent Technologies, USA). The resolution was set to 100,0 – 2000,0.

Infrared Spectroscopy (IR)

The IR spectra were recorded with the Bruker IFS 200 spectrometer. Intensities are reported as follows: s = strong, m = medium, w = weak band.

Fluorescence Lifetime (τ) Measurements

All measurements were carried out in three independent measurements in black clear bottom 96 well plates (µclear, Greiner Bio-One, reference: 655096, Austria). Samples were measured at 150 µM final concentration in 60% propan-1,2-diol, 35% EtOH and 5% glycerol. The sample BODIPY-CO_2H (**22**) + CTZ-400a (**1**) 1:10 contained 150 µM of BODIPY-CO_2H (**22**) and 1.5 mM of CTZ-400a (**1**). For each measurement, 90 µL of the sample solution was added to the wellplate.

The samples were excited at 465nm using a frequency-doubled Ti:Sa-oscillator (Coherent Discovery NX) operated at 930 nm combined with a beta barium borate crystal (Thorlabs NCL08) for second harmonic generation. The repetition rate of 80 MHz was reduced by a pulse picker (APE pulse select) with a division ratio of 15 to avoid accumulation effects. A Mitutoyo Plan-Apo 10x objective was used to focus the beam on the sample and the fluorescence was separated from the laser light using a 490 nm longpass dichroic mirror (Thorlabs DMLP490). The fluorescence of the excited samples was spectrally resolved by a spectrometer (Teledyne Spectra Pro HRS-300) and recorded with a streak camera setup (Optronis SC-10 with a TSU12-10 slow sweep unit).

Lifetimes τ were determined by fitting a monoexponential decay function to the time resolved data from 3-12 ns. Short and long timescales were excluded to minimize the effect of nonlinear effects (at early times because of high excitation densities) and noise (at long timescales because the signal decays). FRET-efficiencies were determined as $E = 1 - \frac{\tau_{DA}}{\tau_D}$.

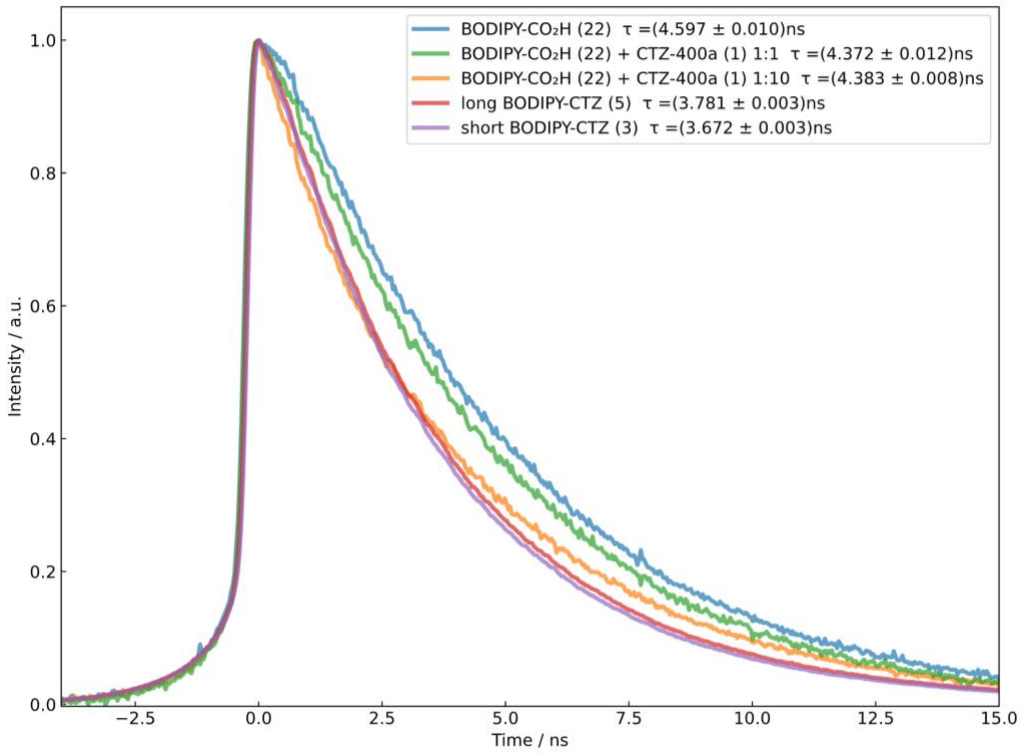

Figure S1: Fluorescence lifetime measurement in 60% propan-1,2-diol, 35% EtOH and 5% glycerol, transients plotted with linear intensity axis, first replicate.

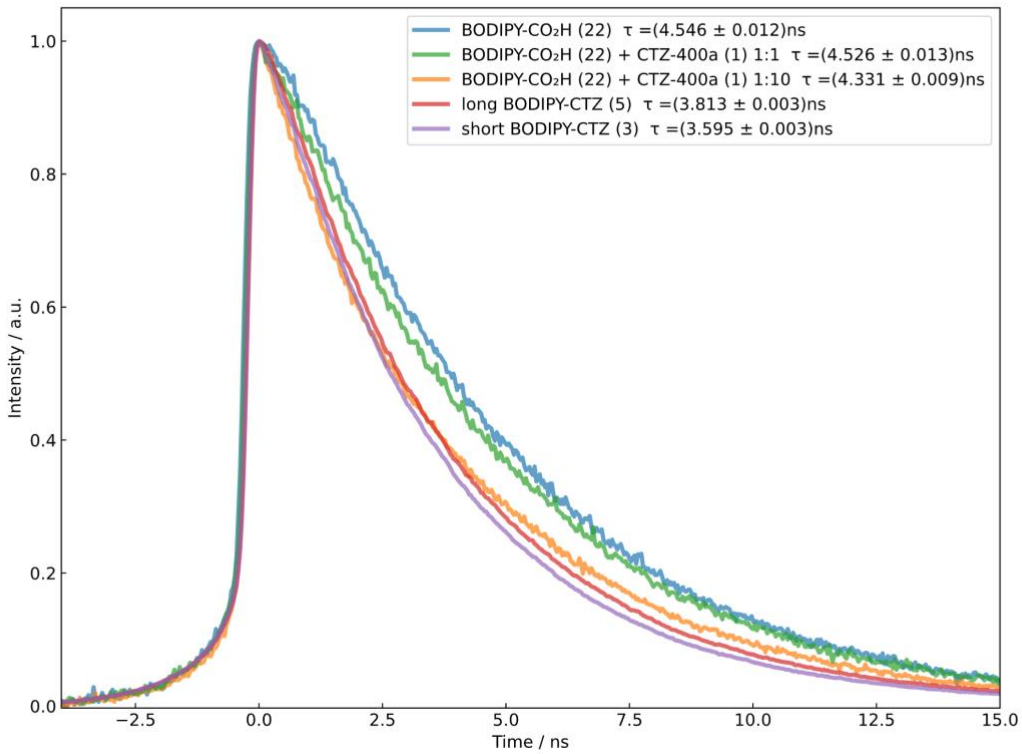

Figure S2: Fluorescence lifetime measurement in 60% propan-1,2-diol, 35% EtOH and 5% glycerol, , transients plotted with linear intensity axis, second replicate.

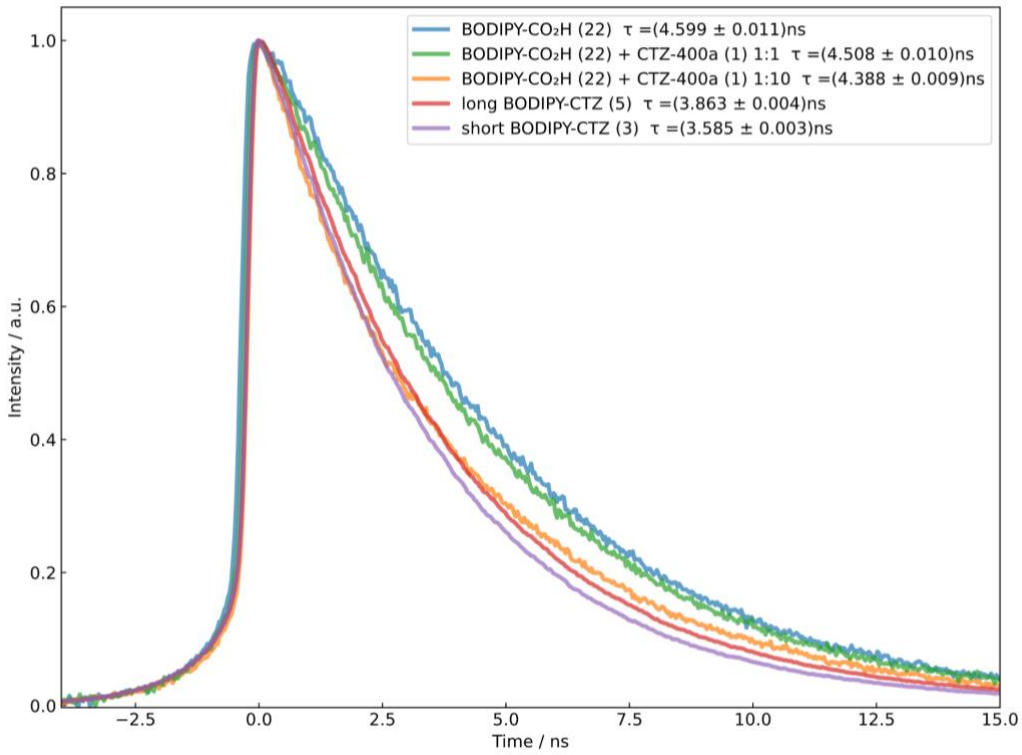

Figure S3: Fluorescence lifetime measurement in 60% propan-1,2-diol, 35% EtOH and 5% glycerol, , transients plotted with linear intensity axis, third replicate.

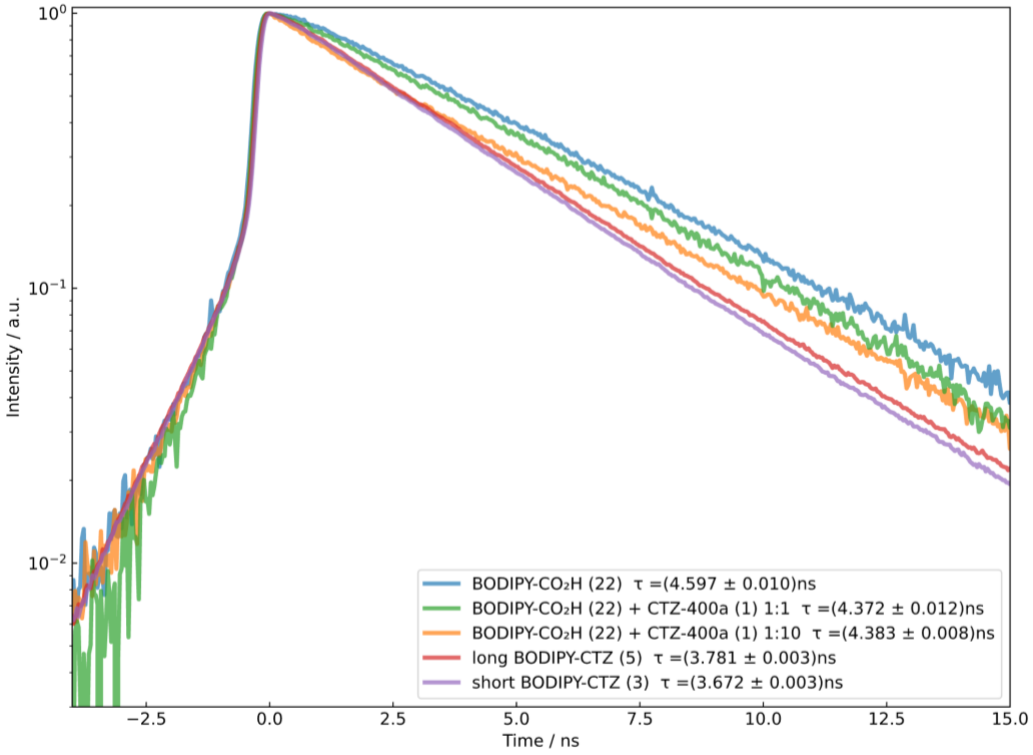

Figure S4: Fluorescence lifetime measurement in 60% propan-1,2-diol, 35% EtOH and 5% glycerol, transients plotted with logarithmic intensity axis, first replicate.

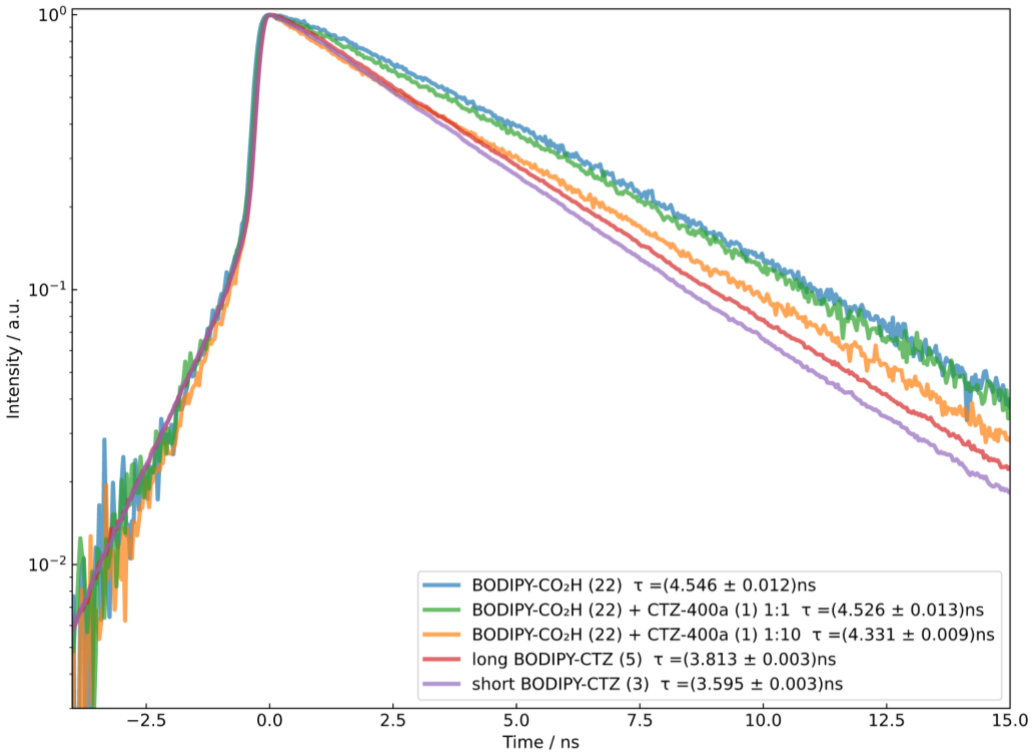

Figure S5: Fluorescence lifetime measurement in 60% propan-1,2-diol, 35% EtOH and 5% glycerol, transients plotted with logarithmic intensity axis, second replicate.

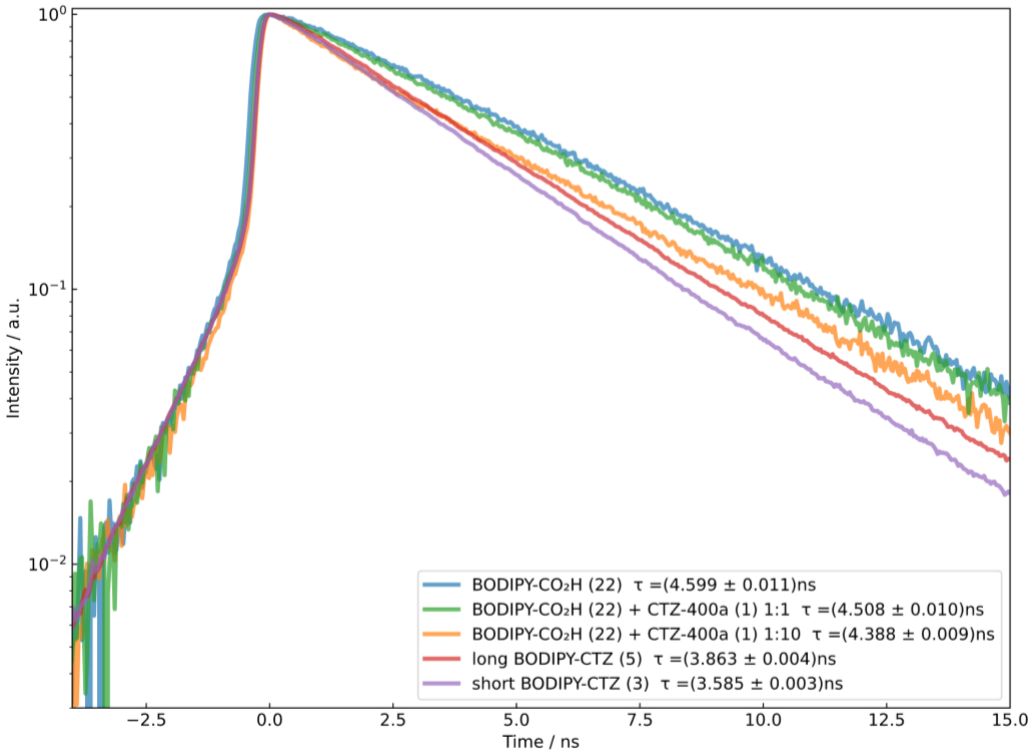

Figure S6: Fluorescence lifetime measurement in 60% propan-1,2-diol, 35% EtOH and 5% glycerol, transients plotted with logarithmic intensity axis, third replicate.

Table S1: Fluorescence lifetimes τ measured in 60% propan-1,2-diol, 35% EtOH and 5% glycerol of 150 µM stocks.

	BODIPY-CO_2H (22)	**BODIPY-CO_2H (22) + CTZ-400a (1) 1:1**	**BODIPY-CO_2H (22) + CTZ-400a (1) 1:10**	**Long BODIPY-CTZ (5)**	**Short BODIPY-CTZ (3)**
Replicate 1	4.597	4.372	4.383	3.781	3.672
Replicate 2	4.546	4.526	4.331	3.813	3.595
Replicate 3	4.599	4.508	4.388	3.863	3.585
Mean ± SD	4.581 ± 0.030	4.469 ± 0.084	4.367 ± 0.032	3.819 ± 0.041	3.617 ± 0.048

Table S2: FRET efficiencies in percent measured in 60% propan-1,2-diol, 35% EtOH and 5% glycerol of 150 µM stocks.

	BODIPY-CO_2H (22) + CTZ-400a (1) 1:1	**BODIPY-CO_2H (22) + CTZ-400a (1) 1:10**	**Long BODIPY-CTZ (5)**	**Short BODIPY-CTZ (3)**
Replicate 1	4.56	4.32	17.46	19.84
Replicate 2	1.20	5.46	16.76	21.52
Replicate 3	1.59	4.21	15.67	21.74
Mean ± SD	2.45 ± 1.84	4.66 ± 0.69	16.63 ± 0.90	21.03 ± 1.03

Fluorescence Quantum Yield (Φ_F) Determination

Fluorescence intensity values for the quantum yields were determined on a FP-6500 spectrofluorometer (Jasco) in a 3400 µL fluorescence quartz cuvette (HellmaAnalytics, 104F-QS, 10 x 10 mm light path) in triplicate using the following settings:

Excitation: 500 nm, 3 nm bandwidth
Emission wavelength scan: 505-650 nm, 3 nm bandwidth.

Absorbance values were measured on a Tecan (Switzerland) Spark 20M multimode microplate reader at room temperature (rt) in triplicate. From all spectra the corresponding background signal was subtracted. All measurements were following the procedure of Horiba[3] and using the equation:

$$\Phi_F = \Phi_{ST} \cdot \frac{Grad_x}{Grad_{ST}} \cdot \frac{\eta_X^2}{\eta_{ST}^2}$$

Φ_F: Fluorescence quantum yield.

$Grad_x$ and $Grad_{ST}$: Gradient from the plot of integrated fluorescence intensity vs absorbance.
η_X and η_{ST}: Refractive index of the used solvent.

As reference compounds, fluorescein in 0.1 M NaOH (Φ_F = 0.790[4], η = 1.3300[5]) and rhodamine B in EtOH (Φ_F = 0.490[6], η = 1.3612[7]) were used.

High-Performance Liquid Chromatography (HPLC)

For analytical HPLC analysis, an Agilent 1260 Series analytical HPLC-system (Agilent Technologies) with a flow rate of 1 mL/min at 55 °C was applied. As solvents, ultrapure water with an addition of 0.05% TFA (A) and MeCN with an addition of 0.03% TFA (B) were used.

Table S3: Columns for analytical HPLC-MS. All analytical runs were performed at 55 °C with a flow rate of 1 mL/min. The specific column and gradient used are noted at the corresponding chromatogram.

Column	Column specifications
Column 1	Eclipse XDB-C18 80 Å column (1.8 µm, 50 × 4.6 mm; Agilent), 1 mL/min
Column 2	Kinetex XB-C18 100 Å column (5 µm, 150 × 4.6 mm; Phenomenex), 1 mL/min

Preparative HPLC for peptide purification was carried out at 25 °C by an Agilent 1260 Series preparative HPLC system (Agilent Technologies). Ultrapure water (A) and MeCN (B) were employed as eluents with an addition of 0.1 % of TFA for both solvents. The flow rates used are listed in the table below.

Table S4: Columns for preparative HPLC. All preparative runs were performed at 25 °C.

Column	Column specifications
Column 3	Nucleodur EC 125/2 100-C18 (Macherey & Nagel), 250 x 21 mm, 5 µm, 10 mL/min

Singlet Oxygen Quantum Yield (Φ_Δ) Determination

The singlet oxygen quantum yield (Φ_Δ) determination was performed based on the protocol reported by Linden *et al*.[8] using DPBF (**21**) as singlet oxygen sensor. All measurements were carried out in triplicates in three independent measurements in black clear bottom 96 well plates (µclear, Greiner Bio-One, reference: 655096, Austria). While a cuvette could also be used, the plate reader improves our efficiency. For this purpose, the compound of interest (c_{final} = 0.54 µM, added from 5.4 µM stock solution for samples measured in MeCN and c_{final} = 1.00 µM, added from 10.0 µM stock solution for samples measured in MeOH) was mixed with the singlet oxygen trap (**22**, c_{final} = 200 µM, added from 800 µM stock solution) in 200 µL MeCN or MeOH. The concentrations of the stock solution were determined using their molar extinction coefficients (Table S5) except for the DPBF stock solution, which was prepared by weighting. In addition, wells containing: i) 200 µL of MeCN or MeOH and ii) DPBF (**21**, 200 µM) in MeCN or MeOH were used as controls. Irradiation was performed with a custom-made 96-LED-array (λ_{max} = 517 nm, luminous intensity: 16000-27000 mcd, viewing angle: 23°, AVAGO HLMP-CM2B-120DD, Broadcom Limited, United States). Previously, the luminous intensity was measured with a photometer (detector integration time: 5 s, 300 scans) for each well in triplicate. The mean luminous intensity of each well was determined followed by calculating the average luminous intensity of all wells. For the Φ_Δ determination, only LEDs with an intensity ± 5% of the average luminous intensity were used for irradiation. The decrease of the DPBF absorbance at 410 nm was recorded with a Spark 20M plate reader (Tecan) at 25 °C every 10 s of irradiation, starting with an initial dark measurement. Φ_Δ was determined of the following photosensitizers: 2I-BODIPY-CO_2H (**2**), short 2I-BODIPY-CTZ conjugate **4**, long 2I-BODIPY-CTZ conjugate **6** using rose bengal (**20**, Φ_Δ (MeCN) = 0.53[9]) or erythrosine B Φ_Δ ((MeOH) = 0.62[10]) as reference molecule. All photosensitizers as well as DPBF (**21**) were handled protected from light.

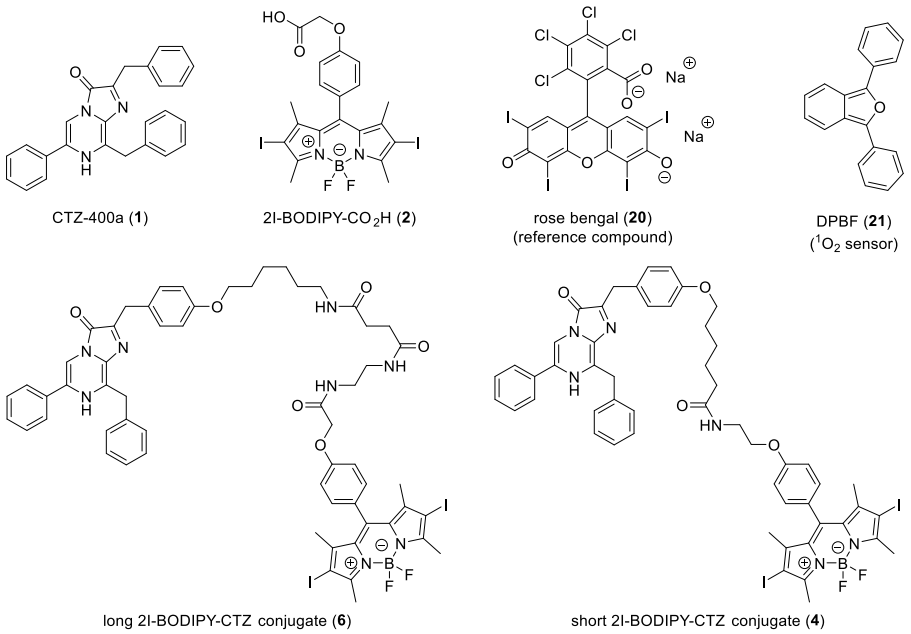

Figure S7: Structures of molecules used during singlet oxygen quantum yield (Φ_Δ) determination.

After the measurement, Φ_Δ was calculated from the following equation[8]:

$$\Phi_\Delta^x = \Phi_\Delta^{ref} \cdot \frac{k_x}{k_{ref}} \cdot \frac{I_a^{ref}}{I_a^x}$$

Φ_Δ^x: Singlet oxygen quantum yield.

k_x and k_{ref}: First-order rate constants (10^{-3} s^{-1}) of DPBF consumption in the presence of the to-be-determined compound and reference, i.e., rose bengal (**20**), respectively.

I_a^x and I_a^{ref}: Absorbance value of the to-be-determined compound and reference, i.e., rose bengal (**20**), respectively, at the irradiation wavelength (517 nm).

The corresponding background signal was subtracted for all values.

UV-Vis Spectroscopy

Concentration determinations and UV-vis measurements were performed on a Tecan (Switzerland) Spark 20M multimode microplate reader at rt. All steady-state measurements were performed in a quartz cuvette (Hellma Analytics (282-QS)) with a pathlength of 1 cm in an initial volume of 800 µL or in a quartz cuvette (black, Hellma Analytics (105.200 QS)) with a pathlength of 1 cm in an initial volume of 100 µL. To determine the concentration, 2 µL were titrated into the cuvette at least four times without exceeding 10% of the initial volume. The concentration of the stock solution was calculated for each titration using the Lamber-Beer law. The extinction coefficients used are summarized in table S5.

$$A = \varepsilon \cdot c \cdot l$$

A = absorbance
ε = molar extinction coefficient
c = concentration
l = path length

Table S5: Extinction coefficients used for concentration determination.

Compound	**Extinction Coefficient**
BODIPY-CO_2H (**22**)	ε(MeCN, 496 nm) = 86086 $M^{-1}cm^{-1}$[11]
HiBiT peptide (H_2N-VSG**W**RLFKKIS-$CONH_2$, **19**)	ε(H_2O, 280 nm) = 5800 $M^{-1}cm^{-1}$[12]
rose bengal (**20**)	ε(MeOH, 558 nm) = 104700 $M^{-1}cm^{-1}$[13]
CTZ-400a (**2**)	ε(MeOH, 249 nm) = 23086 $M^{-1}cm^{-1}$[14]

For 2I-BODIPY-CO_2H (**2**) we used the extinction coefficient of the similar compound **17** whose determination is described in the section: Molecular Extinction Coefficients. For conjugates **3-5** and **4-6** we used the ones for BODIPY-CO_2H (**22**) and **17**, respectively since the coelenterazine moiety does not absorb at the corresponding wavelength maxima.

Finally, the mean value of the stock solutions from at least four independent measurements was calculated, ensuring that the difference among any single measurement was below 9%.

Absorbance Spectra

Absorbance spectra were measured at 5.4 µM of the corresponding compound (Figure S2) in MeCN using a Tecan (Switzerland) Spark 20M multimode microplate reader at room temperature (rt) in a quartz cuvette (black, Hellma Analytics (105.200 QS)) with a pathlength of 1 cm and 100 µL volume. All spectra derived from two independent experiments, i.e., from 2 different stock solutions.

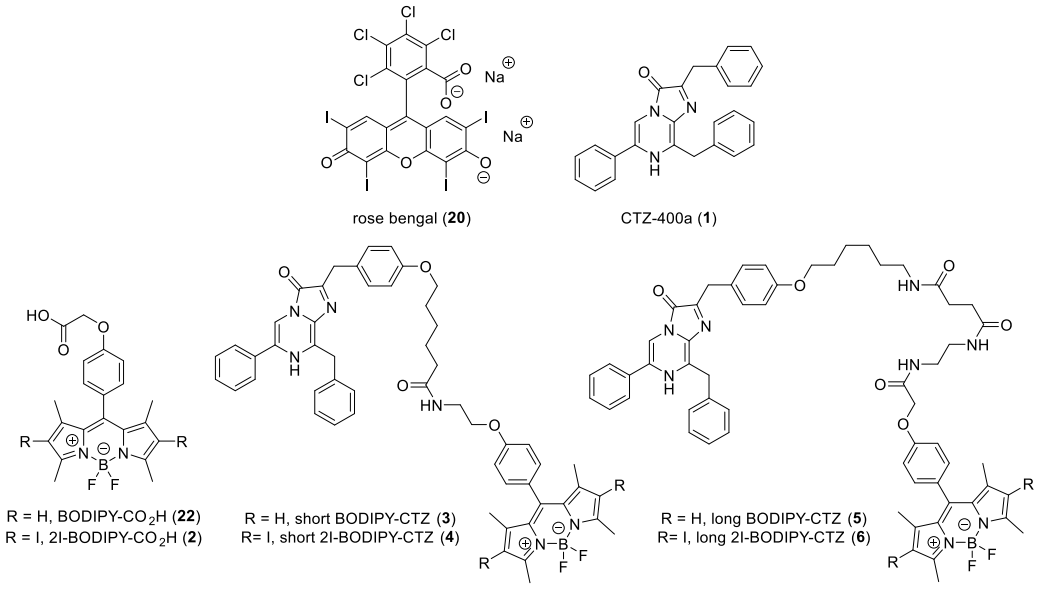

Figure S8: Structures of molecules used in the absorbance and fluorescence measurements.

Fluorescence Spectroscopy

Fluorescence spectra were recorded with a FP-6500 spectrofluorometer (Jasco) in a 200 µL fluorescence quartz cuvette (black, Hellma Analytics, 10 x 2 mm light path) in duplicate from two independent experiments, i.e., from 2 different stock solutions, with the following settings:

For BODIPY derivatives: Excitation: 480 nm, 3 nm bandwidth
Emission wavelength scan: 490-600 nm, 3 nm bandwidth.

For 2I-BODIPY derivatives: Excitation: 528 nm, 3 nm bandwidth
Emission wavelength scan: 535-645 nm, 3 nm bandwidth.

All fluorescence spectra were recorded in MeCN. Solvent blank values were subtracted for every measurement.

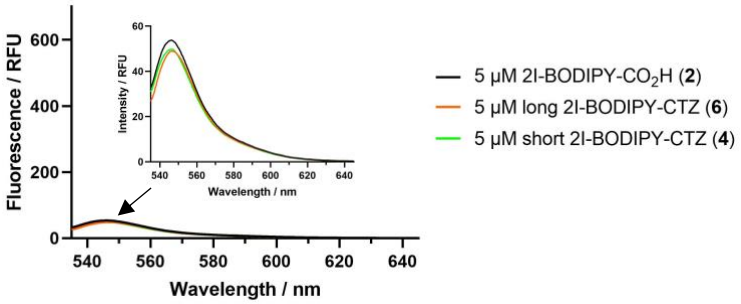

Figure S9: Fluorescence spectra of iodinated BODIPY derivatives **2**, **4**, **6** in MeCN measured in duplicate (solid line: first replicate, dashed line: 2. replicate).

Luminescence Quantum Yield (Φ_{BL}) Determination

Luminescence measurements for the luminescence quantum yield determination were performed with an ORION L microplate luminometer MPL4 (Berthold). For absolute calibration of the luminometer, a luminol solution with known photon emission was used. According to Lee *et al.*[15], 1.00 mL of a luminol solution ($A_{360\ nm}$ = 1.00) in DMSO emits a total of 9.75 × 10^{14} photons, thus 100 µL of a luminol solution ($A_{360\ nm}$ = 0.01) in DMSO emits a total of 9.75 × 10^{11} photons. All measurements were performed as three independent experiments, i.e., from 3 different stock solutions.

Measurement of the Luminol Reference Solution

Based on the procedure of Lee *et al.*[15], a solution of luminol ($A_{360\ nm}$ = 0.01) in dry DMSO and a saturated solution of potassium *tert*-butoxide in dry *tert*-butanol were prepared freshly. To a white 96-well microtiter plate (Greiner Bio-One, reference: 655074, Austria), 100 µL of the luminol solution was added. For blank measurements, 100 µL of dry DMSO was added to the well plate. The solvent lines of the luminometer injection mechanism were primed with the potassium *tert*-butoxide solution immediately before the experiment was started. 10 µL of the saturated potassium *tert*-butoxide solution were injected to the samples and the luminescence was recorded over 20 min. The AUC (area under the curve) of the obtained luminescence spectra was integrated, and the obtained value was used for the calculation of the absolute response of the luminometer (*A*).

Equation for calculating the absolute response of the luminometer (A)[16]:

$$A = \frac{photons}{total\ counts}$$

A: absolute response of the luminometer
$total\ counts$: AUC of the luminescence spectra

Measurement of the LgBiT-HiBiT Enzyme Complex + CTZ-400a (1) Sample Solution

Firstly, the active NLuc enzyme[17] was formed using a LgBiT/-His-tagged fusion protein (40 µM stock solution in 25 mM Tris pH 7.5, 150 mM NaCl, 50% glycerol, 0.05% tergitol). For complementation, 50 µL of a solution containing 8.0 nM LgBiT/His-tagged and 400 nM HiBiT (**19**, 50.0 eq) in Tris buffer (50 mM Tris, 150 mM NaCl, 0.005% Igepal CA-630, pH 7.5) containing BSA (0.1 g/L) was prepared and incubated (rt, 5 min, 300 rpm). Afterwards, the enzyme mix was diluted by adding 950 µL Tris buffer. The diluted enzyme mix was further incubated (rt, 10 min, 300 rpm) and then stored at rt for further 30 min. In the meantime, a solution of 47.44 µM CTZ-400a (**1**) in Tris buffer was prepared and the lines of the luminometer were primed with that solution. To a white 96-well microtiter plate (Greiner Bio-One, reference: 655074, Austria), 35 µL of Tris buffer and 25 µL of 4-fold enzyme mix containing: i) LgBiT/His-tagged ($c_{4\text{-fold stock}}$ = 400 pM; c_{final} = 100 pM) and ii) HiBiT (**19**, 50 eq; $c_{4\text{-fold stock}}$ = 20 nM; c_{final} = 5 nM) were added. For blank measurements, 60 µL of Tris buffer was added to the well plate. 50 µL of the CTZ-400a (**1**) solution were injected to the samples and the luminescence was recorded over 160 min. The AUC of the obtained luminescence spectra was integrated, and the obtained value together with the previously determined absolute response of the luminometer (*A*) allowed the calculation of the luminescence quantum yield of NLuc oxidizing CTZ-400a (**1**).

Equation for calculating the luminescence quantum yield (Φ_{BL})[16]:

$$\Phi_{BL} = \frac{total\ counts\ \cdot A}{number\ of\ luciferins}$$

Φ_{BL}: luminescence quantum yield
A: absolute response of the luminometer
$total\ counts$: AUC of the luminescence spectra

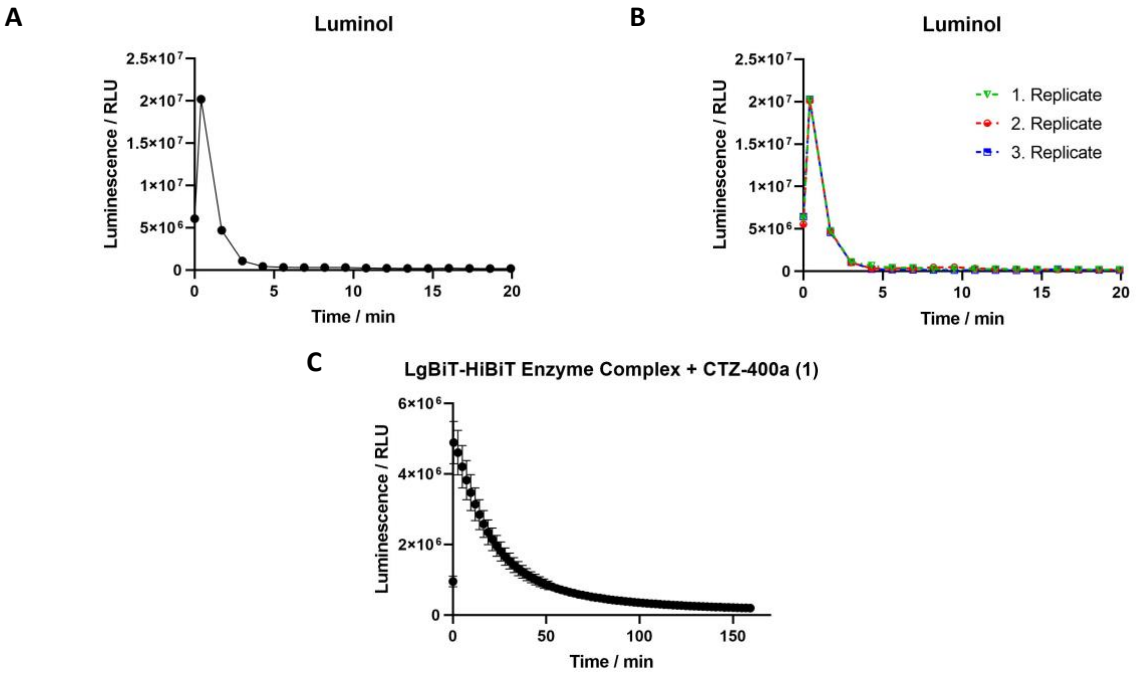

Figure S10: Luminescence measurements for the luminescence quantum yield determination. A) Luminescence decay of the luminol reference solution. B) Three independent replicates of the luminol reference solution luminescence decay shown separately. C) Luminescence decay of the enzymatic conversion of CTZ-400a (**1**) by the LgBiT-HiBiT enzyme complex. The plots derived from three independent experiments, i.e., from 3 different stock solutions.

Table S6: Results of the Φ_{BL} determination of LgBiT-HiBiT enzyme complex oxidizing CTZ-400a (**1**). All values obtained are mean values derived from three independent experiments. Photons emitted by the luminol solution ($A_{360\,nm}$ = 0.01) in DMSO: 9.75 × 10^{11} photons; number of luciferins (CTZ-400a, **1**): 1.4284 ×10^{15} molecules.

	Mean ± SD	**SD [%]**
AUC (luminol)	30031378 ± 1378517	4.6
A (photons/count)	32512.9 ± 1532.0	4.7
AUC (luciferin)	153282745 ± 4666686	3.0
Φ_{BL}(NLuc + CTZ-400a, 1)	3.49 × 10^{-3} ± 0,107	3.1

Michaelis Menten Constant (K_m) Determination

The experiments were carried out in Tris buffer (50 mM Tris, 150 mM NaCl, 0.005% Igepal CA-630, pH 7.5). BSA (0.1 g/L) was added from a freshly prepared 10-fold stock solution in Tris buffer before each experiment. First, concentration determination of freshly prepared stocks of HiBiT peptide **19** in ultrapure water was performed. To form the active NLuc enzyme[17], a LgBiT/-His-tagged fusion protein (40 µM stock solution in 25 mM Tris pH 7.5, 150 mM NaCl, 50% glycerol, 0.05% tergitol) was used. For complementation, 150 µL of a solution containing 1.6 µM LgBiT/His-tagged and 80 µM HiBiT (50.0 eq) in Tris buffer containing BSA (0.1 g/L) was prepared and incubated (rt, 5 min, 300 rpm). Afterwards, the enzyme mix was diluted by adding 2.85 mL Tris buffer. The diluted enzyme mix was further incubated (rt, 10 min, 300 rpm) and then stored at rt for further 30 min. In the meantime, a 2-fold dilution series of BODIPY-CTZ conjugates **3** and **5** (2:1) in Tris buffer starting with 100 µM concentration of the 2-fold stock (11 concentrations) were prepared. The conjugates **3** and **5** were always handled in the dark.

In this assay, a total volume of 80 µL per well (20 µL Tris buffer, 40 µL of corresponding 2-fold conjugate dilution and 20 µL 4-fold enzyme mix containing: i) LgBiT/His-tagged ($c_{4\text{-fold stock}}$ = 80 nM; c_{final} = 20 nM) and ii) HiBiT (50 eq; $c_{4\text{-fold stock}}$ = 4 µM; c_{final} = 1 µM) was used in a white 96-well microtiter plate (Greiner Bio-One, reference: 655074, Austria). In addition, wells only containing: i) the enzyme mix (20 µL of 4-fold enzyme mix (80 nM LgBiT/His-tagged, 4 µM HiBiT) and 60 µL Tris-buffer) and ii) Tris-buffer (80 µL) were prepared as controls. Furthermore, wells containing 40 µL of 2-fold conjugate dilution (c_{final} = 50 µM) and 40 µL Tris buffer were prepared. The addition to the 96 well plate was always carried out in the same order. First, Tris buffer was added followed by the addition of the conjugate dilution. After 45 min preincubation time, 20 µL of 4-fold enzyme mix (80 nM LgBiT/His-tagged, 4 µM HiBiT) was added to the 96 well plate and the solutions in the wells were mixed by pipetting 40 µL up and down 10 times within 3.5 min. The 96 well plate was shaken at 150 rpm at rt in the dark for 1.5 min. 5 min after substrate (BODIPY-CTZ conjugate **3** and **5**) addition, luminescence (100 ms integration time) was recorded with a Spark 20M platereader (Tecan) at 25 °C.

Michaelis Menten equation[18]:

$$y = \frac{V_{max} \cdot x}{K_m + x}$$

V_{max}: maximum enzyme velocity
K_m: Michaelis-Menten constant

Equation for substrate inhibition[19]:

$$y = \frac{V_{max} \cdot x}{K_m + x + \frac{x^2}{K_I}}$$

V_{max}: maximum enzyme velocity
K_m: Michaelis-Menten constant
K_I: dissociation constant of second bound substrate

Luminescence Spectroscopy

Luminescence spectra were measured with a Spark 20M platereader (Tecan) in duplicate from 2 different stock solutions using 20 nM LgBiT/-His-tagged protein and 1 µM of tested HiBiT peptide (H_2N-GGGGS-VSGWRLFKKIS-$CONH_2$, **19**) in the buffer: 50 mM Tris pH 7.5, 150 mM NaCl, 0.005% Igepal CA-630 in which BSA (0.1 g/L) was added from a freshly prepared 10-fold BSA stock solution. The obtained enzyme stock was preincubated for 45 min before the addition of the substrate (short BODIPY-CTZ conjugate **3** and long BODIPY-CTZ conjugate **5**: 14.8 µM). The readout was performed 5 min after substrate addition.

Fluorescence-based Detection of Singlet Oxygen

The experiments were conducted in a mixture of 80% phosphate buffer (10 mM phosphate, 100 mM NaCl, pH 7.4) and 20% glycerol. All samples were handled protected from light.

First, concentration determination of freshly prepared stocks of HiBiT peptide **19** in ultrapure water was performed. To form the active NLuc enzyme[17], a LgBiT/-His-tagged fusion protein (40 µM stock solution in 25 mM Tris pH 7.5, 150 mM NaCl, 50% glycerol, 0.05% tergitol) was used. For complementation, 150 µL of a solution containing 20.8 µM LgBiT/His-tagged and 31.2 µM HiBiT (**19**, 1.5 eq) in phosphate buffer containing 20% glycerol was prepared and incubated (rt, 5 min, 300 rpm). Afterwards, the enzyme mix was diluted by adding 2.85 mL phosphate buffer. The diluted enzyme mix was further incubated (rt, 10 min, 300 rpm) and then stored at rt for further 30 min. In the meantime, substrate 4-fold stock solutions of compounds **5** and **6** were prepared.

In this assay, a total volume of 100 µL per well in a black 96-well microtiter plate (Greiner Bio-One, reference: 655076, Austria) was used. Samples contained phosphate buffer (47.5 µL), the corresponding substrate (compound **5** or **6**) added from a 4-fold stock solution (25 µL, $c_{4\text{-fold stock}}$(compound **6**) = 27.2 µM, $c_{4\text{-fold stock}}$(compound **5**) = 50.0 µM) as well as the enzyme mix added from a 4-fold stock solution (25 µL) containing: i) LgBiT/His-tagged ($c_{4\text{-fold stock}}$ = 1.04 µM; c_{final} = 0.26 µM) and ii) HiBiT (**19**, 1.5 eq; $c_{4\text{-fold stock}}$ = 1.56 µM; c_{final} = 0.39 µM). Si-DMA was added from a 40-fold stock in DMSO ($c_{40\text{-fold stock}}$ = 1.00 mM; c_{final} = 25.0 µM).

In addition, wells containing:

a) 25 µL of 4-fold substrate 25 µL, $c_{4\text{-fold stock}}$(compound **6**) = 27.2 µM, $c_{4\text{-fold stock}}$(compound **5**) = 50.0 µM); 2.5 µL of 40-fold Si-DMA in DMSO ($c_{40\text{-fold stock}}$ = 1.00 mM) and phosphate buffer (72.5 µL)

b) 25 µL of 4-fold substrate 25 µL, $c_{4\text{-fold stock}}$(compound **6**) = 27.2 µM, $c_{4\text{-fold stock}}$(compound **5**) = 50.0 µM) and phosphate buffer (75 µL)

c) 25 µL of 4-fold substrate, $c_{4\text{-fold stock}}$(compound **6**) = 27.2 µM, $c_{4\text{-fold stock}}$(compound **5**) = 50.0 µM; 25 µL 4-fold of enzyme mix (LgBiT/His-tagged ($c_{4\text{-fold stock}}$ = 1.04 µM) and HiBiT (1.5 eq; $c_{4\text{-fold stock}}$ = 1.56 µM) and phosphate buffer (75 µL)

d) 25 µL 4-fold of enzyme mix (LgBiT/His-tagged ($c_{4\text{-fold stock}}$ = 1.04 µM) and HiBiT (1.5 eq; $c_{4\text{-fold stock}}$ = 1.56 µM); 2.5 µL of 40-fold Si-DMA in DMSO ($c_{40\text{-fold stock}}$ = 1.00 mM) and phosphate buffer (72.5 µL)

e) 2.5 µL of 40-fold Si-DMA in DMSO ($c_{40\text{-fold stock}}$ = 1.00 mM) and phosphate buffer (97.5 µL)

were prepared as controls.

The addition to the 96 well plate was always carried out in the same order. First, phosphate buffer was added to the 96 well plate followed by the addition of the substrate (compound **5** or **6**). After 45 min preincubation time of the enzyme mix, Si-DMA was added followed by the addition of the 4-fold enzyme mix (80 nM LgBiT/His-tagged, 4 µM HiBiT). The solutions in the wells were mixed by pipetting 50 µL up and down 10 times. The 96 well plate was shaken at 150 rpm at rt in the dark for 40 min. After

that time, fluorescence (excitation: 630 nm, 15 nm bandwidth; emission: 490-600 nm, 15 nm bandwidth; gain: 180; Z-position: 17240) was recorded with a Spark 20M platereader (Tecan) at 25 °C.

Molar Extinction Coefficients

The molar extinction coefficient of 2I-BODIPY-NH_2 (**17**) was determined in MeCN at 528 nm. For this purpose, a specific amount (>5.00 mg) of the compound was weighted on a Mettler Toledo XP6 micro balance to prepare a solution of known concentration. Absorbance was measured in a 1400 µL quartz cuvette (Hellma Analytics, 104F-QS) with a pathlength of 1 cm in a volume of 800 µL. Increasing amounts of the corresponding stock solution (2 µL per addition) were added without exceeding 10 % of the initial volume of the cuvette. Solvent blank values were subtracted for every measurement. The recorded absorbance was between 0.1 and 1 AU to be in concordance with Lambert-Beer law:

$$A = \varepsilon \cdot c \cdot l$$

A = absorbance
ε = molar extinction coefficient
c = concentration
l = path length

The linear regression of the obtained absorbance versus the concentration of the corresponding compound gave the molar extinction coefficient and the regression value (R^2). The experiment was performed three times independently, i.e., from 3 different stock solutions.

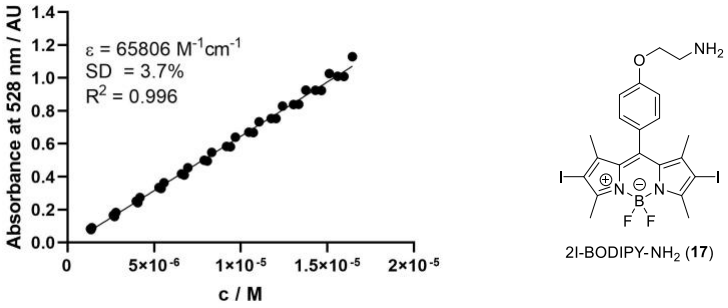

Figure S11: Extinction coefficient determination of 2I-BODIPY-NH_2 (**17**) in MeCN at 528 nm.

Cell-Based Experiments

General Culture and Handling

All studies were conducted with a stable HEK-293t cell line carrying a vector for the expression of the NLuc enzyme. HEK-293t cells were grown in flat-bottomed culture flasks (T75, Sarstedt, Germany) in a humidified cell-culture incubator (Galaxy CO-170 S incubator, New Brunswick Scientific, USA) at 37 °C under CO_2 (g) (5 % v/v). As growth medium, DMEM supplemented with FBS (5% v/v), penicillin (100 units mL^{-1}), and streptomycin (100 µg mL^{-1}) was used. Additives and trypsin were stored at -20 °C, DMEM and DPBS were stored at 4 °C. All solutions were tempered to 37 °C with a water bath before usage. Cells were grown to confluency and passaged every 1-3 days using trypsin-EDTA solution till passage 14. All cell-based assays were performed with media containing 5% FBS.

Cell Viability Studies

Seeding: For the determination of seeding densities, cells were counted with a Neubauer cell counter. 200 µL of cell suspension (1.5× 10^5 cells/mL, DMEM supplemented with FBS (5% v/v)) were added to the wells of a black 96-well cell culture microplate (Greiner Bio-One, 655086, Austria). The plates were incubated for 24 h.

Treatment: The next day, the following amounts of cell media were removed: 120 µL for samples, 110 µL for solvent control and 100 µL for untreated cells and background measurements. Afterwards, 10-fold concentrated conjugate stocks (10 µL per well, final concentration 200 – 0.78 µM) in DMEM media supplemented with FBS (5% v/v)) containing 5 % DMSO (c_{final} = 0.5%) were added to the cells under red light irradiation and mixed by pipetting up and down 50 µL of the respective solution 10 times. To wells containing the solvent control, 10 µL DMEM media supplemented with FBS (5% v/v)) containing 5 % DMSO were given (c_{final} = 0.5%). The plate was covered with alumina foil and incubated for 24 h in a humidified cell-culture incubator (Galaxy CO-170 S incubator, New Brunswick Scientific, USA) at 37 °C under CO_2 (g) (5% v/v).

Data evaluation: After incubation, 20 µL of a 1.63 mM resazurin solution in DPBS was added to each well and mixed by pipetting up and down 60 µL of the respective solution 10 times. Fluorescence was measured using a Tecan (Switzerland) Spark 20M multimode microplate reader at rt with the following settings: excitation wavelength: 560 nm, emission wavelength: 590 nm, bandwidth for excitation and emission: 10 nm, gain: 80, Z-position: 20000 µm. The measurements were carried out at 30-minute intervals as long as the fluorescence of the untreated cells increased linearly. The cell survival of untreated cells was assumed as 100% and the slope of each individual well was calculated. Relative viability = (experimental slope - background slope)/(slope of untreated control-background slope) × 100 %. All values were obtained in triplicates. At least two independent measurements, i.e., from different stock solutions, were performed.[8]

LgBiT/His-tagged Expression and Purification

Single colonies of *E. coli* Bl21De3 harbouring LgBiT/His-tagged plasmid (Promega) were used to inoculate starter cultures. The cultures were grown for 18 h at 37 °C in LB media containing kanamycin (50 µg/mL). The overnight culture was diluted 1:100 into a flask containing 500 mL of the same media and grown for 20 h at 37 °C. Overexpression was induced by IPTG (500 µM) when an OD_{600} of 0.5 was reached. Cells were pelleted and re-suspended in a Tris-buffered saline solution (TBS, pH 7.5) with 0.2 mg/mL lysozyme and 1 tablet of ROCHE cOmplete™ protease inhibitor cocktail. For lysate preparation, the sample was subject to three freeze/thaw cycles and short sonication. The lysate was centrifuged, and the supernatant was loaded to a nickel-sepharose column (HisTrap FF 1 ml; Cytiva) and then washed with 6–10 column volumes of buffer A: 25 mM Tris (pH 7.5), 300 mM NaCl, 5% glycerol, 2 mM imidazole, 0.5 % Tween. Fractions were eluated with buffer B: 25 mM Tris (pH 7.5), 300 mM NaCl, 5% glycerol, 200 mM imidazole, 0.5 % Tween, collected, pooled, and dialyzed against 50 mM Tris pH 7.5, 500 mM NaCl, 0.005% tergitol and 10% glycerol.

Pet28-LgBit, H6-LgBiT

Sequence:

MGSSHHHHHHSSGLVPRGSHMASMTGGQQMGRGSVGAQGNSGSSGGGGSGGGGSSGVFTLEDFVGDWEQT
AAYNLDQVLEQGGVSSLLQNLAVSVTPIQRIVRSGENALKIDIHVIIPYEGLSADQMAQIEEVFKVVYPVDDHHFKVIL
PYGTLVIDGVTPNMLNYFGRPYEGIAVFDGKKITVTGTLWNGNKIIDERLITPDGSMLFRVTINSGSSGSAGSSGSKSK
LAAALEHHHHHH

Number of amino acids: 240
Molecular weight: 25318.26
Theoretical pI: 6.21
ε(280 nm, ultrapure H_2O): 19940 M^{-1} cm^{-1}

Purification

Buffer A: 25 mM Tris (pH 7.5), 300 mM NaCl, 5% glycerol, 2 mM imidazole, 0.5 % Tween
Buffer B: 25 mM Tris (pH 7.5), 300 mM NaCl, 5% glycerol, 200 mM imidazole, 0.5 % Tween

The final sample was diluted to a 40 µM stock containing 25 mM Tris pH 7.5, 150 mM NaCl, 50% glycerol, 0.05% tergitol.

Organic Synthesis

2,8-Dibenzyl-6-phenylimidazo[1,2-a]pyrazin-3-yl acetate (Ac-CTZ-400a, 27)

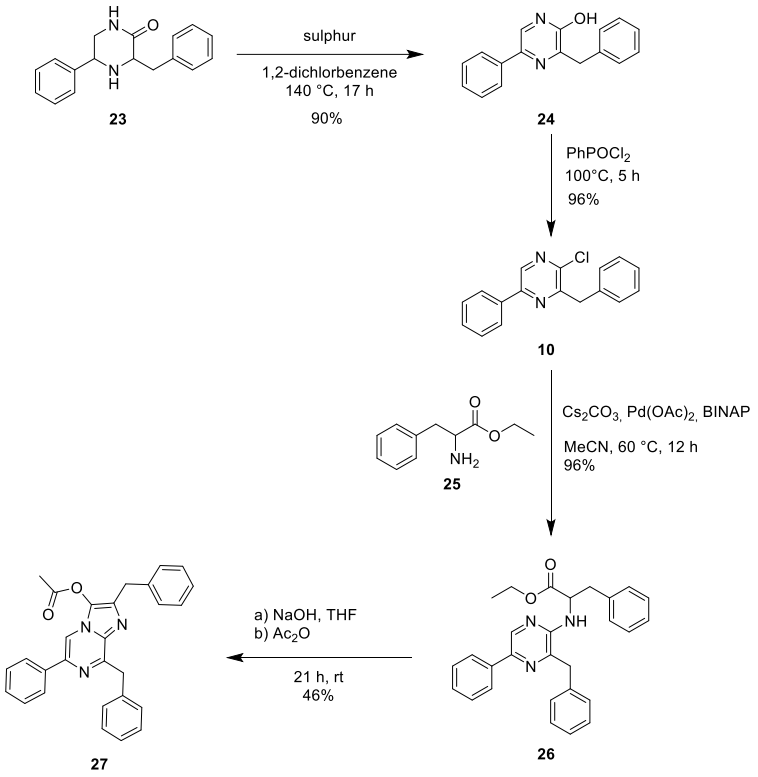

Scheme S1: Synthesis of Ac-CTZ-400a (**27**) reported by Coutant *et al.*[20]

Ac-CTZ-400a (**27**) was synthesized following the procedure of Coutant *et al.*[20] First, compound **$9** was oxidized using sulphur, which led to the aromatization. Afterwards, chlorination with phenyl phosphonic dichloride resulted in the formation of pyrazine **10**. Next, compound **26** was synthesized by a Hartwig-Buchwald cross coupling reaction, which was finally converted into Ac-CTZ-400a (**27**).[20]

TLC (UV_{254nm}): R_f = 0.94 (DCM/MeOH 20:1, v/v).

^{1}H-NMR (300 MHz, DMSO-d_6): δ = 8.74 (s, 1H), 8.05 (d, ^3J(H,H) = 7.1 Hz, 2H), 7.53 – 7.35 (m, 5H), 7.35 – 7.19 (m, 8H), 4.48 (s, 2H), 4.09 (s, 2H), 2.37 (s, 3H) ppm.

^{13}C-NMR (75 MHz, $CDCl_3$): δ = 167.2 (*C*O), 153.1 (C_q), 139.2 (C_q), 138.2 (C_q), 138.0 (C_q), 137.0 (C_q), 135.4 (C_q), 133.8 (C_q), 129.9 (2C; *C*H), 129.2 (2C; *C*H), 128.9 (2C; *C*H), 128.7 (*C*H), 128.6 (2C; *C*H), 128.4 (2C; *C*H), 126.6 (*C*H), 126.6 (2C; *C*H), 126.6 (2C; *C*H), 109.0 (*C*H), 39.6 (CH_2), 34.4 (CH_2), 20.0 (CH_3) ppm.

HRMS-ESI (*m/z*): $[M + Na]^+$ calcd for $C_{28}H_{23}N_3O_2Na$: 456.1682; found: 456.1684.

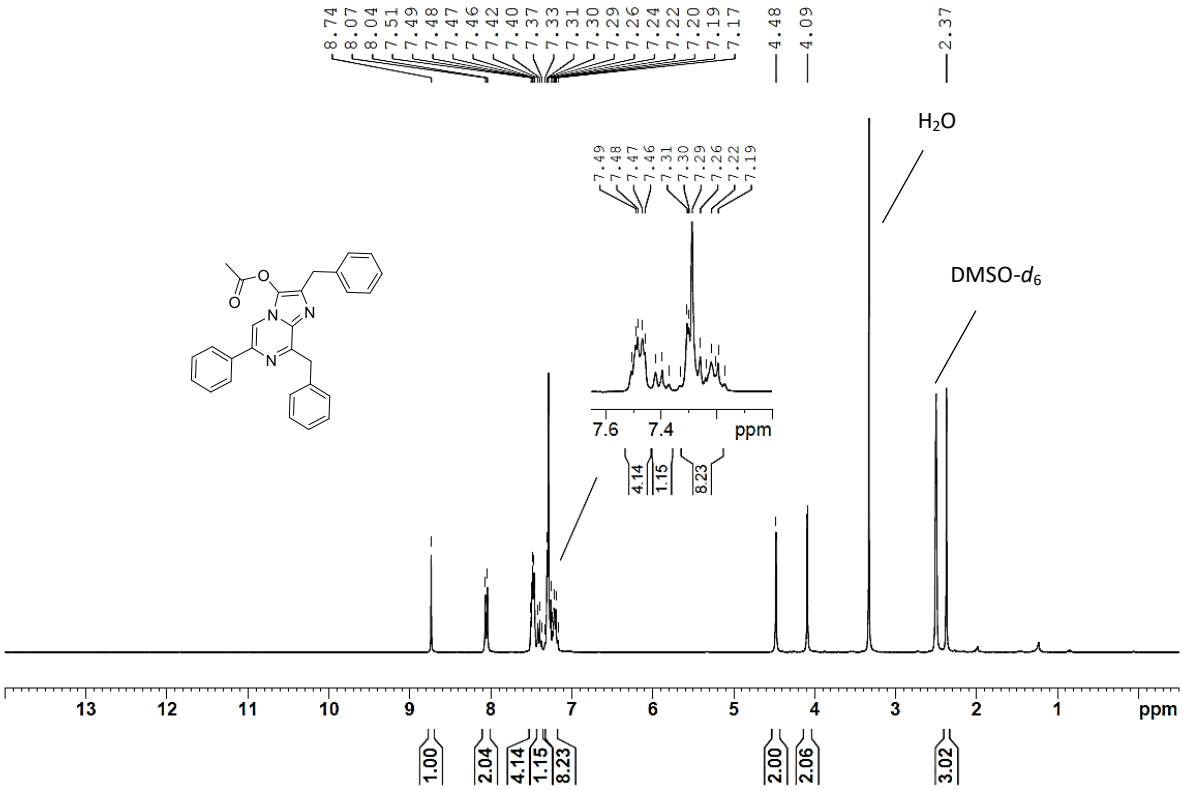

Figure S12: ^{1}H-NMR (300 MHz) spectrum of compound **27** in DMSO-d_6.

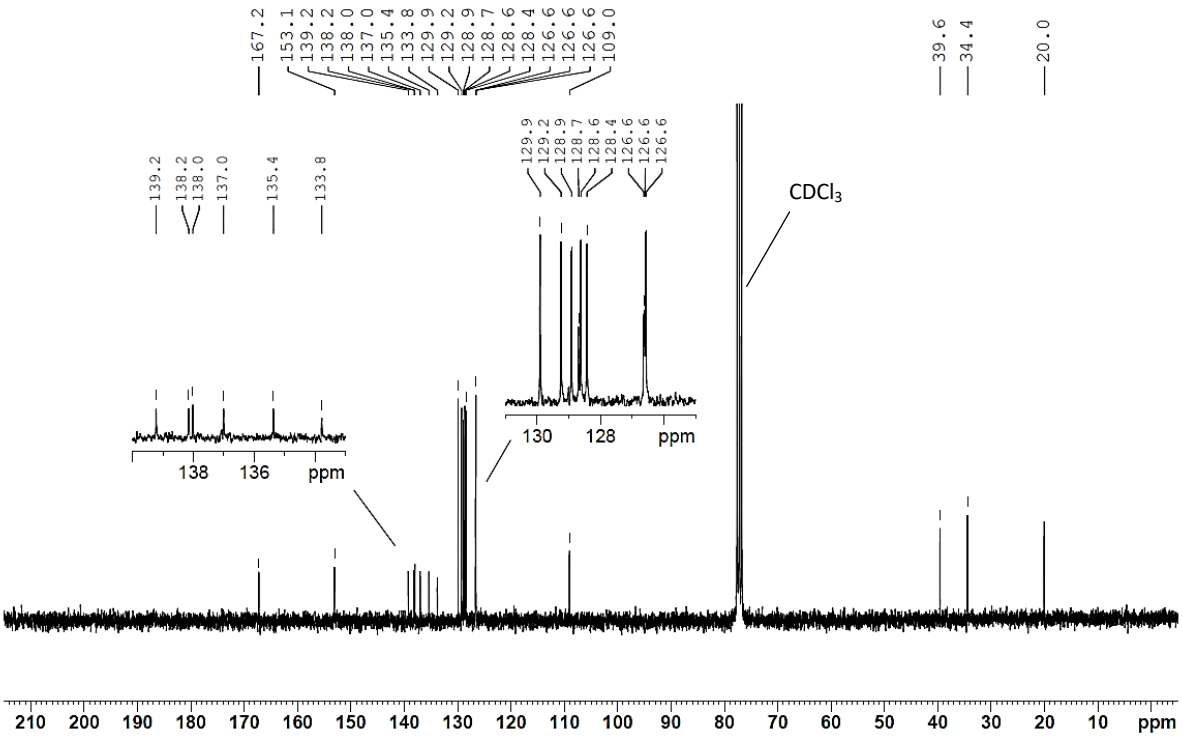

Figure S13: ^{13}C-NMR (75 MHz) spectrum of compound **27** in $CDCl_3$.

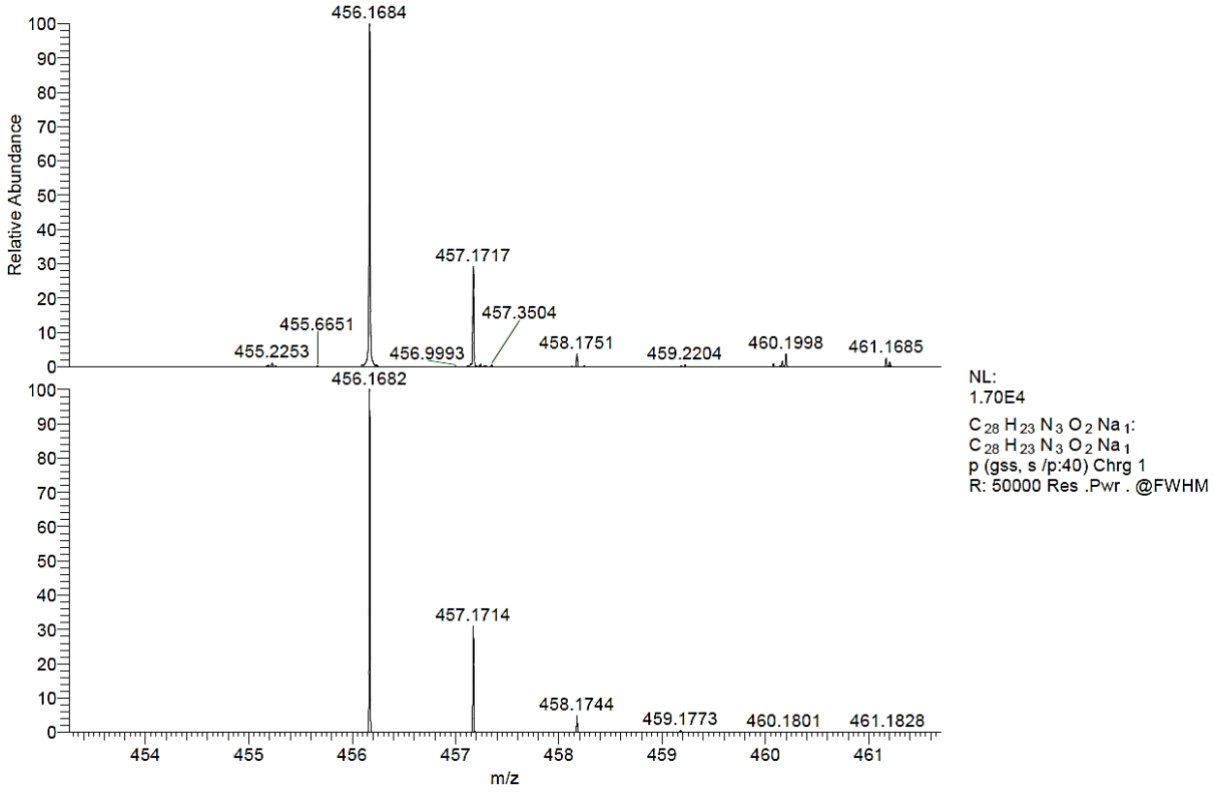

Figure S14: Measured (top) and calculated (bottom) HRMS-ESI spectrum of **27** in positive ion mode.

Deacetylation of Coelenterazine (Ac-CTZ-400a, 27)

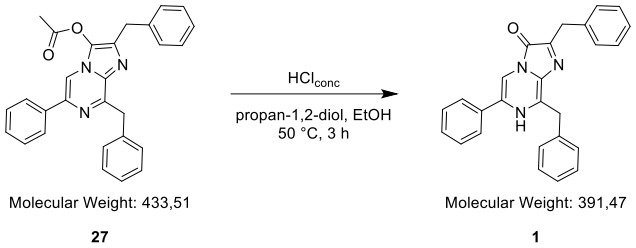

Scheme S2: Deacetylation of Ac-CTZ-400a (**27**) for in vitro experiments.

A part of Ac-CTZ-400a (**27**) was deacetylated for *in vitro* experiments using a protocol based on the procedure reported by Coutant *et al.*[20] For this purpose, Ac-CTZ-400a (**27**, 1.80 mg, 4.15 µmol, 1.00 eq) was dissolved propan-1,2-diol (1.20 mL). Ethanol (500 µL) and concentrated HCl (5.00 µL) were added, and the reaction mixture was shaken at 50 °C for 3 h. After confirmation of full conversion of the starting material by HPLC, further EtOH (200 µL) and glycerol (100 µL) were added to obtain a final solvent composition of 60% propan-1,2-diol, 35% EtOH and 5% glycerol. The obtained stock solution was centrifuged (rt, 1 min, 14000 rpm) and the concentration (~1.5 mM) was rechecked via absorbance titration as described in the UV-Vis section. The stock was stored in the dark at -80 °C.

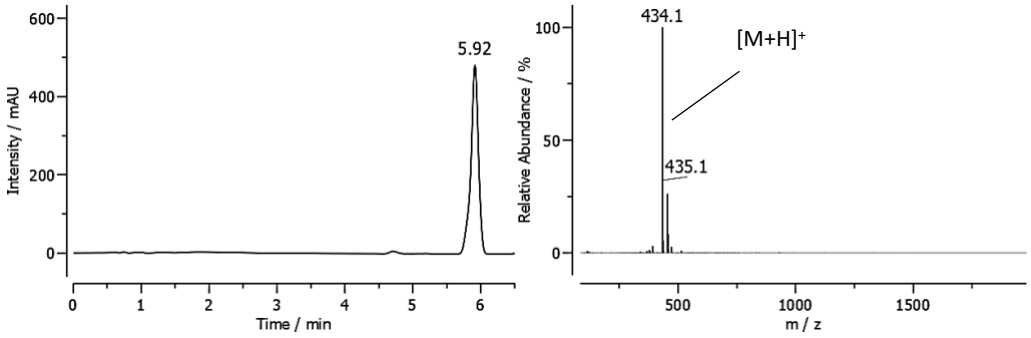

Figure S15: HPLC chromatogram (220 nm, 5 – 95% of solvent B in 6.5 min, column 1) of coelenterazine deacetylation at t_0.

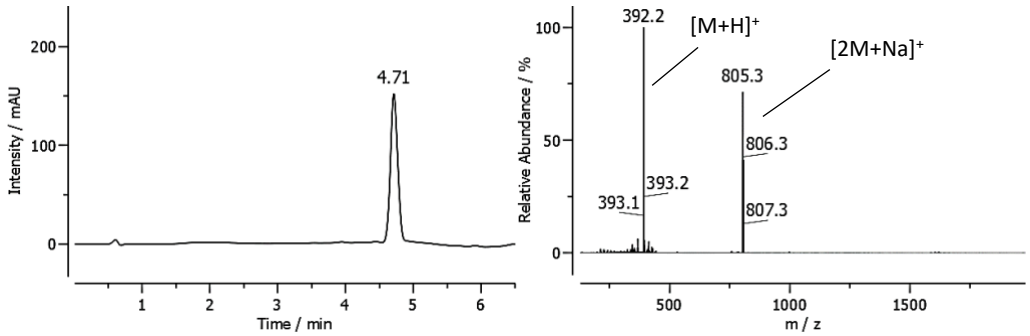

Figure S16: HPLC chromatogram (220 nm, 5 – 95% of solvent B in 6.5 min, column 1) of coelenterazine deacetylation after 3 h.

HRMS-ESI (*m/z*): $[M + H]^+$ calcd for $C_{26}H_{22}N_3O$: 392.1757; found: 392.1747.

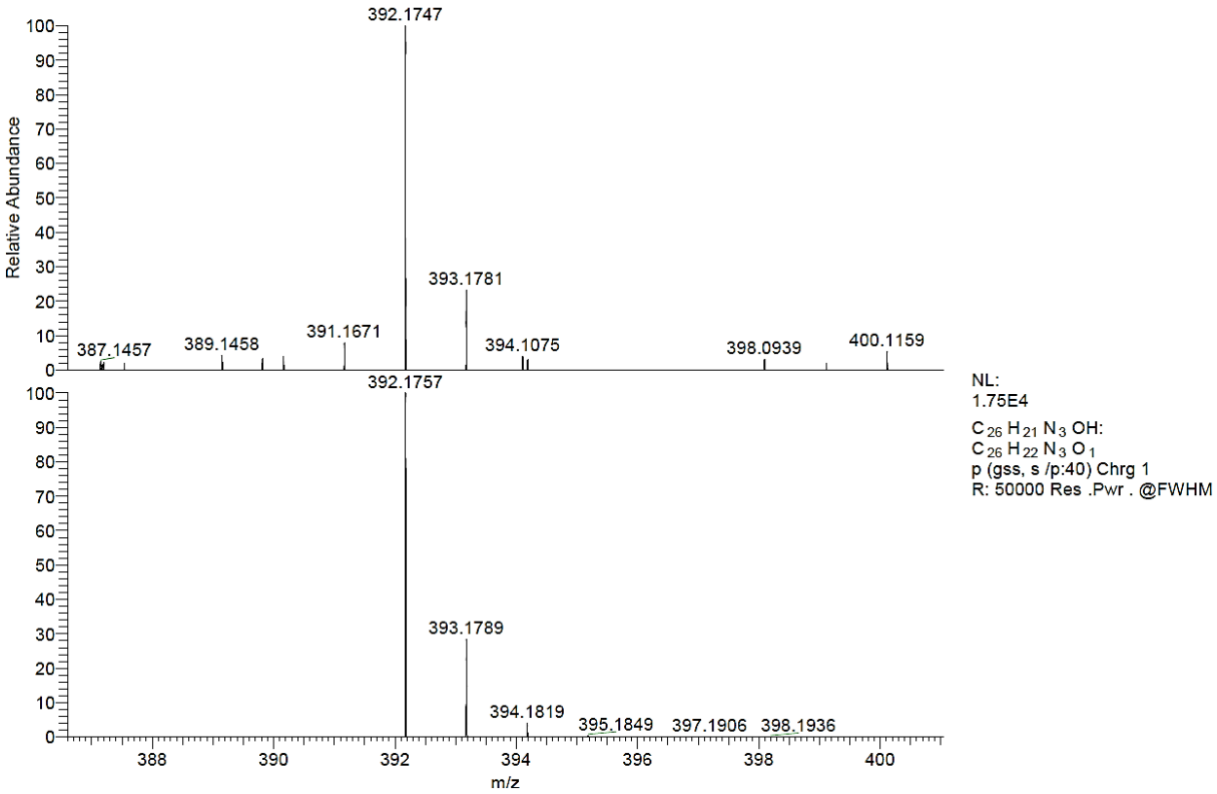

Figure S17: Measured (top) and calculated (bottom) HRMS-ESI spectrum of **1** in positive ion mode.

Allyl (6-hydroxyhexyl)carbamate (30)

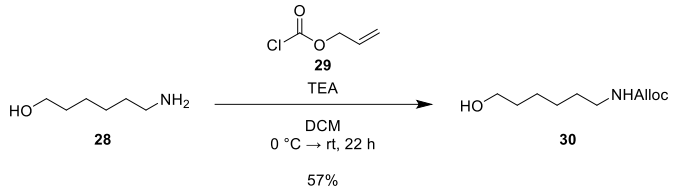

Scheme S3: Synthesis of allyl (6-hydroxyhexyl)carbamate (**30**).[21]

According to the procedure of Dufour *et al.*[21], 6-aminohexan-1-ol (**28**, 1.00 g, 8.53 mmol, 1.00 eq) was dissolved in dry DCM (40.0 mL) under nitrogen atmosphere. TEA (3.00 mL, 21.33 mmol, 2.50 eq) was added. After cooling the reaction mixture to 0 °C, allyl chloroformate (**29**, 1.00 mL, 9.39 mmol, 1.10 eq) was added slowly. The reaction mixture was heated to rt for 22 h with stirring. Afterwards, the reaction was washed with distilled water (~150 mL, 2×), an aqueous solution adjusted to pH 2 with 1 M HCl (~150 mL, 2×) and brine (~150 mL). Afterwards, the organic phase was dried over Na_2SO_4, filtered, and concentrated under reduced pressure. The crude was purified by flash column chromatography using *n*-pentane/ EtOAc (1:1, v/v) to give **30** (0.97 g, 4.83 mmol, 57%) as colourless crystals. The characterization is in agreement with the literature.[21]

TLC (permanganate developer): R_f = 0.24 (*n*-pentane/EtOAc 1:1, v/v).

^{1}H-NMR (300 MHz, $CDCl_3$): δ = 5.98-5.85 (m, 1H), 5.29 (dd, ^3J(H,H) = 17.2 Hz, ^2J(H,H) = 1.6 Hz, 1H), 5.20 (dd, ^3J(H,H) = 10.5 Hz, ^2J(H,H) = 1.3 Hz, 1H), 4.69 (s, 1H), 4.56 (d, ^3J(H,H) = 5.5 Hz, 1H), 3.63 (t, ^3J(H,H) = 6.5 Hz, 2 H), 3.18 (t, ^3J(H,H) = 7.0 Hz, 2 H), 1.61-1.47 (m, 4H), 1.41-1.33 (m, 4H) ppm.

^{13}C-NMR (75 MHz, $CDCl_3$): δ = 156.5 (C_q), 133.1 (*C*H), 117.7 (*C*H_2), 65.6 (*C*H_2), 62.9 (*C*H_2), 41.0 (*C*H_2), 32.7(*C*H_2), 30.1 (*C*H_2), 26.5 (*C*H_2), 25.4 (*C*H_2) ppm.

HRMS-ESI (*m/z*): $[M+H]^+$ calcd for $C_{10}H_{20}NO_3$: 202.1438; found: 202.1439.

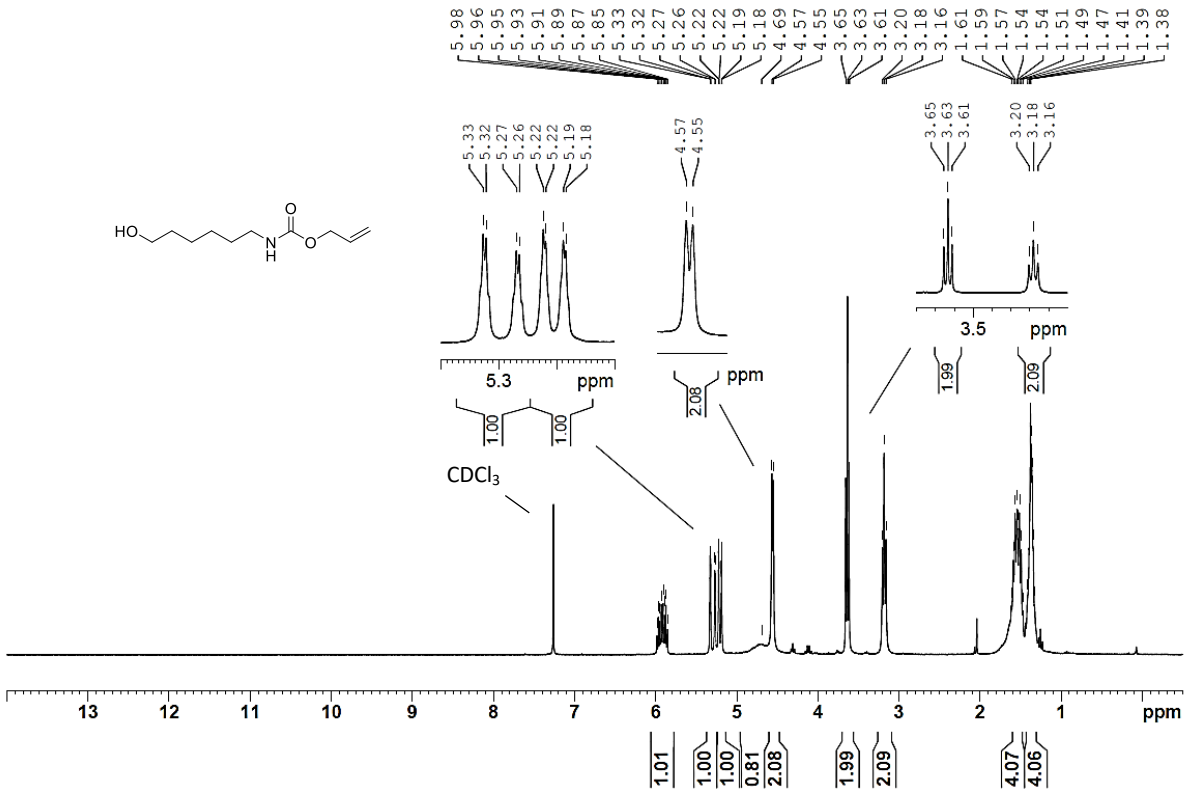

Figure S18: ^{1}H-NMR (300 MHz) spectrum of compound **30** in $CDCl_3$.

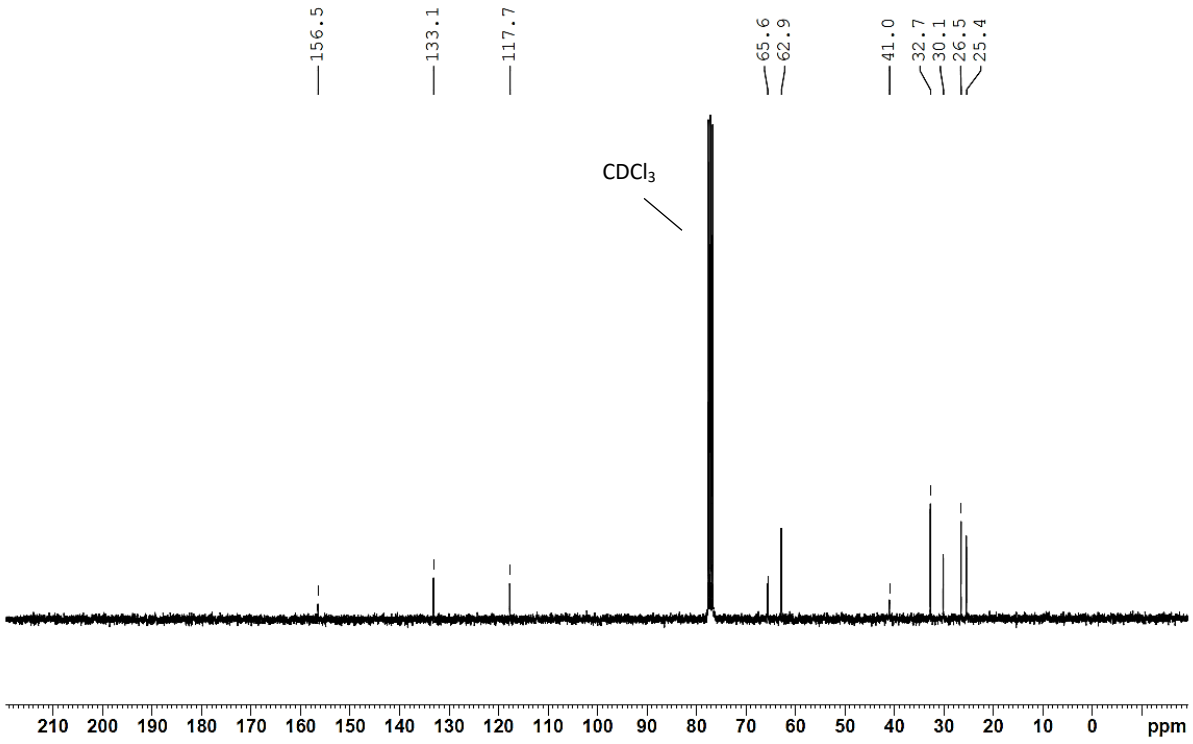

Figure S19: ^{13}C-NMR (75 MHz) spectrum of compound **30** in $CDCl_3$.

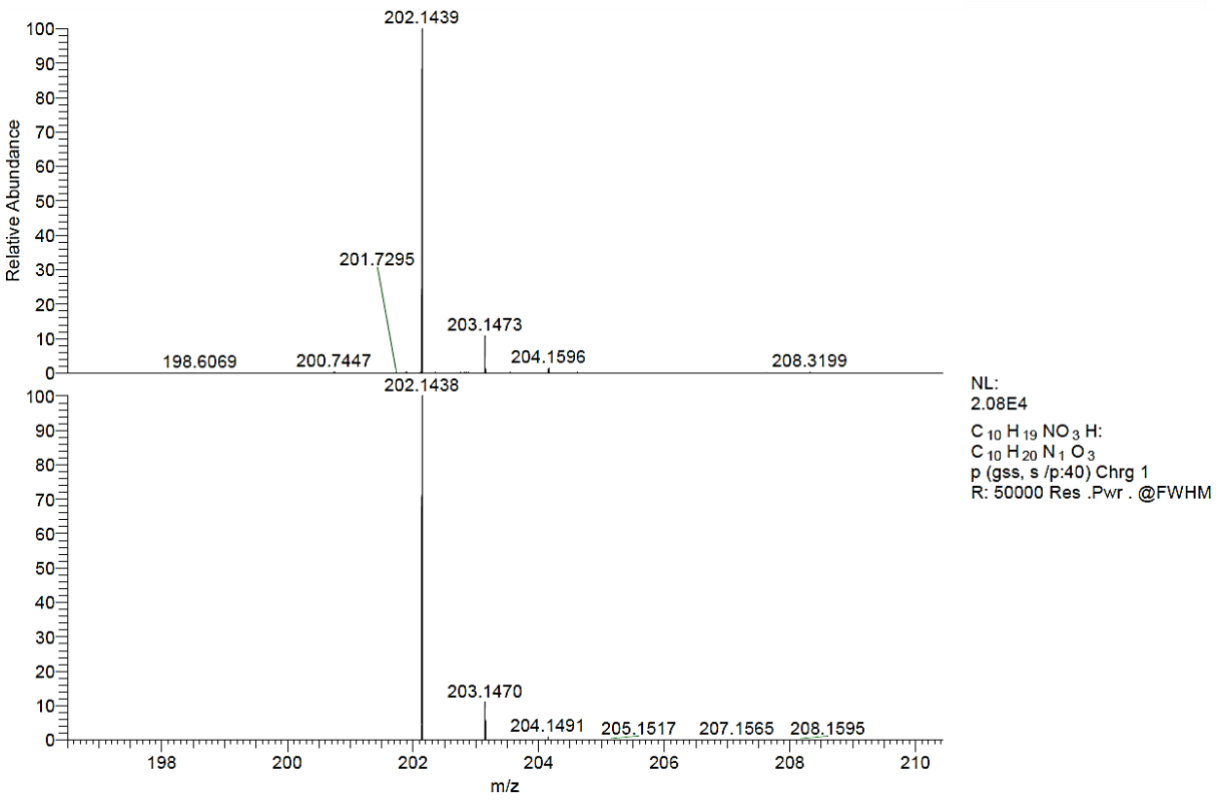

Figure S20: Measured (top) and calculated (bottom) HRMS-ESI spectrum of **30** in positive ion mode.

Allyl (6-bromohexyl)carbamate (31)

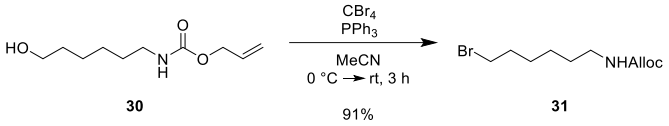

Scheme S4: Synthesis of allyl (6-bromohexyl)carbamate (**31**).

Based on a procedure of Chatterjee *et al.*[22], allyl (6-hydroxyhexyl)carbamate (**30**, 1.00 g, 4.97 mmol, 1.00 eq) was dissolved in dry MeCN (37.0 mL) under nitrogen atmosphere. The solution was cooled to 0 °C and carbon tetrabromide (3.13 g, 9.44 mmol, 1.90 eq) was added followed by slow addition of triphenylphosphine (2.61 g, 9.94 mmol, 2.00 eq). After 30 min, the solution was warmed to rt and stirring was continued for 2.5 h. When TLC (permanganate developer) showed complete conversion of the starting material, the solvent was evaporated, and the remaining residue was dissolved in distilled water/ EtOAc (~200 mL, 1:1). The organic phase was washed with distilled water (~200 mL, 3×). Afterwards, the combined aqueous phases were extracted with EtOAc (~200 mL, 2×). The combined organic phases were washed with brine (~200 mL, 1×) and dried over $MgSO_4$. The solvent was removed under reduced pressure, and the crude was purified by flash column chromatography (*n*-pentane/EtOAc 9:1 → 4:1 (v/v)) to give the desired product **31** (1.20 g, 4.55 mmol, 91%) as a colourless oil.

TLC (permanganate developer): R_f = 0.76 (*n*-pentane/EtOAc 1:1, v/v).

^{1}H-NMR (300 MHz, $CDCl_3$): δ = 5.95 – 5.86 (m, 1H), 5.33 – 5.19 (m, 2H), 4.70 (s, 1H), 5.56 (d, ^3J(H,H) = 3.3 Hz, 2H), 3.40 (t, ^3J(H,H) = 6.7 Hz, 2H), 3.18 (q, ^3J(H,H) = 6.4 Hz, 2H), 1.86 (quint, ^3J(H,H) = 7.2 Hz, 2H), 1.57 – 1.43 (m, 6H) ppm.

^{13}C-NMR (125 MHz, $CDCl_3$): δ = 156.4 (-*C*OO-), 133.1 (*C*H), 117.8 (CH_2), 65.6 (CH_2), 41.0 (CH_2), 33.9 (CH_2), 32.7 (CH_2), 30.0 (CH_2), 27.9 (CH_2), 26.0 (CH_2) ppm.

HRMS-ESI (*m/z*): $[M+Na]^+$ calcd for $C_{10}H_{18}BrNO_2Na$: 286.0413; found: 286.0418.

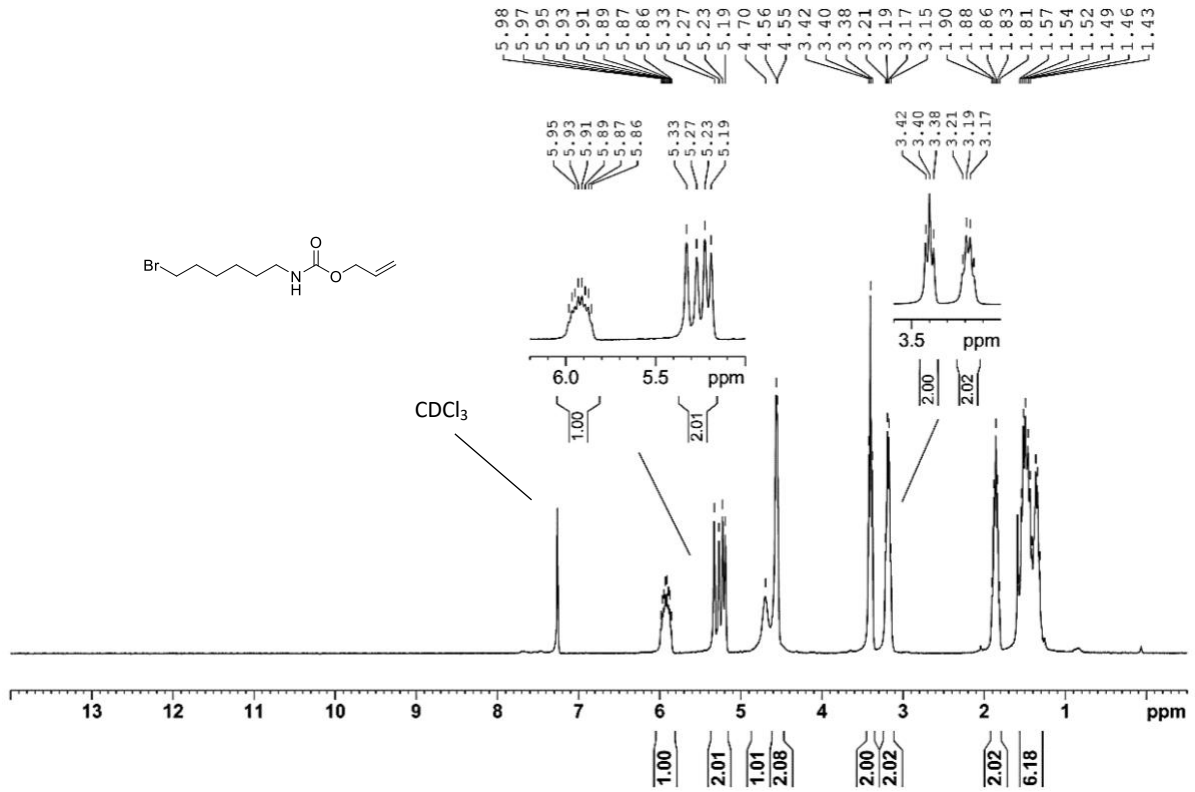

Figure S21: ^{1}H-NMR (300 MHz) spectrum of compound **31** in $CDCl_3$.

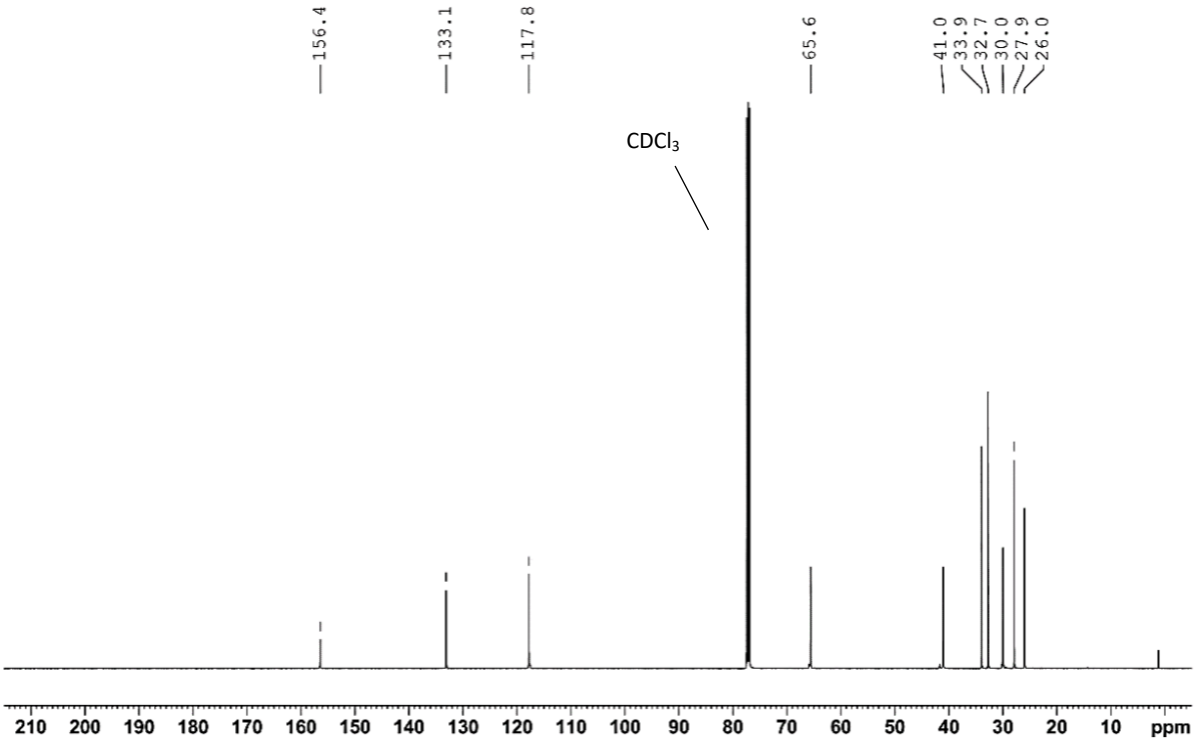

Figure S22: ^{13}C-NMR (125 MHz) spectrum of compound **31** in $CDCl_3$.

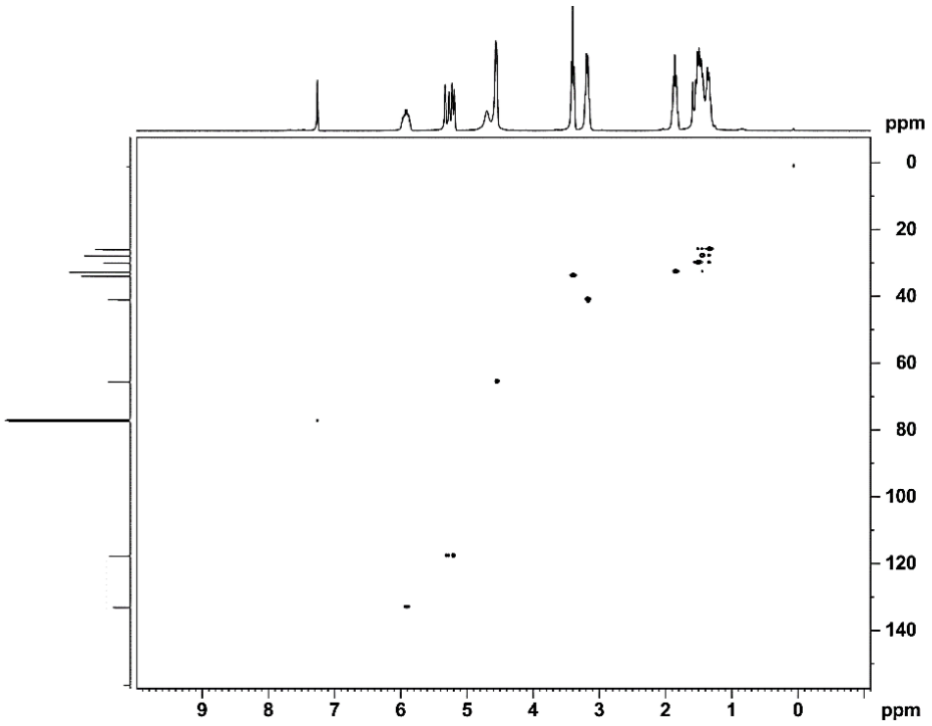

Figure S23: HSQC spectrum of compound **31** (^{1}H-NMR: 300 MHz, ^{13}C-NMR: 125 MHz, $CDCl_3$).

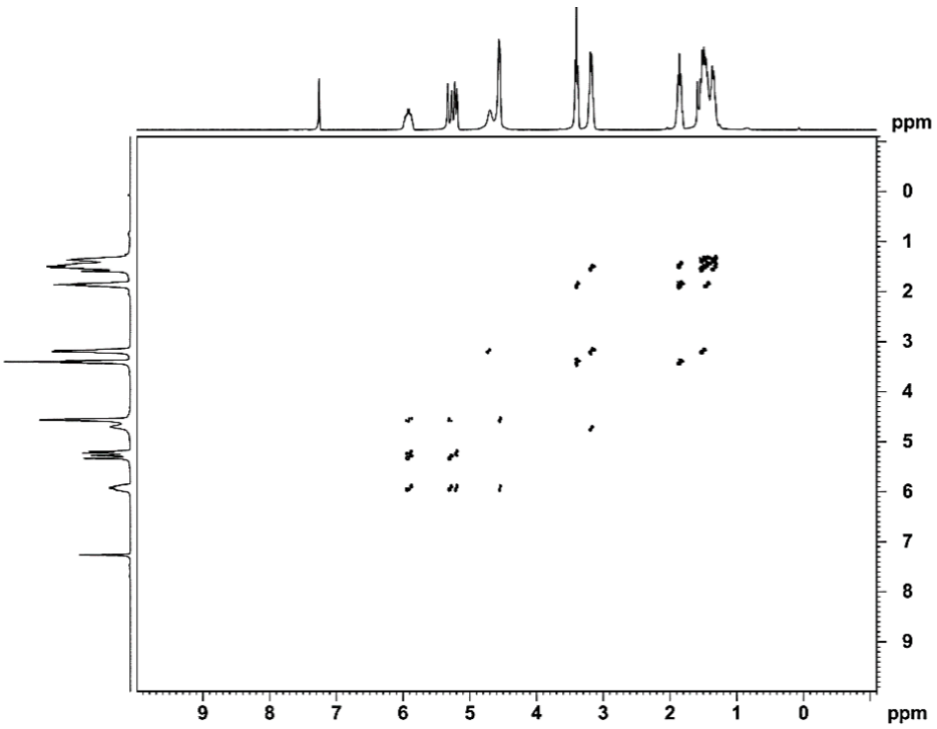

Figure S24: COSY spectrum of compound **31** (^{1}H-NMR: 300 MHz, $CDCl_3$).

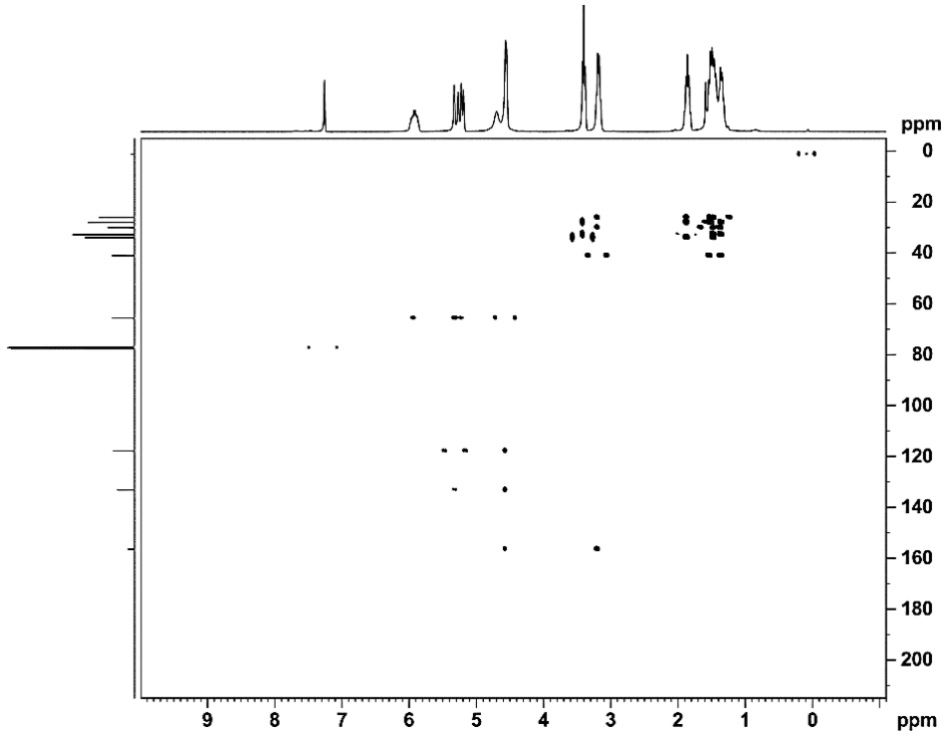

Figure S25: HMBC spectrum of compound **31** (^{1}H-NMR: 300 MHz, ^{13}C-NMR: 125 MHz, $CDCl_3$).

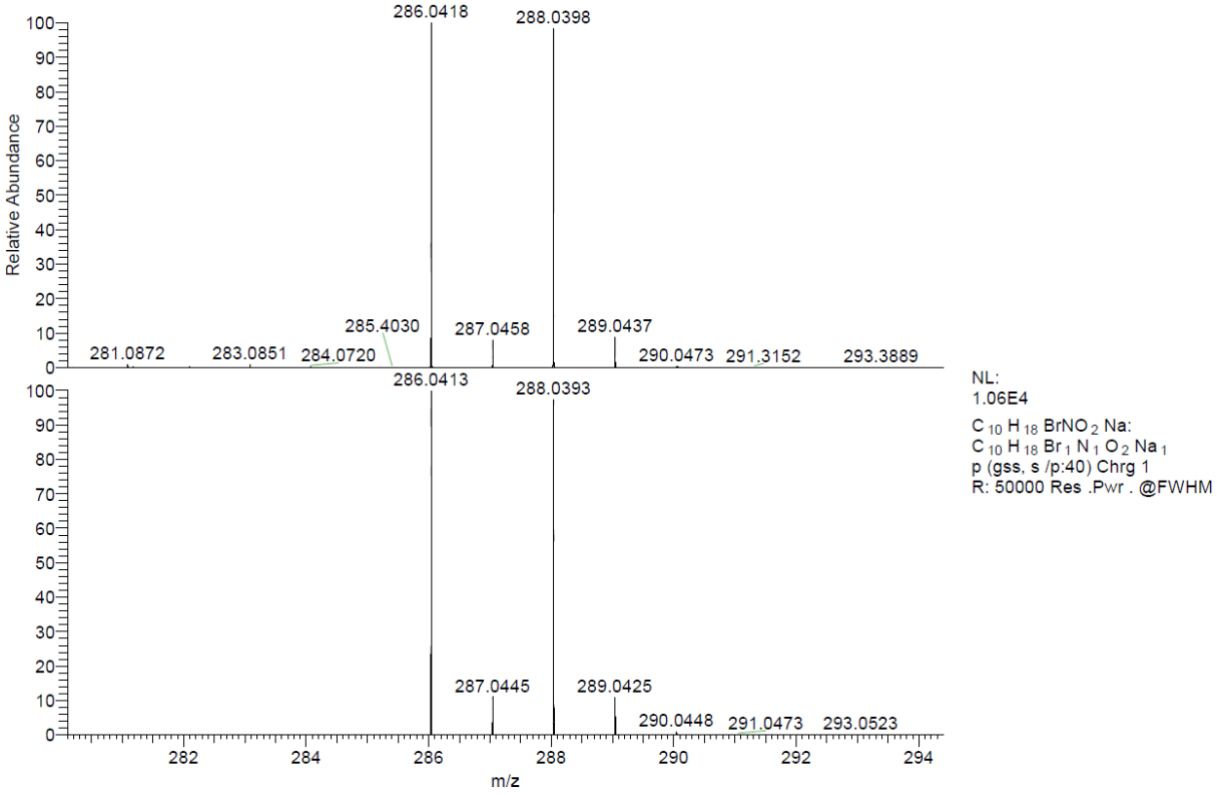

Figure S26: Measured (top) and calculated (bottom) HRMS-ESI spectrum of **31** in positive ion mode.

Allyl (6-(4-formylphenoxy)hexyl)carbamate (8)

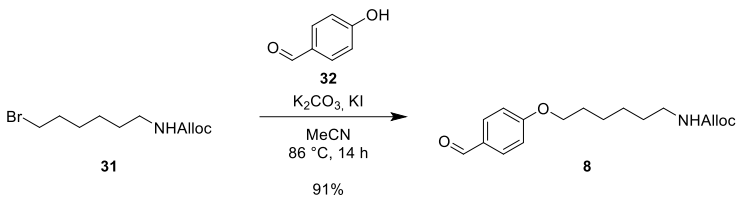

Scheme S5: Synthesis of allyl (6-(4-formylphenoxy)hexyl)carbamate (**8**).

Adapted from the protocol of Yoo *et al.*[23], 4-hydroxybenzaldehyde (**32**, 0.46 g, 3.79 mmol, 1.00 eq), potassium carbonate (1.26 g, 9.09 mmol, 2.40 eq) and potassium iodine (0.06 g, 0.38 mmol, 0.10 eq) were suspended in dry MeCN (9.00 mL) under nitrogen atmosphere. Allyl-6-bromohexylcarbamate (**31**, 1.20 g, 4.54 mmol, 1.20 eq) was dissolved in dry MeCN (4.10 mL) and added to the suspension. The reaction mixture was heated to 86 °C and refluxed for 14 h. Afterwards, the solid was removed by filtration and the solvent was evaporated. The residue was purified by flash column chromatography (*n*-pentane/EtOAc 3:1 → 1:1 (v/v)) to yield compound **8** (1.05 g, 3.43 mmol, 91%) as a white solid.

TLC ($UV_{254\ nm}$): R_f = 0.36 (*n*-pentane/EtOAc 3:1, v/v).

^{1}H-NMR (300 MHz, DMSO-d_6): δ = 9.86 (s, 1H), 7.85 (dt, ^4J(H,H) = 2.3 Hz, ^3J(H,H) = 8.7 Hz, 2H), 7.17 (t, ^3J(H,H) = 5.4 Hz, 1H), 7.11 (dt, ^4J(H,H) = 2.3 Hz, ^3J(H,H) = 8.7 Hz, 2H), 5.96-5.83 (m, 1H), 5.25 (dq, ^3J(H,H) = 17.2 Hz, ^2J(H,H) = 1.7 Hz, 1H), 5.15 (dq, ^3J(H,H) = 10.4 Hz, ^2J(H,H) = 1.4 Hz, 1H), 4.44 (d, ^3J(H,H) = 5.3 Hz, 2H), 4.08 (t, ^3J(H,H) = 6.5 Hz, 2H), 2.98 (q, ^3J(H,H) = 6.6 Hz, 2H), 1.73 (qi, ^3J(H,H) = 6.8 Hz, 2H), 1.46-1.28 (m, 6H) ppm.

^{13}C-NMR (125 MHz, DMSO-d_6): δ = 191.2 (C_q), 163.7 (C_q), 155.9 (C_q), 133.9 (*C*H), 131.8 (2C; *C*H), 129.5 (C_q), 116.8 (CH_2), 114.9 (2C; *C*H), 68.0 (CH_2), 64.0 (CH_2), 40.1 (CH_2), 29.3 (CH_2), 28.4 (CH_2), 25.9 (CH_2), 25.1 (CH_2) ppm.

HRMS-ESI (*m/z*): $[M+Na]^+$ calcd for $C_{17}H_{23}NO_4Na$: 328.1519; found: 328.1520.

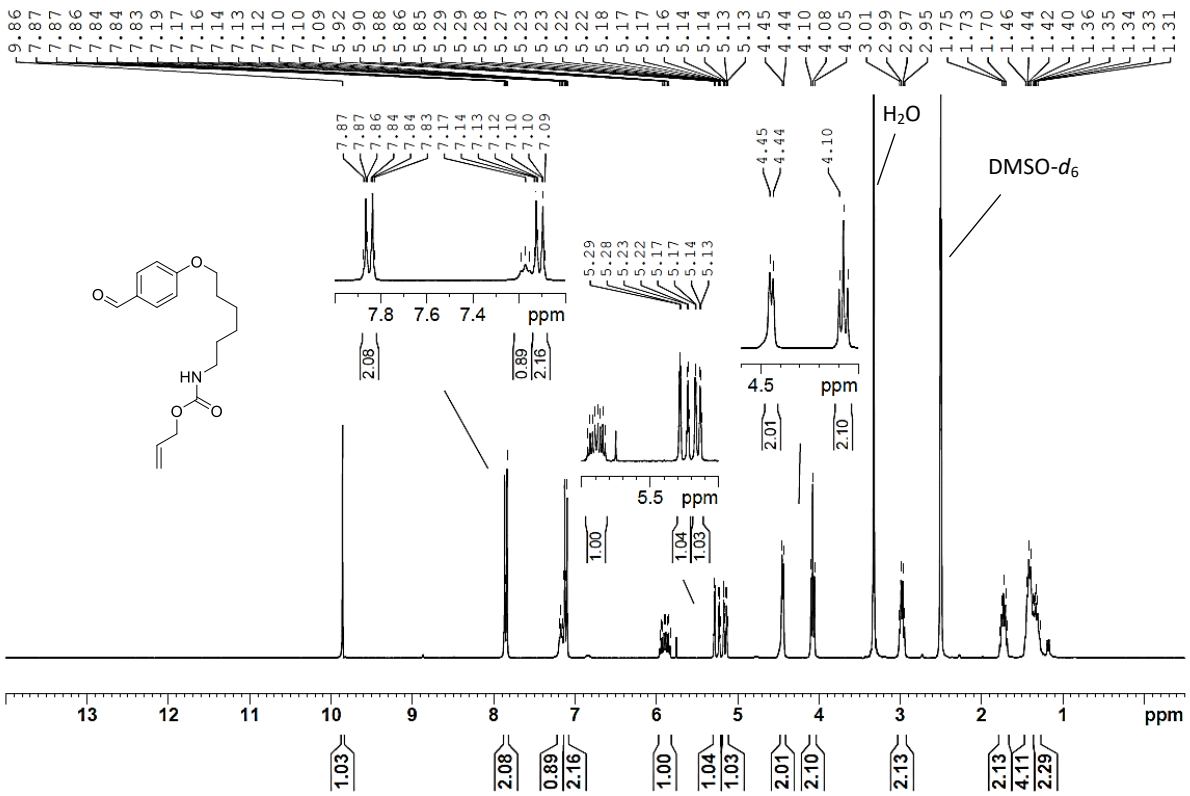

Figure S27: ^{1}H-NMR (300 MHz) spectrum of compound **8** in DMSO-d_6.

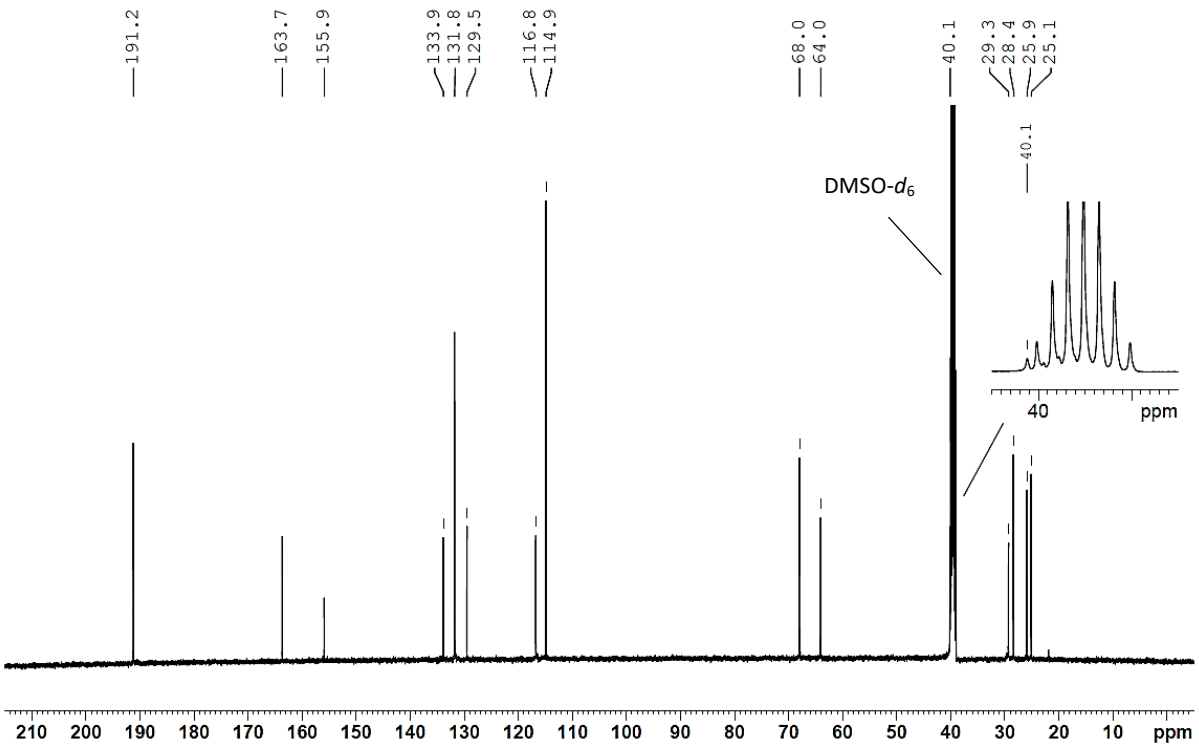

Figure S28: ^{13}C-NMR (125 MHz) spectrum of compound **8** in DMSO-d_6.

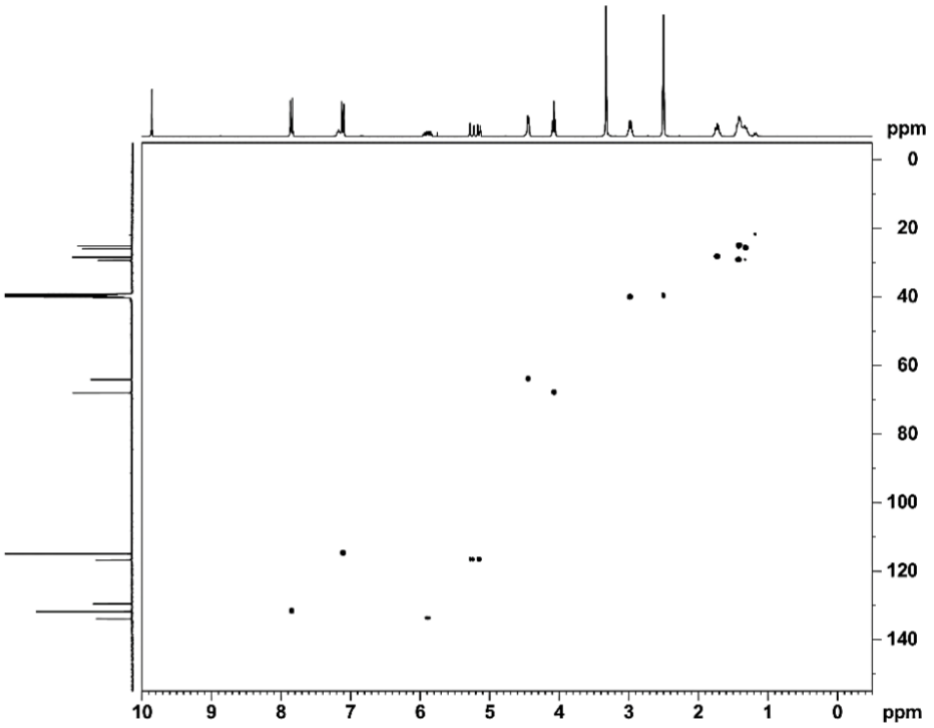

Figure S29: HSQC spectrum of compound **8** (^{1}H-NMR: 300 MHz, ^{13}C-NMR: 125 MHz, DMSO-d_6).

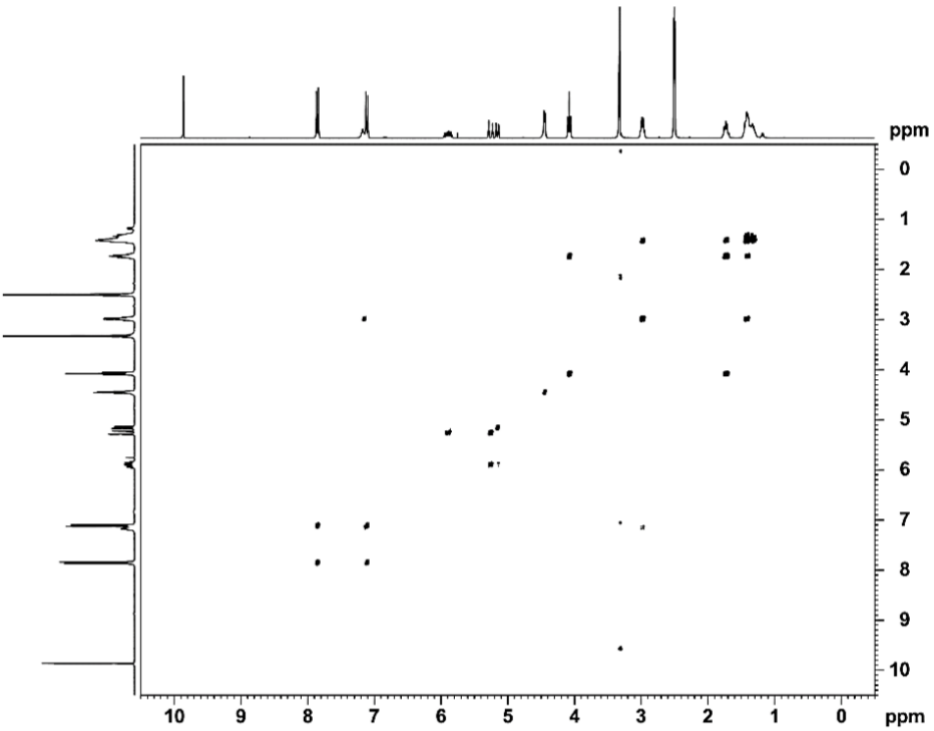

Figure S30: COSY spectrum of compound **8** (^{1}H-NMR: 300 MHz, DMSO-d_6).

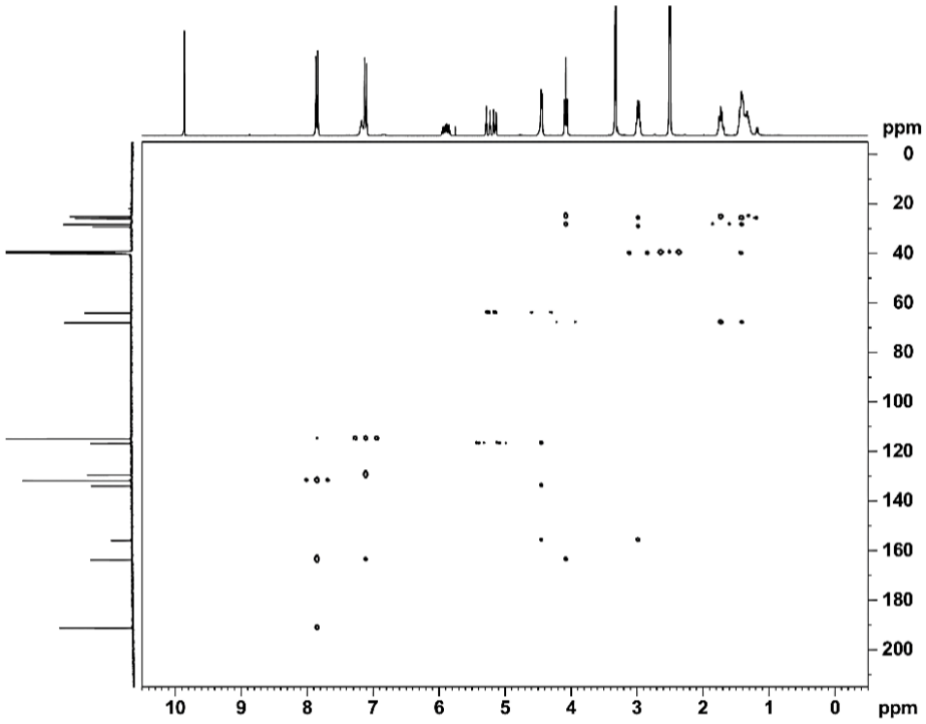

Figure S31: HMBC spectrum of compound **8** (^{1}H-NMR: 300 MHz, ^{13}C-NMR: 125 MHz, DMSO-d_6).

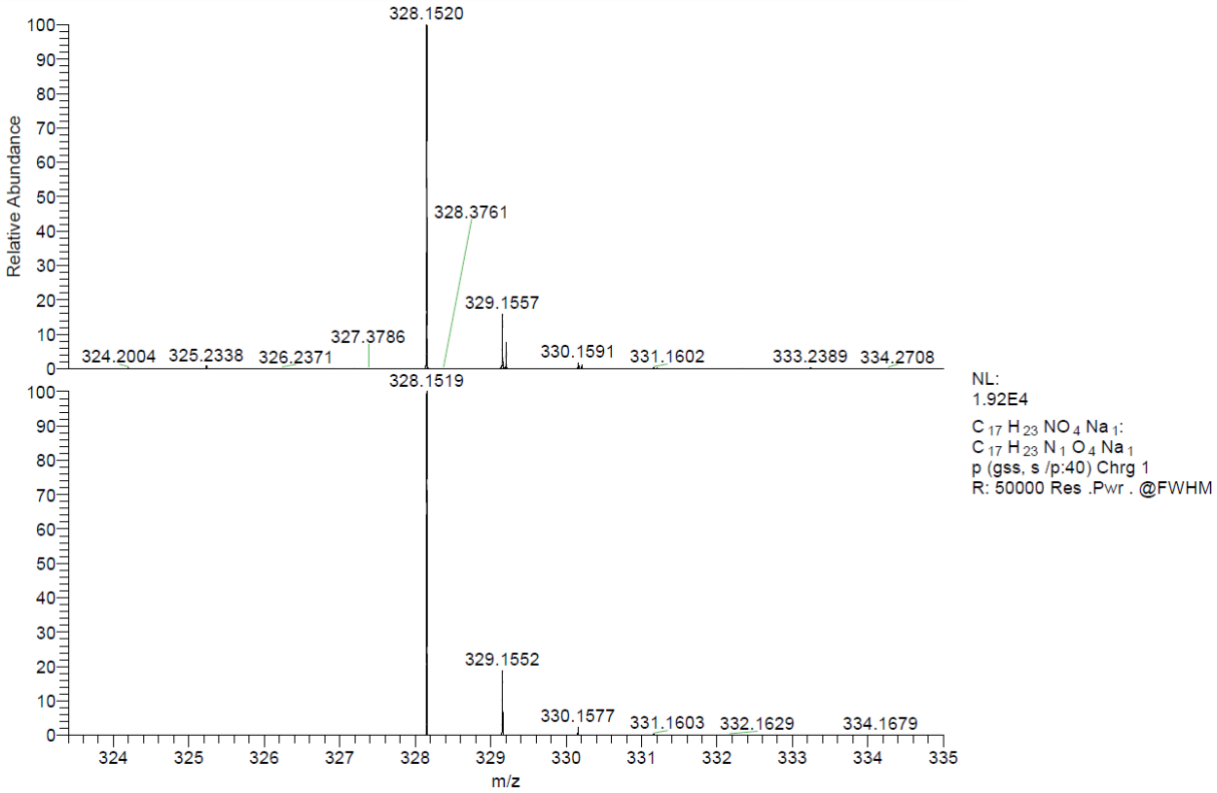

Figure S32: Measured (top) and calculated (bottom) HRMS-ESI spectrum of **8** in positive ion mode.

3-Benzyl-5-bromopyrazin-2-amine (35)

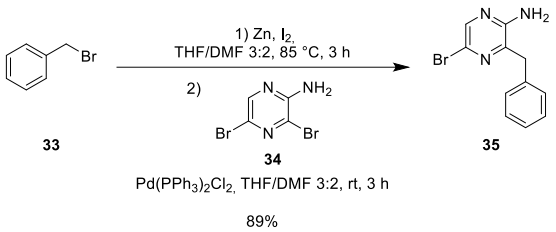

Scheme S6: Synthesis of 3-benzyl-5-bromopyrazin-2-amine (**35**).[24]

Adapted from the procedure of Yuan *et al.*[24] a solution of iodine (491 mg, 1.94 mmol, 0.10 eq) in dry THF (30.0 mL) and HPLC-grade DMF (20.0 mL) was added to zinc dust (4.91 g, 75.1 mmol, 3.80 eq) under nitrogen atmosphere using a syringe. The reaction mixture was stirred at rt until the brown colour of the iodine disappeared. Benzyl bromide (**33**, 3.52 mL, 29.7 mmol, 1.50 eq) was added slowly using a syringe and the reaction mixture was heated to 85 °C to reflux. After cooling to rt, 2-amino-3,5-dibromopyrazine (**34**, 5.00 mg, 19.8 mmol, 1.00 eq) and a suspension of $Pd(PPh_3)_2Cl_2$ (550 mg, 0.78 mmol, 0.04 eq) in THF/DMF 3:2 (75.0 mL) was added. The mixture was stirred at rt while monitoring the reaction by TLC ($UV_{254\ nm}$). After 3 h, complete conversion was confirmed, and the mixture was filtered through celite using EtOAc. The filtrate was washed with distilled water (~200 mL, 2×). The aqueous phase was extracted with EtOAc (~200 mL, 2×). The combined organic phases were washed with brine (~200.0 mL, 1×), dried over Na_2SO_4 and concentrated under reduced pressure. To purify the remaining residue, silica gel column chromatography (*n*-pentane/EtOAc 4:1 ⟶ 3:1 ⟶ 3:2 ⟶ 1:1 (v/v)) was used, yielding the desired product (**35**, 4.66 g, 17.6 mmol, 89%) as a yellow viscous oil. The characterization is in agreement with the literature.[24]

TLC ($UV_{254\ nm}$): R_f = 0.45 (*n*-pentane/EtOAc 2:1, v/v).

^{1}H-NMR (300 MHz, $CDCl_3$): δ = 8.01 (s, 1H), 7.35-7.27 (m, 3H), 7.23-7.20 (m, 2H), 4.42 (s (br), 2H), 4.07 (s, 2H) ppm.

^{13}C-NMR (75 MHz, $CDCl_3$): δ = 152.2 (C_q), 142.4 (C_q), 142.0 (*C*H), 135.8 (C_q), 129.2 (2C; *C*H), 128.6 (2C; *C*H), 127.4 (*C*H), 126.4 (C_q), 40.9 (CH_2) ppm.

HRMS-ESI (*m/z*): $[M+H]^+$ calcd for $C_{11}H_{11}BrN_3$: 264.0131; found: 264.0141.

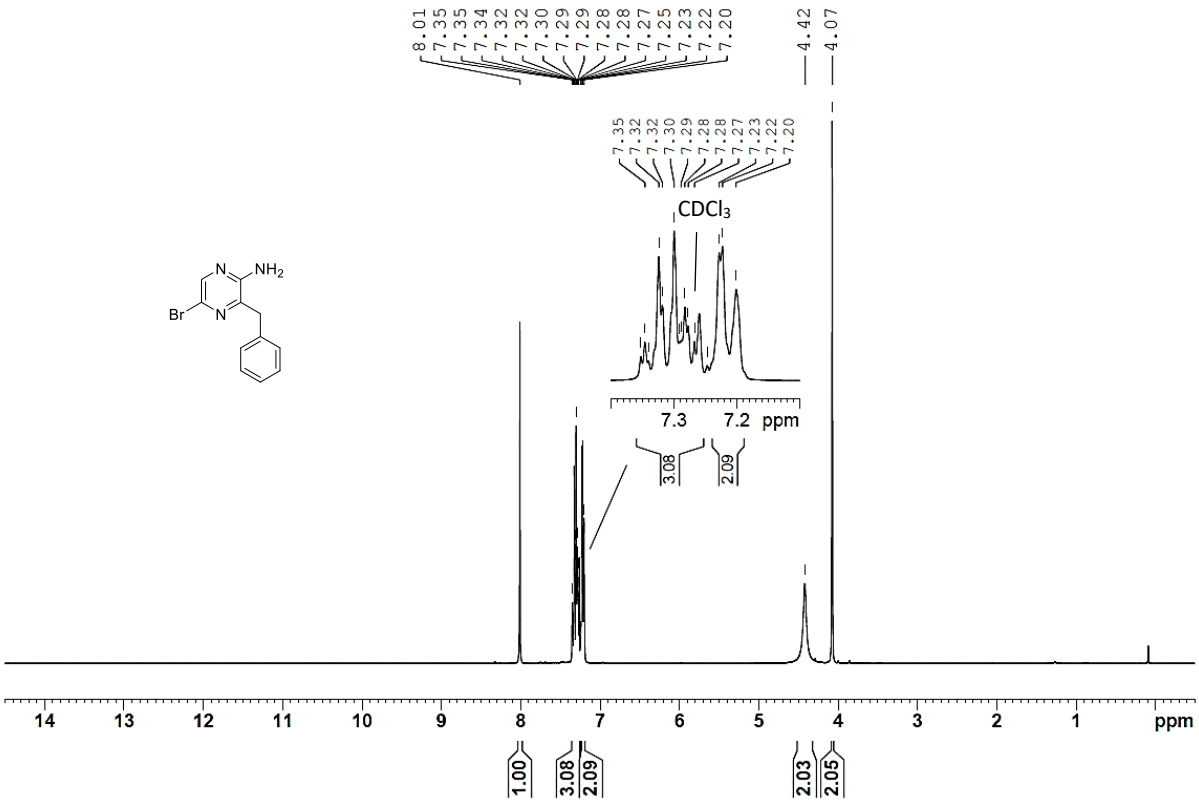

Figure S33: ^{1}H-NMR (300 MHz) spectrum of compound **35** in $CDCl_3$.

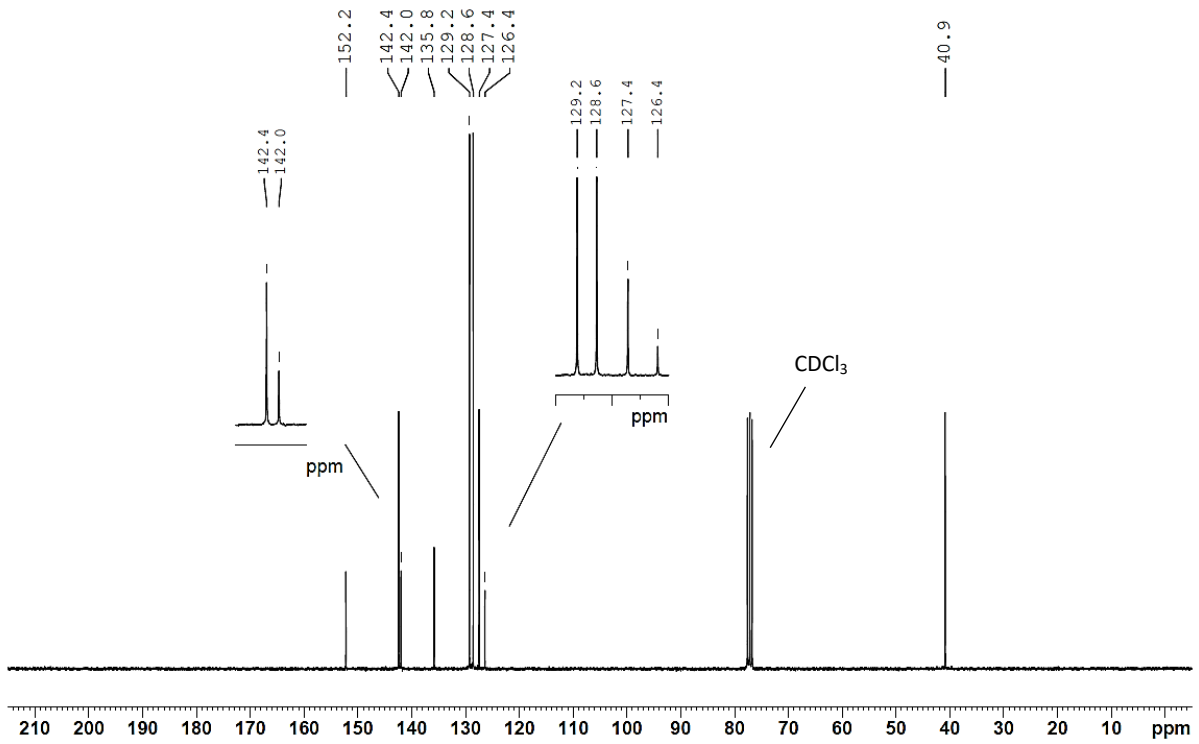

Figure S34: ^{13}C-NMR (75 MHz) spectrum of compound **35** in $CDCl_3$.

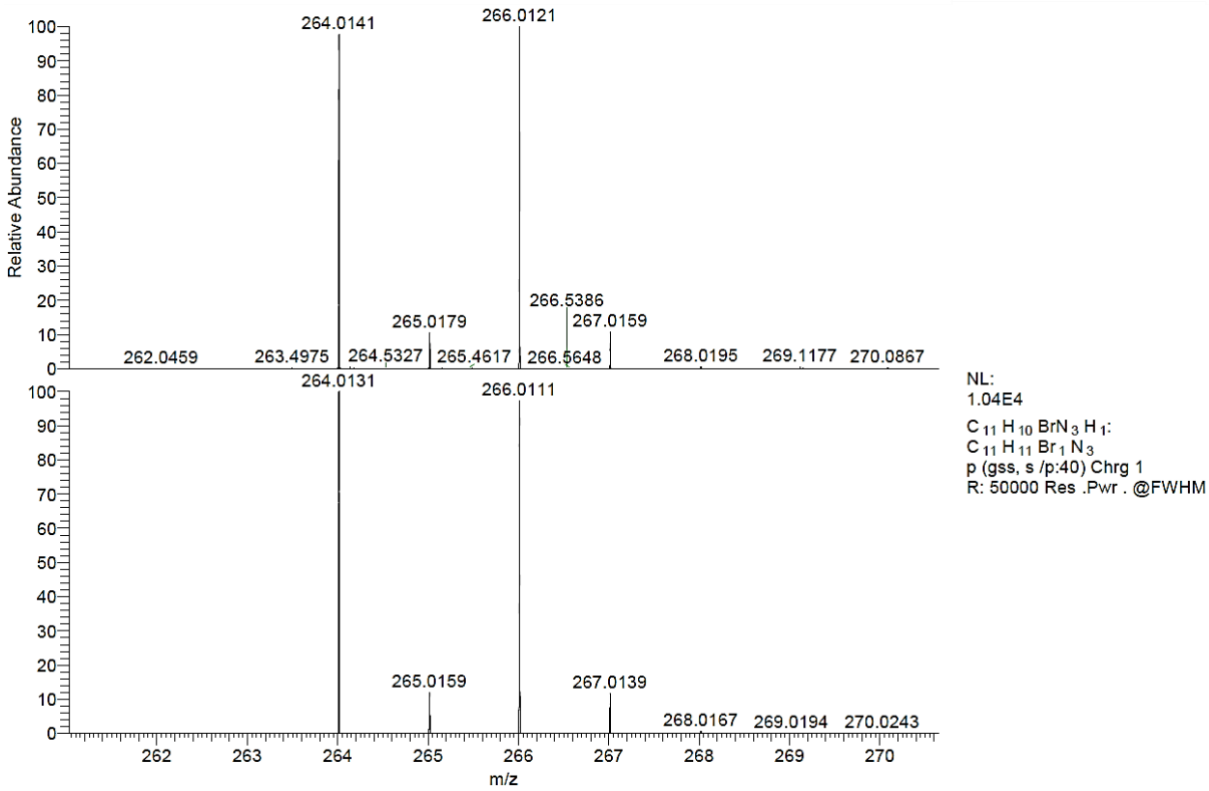

Figure S35: Measured (top) and calculated (bottom) HRMS-ESI spectrum of **35** in positive ion mode.

3-Benzyl-5-phenylpyrazin-2-amine (37)

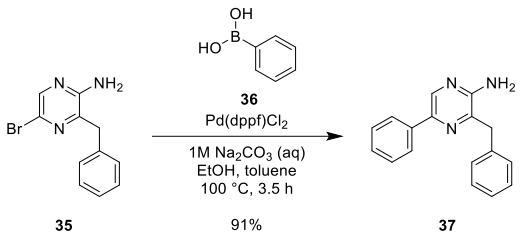

Scheme S7: Synthesis of 3-benzyl-5-phenylpyrazin-2-amine (**37**).[24]

Based on the procedure of Yuan *et al.*[24], 3-benzyl-5-bromopyrazine-2-amine (**35**, 414.7 mg, 1.57 mmol, 1.00 eq) and phenylboronic acid (**36**, 287.1 mg, 2.36 mmol, 1.50 eq) were dissolved in toluene (22.0 mL) at rt under nitrogen atmosphere. Absolute EtOH (6.20 mL) and a 1 M Na_2CO_3 (aq) solution (15.0 mL) were added. Pd(dppf)Cl_2 (57.8 mg, 0.08 mmol, 0.05 eq) was suspended in toluene (9.50 mL) and added to the reaction mixture. The mixture was stirred for 3.5 h at 100 °C. After cooling to rt, the solution was filtered through celite and washed with EtOAc (~150 mL, 1×). The organic phase was washed with distilled water (~150 mL, 2×) and brine (~150 mL, 1×), dried over Na_2SO_4 and evaporated. Purification was done by silica gel column chromatography (*n*-pentane/EtOAc 2:1 → 1:1 (v/v)) yielding 3-benzyl-5-phenylpyrazin-2-amine (**37**, 373 mg, 1.43 mmol, 91%) as a pale-yellow solid. The characterization is in agreement with the literature.[24]

TLC ($UV_{254\ nm}$): R_f = 0.28 (*n*-pentane/EtOAc 2:1, v/v).

^{1}H-NMR (300 MHz, DMSO-d_6): δ = 8.42 (s, 1H), 7.92-7.89 (m, 2H), 7.43-7.34 (m, 4H), 7.32-7.26 (m, 3H), 7.21-7.17 (m, 1H), 6.41 (s, 2H), 4.08 (s, 2H) ppm.

^{13}C-NMR (75 MHz, DMSO-d_6): δ = 152.7 (C_q), 140.0 (*C*H), 138.7 (C_q), 138.1 (C_q), 137.1 (C_q), 136.9 (C_q), 128.9 (2C; *C*H), 128.6 (2C; *C*H), 128.2 (2C; *C*H), 127.3 (*C*H), 126.1 (*C*H), 124.7 (2C; *C*H), 38.6 (CH_2) ppm.

HRMS-ESI (*m/z*): $[M+H]^+$ calcd for $C_{17}H_{16}N_3$: 262.1339; found: 262.1342.

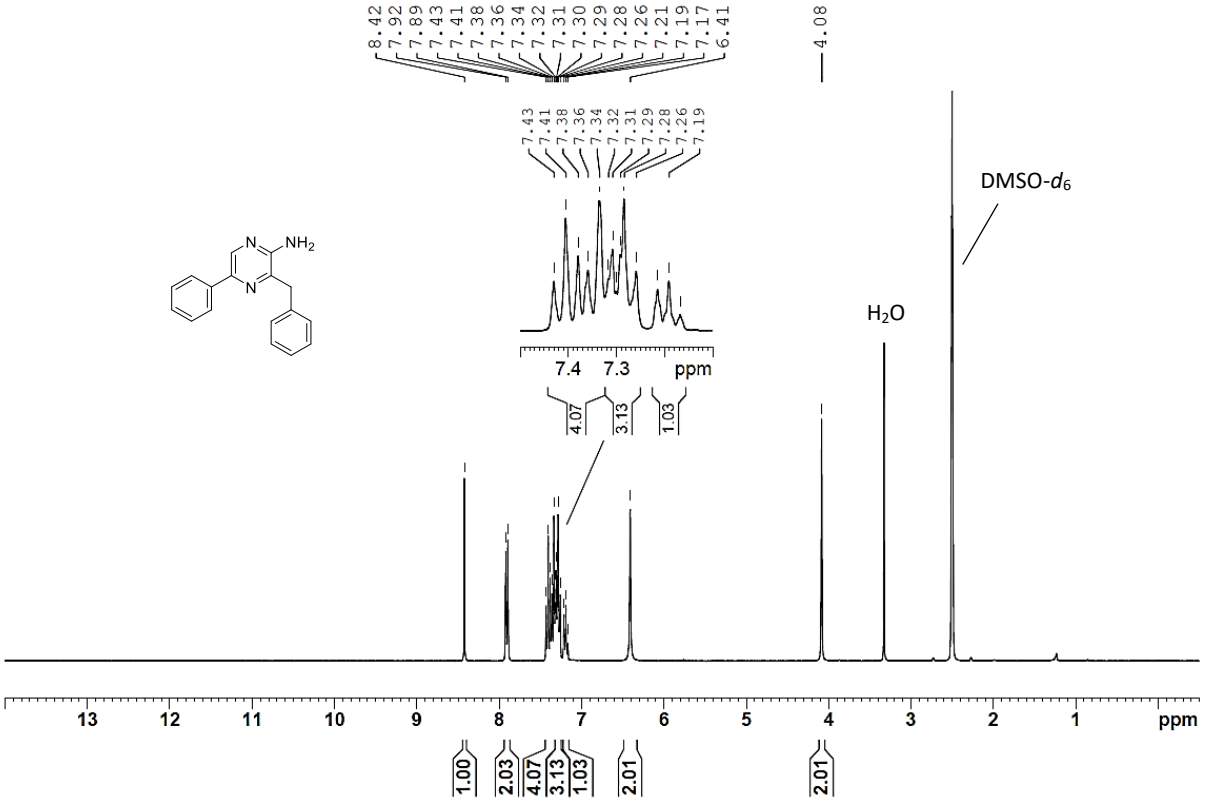

Figure S36: ^{1}H-NMR (300 MHz) spectrum of compound **37** in DMSO-d_6.

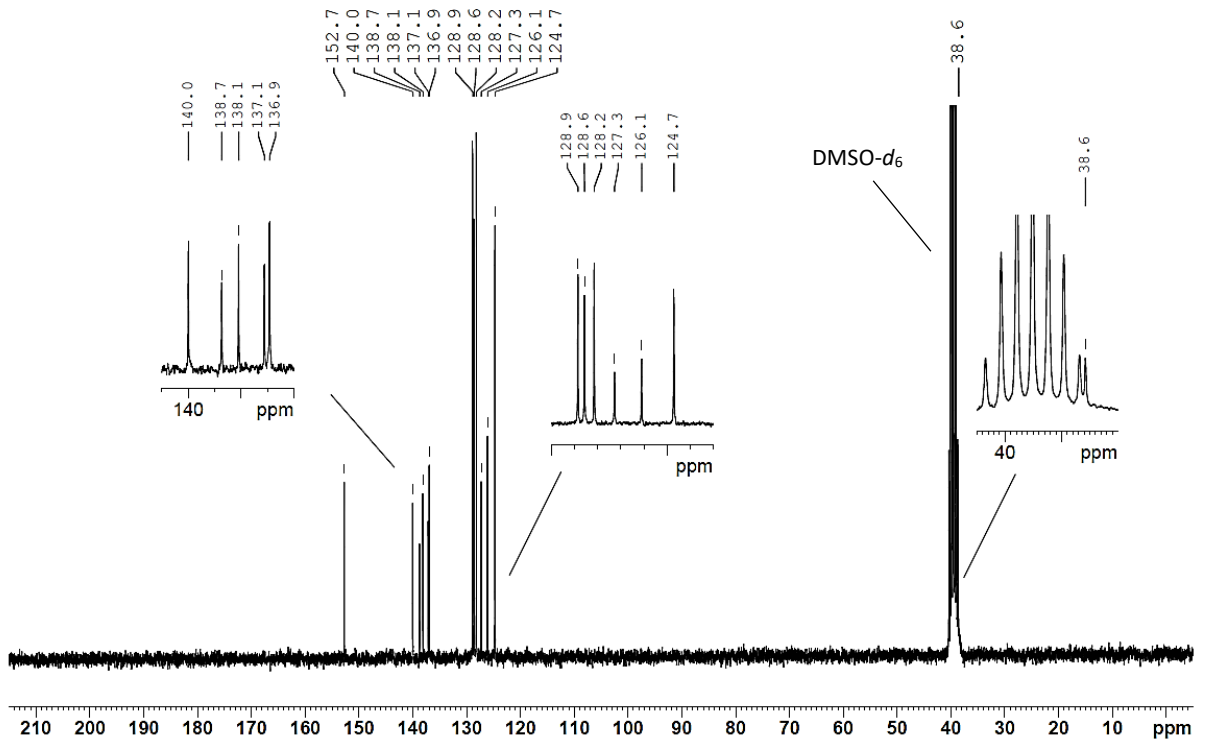

Figure S37: ^{13}C-NMR (75 MHz) spectrum of compound **37** in DMSO-d_6.

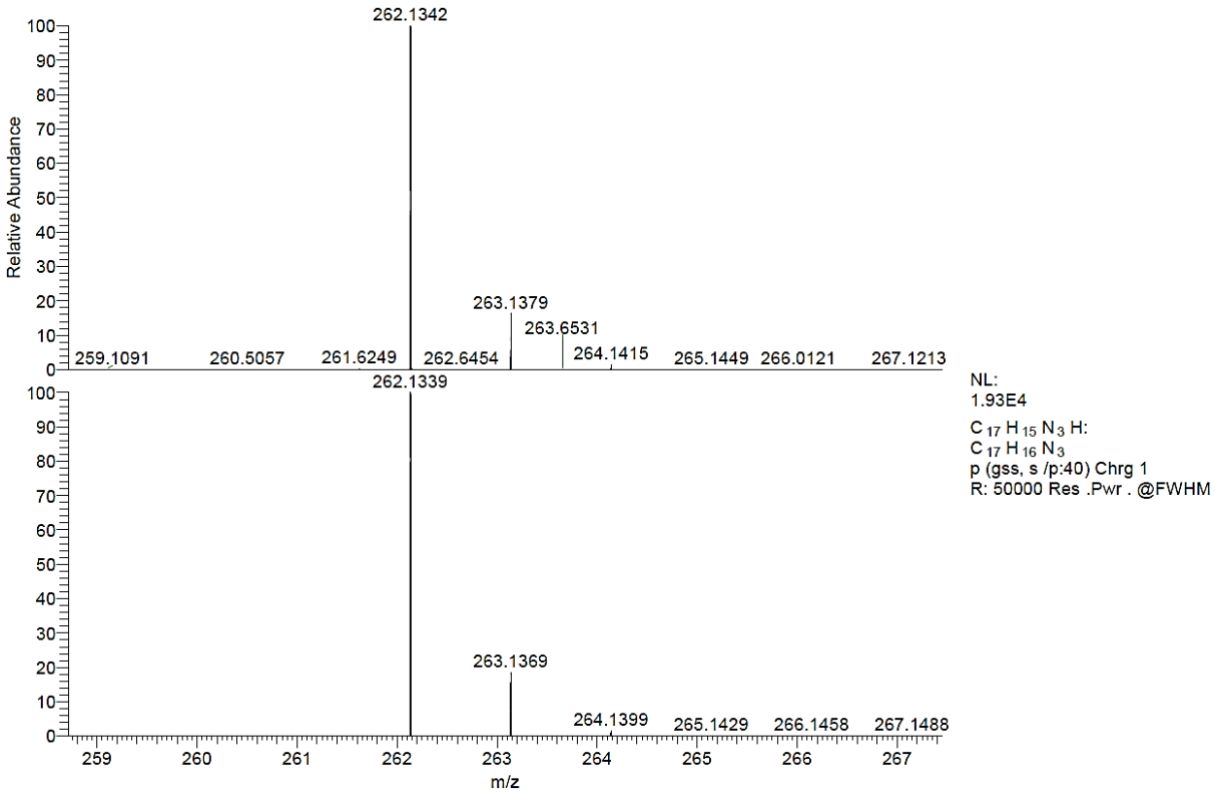

Figure S38: Measured (top) and calculated (bottom) HRMS-ESI spectrum of **37** in positive ion mode.

Ethyl-2-diazo-2-(diethoxyphosphoryl)acetate (39)

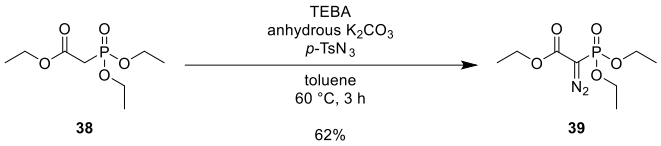

Scheme S8: Synthesis of ethyl-2-diazo-2-(diethoxyphosphoryl)acetate (**39**).[25]

Following an adapted procedure of Jászay *et al*.[25], TEBA (0.25 g, 1.12 mmol, 0.10 eq) and ground anhydrous potassium carbonate (6.17 g, 44.6 mmol, 4.00 eq) were suspended in dry toluene (28.4 mL) under nitrogen atmosphere. Ethyl-2-(diethoxyphosphoryl)-acetate (**38**, 2.2 mL, 11.2 mmol, 1.00 eq) was added using a syringe and the reaction mixture was heated to 60 °C. A solution of tosyl azide in toluene (11-15% (w/w), 16.3 mL, 11.2 mmol, 1.00 eq) was added and the mixture was stirred at 60 °C for 3 h. The complete conversion was confirmed using TLC (permanganate developer). After cooling to rt, the precipitate was filtered and washed with EtOAc (~150 mL, 2×). The filtrate was washed with 0.5 M NaOH (~150 mL, 2×), distilled water (~150 mL, 2× 150) and brine (~150 mL, 1×), dried over $MgSO_4$ and concentrated under reduced pressure. The residue was purified by silica gel column chromatography (*n*-pentane/EtOAc 4:1 → 2:1 → 1:1 → EtOAc, (v/v)) to yield the desired diazo compound **39** (1.74 g, 6.95 mmol, 62%) as a colorless liquid. The characterization is in agreement with the literature.[25]

TLC (permanganate developer): R_f = 0.18 (*n*-pentane/EtOAc 2:1, v/v).

^{1}H-NMR (300 MHz, $CDCl_3$): δ = 4.29-4.09 (m, 6H), 1.41-1.24 (m, 9H) ppm.

^{13}C-NMR (75 MHz, $CDCl_3$): δ = 163.6 (C_q), 163.5 (C_q), 63.8 (CH_2), 63.7 (CH_2), 61.8 (CH_2), 16.3 (CH_3), 16.2 (CH_3), 14.5 (CH_3) ppm.

IR: $\tilde{\nu}$ = 2984 (w), 2937 (w), 2909 (w), 2124 (s), 1701 (s), 1477 (w), 1446 (w), 1392 (w), 1368 (w), 1273 (s), 1216 (w), 1165 (w), 1095 (w), 1015 (s), 976 (w), 860 (w), 797 (w), 747 (m), 588 (w), 558 (m), 509 (w), 478 (w) cm^{-1}.

HRMS-ESI (*m/z*): $[M+Na]^+$ calcd for $C_8H_{15}N_2O_5PNa$: 273.0611; found: 273.0622.

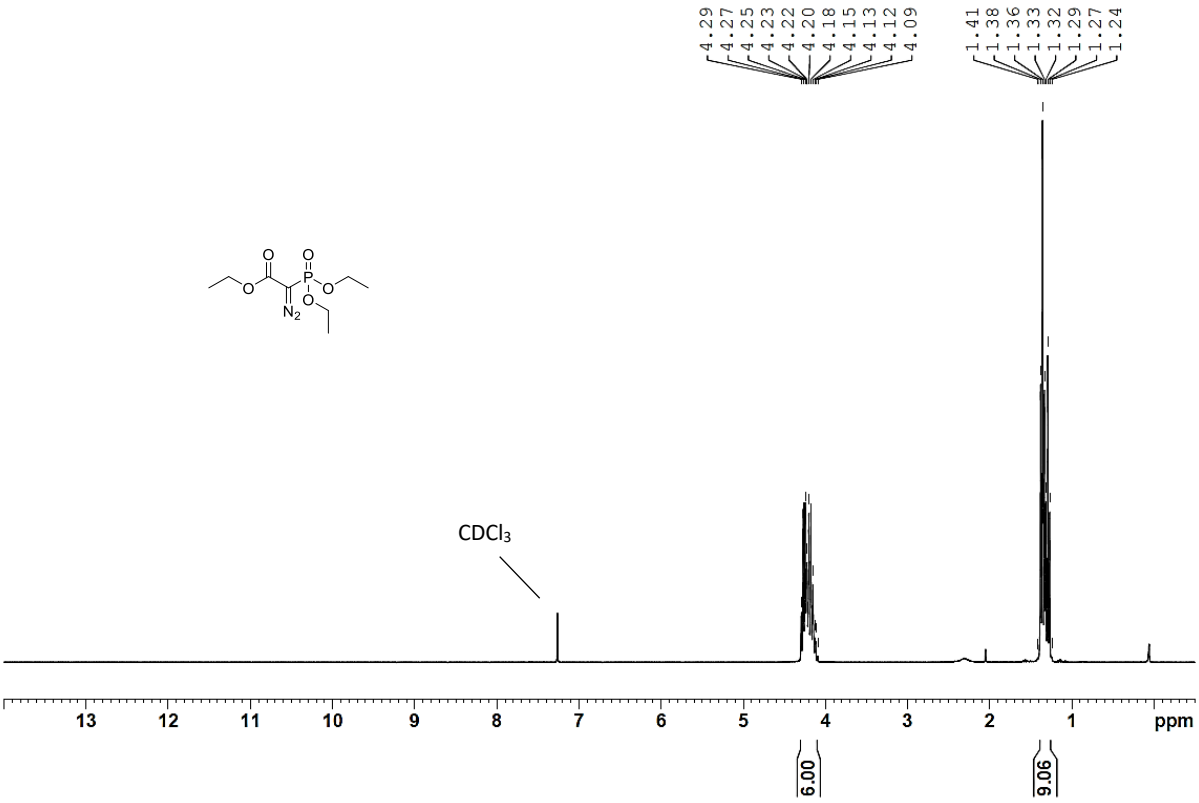

Figure S39: ^{1}H-NMR (300 MHz) spectrum of compound **39** in $CDCl_3$.

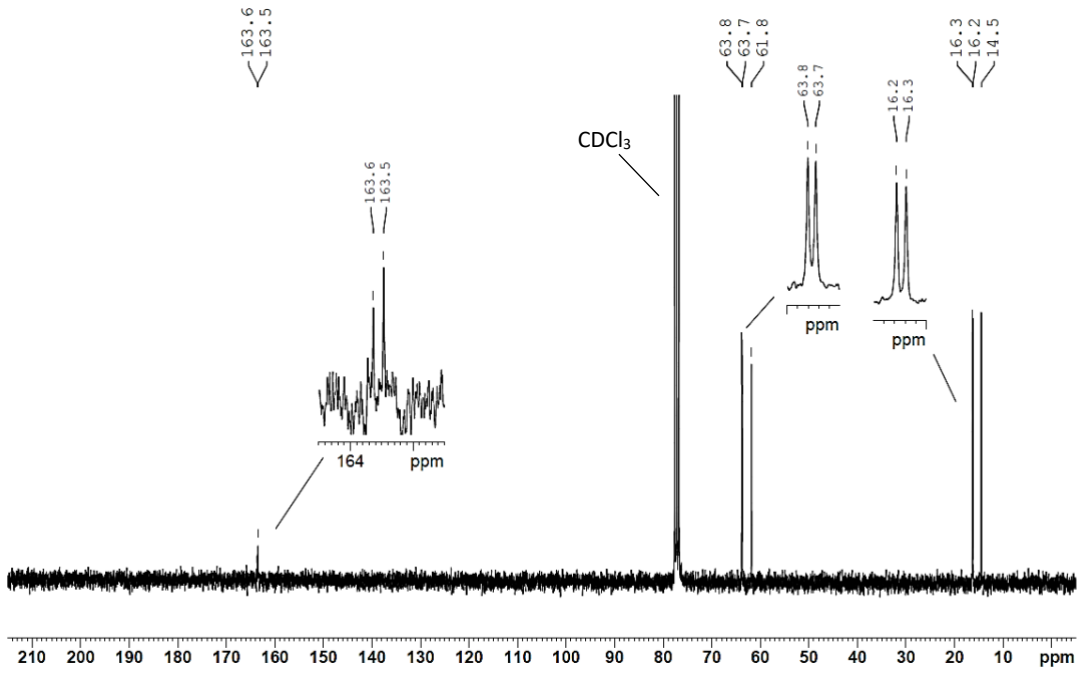

Figure S40: ^{13}C-NMR (75 MHz) spectrum of compound **39** in $CDCl_3$.

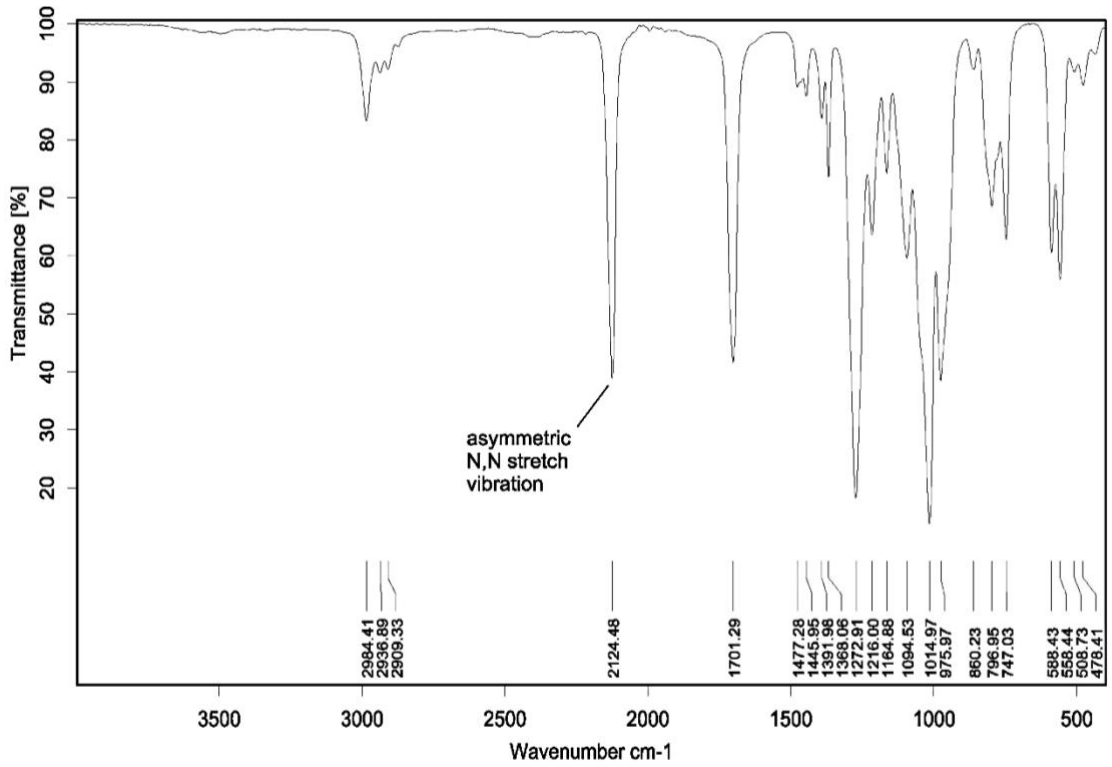

Figure S41: IR-spectrum of compound **39**. The band at 2124.48 cm^{-1} corresponds to the asymmetric *N,N*-stretch vibration, which confirms the presence of the diazo group in the molecule.[26]

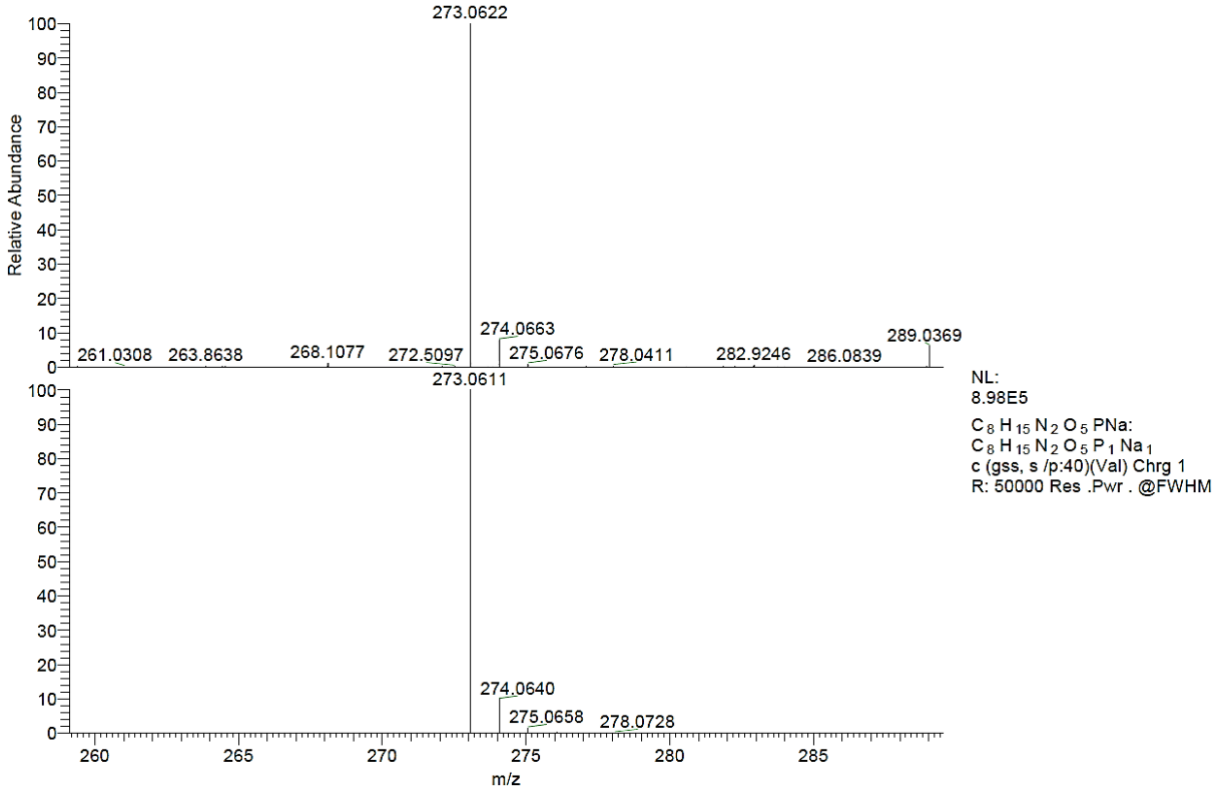

Figure S42: Measured (top) and calculated (bottom) HRMS-ESI spectrum of **39** in positive ion mode.

Compound 37

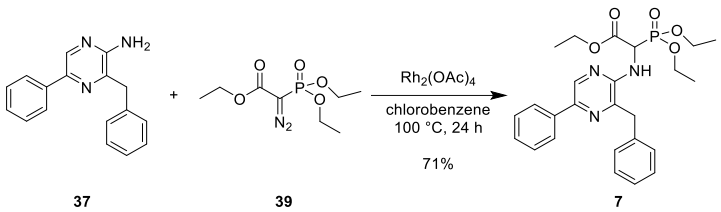

Scheme S9: Synthesis of ethyl-2-((3-benzyl-5-phenylpyrazin-2-yl)amino)-2-(diethoxyphosphoryl)acetate (**7**).

Based on a procedure reported by Shakhim *et al*.[27], chlorobenzene (7.10 mL) was added to aminopyrazine **37** (1.21 g, 4.64 mmol, 1.00 eq) and $Rh_2(OAc)_4$ (205 mg, 0.46 mmol, 0.10 eq) under nitrogen atmosphere. Next, the diazo compound **39** (1.48 mL, 6.95 mmol, 1.50 eq) was given. The reaction mixture was refluxed at 100 °C. After 24 h, the reaction mixture was filtered over celite to remove the catalyst, followed by purification using silica gel column chromatography (*n*-pentane/EtOAc 3:2 → 1:1 → 2:3 → pure EtOAc, (v/v)). The desired product **7** (1.59 g, 3.28 mmol, 71%) was isolated as a brown solid.

TLC ($UV_{254\ nm}$): R_f = 0.22 (*n*-pentane/EtOAc 3:2, v/v).

^{1}H-NMR (500 MHz, DMSO-d_6): δ = 8.57 (s, 1H), 7.97 (d, ^3J(H,H) = 7.4 Hz, 2H), 7.44 (t, ^3J(H,H) = 7.6 Hz, 2H), 7.36-7.33 (m, 3H), 7.31-7.28 (m, 2H), 7.23-7.20 (m, 1H), 6.58 (dd, *J*(H,H) = 8.8 Hz, 4.4 Hz, 1H), 5.30-5.23 (m, 1H), 4.36 (d, ^2J(H,H) = 15.1 Hz, 1H), 4.22 (d, ^2J(H,H) = 15.1 Hz, 1H), 4.18-4.11 (m, 2H), 4.10-3.87 (m, 4H), 1.20 (t, ^3J(H,H) = 7.1 Hz, 3H), 1.18 (t, ^3J(H,H) = 7.1 Hz, 3H), 1.11 (t, ^3J(H,H) = 7.1 Hz, 3H) ppm.

^{13}C-NMR (125 MHz, DMSO-d_6): δ = 167.4 (C_q), 149.9 (C_q), 142.0 (C_q), 140.4 (C_q), 137.5 (C_q), 136.5 (C_q), 136.1 (*C*H), 128.8 (2C; *C*H), 128.8 (2C; *C*H), 128.5 (2C; *C*H), 128.0 (*C*H), 126.5 (*C*H), 125.3 (2C; *C*H), 63.1 (CH_2), 63.0 (CH_2), 61.5 (CH_2), 52.5 (*C*H), 38.7 (CH_2), 16.2 (2C; CH_3), 13.9 (CH_3) ppm.

HRMS-ESI (*m/z*): $[M+Na]^+$ calcd for $C_{25}H_{30}N_3O_5PNa$: 506.1815; found: 506.1820.

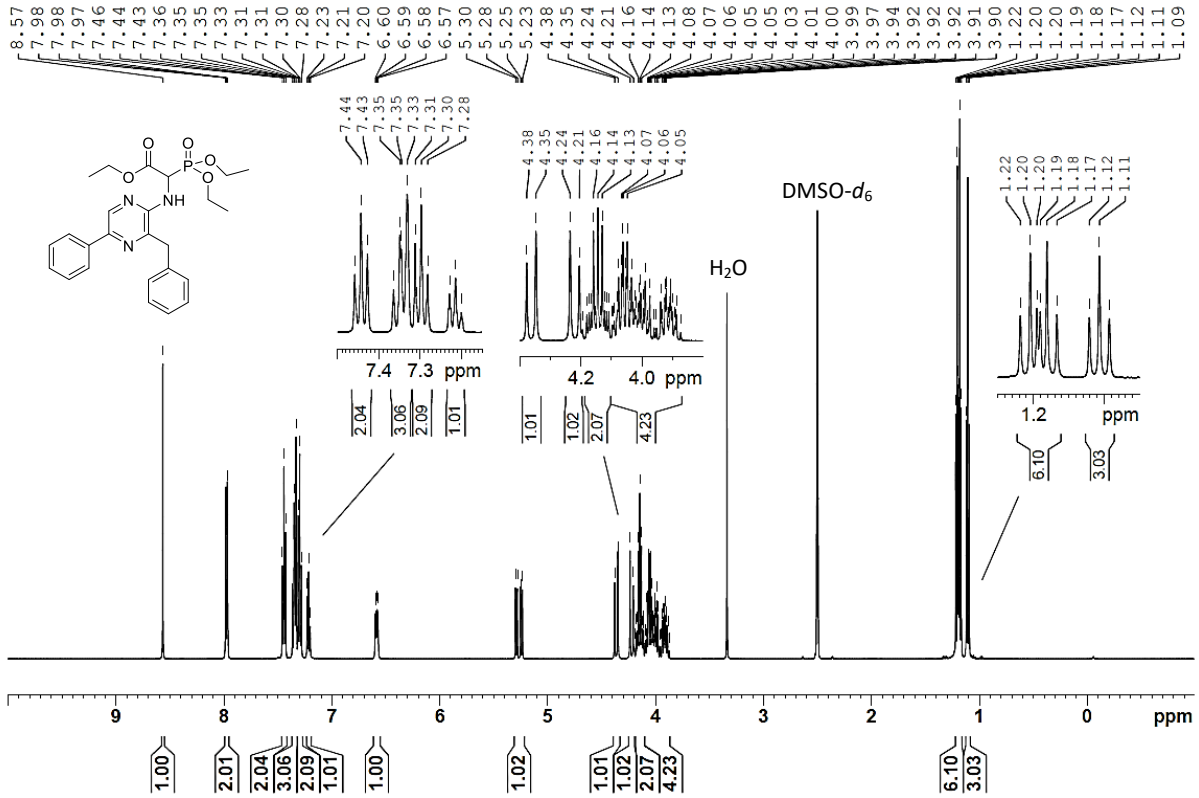

Figure S43: ^{1}H-NMR (500 MHz) spectrum of compound **7** in DMSO-d_6.

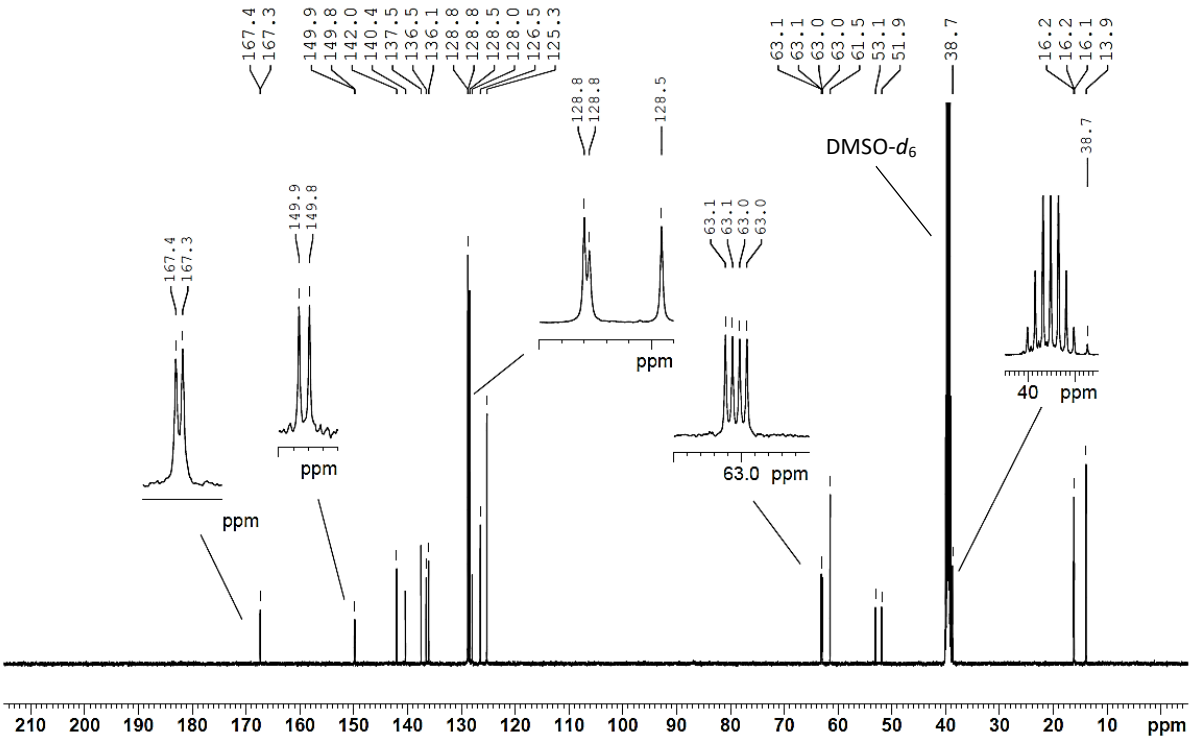

Figure S44: ^{13}C-NMR (125 MHz) spectrum of compound **7** in DMSO-d_6.

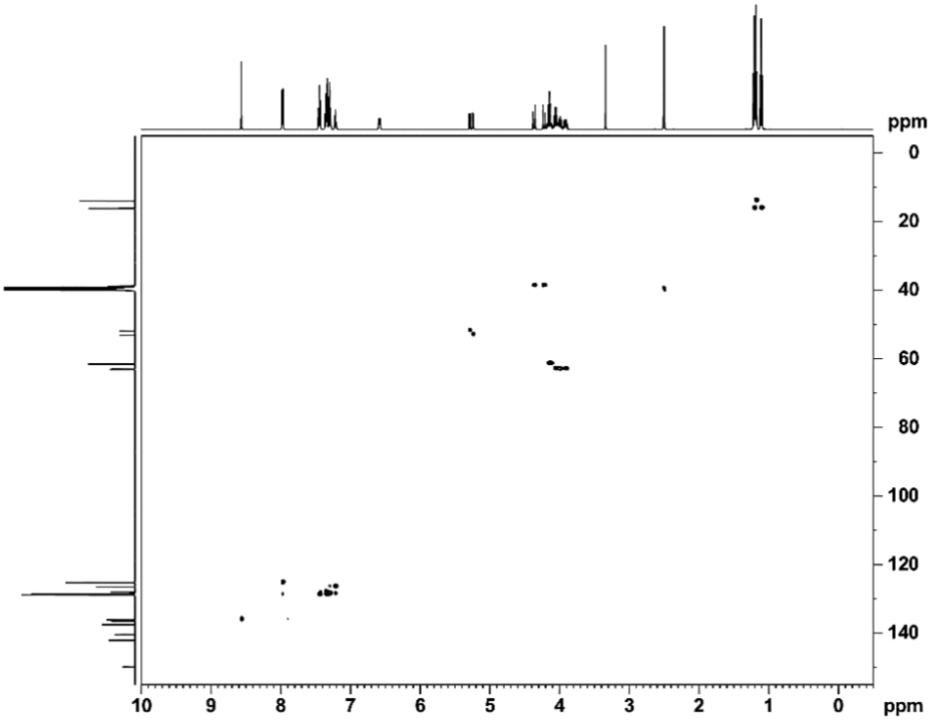

Figure S45: HSQC spectrum of compound **7** (^{1}H-NMR: 500 MHz, ^{13}C-NMR: 125 MHz, DMSO-d_6).

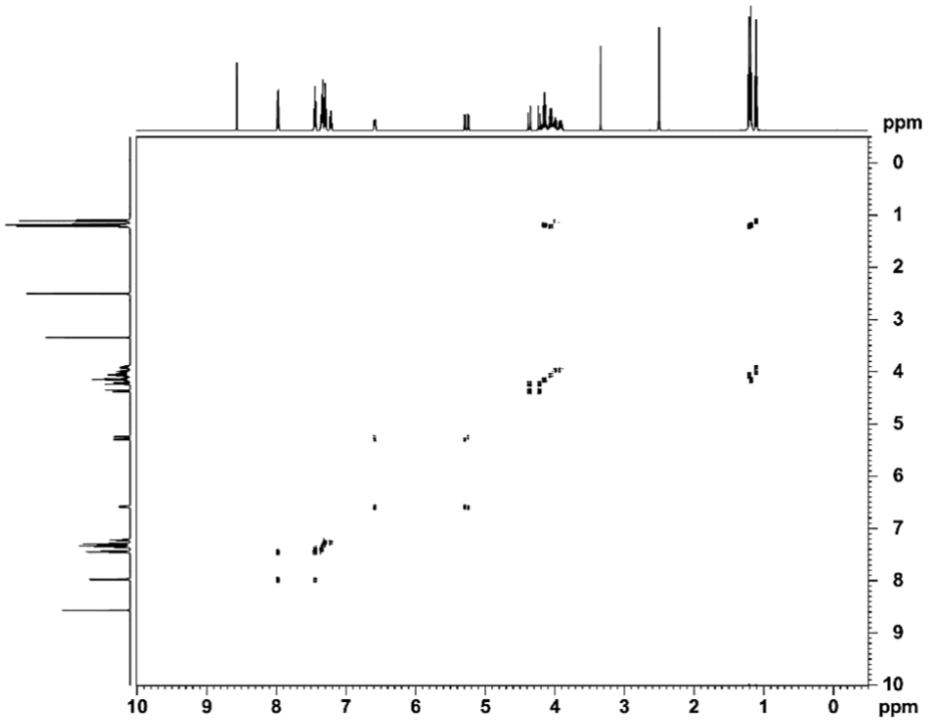

Figure S46: COSY spectrum of compound **7** (^{1}H-NMR: 500 MHz, DMSO-d_6).

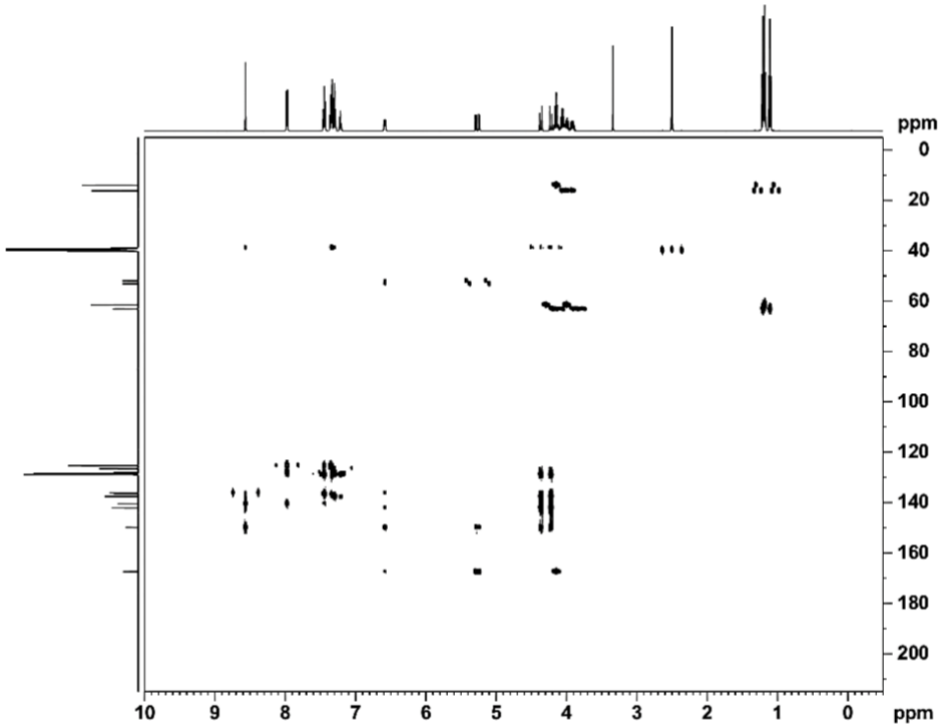

Figure S47: HMBC spectrum of compound **7** (^{1}H-NMR: 500 MHz, ^{13}C-NMR: 125 MHz, DMSO-d_6).

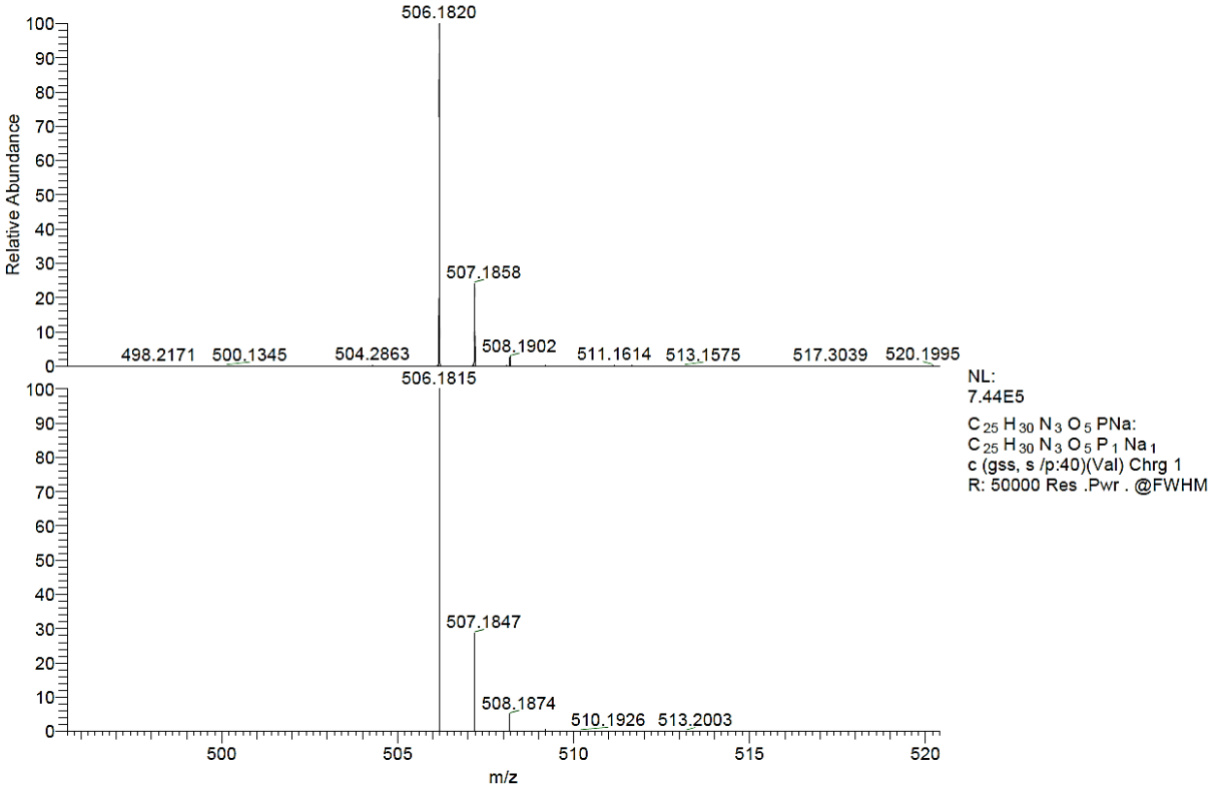

Figure S48: Measured (top) and calculated (bottom) HRMS-ESI spectrum of **7** in positive ion mode.

Compound (9)

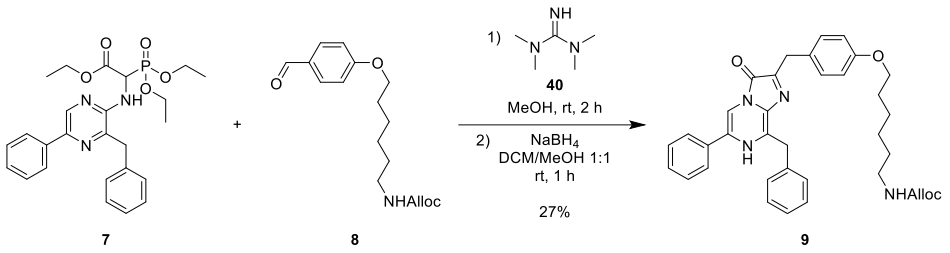

Scheme S10: Synthesis of compound **9**.

Adapted from the procedures of Shakhim *et al.*[27] and Hall *et al.*[28], pyrazine **7** (317 mg, 0.66 mmol, 1.00 eq) and aldehyde **8** (200 mg, 0.66 mmol, 1.00 eq) were dissolved in dry MeOH (16.0 mL) in the dark and added to a flask under nitrogen atmosphere using a syringe. Tetramethyl guanidine (**40**, 0.94 mL, 7.53 mmol, 11.5 eq) was added and the reaction mixture was stirred at rt for 2 h. When TLC ($UV_{254\ nm}$) showed no further conversion, the reaction was poured into a mixture of EtOAc/ 0.1 M HCl (1:1). The product was extracted with EtOAc (150 mL, 3×). The organic phase was washed with brine (150 mL, 1×), dried over Na_2SO_4 and the solvent was removed under reduced pressure. The remaining residue was purified by flash column chromatography (DCM/MeOH 200:1 → 100:1 → 50:1, (v/v)) to receive a red solid. The red solid was dissolved in DCM/ dry MeOH (1:1, 5.40 mL) and treated with an excess of $NaBH_4$ (248 mg, 6.55 mmol, 10.0 eq). The mixture was stirred for 1 h at rt until TLC ($UV_{254\ nm}$) showed complete conversion. The reaction was quenched with distilled water (~150 mL). Subsequently, the aqueous phase was extracted with DCM (~150 mL, 3×) and the combined organic phases were washed with brine (~150 mL, 1×), dried over Na_2SO_4 and concentrated under reduced pressure. The residue was purified by flash column chromatography (DCM/MeOH 200:1 → 100:1 → 100:2 → 100:3 → 95:5 → 90:10, (v/v)) to isolate the desired coelenterazine (**9**, 105 mg, 0.18 mmol, 27%) as an orange solid.

TLC ($UV_{254\ nm}$): R_f = 0.17 (DCM/MeOH 100:1, v/v).

^{1}H-NMR (500 MHz, MeOD-d_4): δ = 7.62 (s, 2H), 7.46-7.41 (m, 3H), 7.39 (d, ^3J(H,H) = 7.6 Hz, 2H), 7.31-7.20 (m, 6H), 6.80 (d, ^3J(H,H) = 8.6 Hz , 2H), 5.94-5.86 (m, 1H), 5.27 (dd, ^3J(H,H) = 17.3 Hz, ^2J(H,H) = 1.5 Hz, 1H), 5.14 (dd, ^3J(H,H) = 10.5 Hz, ^2J(H,H) = 1.0 Hz, 1H), 4.49 (d, ^3J(H,H) = 5.2 Hz, 2H), 4.40 (s, 2H), 4.09 (s, 2H), 3.91 (t, ^3J(H,H) = 6.4 Hz, 2H), 3.09 (t, ^3J(H,H) = 6.7 Hz, 2H), 1.73 (qi, ^3J(H,H) = 7.0 Hz, 2H), 1.53-1.43 (m, 4H), 1.40-1.35 (m, 2H) ppm.

^{13}C-NMR (125 MHz, MeOD-d_4): δ = 159.2 (2C; C_q), 158.8 (C_q), 138.1 (2C; C_q), 134.6 (*C*H), 131.7 (C_q), 130.8 (2C; *C*H), 130.6 (2C; C_q), 130.1 (2C; *C*H), 129.9 (C_q), 129.8 (2C; *C*H), 129.8 (2C; *C*H), 128.2 (2C; *C*H), 127.9 (2C; *C*H), 126.7 (C_q), 117.3 (CH_2), 115.6 (2C; *C*H), 108.9 (*C*H), 68.9 (CH_2), 66.2 (CH_2), 41.7 (CH_2), 30.8 (CH_2), 30.3 (2C; CH_2), 27.6 (2C; CH_2), 26.8 (CH_2) ppm.

HRMS-ESI (*m/z*): $[M + H]^+$ calcd for $C_{36}H_{39}N_4O_4$: 591.2966; found: 591.2967.

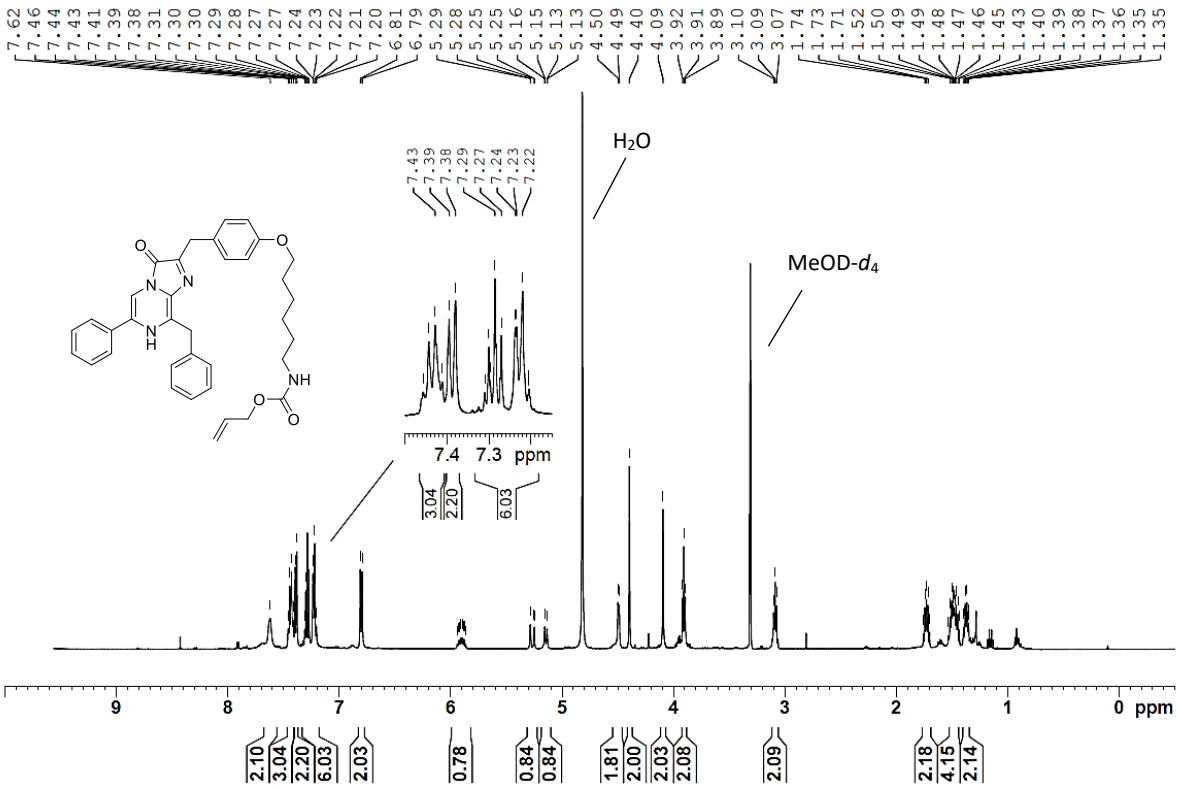

Figure S49: ^{1}H-NMR (500 MHz) spectrum of compound **9** in MeOD-d_4.

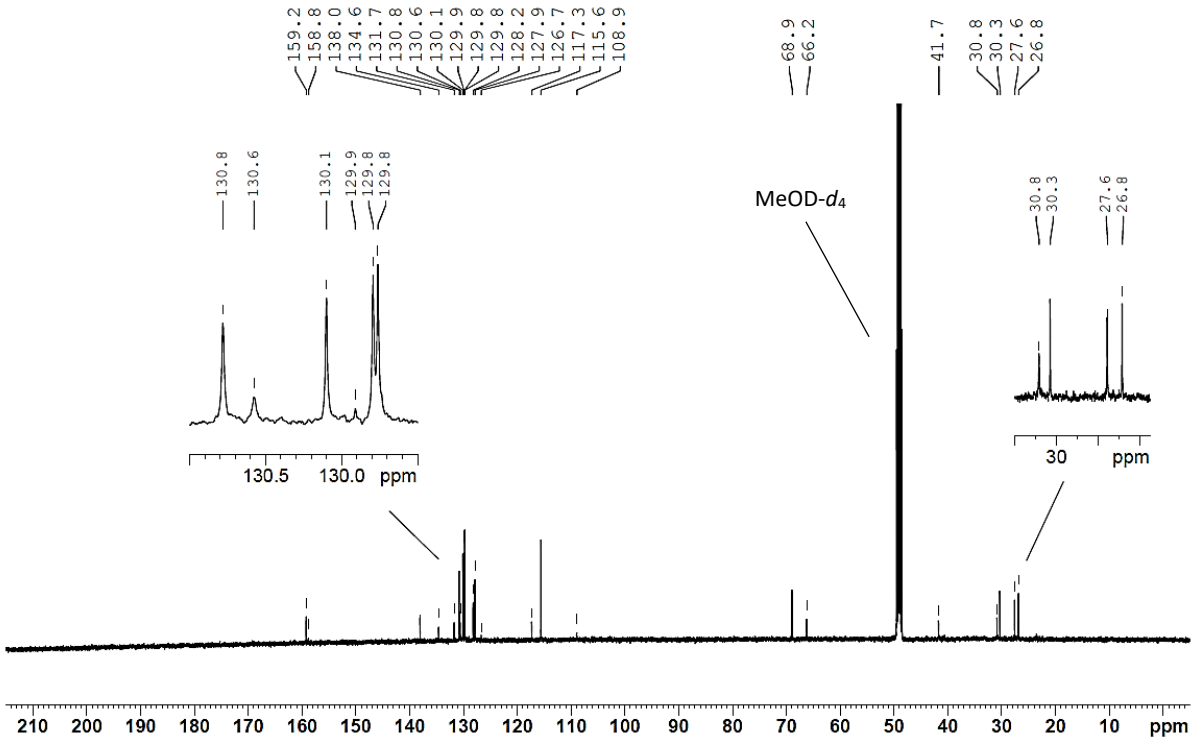

Figure S50: ^{13}C-NMR (125 MHz) spectrum of compound **9** in MeOD-d_4.

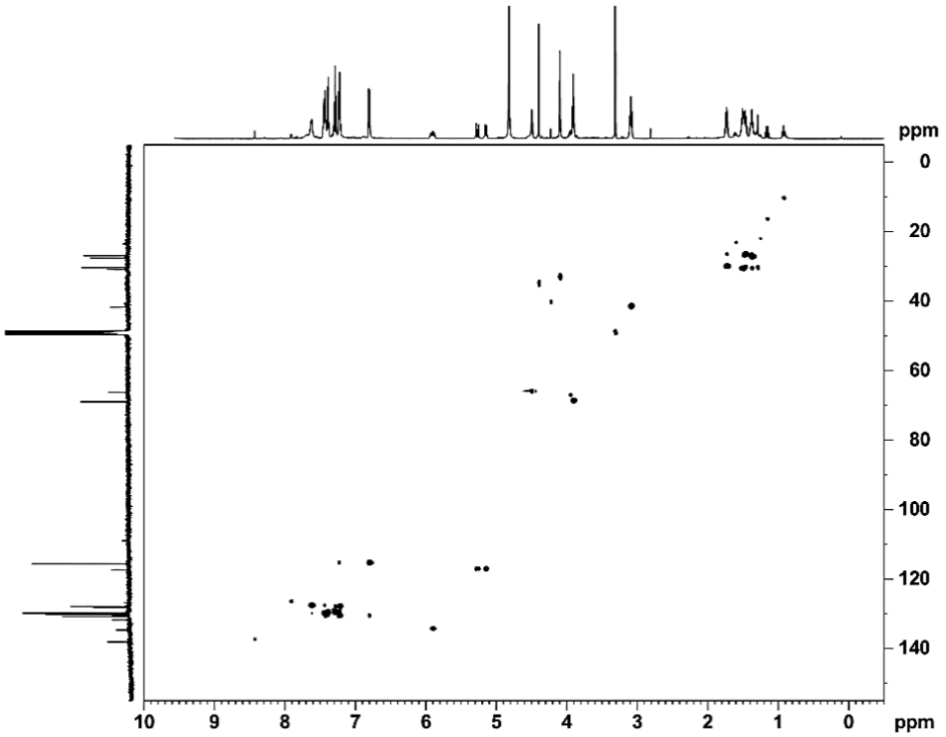

Figure S51: HSQC spectrum of compound **9** (^{1}H-NMR: 500 MHz, ^{13}C-NMR: 125 MHz, MeOD-d_4).

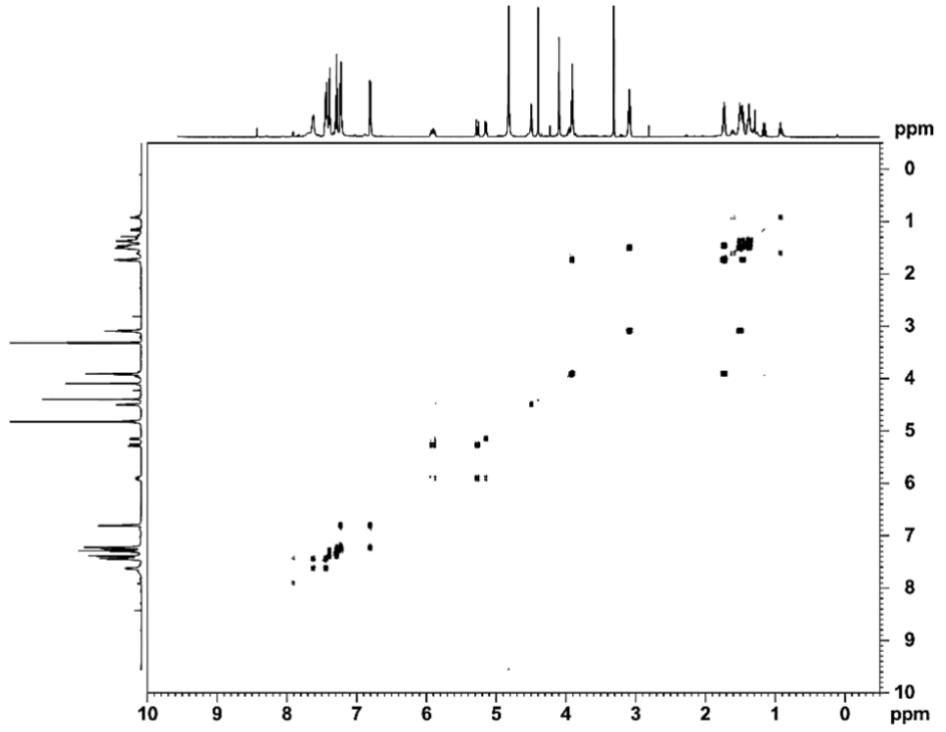

Figure S52: COSY spectrum of compound **9** (^{1}H-NMR: 500 MHz, MeOD-d_4).

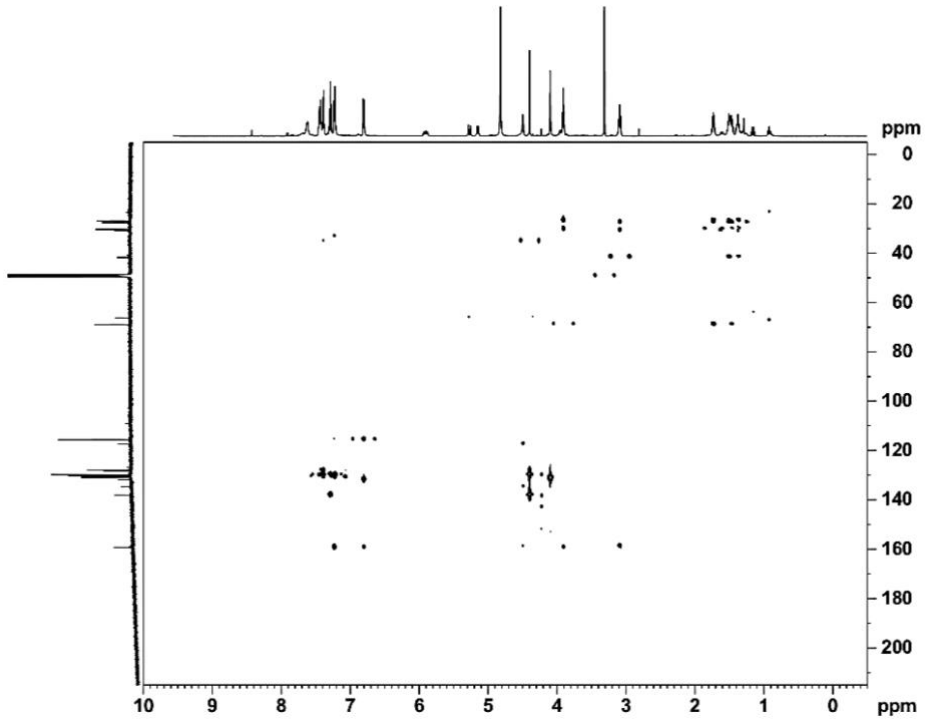

Figure S53: HMBC spectrum of compound **9** (^{1}H-NMR: 500 MHz, ^{13}C-NMR: 125 MHz, MeOD-d_4).

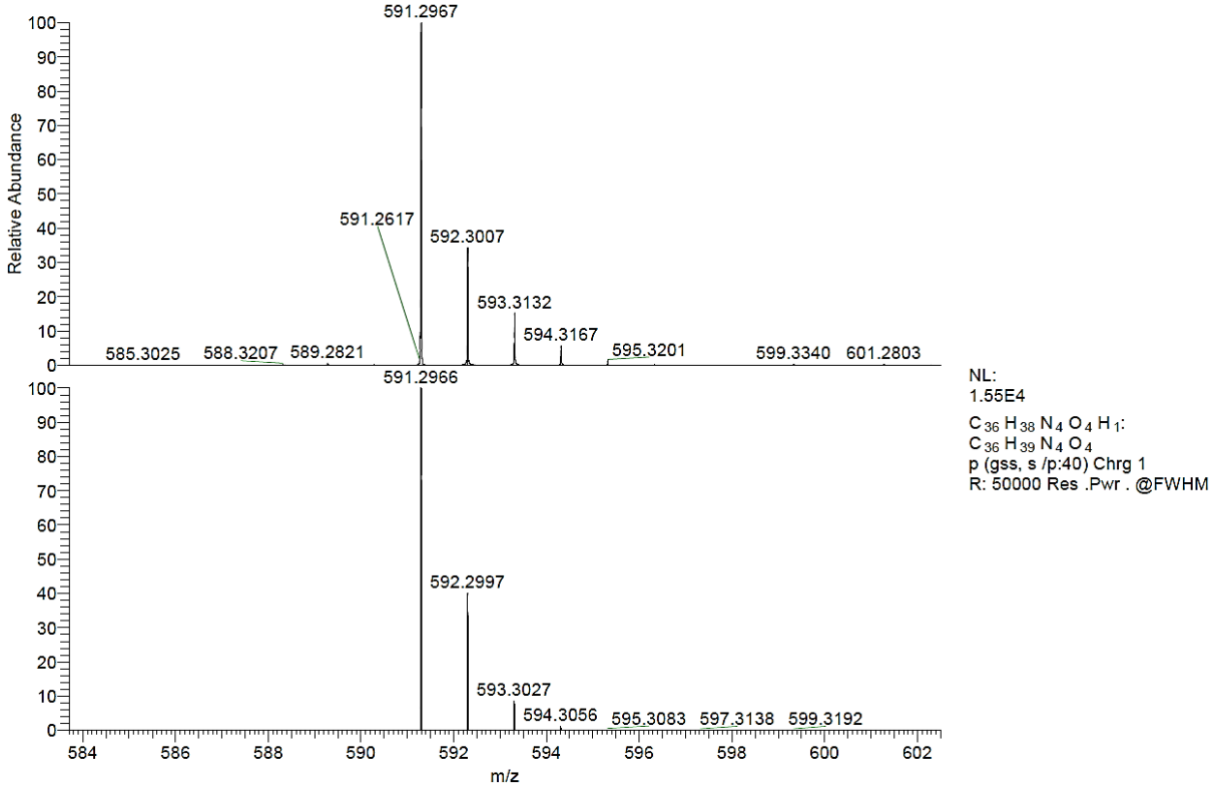

Figure S54: Measured (top) and calculated (bottom) HRMS-ESI spectrum of **9** in positive ion mode.

Compound (13)

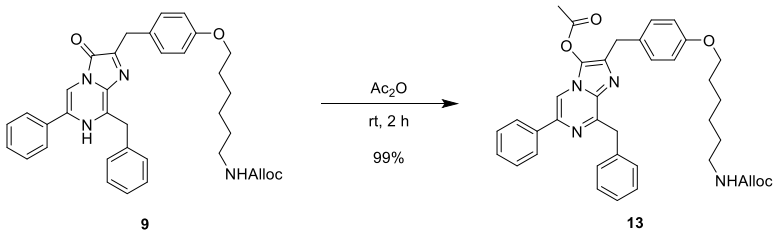

9 13

Scheme S11: Synthesis of compound (**13**).

Based on a procedure reported by Coutant *et al.*[20], coelenterazine **9** (130 mg, 220 µmol, 1.00 eq) was dissolved in acetic anhydride (4.00 mL, 42.2 mmol, 192 eq) and stirred at rt for 2 h in the dark. When TLC ($UV_{254\,nm}$) showed complete conversion of the starting material, the mixture was diluted with EtOAc (~100 mL) and washed with distilled water (~100 mL, 3×) and brine (~100 mL, 1×) followed by drying over Na_2SO_4. The solvent was evaporated, and the crude product was purified by flash column chromatography (DCM/MeOH 100:1 → 100:2, (v/v)) to obtain **13** (139 mg, 218 µmol, 99%) as a red solid.

TLC ($UV_{254\,nm}$): R_f = 0.17 (DCM/MeOH 100:1, v/v).

^{1}H-NMR (300 MHz, MeOD-d_4): δ = 8.29 (s, 1H), 7.91 (d, ^3J(H,H) = 7.1 Hz, 2H), 7.46 (d, ^3J(H,H) = 7.2 Hz, 2H), 7.39-7.30 (m, 3H), 7.24 (t, ^3J(H,H) = 7.5 Hz, 2H), 7.17-7.14 (m, 1H), 7.12 (d, ^3J(H,H) = 8.7 Hz, 2H), 6.79 (d, ^3J(H,H) = 8.7 Hz , 2H), 5.96-5.83 (m, 1H), 5.26 (dd, ^3J(H,H) = 17.2 Hz, ^2J(H,H) = 1.5 Hz, 1H), 5.14 (dd, ^3J(H,H) = 10.5 Hz, ^2J(H,H) = 0.9 Hz, 1H), 4.51 (s, 2H), 4.48 (s, 2H), 4.03 (s, 2H), 3.88 (t, ^3J(H,H) = 6.4 Hz, 2H), 3.07 (t, ^3J(H,H) = 7.0 Hz, 2H), 2.23 (s, 3H), 1.71 (qi, ^3J(H,H) = 6.6 Hz, 2H), 1.53-1.41 (m, 4H), 1.39-1.31 (m, 2H) ppm.

^{13}C-NMR (125 MHz, MeOD-d_4): δ = 169.0 (C_q), 159.2 (C_q), 158.7 (C_q), 153.2 (C_q), 140.2 (C_q), 139.0 (C_q), 137.6 (C_q), 136.8 (C_q), 134.6 (*C*H), 134.5 (*C*H), 131.1 (C_q), 131.0 (2C; *C*H), 130.5 (C_q), 130.4 (2C; *C*H), 129.6 (2C; *C*H), 129.5 (C_q), 129.3 (2C; *C*H), 127.5 (*C*H), 127.4 (2C; *C*H), 117.3 (CH_2), 115.6 (2C; *C*H), 111.1 (*C*H), 68.9 (CH_2), 66.2 (CH_2), 41.7 (CH_2), 39.9 (CH_2), 33.4 (CH_2), 30.8 (CH_2), 30.2 (CH_2), 27.5 (CH_2), 26.8 (CH_2), 20.0 (CH_3) ppm.

HRMS-ESI (*m/z*): $[M + H]^+$ calcd for $C_{38}H_{41}N_4O_5$: 633.3082; found: 633.3100.

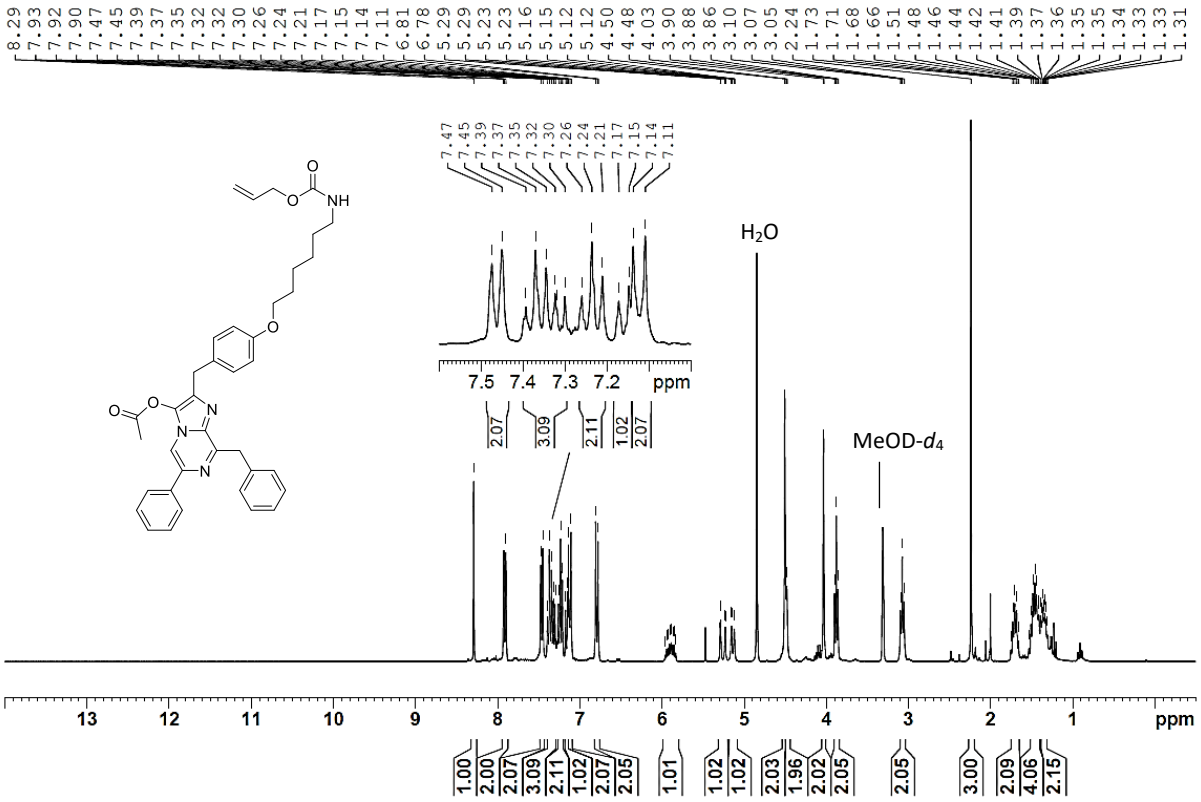

Figure S55: ^{1}H-NMR (300 MHz) spectrum of compound **13** in MeOD-d_4.

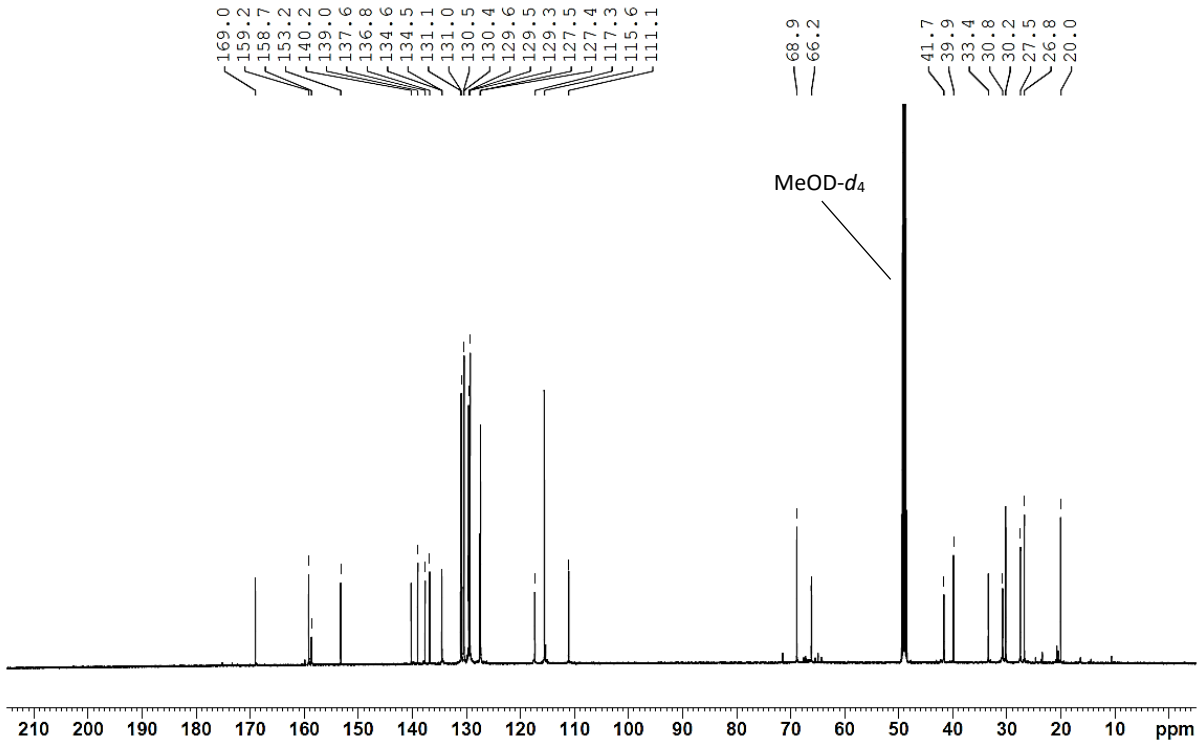

Figure S56: ^{13}C-NMR (125 MHz) spectrum of compound **13** in MeOD-d_4.

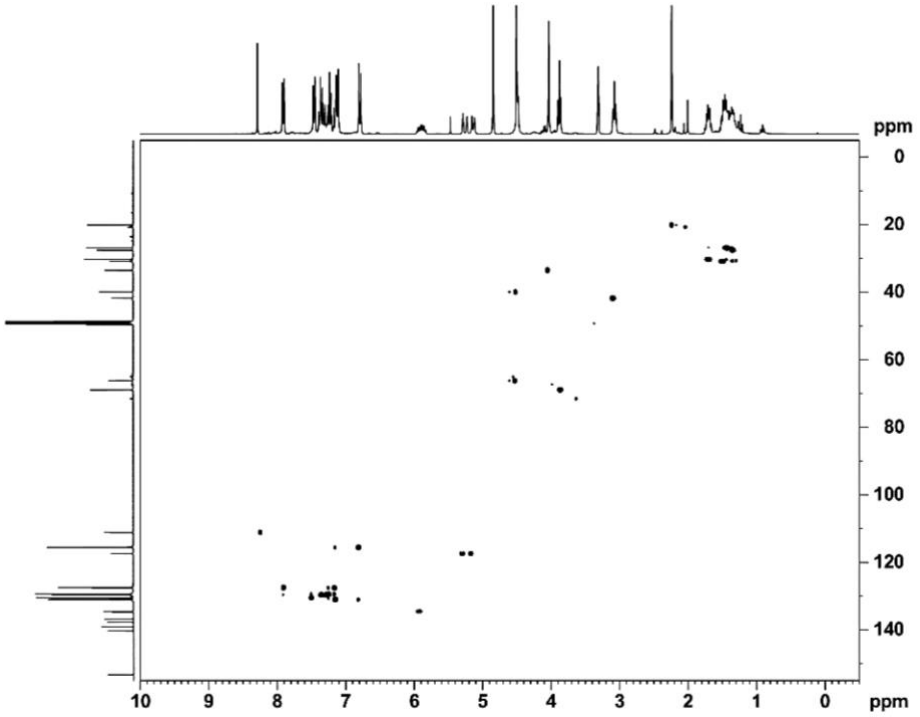

Figure S57: HSQC spectrum of compound **13** (^{1}H-NMR: 300 MHz, ^{13}C-NMR: 125 MHz, MeOD-d_4).

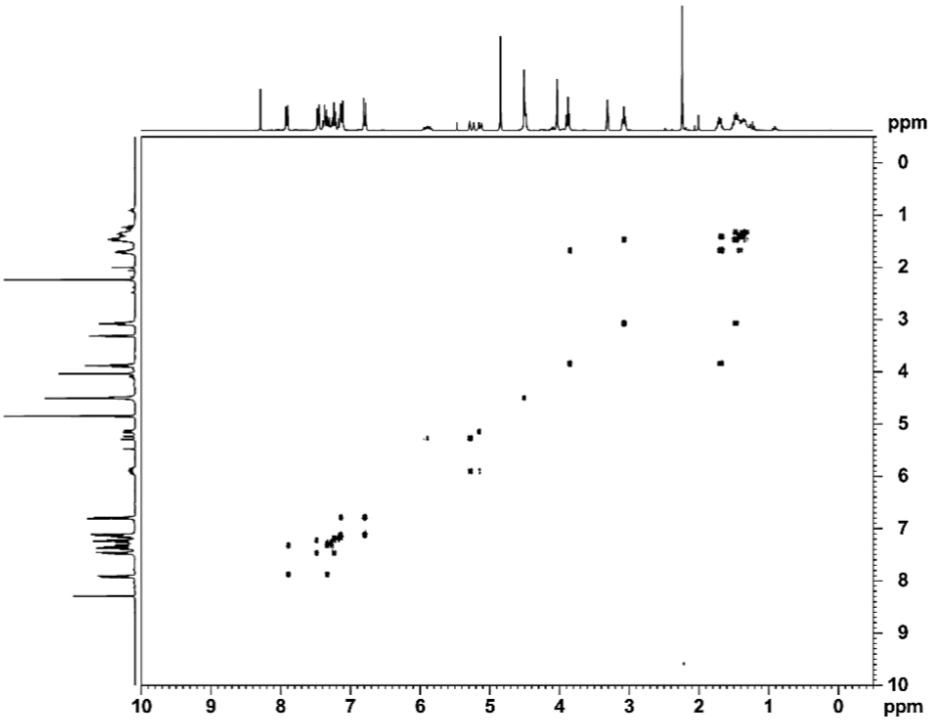

Figure S58: COSY spectrum of compound **13** (^{1}H-NMR: 300 MHz, MeOD-d_4).

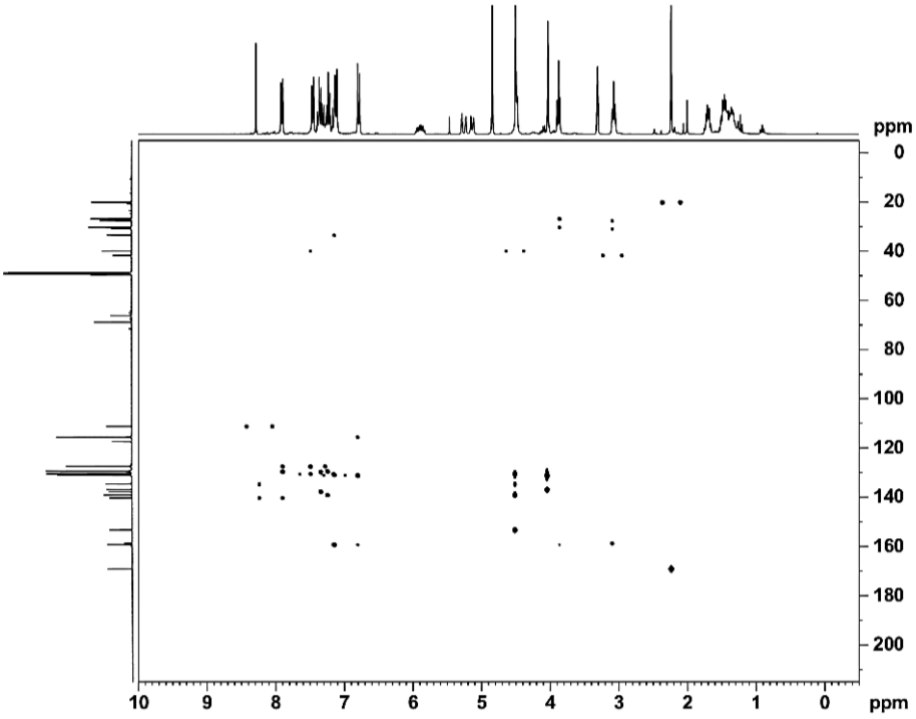

Figure S59: HMBC spectrum of compound **13** (^{1}H-NMR: 300 MHz, ^{13}C-NMR: 125 MHz, MeOD-d_4).

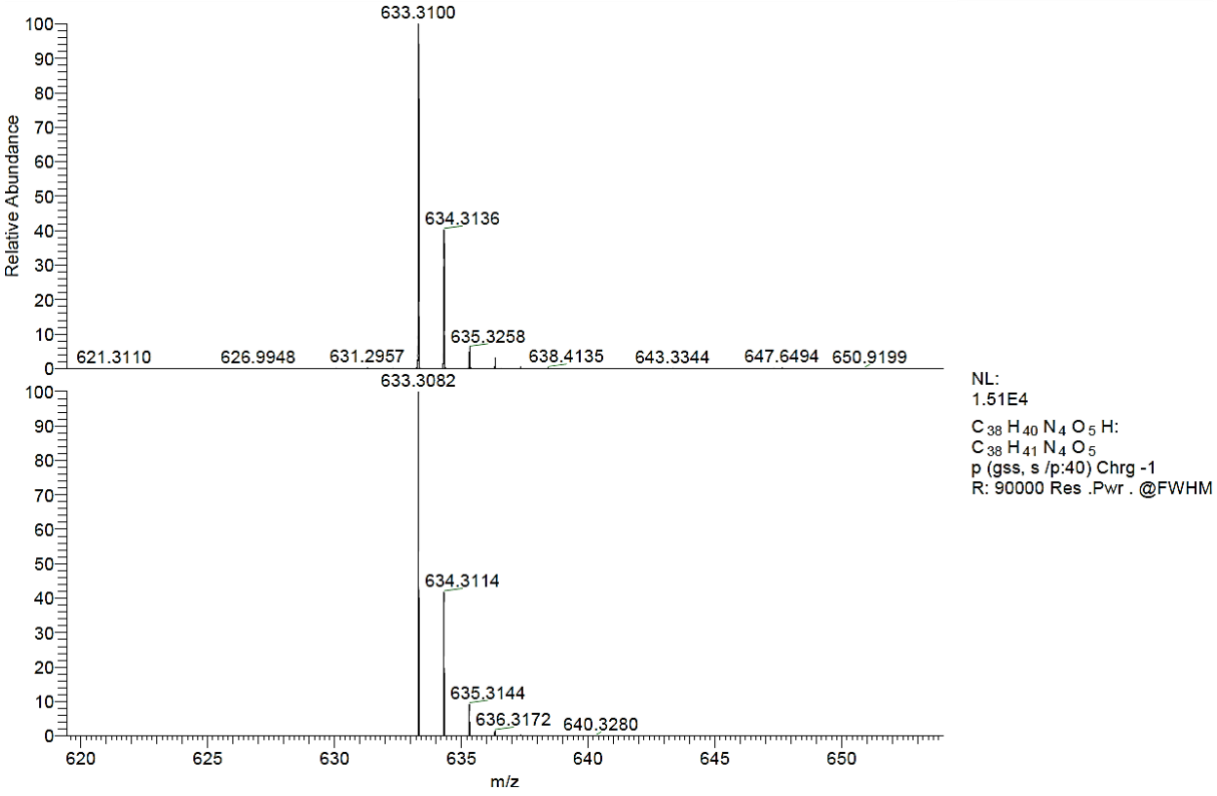

Figure S60: Measured (top) and calculated (bottom) HRMS-ESI spectrum of **13** in positive ion mode.

Compound 42

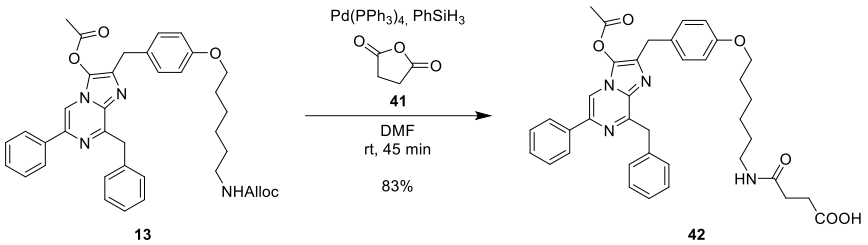

Scheme S12: Synthesis of compound **42**.

Coelenterazine **13** (160 mg, 0.25 mmol, 1.00 eq) and $Pd(PPh_3)_4$ (28.9 mg, 25.0 µmol, 0.10 eq) were added to a solution of succinic anhydride (**41**, 506 mg, 5.06 mmol, 20.0 eq) in DMF (1.00 mL). Afterwards, phenylsilane (274 mg, 2.53 mmol, 10.0 eq) was added and the reaction mixture was stirred under nitrogen atmosphere at rt in the dark for 45 min. Afterwards, the mixture was filtered over celite and the supernatant was purified by using EtOAc. The filtrate was concentrated and purified by flash column chromatography (*n*-pentane → *n*-pentane/EtOAc 1:1 + 1% HOAc (v/v)). The product-containing fractions were combined, and the solvent was evaporated. To remove the remaining DMF and HOAc, the residue was dissolved in EtOAc (~50.0 mL) and washed with distilled water/ brine (9:1, ~50.0 mL, 5×). The aqueous phase was extracted with EtOAc (~50.0 mL, 3×) and the combined organic phases were dried with brine (~50.0 mL) and $MgSO_4$. After evaporation of the solvent, the product **42** (137 mg, 0.21 mmol, 83%) was obtained as an orange oily solid.

TLC ($UV_{254\ nm}$): R_f = 0.22 (*n*-pentane/EtOAc 1:1+ 1% HOAc, v/v).

^{1}H-NMR (500 MHz, MeOD-d_4): δ = 8.39 (s, 1H), 7.98 – 7.96 (m, 1H), 7.65 – 7.64 (m, 1H), 7.49 – 7.34 (m, 5H), 7.31 – 7.23 (m, 3H), 7.20 – 7.14 (m, 2H), 6.84 – 6.81 (m, 2H), 4.54 (s, 1.2H; C$H_{2,\ benzyl}$), 4.40 (s, 0.8H; C$H_{2,\ benzyl}$), 4.10 (s, 0.8H; C$H_{2,\ benzyl}$), 4.07 (s, 1.2H; C$H_{2,\ benzyl}$), 3.95 – 3.90 (m, 2H), 3.18 – 3.14 (m, 2H), 2.58 – 2.55 (m, 2H), 2.45 – 2.42 (m, 2H), 2.28 (s, 1.97H; COOCH_3), 2.24 (s, 0.21H; COOCH_3), 2.09 (s, 0.25H; COOCH_3), 2.01 (s, 0.26H; COOCH_3), 1.99 (s, 0.31H; COOCH_3), 1.78 – 1.71 (m, 2H), 1.55 – 1.44 (m, 4H), 1.42 – 1.36 (m, 2H) ppm.

^{13}C-NMR (125 MHz, MeOD- d_4): δ = 176.3 (*C*OOH), 174.4 (*C*ONH), 169.2 (*C*OCH$_3$), 159.3 (C_q), 153.4 (C_q), 140.5 (C_q), 139.1 (C_q), 137.8 (C_q), 136.9 (C_q), 134.7 (C_q), 131.1 (C_q), 131.0 (*C*H), 130.8 (*C*H), 130.7 (C_q), 130.4 (*C*H), 130.1 (*C*H), 129.8 (*C*H), 129.7 (*C*H), 129.7 (*C*H), 129.4 (*C*H), 128.2 (*C*H), 127.9 (*C*H), 127.6 (*C*H), 127.6 (*C*H), 115.6 (*C*H), 115.5 (*C*H), 111.3 (*C*H), 68.9 (*C*H$_2$), 40.4 (*C*H$_2$), 39.9 (*C*H$_2$), 33.4 (*C*H$_2$), 31.6 (*C*H$_2$), 30.4 (*C*H$_2$), 30.3 (*C*H$_2$), 30.3 (*C*H$_2$), 27.7 (*C*H$_2$), 26.9 (*C*H$_2$), 20.0 (*C*H$_3$) ppm.

HRMS-ESI (*m/z*): $[M - H]^-$ calcd for $C_{38}H_{39}N_4O_6$: 647.2875; found: 647.2871.

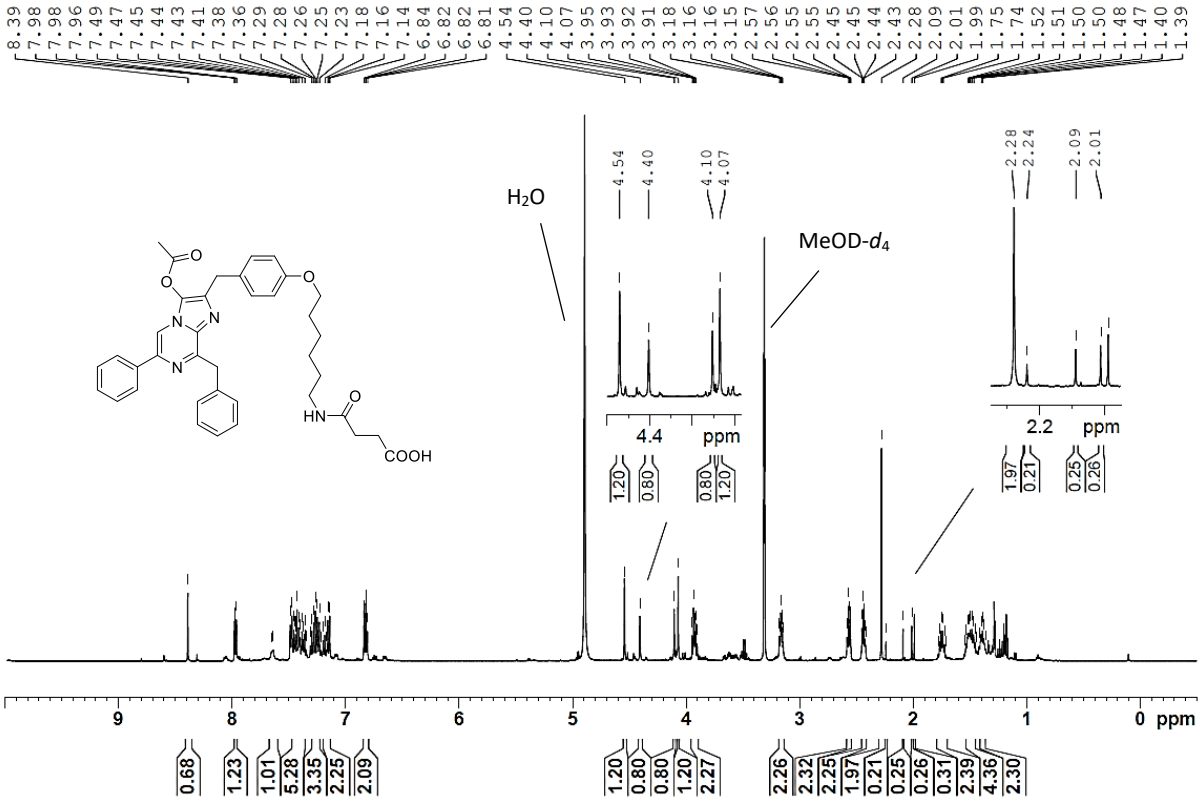

Figure S61: ^{1}H-NMR (500 MHz) spectrum of compound **42** in MeOD-d_4.

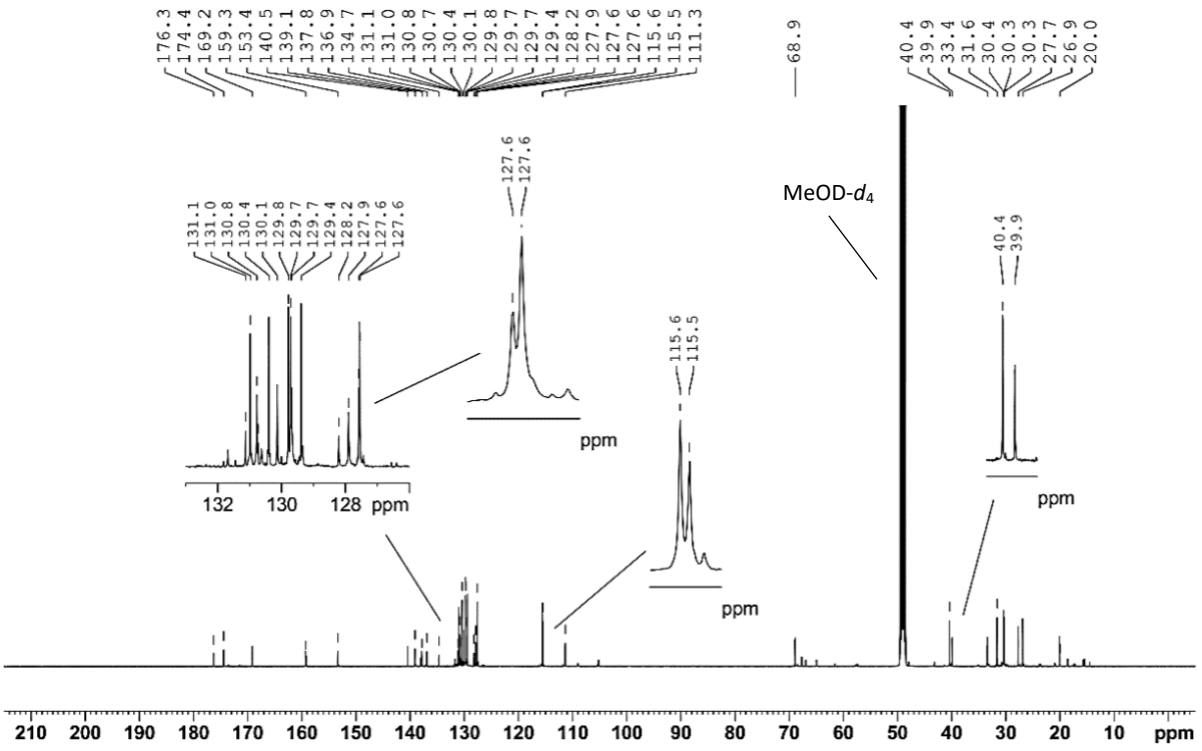

Figure S62: ^{13}C-NMR (125 MHz) spectrum of compound **42** in MeOD-d_4.

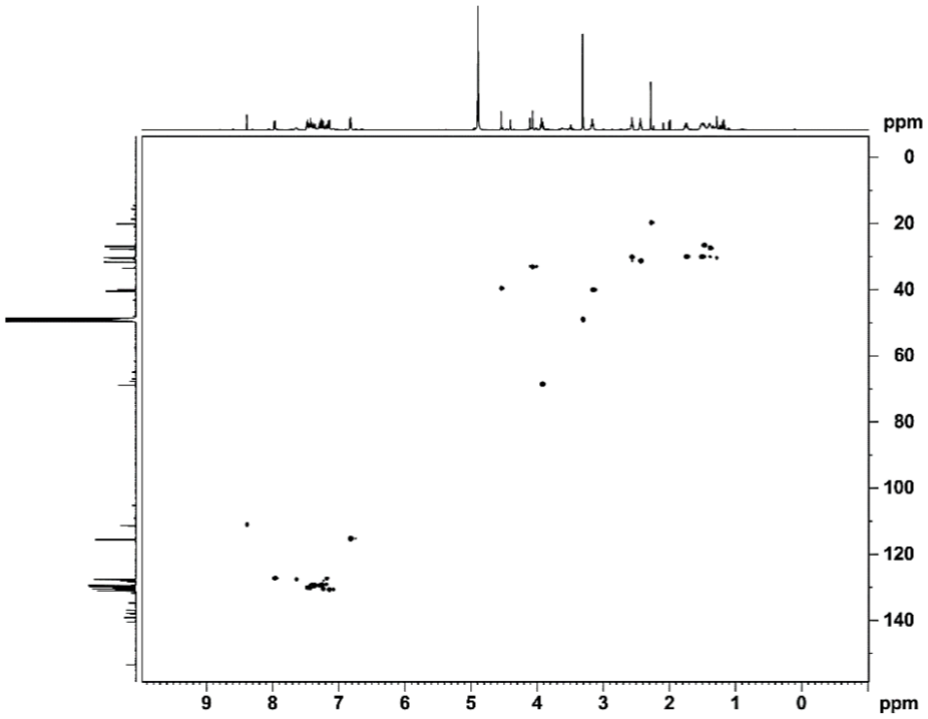

Figure S63: HSQC spectrum of compound **42** (^{1}H-NMR: 500 MHz, ^{13}C-NMR: 125 MHz, MeOD-d_4).

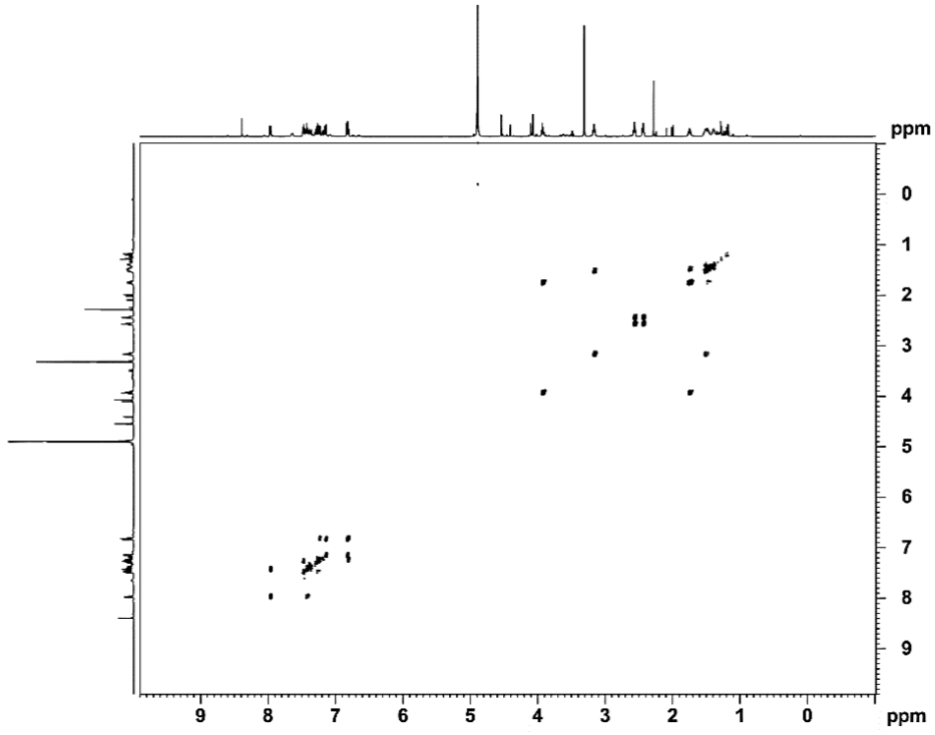

Figure S64: COSY spectrum of compound **42** (^{1}H-NMR: 500 MHz, MeOD-d_4).

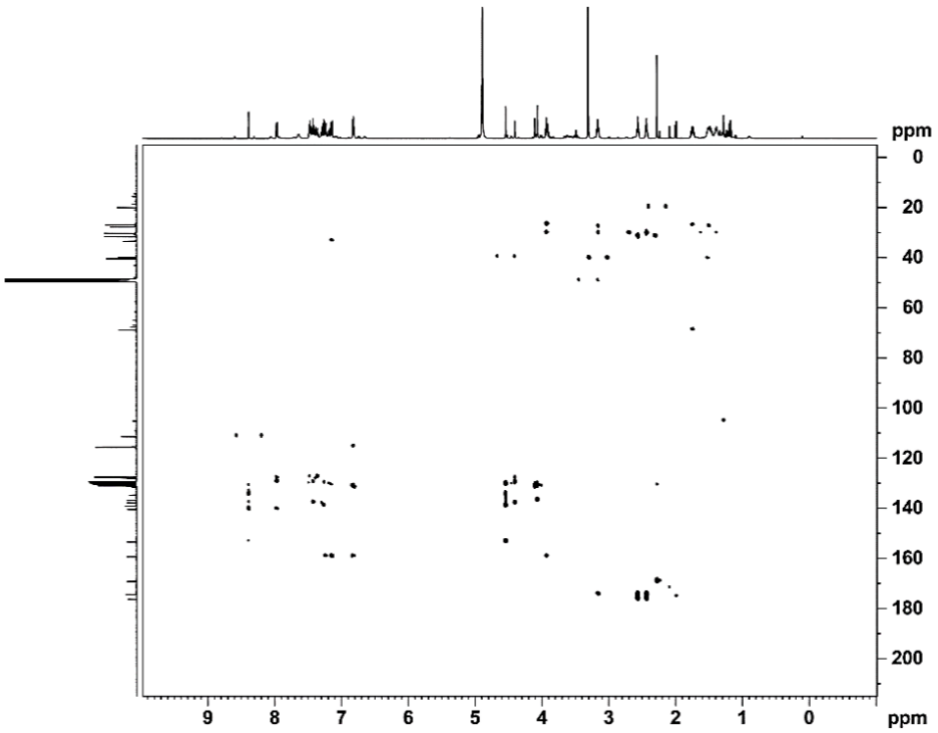

Figure S65: HMBC spectrum of compound **42** (^{1}H-NMR: 500 MHz, ^{13}C-NMR: 125 MHz, MeOD-d_4).

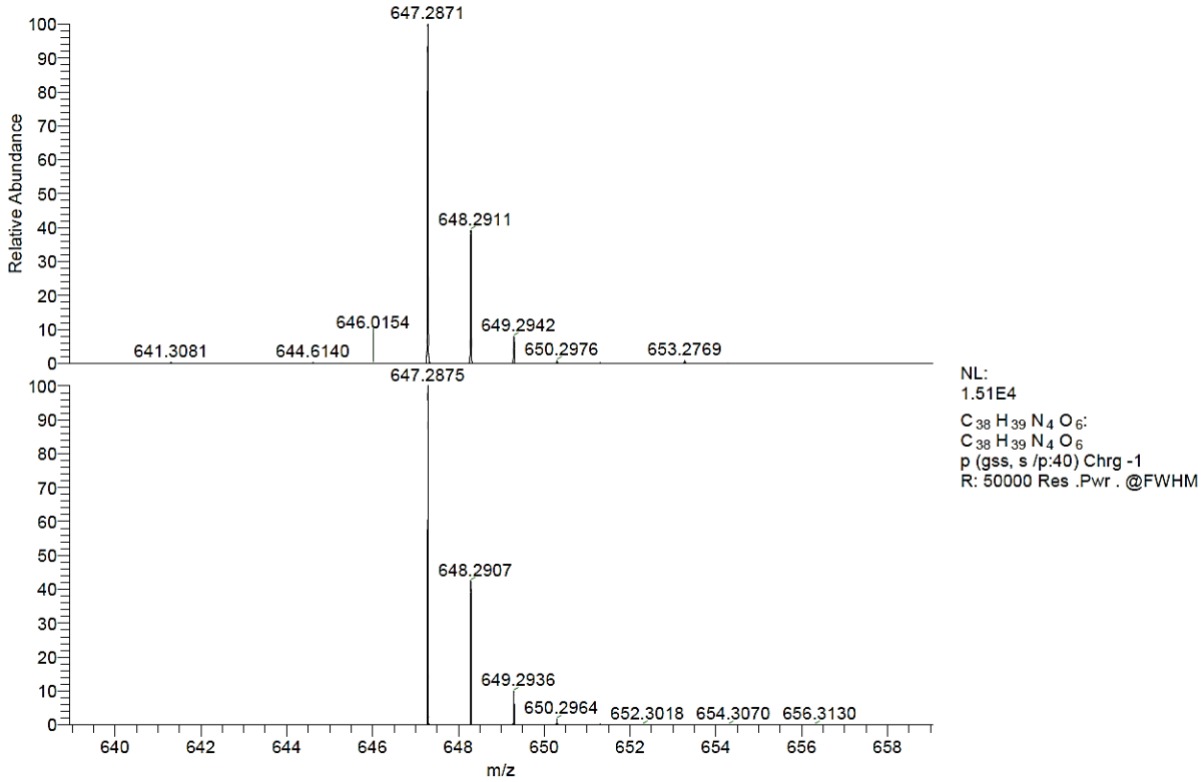

Figure S66: Measured (top) and calculated (bottom) HRMS-ESI spectrum of **42** in negative ion mode.

Compound 44

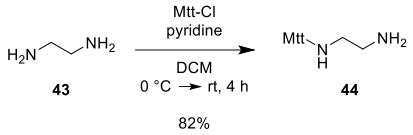

Scheme S13: Synthesis of compound **44**.

Following the procedure of Albert *et al.*[29], ethylene diamine (**43**, 0.92 g, 15.4 mmol, 9.00 eq) was dissolved in DCM (3.50 mL). Pyridine (2.50 mL) was added to the solution. After cooling the reaction mixture to 0 °C, 4-methyltrityl chloride (0.50 g, 1.70 mmol, 1.00 eq) was added portion wise. The solution was allowed to warm to rt and stirred for 4 h. Subsequently, the solvent was removed under reduced pressure. The residue was dissolved in a mixture of DCM and water containing 1% TEA (~100 mL). The aqueous phase was extracted with DCM (~100 mL, 3×). The combined organic phases were dried over $MgSO_4$ followed by removal of the solvent under reduced pressure. The crude was purified by flash column chromatography (EtOAc, 1% TEA) to yield the product (**44**, 0.44 g, 1.40 mmol, 82%) as a pale orange oil. The characterization is in agreement with the literature.[29]

TLC (ninhydrin developer): R_f = 0.20 (EtOAc + 1% TEA).

^{1}H-NMR (300 MHz, $CDCl_3$): δ = 7.48 (dd, ^3J(H,H) = 7.5 Hz, 4H), 7.36 (d, ^3J(H,H) = 8.2 Hz, 2H), 7.29 – 7.23 (m, 4H), 7.19 – 7.15 (m, 2H), 7.08 (d, ^3J(H,H) = 8.0 Hz, 2H), 2.80 (t, ^3J(H,H) = 5.9 Hz, 2H), 2.31 (s, 3H), 2.21 (t, ^3J(H,H) = 5.9 Hz, 2H) ppm.

^{13}C-NMR (75 MHz, $CDCl_3$): δ = 146.4 (2C; C_q), 143.2 (C_q), 135.8 (C_q), 128.7 (4C; *C*H), 128.7 (2C; *C*H), 128.6 (4C; *C*H), 127.8 (2C; *C*H), 126.2 (2C; *C*H), 70.5 (*C*NH), 46.4 (CH_2), 42.8 (CH_2), 21.0 (CH_3) ppm.

HRMS-ESI (*m/z*): $[M + Na]^+$ calcd for $C_{22}H_{24}N_2Na$: 339.1832; found: 339.1840.

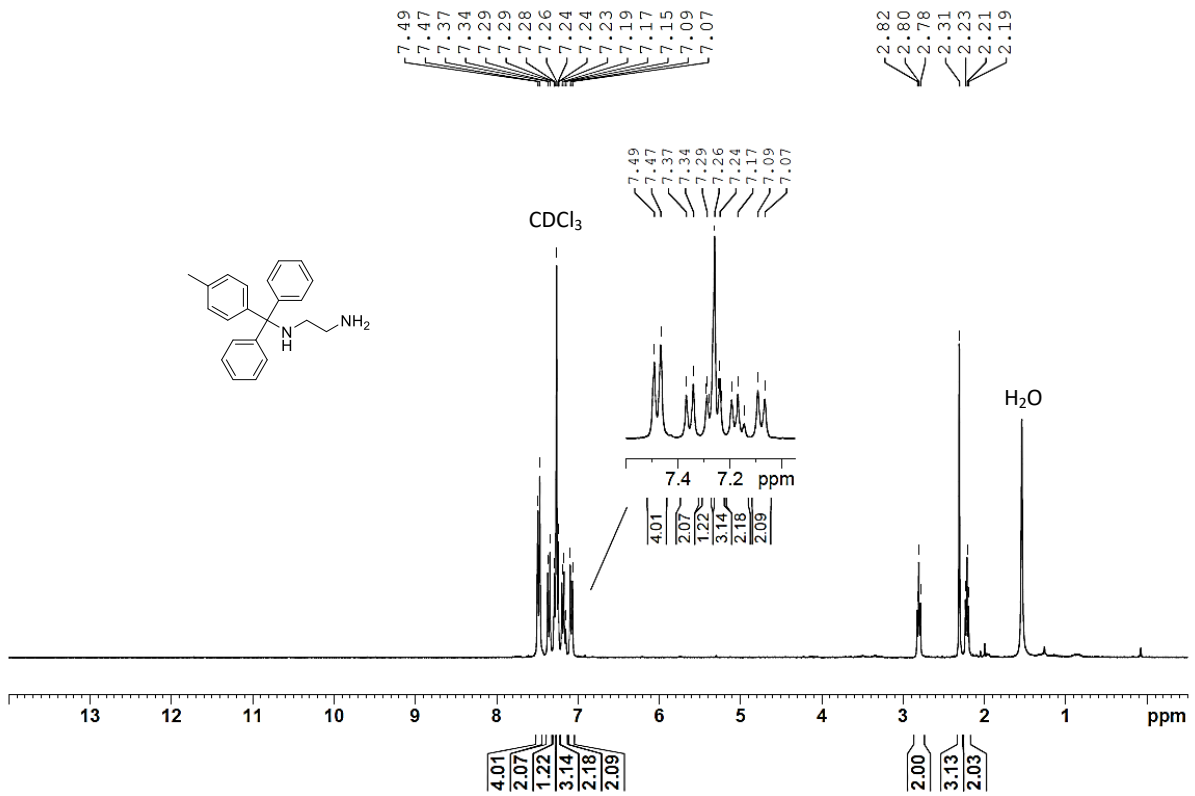

Figure S67: ^{1}H-NMR (300 MHz) spectrum of compound **44** in $CDCl_3$.

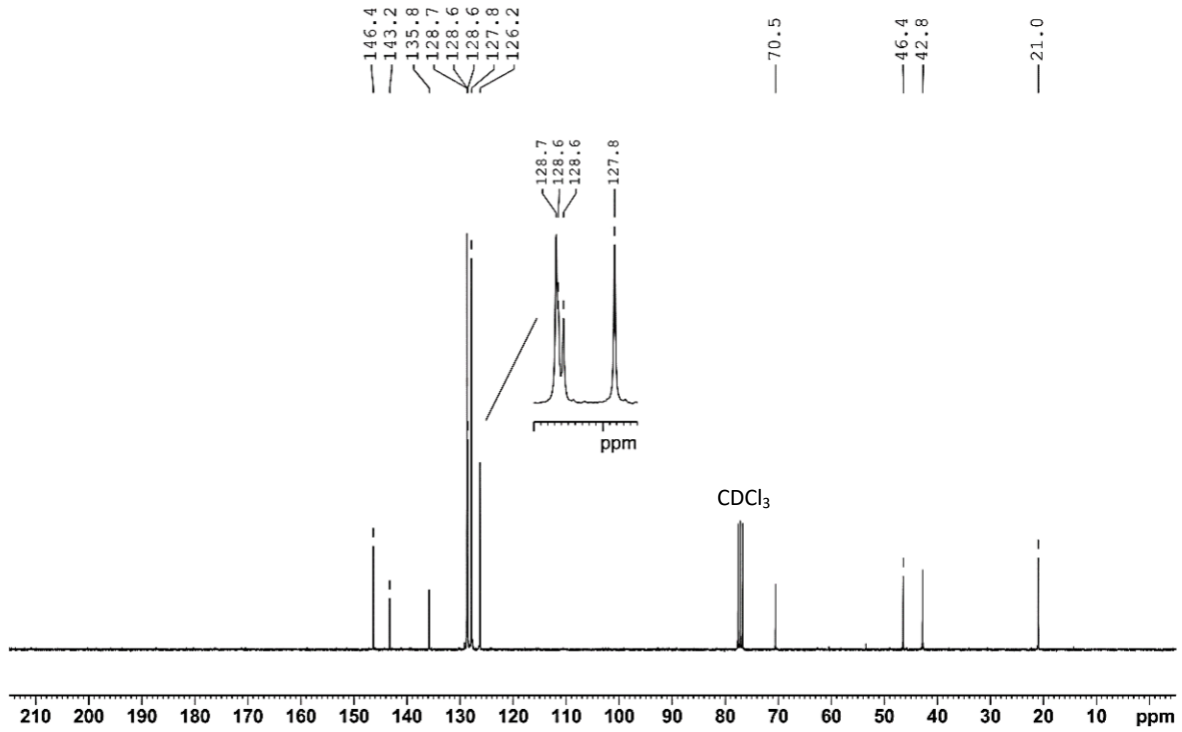

Figure S68: ^{13}C-NMR (75 MHz) spectrum of compound **44** in $CDCl_3$.

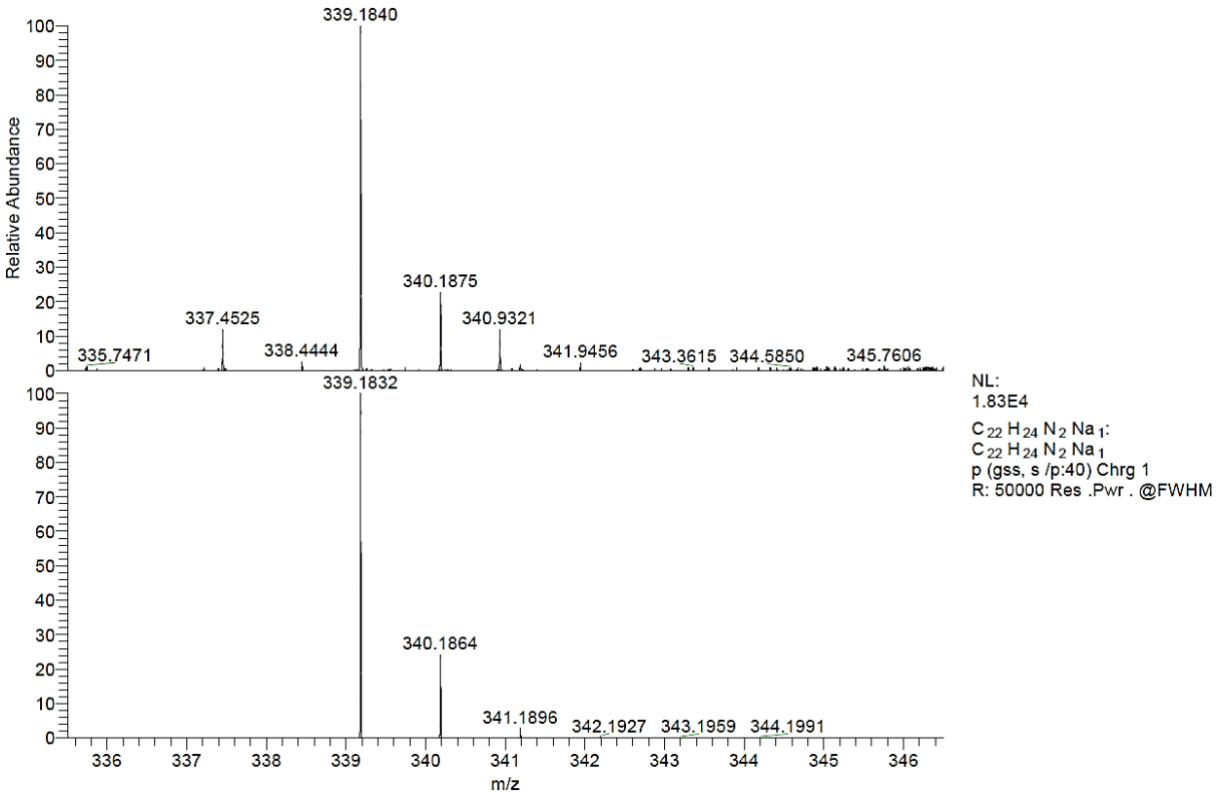

Figure S69: Measured (top) and calculated (bottom) HRMS-ESI spectrum of **44** in positive ion mode.

Benzyl-2-(4-formylphenoxy)acetate (46)

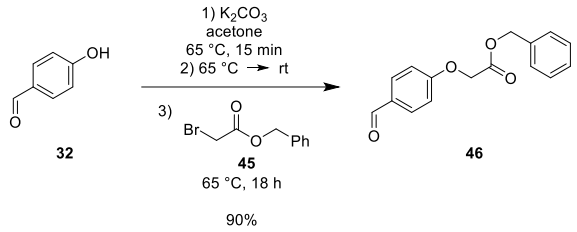

Scheme S14: Synthesis of benzyl-2-(4-formylphenoxy)acetate (**46**).

Adapted from the procedure of Bensinger *et al.*[30], 4-hydroxybenzaldehyde (**32**, 2.30 g, 18.8 mmol, 1.00 eq) was dissolved in acetone (50.0 mL). Potassium carbonate (5.73 g, 41.4 mmol, 2.20 eq) was added and the suspension was heated at 65 °C to reflux for 15 min. Afterwards, the mixture was cooled to rt and benzyl 2-bromoacetate (**45**, 8.63 g, 37.7 mmol, 2.00 eq) was added. The reaction mixture was stirred for 18 h at 65 °C. When complete conversion was observed, distilled water was added (~200 mL), and the aqueous phase was extracted with EtOAc (~200 mL, 3×). The combined organic phases were washed with brine (~200 mL, 1×) and dried over Na_2SO_4. The solvents were removed under reduced pressure and the obtained crude was purified by flash column chromatography (*n*-pentane/EtOAc 5:1 → 2:1 → 1:1 (v/v)) to give the product (**46**, 4.60 g, 17.0 mmol, 90%) as a colourless oil, which crystallized to white solid after one day storage at 4 °C. The characterization is in agreement with the literature.[30]

TLC ($UV_{254\ nm}$): R_f = 0.64 (*n*-pentane/EtOAc 2:1, v/v).

^{1}H-NMR (300 MHz, $CDCl_3$): δ = 9.89 (s, 1H), 7.83 (d, ^3J(H,H) = 8.8 Hz, 2H), 7.39 – 7.31 (m, 5H), 6.99 (d, ^3J(H,H) = 8.8 Hz, 2H), 5.25 (s, 2H), 4.75 (s, 2H) ppm.

^{13}C-NMR (125 MHz, $CDCl_3$): δ = 190.8 (*C*HO), 168.1 (*C*OO), 162.7 (C_q), 135.1 (C_q), 132.1 (2C; *C*H$_q$), 130.9 (C_q), 128.8 (*C*H), 128.8 (2C; *C*H), 128.7 (2C; *C*H), 115.1 (2C; *C*H), 67.4 (*C*H$_2$), 65.3 (*C*H$_2$) ppm.

HRMS-ESI (*m/z*): $[M + H]^+$ calcd for $C_{16}H_{15}O_4$: 271.0965; found: 271.0959.

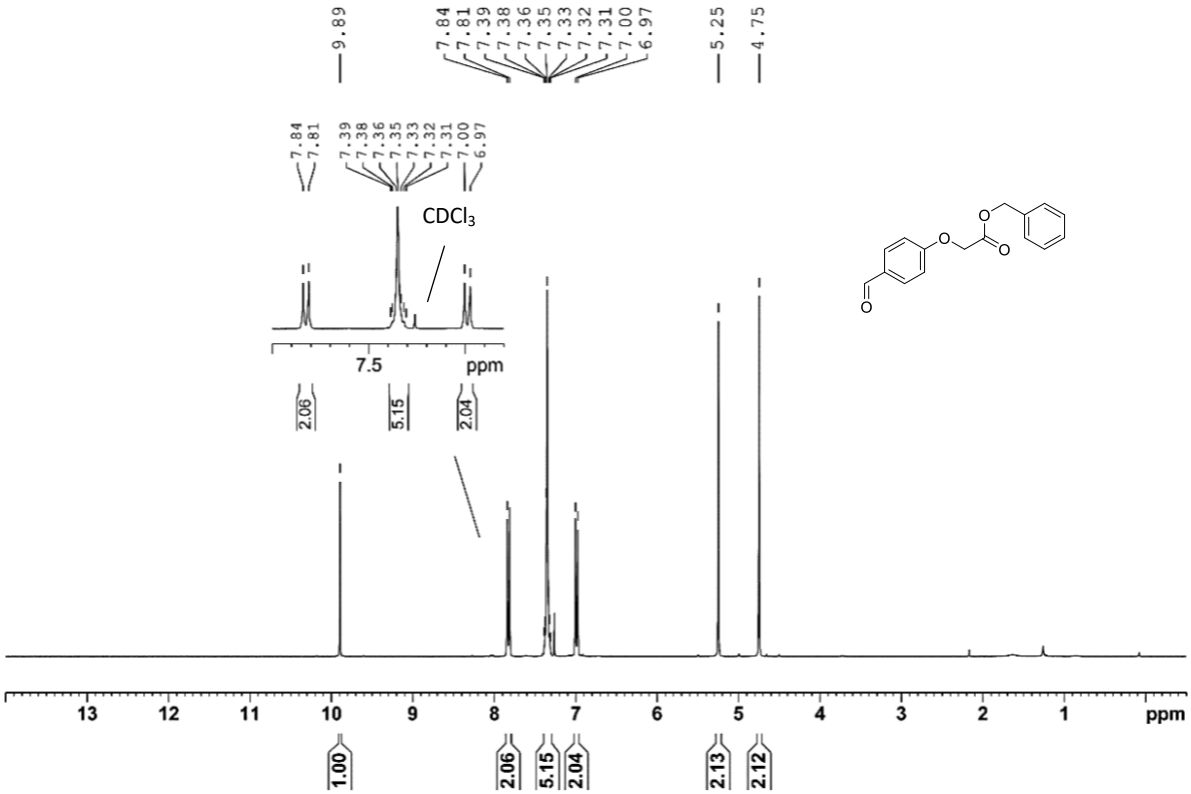

Figure S70: ^{1}H-NMR (300 MHz) spectrum of compound **46** in $CDCl_3$.

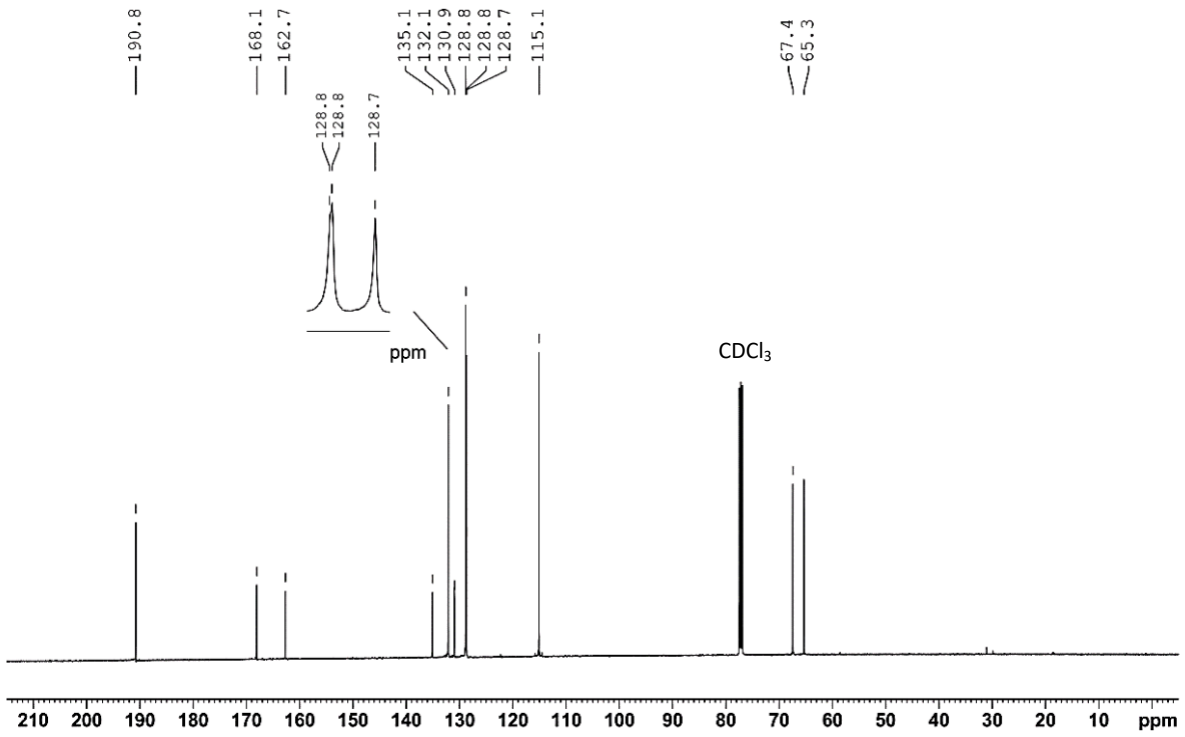

Figure S71: ^{13}C-NMR (125 MHz) spectrum of compound **46** in $CDCl_3$.

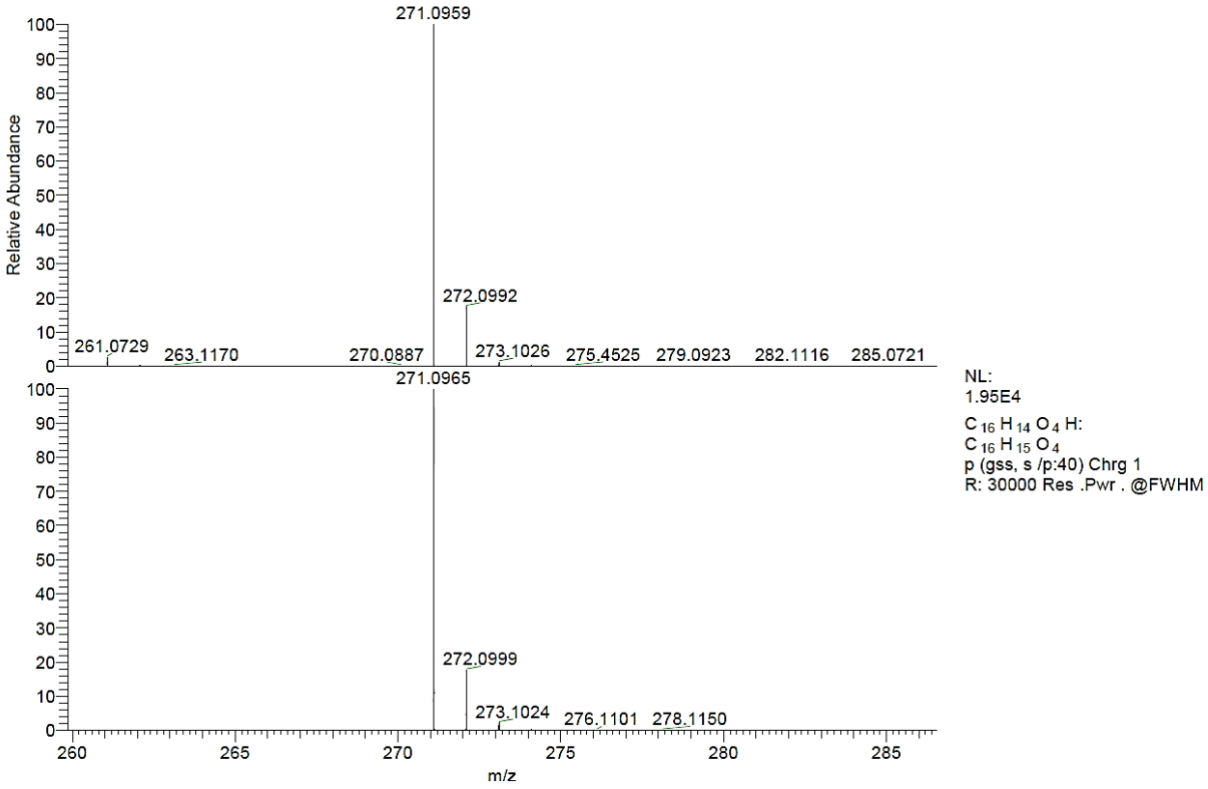

Figure S72: Measured (top) and calculated (bottom) HRMS-ESI spectrum of **46** in positive ion mode.

BODIPY-CO_2H (22)

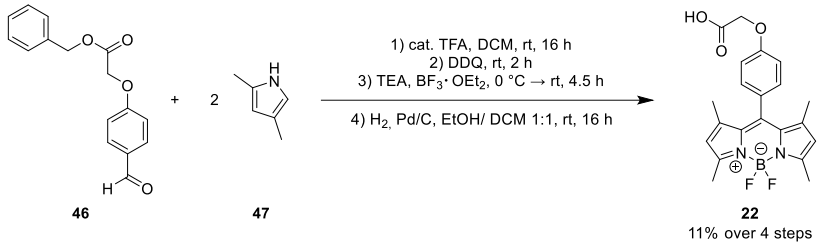

Scheme S15: Synthesis of BODIPY-CO_2H (**22**).

Adapted from the conditions described by Kolemen *et al*.[31] and Romanelli *et al*.[32], benzyl-protected 4-carboxybenzaldehyde (**46**, 100 mg, 0.37 mmol, 1.00 eq) and 2,4-dimethyl pyrrole (**47**, 0.08 mL, 0.77 mmol, 2.10 eq) were dissolved in degassed DCM (7.00 mL) under nitrogen atmosphere. A drop of TFA was added and the mixture was stirred for 16 h at rt in the dark. After the consumption of the starting material was confirmed by TLC ($UV_{254\ nm}$), DDQ (83.3 mg, 0.37 mmol, 1.00 eq) and degassed DCM (2.00 mL) was added to the mixture. Stirring was continued at rt for 2 h in the dark. Then, TEA (0.51 mL, 3.67 mmol, 10.0 eq) was added. The reaction mixture was cooled to 0 °C, then boron trifluoride-diethyl ether complex (0.47 mL, 3.67 mmol, 10.0 eq) was added dropwise and the stirring was continued for 4.5 h at rt. Afterwards, the reaction mixture was washed with $NaHCO_3$ (~150.0 mL, 1×) and distilled water (~150 mL, 2×). The aqueous phase was extracted with DCM (~150 mL, 3×) and the combined organic phases were washed using brine (~200 mL, 1×) and dried over Na_2SO_4. After evaporating the solvent, the gained crude was purified by flash column chromatography (*n*-pentane/EtOAc 9:1 → 4:1 → 2:1 (v/v)). The obtained substance was dissolved in a 1:1 mixture of EtOH/ DCM (50.0 mL). Pd/C (27.5 mg) was added, and the reaction mixture was stirred strongly under hydrogen atmosphere at rt in the dark. After 16 h, all solid components were removed by filtration of the reaction mixture over celite and washed with EtOAc. The solvent was evaporated, and the product was purified by flash column chromatography (*n*-pentane/EtOAc 1:1 (v/v) → EtOAc, 1% formic acid) to yield the product **22** (15.6 mg, 0.04 mmol, 11%) as an orange solid.

TLC ($UV_{254\ nm}$): R_f = 0.21 (DCM/MeOH 50:1 + 1% formic acid, v/v).

^{1}H-NMR (500 MHz, $CDCl_3$): δ = 7.22 (dt, ^3J(H,H) = 8.7 Hz, ^4J(H,H) = 2.5 Hz, 2H), 7.05 (dt, ^3J(H,H) = 8.7 Hz, ^4J(H,H) = 2.5 Hz, 2H), 5.97 (s, 2H), 4.76 (s, 2H), 2.55 (s, 6H), 1.41 (s, 6H) ppm.

^{13}C-NMR (125 MHz, $CDCl_3$): δ = 172.7 (C_q), 164.3 (C_q), 158.2 (2C; C_q), 155.7 (C_q), 143.2 (C_q), 141.3 (C_q), 131.9 (C_q), 131.9 (C_q), 129.7 (2C; *C*H), 128.8 (C_q), 121.4 (*C*H), 121.4 (*C*H), 115.5 (2C; *C*H), 65.0 (CH_2), 14.7 (2C; CH_3), 14.7 (2C; CH_3) ppm.

^{19}F-NMR (282 MHz, $CDCl_3$): δ = -146.2 (dd, ^1J(B, F) = 33.1 Hz, 2F, BF_2) ppm.

HRMS-ESI (*m/z*): $[M - H]^-$ calcd for $C_{21}H_{20}BF_2N_2O_3$: 397.1544; found: 397.1543.

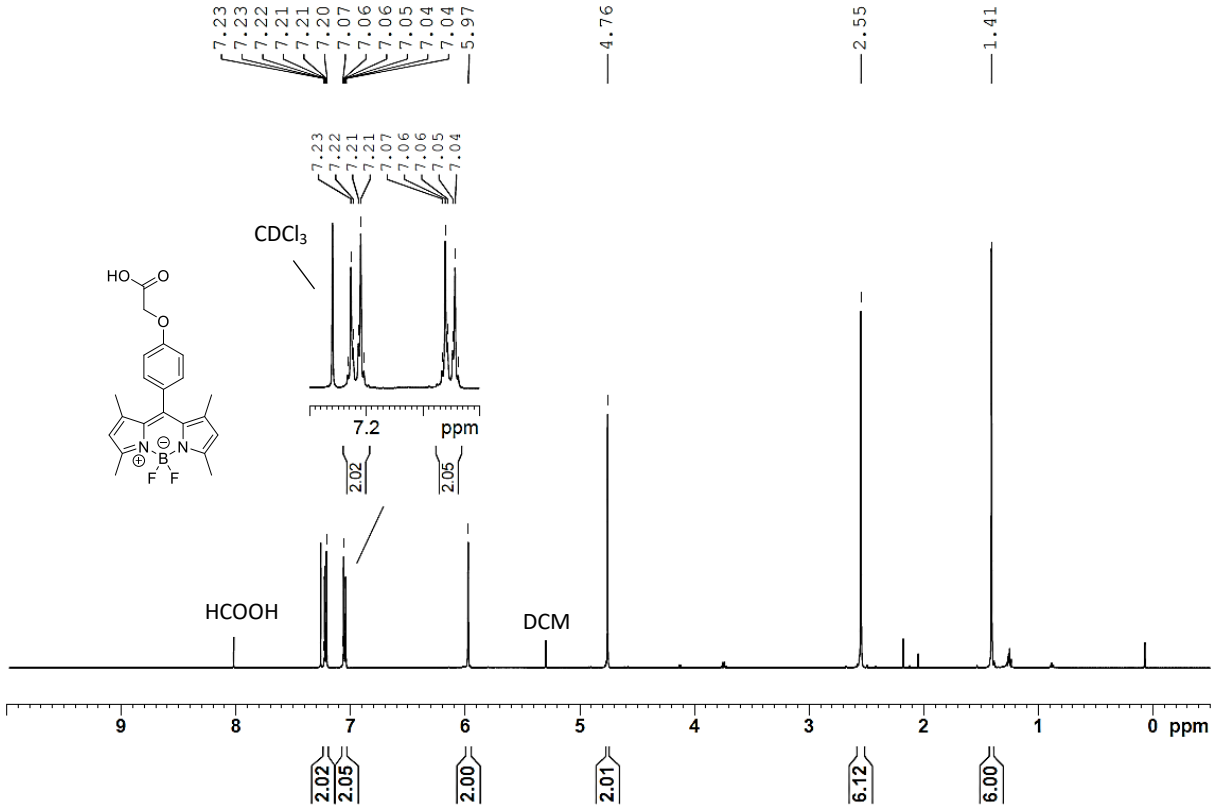

Figure S73: ^{1}H-NMR (500 MHz) spectrum of compound **22** in $CDCl_3$.

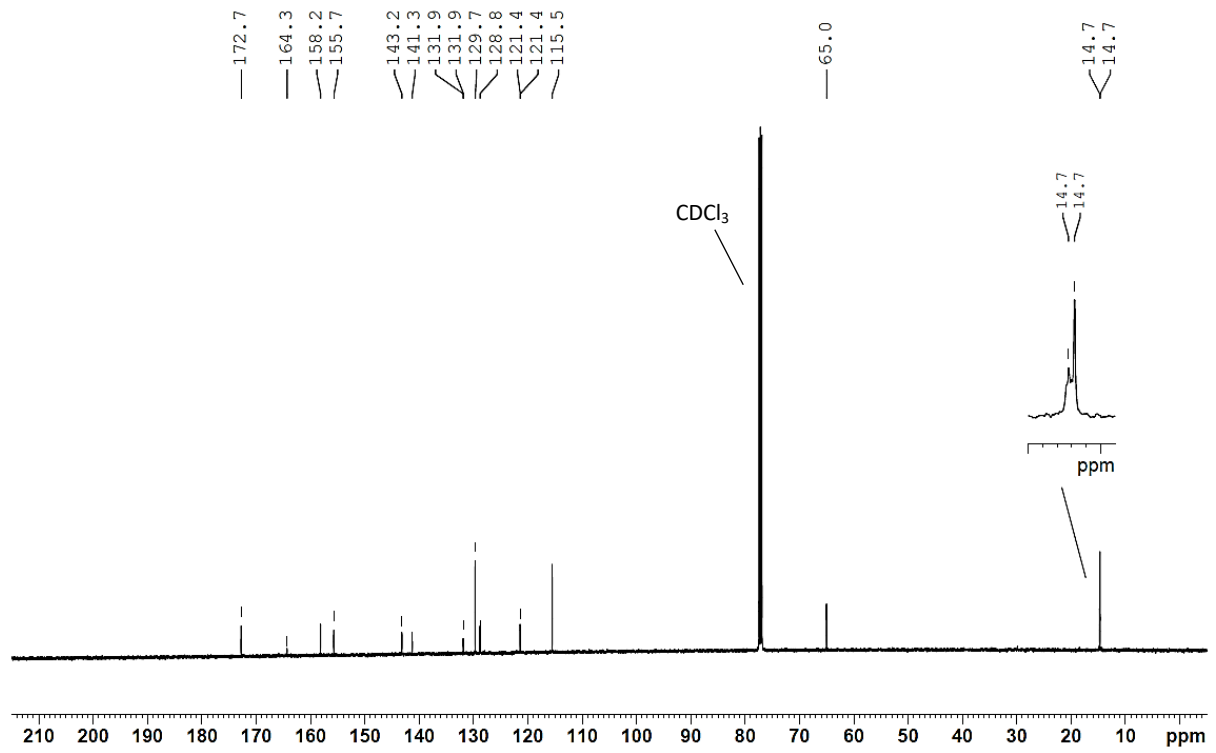

Figure S74: ^{13}C-NMR (125 MHz) spectrum of compound **22** in $CDCl_3$.

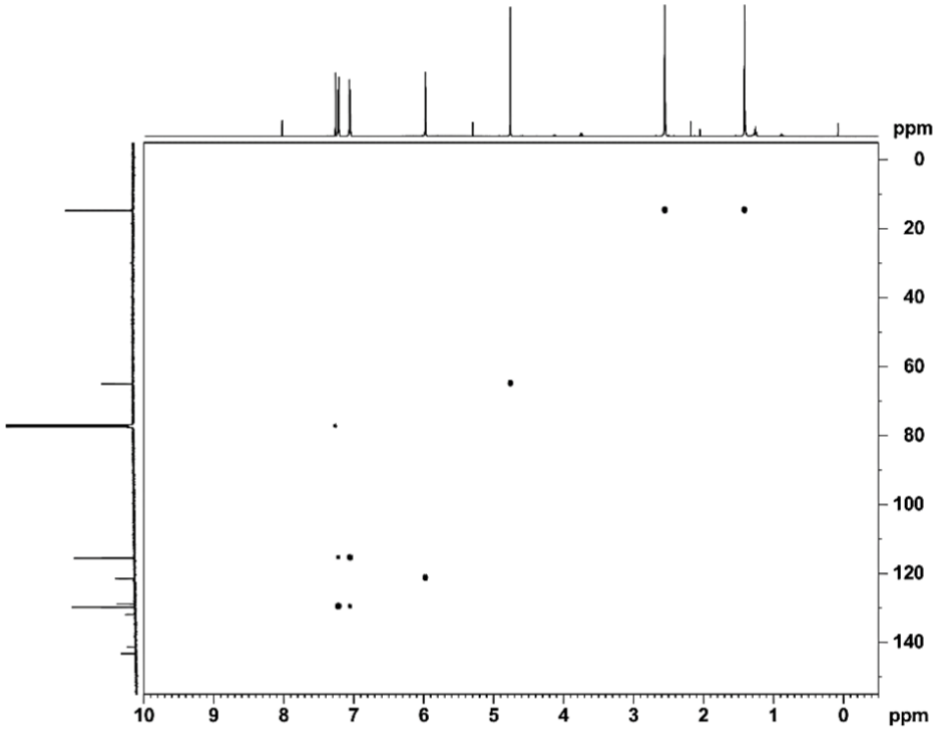

Figure S75: HSQC spectrum of compound **22** (^{1}H-NMR: 500 MHz, ^{13}C-NMR: 125 MHz, $CDCl_3$).

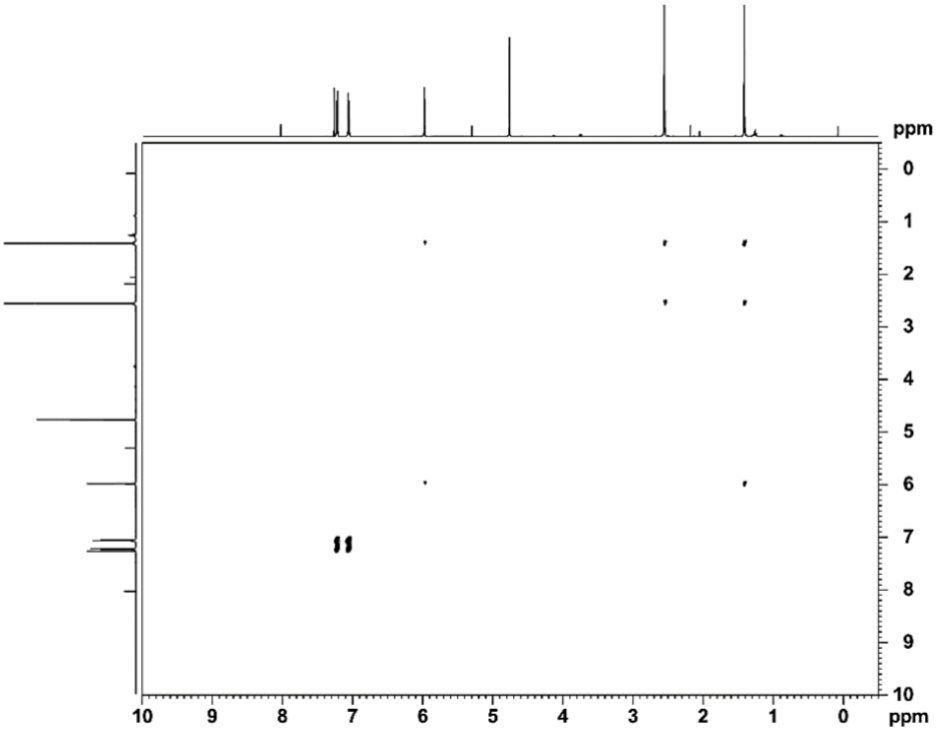

Figure S76: COSY spectrum of compound **22** (^{1}H-NMR: 500 MHz, $CDCl_3$).

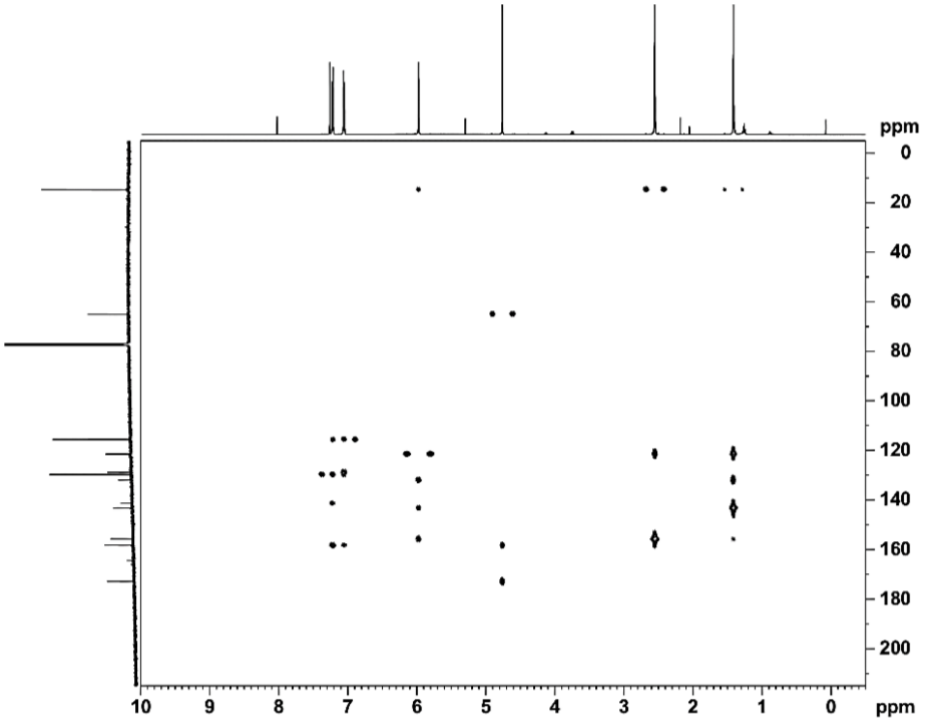

Figure S77: HMBC spectrum of compound **22** (^{1}H-NMR: 500 MHz, ^{13}C-NMR: 125 MHz, $CDCl_3$).

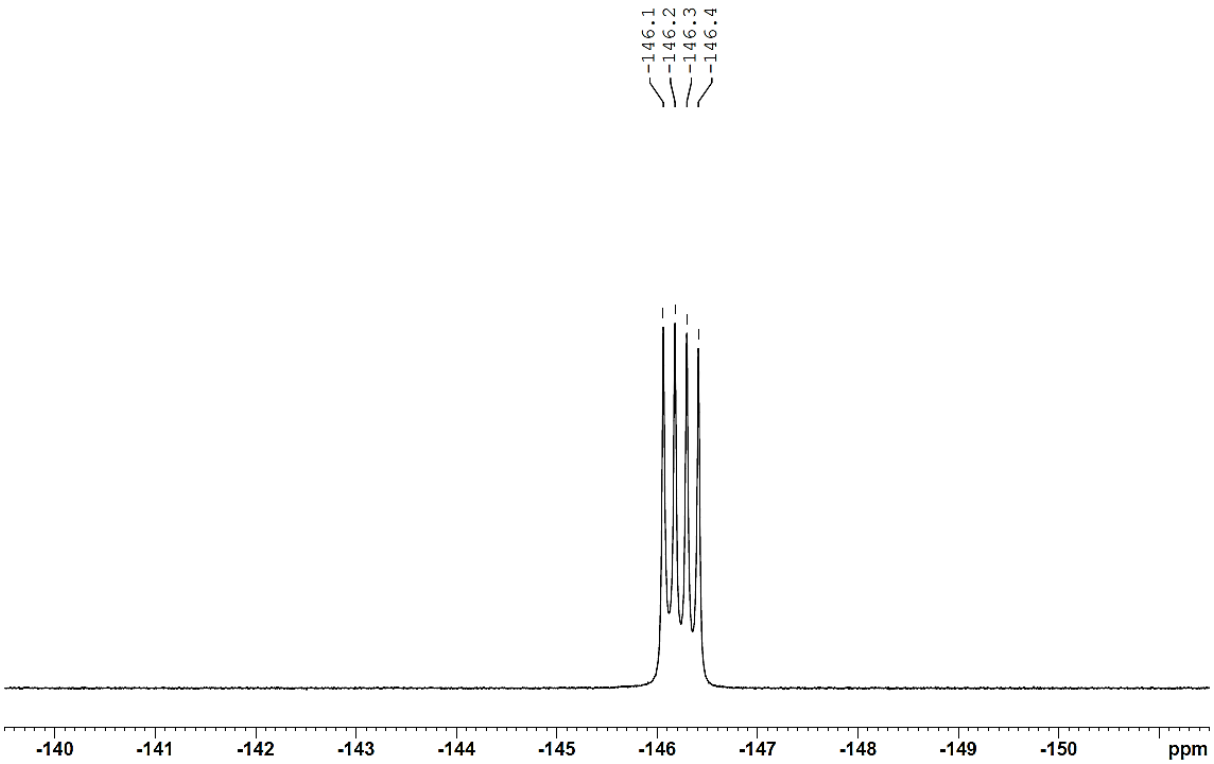

Figure S78: ^{19}F-NMR (282 MHz) spectrum of compound **22** in $CDCl_3$.

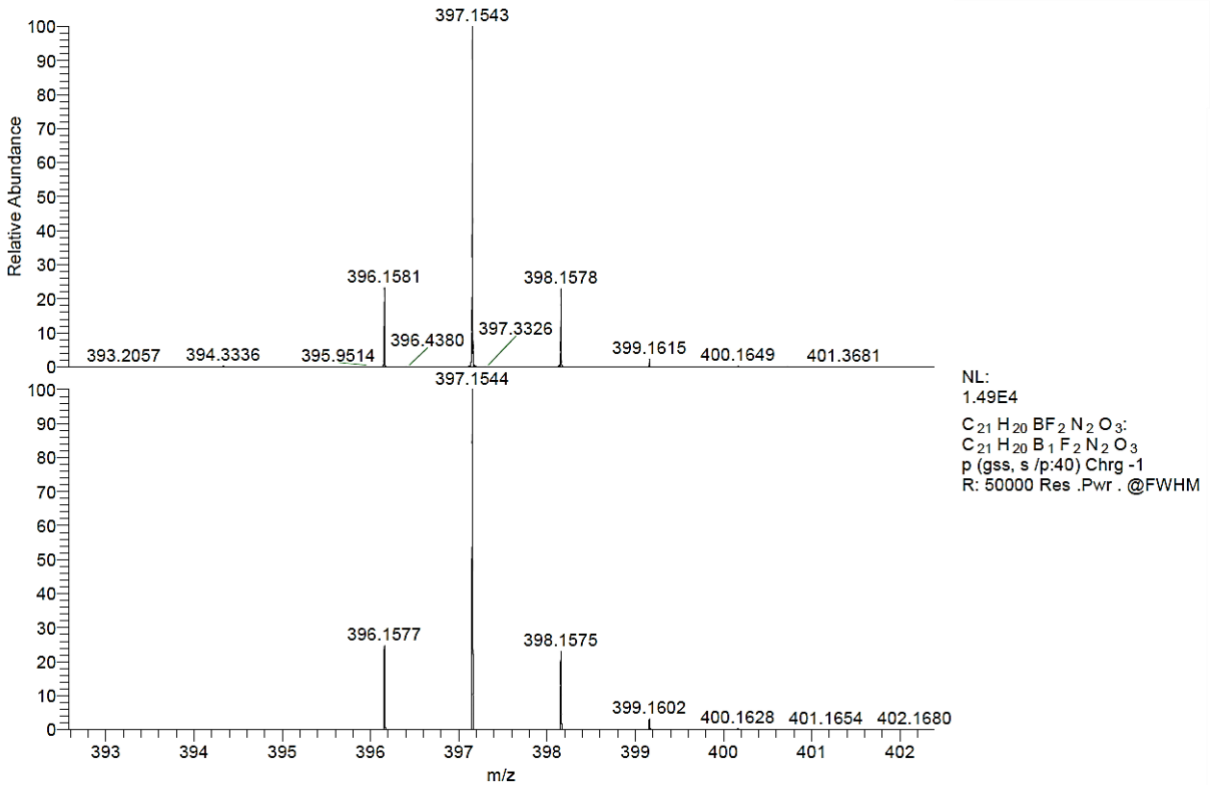

Figure S79: Measured (top) and calculated (bottom) HRMS-ESI spectrum of **22** in negative ion mode.

2I-BODIPY-CO_2H (2)

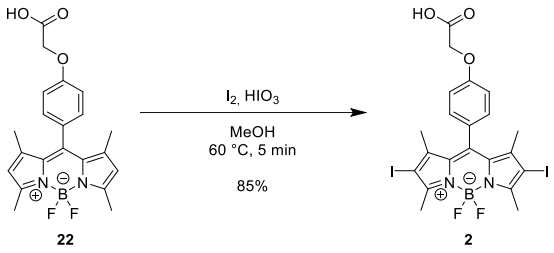

Scheme S16: Synthesis of 2I-BODIPY-CO_2H (**2**)**.**

To a solution of the BODIPY **22**(150 mg, 0.38 mmol, 1.00 eq) and iodine (239 mg, 0.94 mmol, 2.50 eq) in MeOH (15.0 mL), a solution of iodic acid (133 mg, 0.75 mmol, 2.00 eq) in distilled water (0.55 mL) was added. The reaction mixture was stirred at 60 °C for 5 min, cooled to rt, and then diluted with chloroform (~100 mL). The organic phase was washed with saturated $Na_2S_2O_3$ solution (~100 mL, 3×) in water followed by extraction of the aqueous phase with chloroform (100 mL, 3×). The combined organic phase was washed with brine (~150 mL, 1×) and dried over Na_2SO_4, the solvent was removed under reduced pressure and the crude was purified by flash column chromatography (*n*-pentane/EtOAc 2:1 ⟶ 1:1 (v/v), 1% formic acid) to yield the iodinated BODIPY **2** (208 mg, 0.32 mmol, 85%) as an intense pink solid.

TLC ($UV_{254\ nm}$): R_f = 0.74 (EtOAc + 1% formic acid).

^{1}H-NMR (300 MHz, $CDCl_3$): δ = 7.19 (dt, ^3J(H,H) = 8.8 Hz, ^4J(H,H) = 2.3 Hz, 2H), 7.08 (dt, ^3J(H,H) = 8.8 Hz, ^4J(H,H) = 2.3 Hz, 2H), 4.78 (s, 2H), 2.64 (s, 6H), 1.42 (s, 6H) ppm.

^{13}C-NMR (125 MHz, $CDCl_3$): δ = 172.6 (C_q), 164.2 (C_q), 158.4 (2C; C_q), 157.0 (C_q), 145.4 (C_q), 140.9 (C_q), 131.7 (2C; C_q), 129.5 (2C; *C*H), 128.4 (C_q), 115.8 (2C; *C*H), 85.9 (2C; C_q), 64.9 (CH_2), 17.3 (2C; CH_3), 16.2 (2C; CH_3) ppm.

^{19}F-NMR (282 MHz, $CDCl_3$): δ = -145.6 (dd, ^1J(B,F) = 32.3 Hz, 2F; BF_2) ppm.

HRMS-ESI (*m/z*): $[M - H]^-$ calcd for $C_{21}H_{18}BF_2I_2N_2O_3$: 648.9477; found: 648.9479.

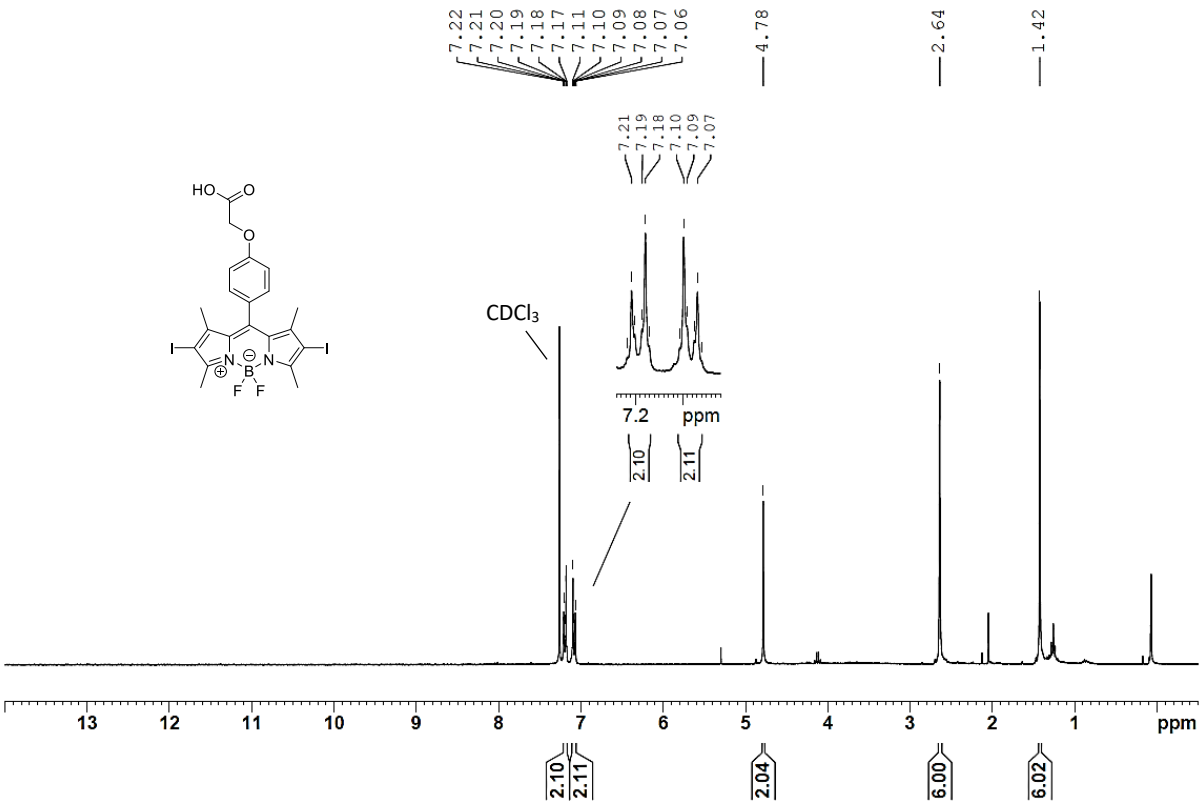

Figure S80: ^{1}H-NMR (300 MHz) spectrum of compound **2** in $CDCl_3$.

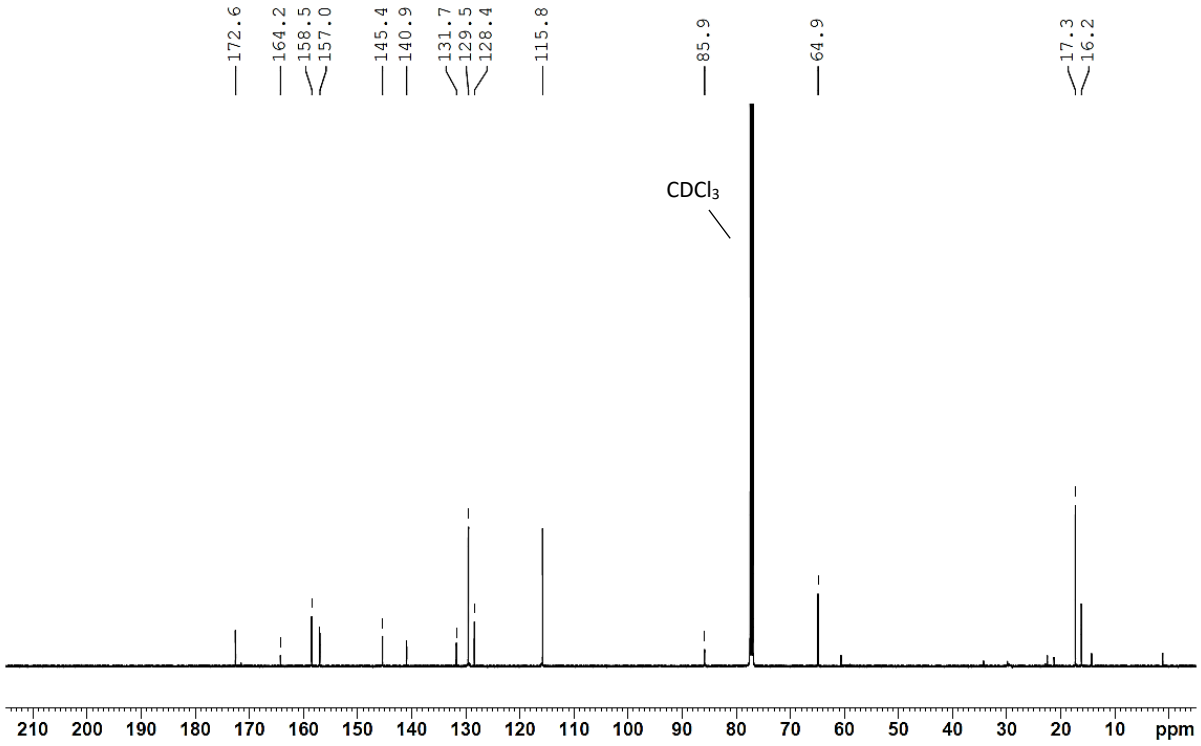

Figure S81: ^{13}C-NMR (125 MHz) spectrum of compound **2** in $CDCl_3$.

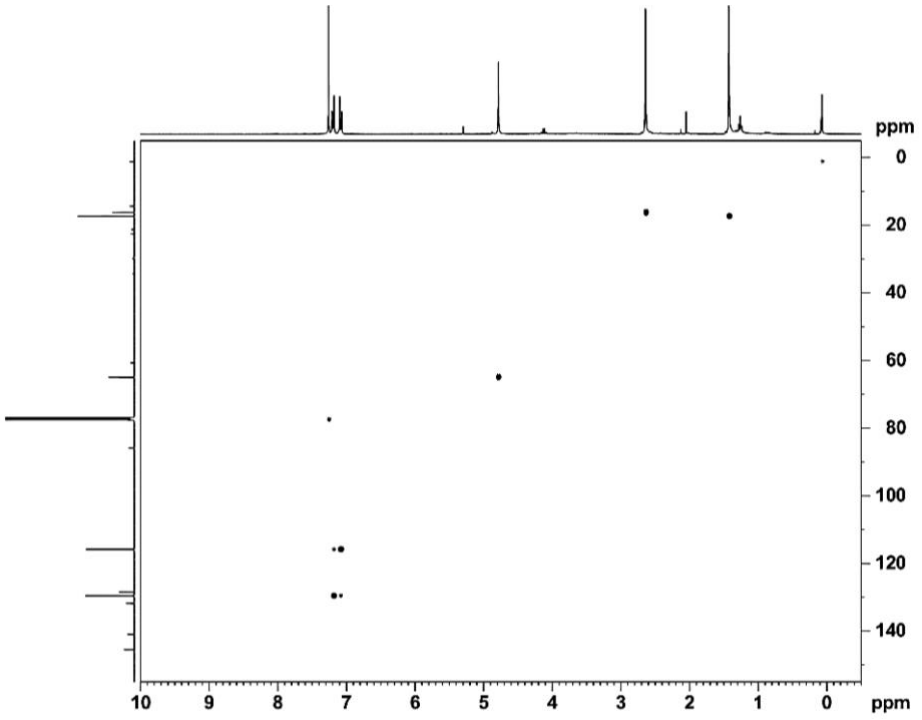

Figure S82: HSQC spectrum of compound **2** (^{1}H-NMR: 300 MHz, ^{13}C-NMR: 125 MHz, $CDCl_3$).

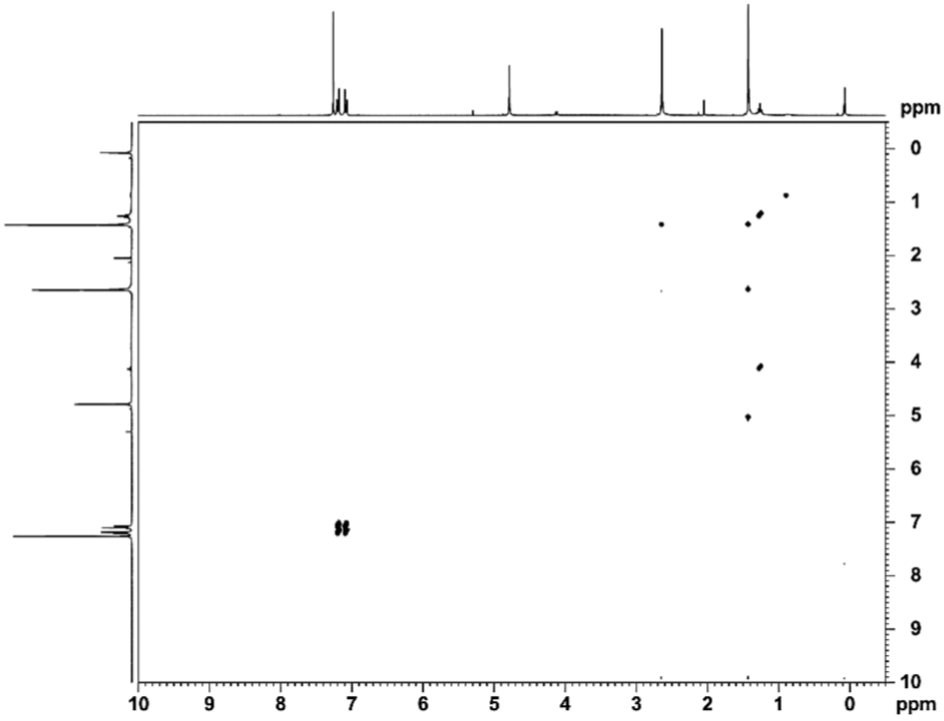

Figure S83: COSY spectrum of compound **2** (^{1}H-NMR: 300 MHz, $CDCl_3$).

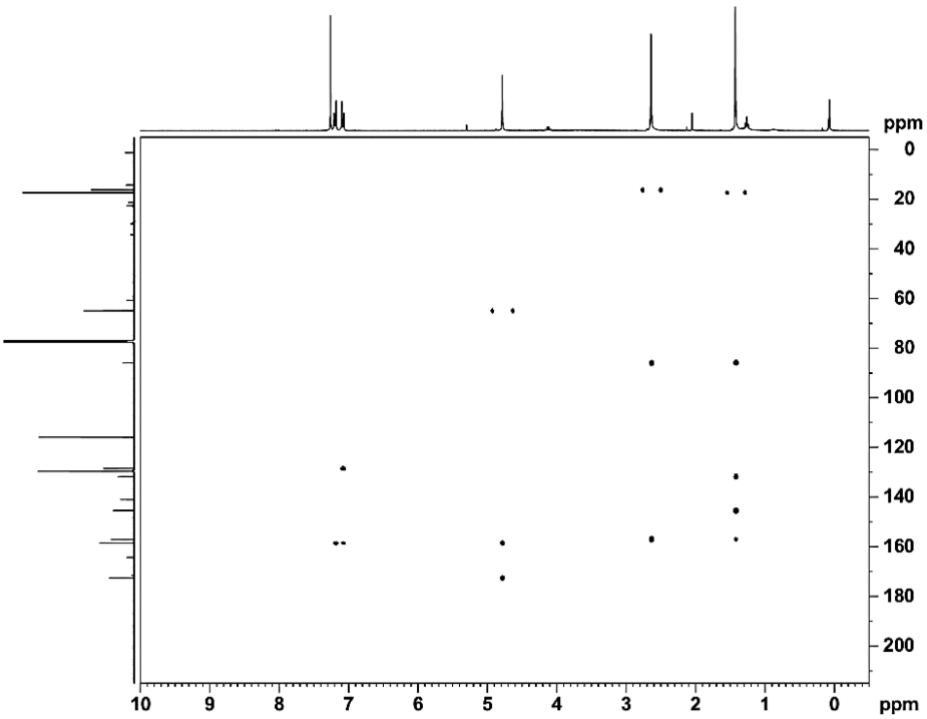

Figure S84: HMBC spectrum of compound **2** (^{1}H-NMR: 300 MHz, ^{13}C-NMR: 125 MHz, $CDCl_3$).

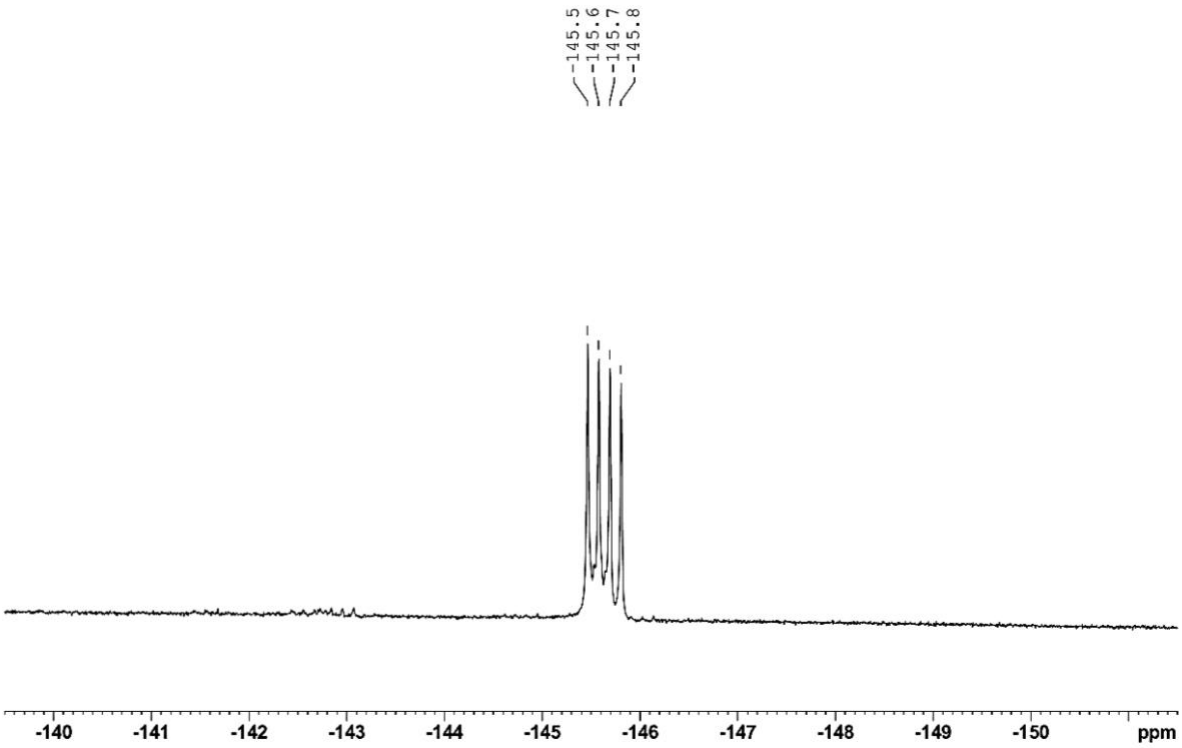

Figure S85: ^{19}F-NMR (282 MHz) spectrum of compound **2** in $CDCl_3$.

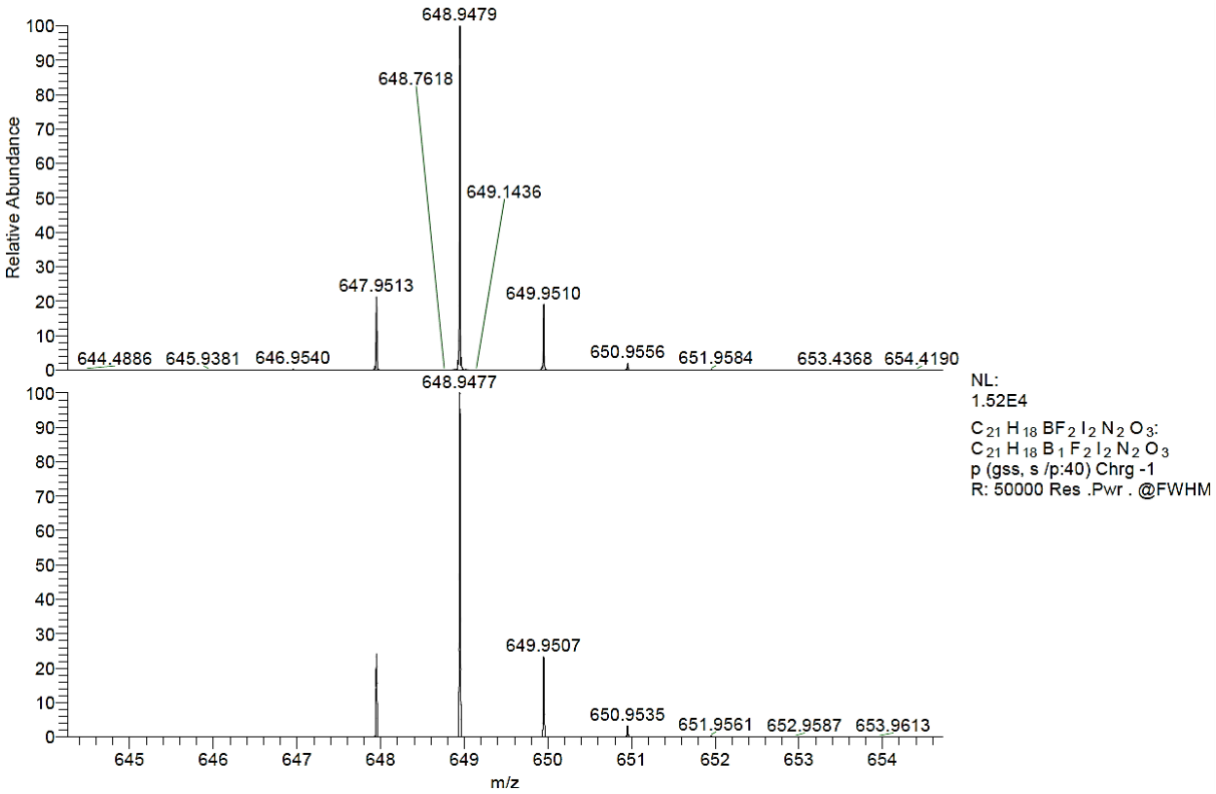

Figure S86: Measured (top) and calculated (bottom) HRMS-ESI spectrum of **2** in negative ion mode.

BODIPY-CONH-NH_2 (15)

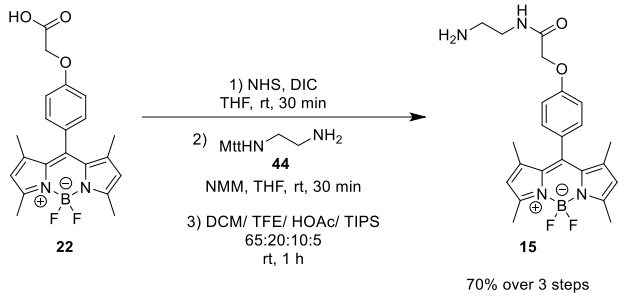

Scheme S17: Synthesis of BODIPY-CONH-NH_2 (**15**).

Based on synthetic procedures described by Akizawa *et al*.[33] and Bollhagen *et al*.[34], BODIPY **22** (150 mg, 0.45 mmol, 1.00 eq) and *N*-hydroxysuccinimide (54.2 mg, 0.56 mmol, 1.25 eq) were dissolved in dry THF (984 µL). DIC (64.0 µL, 0.49 mmol, 1.10 eq) was added and the reaction mixture was shaken at rt for 30 min under nitrogen atmosphere. During this time, Mtt-protected ethylenediamine (**44**, 572 mg, 1.81 mmol, 4.00 eq) was dissolved in dry THF (800 µL) followed by addition of NMM (199 µL, 1.81 mmol, 4.00 eq). When complete NHS ester formation was shown by TLC ($UV_{254\ nm}$), the prepared amine solution was added to the reaction mixture. The mixture was shaken for further 30 min at rt under nitrogen atmosphere. After complete conversion, the mixture was diluted with DCM (~50 mL) and washed with brine (~50 mL, 2×) acidified with citric acid. The aqueous phase was extracted with DCM (~50 mL, 3×). The combined organic phase was concentrated under reduced pressure. For the last step, the crude was dissolved in dry DCM/ TFE/ HOAc/ TIPS (65:20:10:5, 22.9 mL). The reaction mixture was stirred at rt under nitrogen atmosphere. After 1 h, complete conversion was confirmed by TLC ($UV_{254\ nm}$). The solvent was evaporated, and the remaining residue was purified by flash column chromatography ($DCM{\cdot}NH_3$/MeOH 9:1 (v/v)) to give compound **15** (140 mg, 0.32 mmol, 70%) as an orange solid.

TLC ($UV_{254\ nm}$): R_f = 0.20 (DCM/MeOH 9:1 + 0.2% DEA, v/v).

^{1}H-NMR (300 MHz, MeOD-d_4):[a] δ = 7.26 (d, ^3J(H,H) = 8.8 Hz, 2H), 7.19 (d, ^3J(H,H) = 8.8 Hz, 2H), 6.06 (s, 2H), 4.61 (s, 2H), 3.38 (t, ^3J(H,H) = 6.2 Hz, 2H), 2.79 (t, ^3J(H,H) = 6.2 Hz, 2H), 2.48 (s, 6H), 1.45 (s, 6H) ppm.

^{13}C-NMR (125 MHz, MeOD-d_4): δ = 173.8, 171.9, 171.1, 159.9, 159.8, 156.6, 156.6, 144.5, 144.5, 143.3, 143.2, 132.9, 130.8, 130.7, 129.5, 129.4, 122.2, 116.7, 116.7, 68.2, 41.2, 40.1, 39.9, 38.9, 14.8, 14.8, 14.8, 14.5 ppm.[a]

^{19}F-NMR (282 MHz, $CDCl_3$): δ = -147.0 (dd, ^1J(B,F) = 32.5 Hz, 2F; BF_2) ppm.

HRMS-ESI (*m/z*): $[M + H]^+$ calcd for $C_{23}H_{28}BF_2N_4O_2$: 441.2272; found: 441.2265.

[a] In ^{13}C spectra, two closely spaced signal sets (≥ 0.1 ppm) were observed for nearly all while only one signal set was found in the ^{1}H-NMR was found. This may be due to an overlap of signals caused by the high similarity of the two conformational isomers. A possible explanation might be the double bond character of the amide bond.[35]

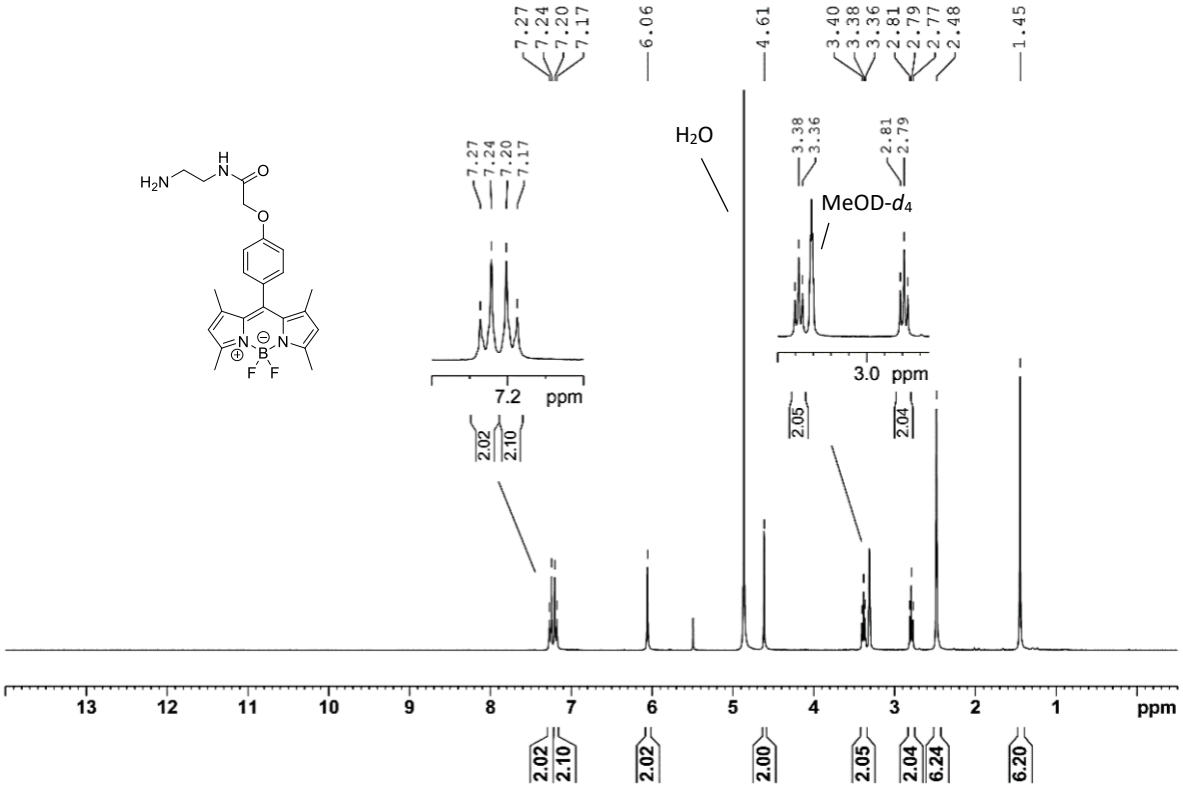

Figure S87: ^{1}H-NMR (300 MHz) spectrum of compound **15** in MeOD-d_4.

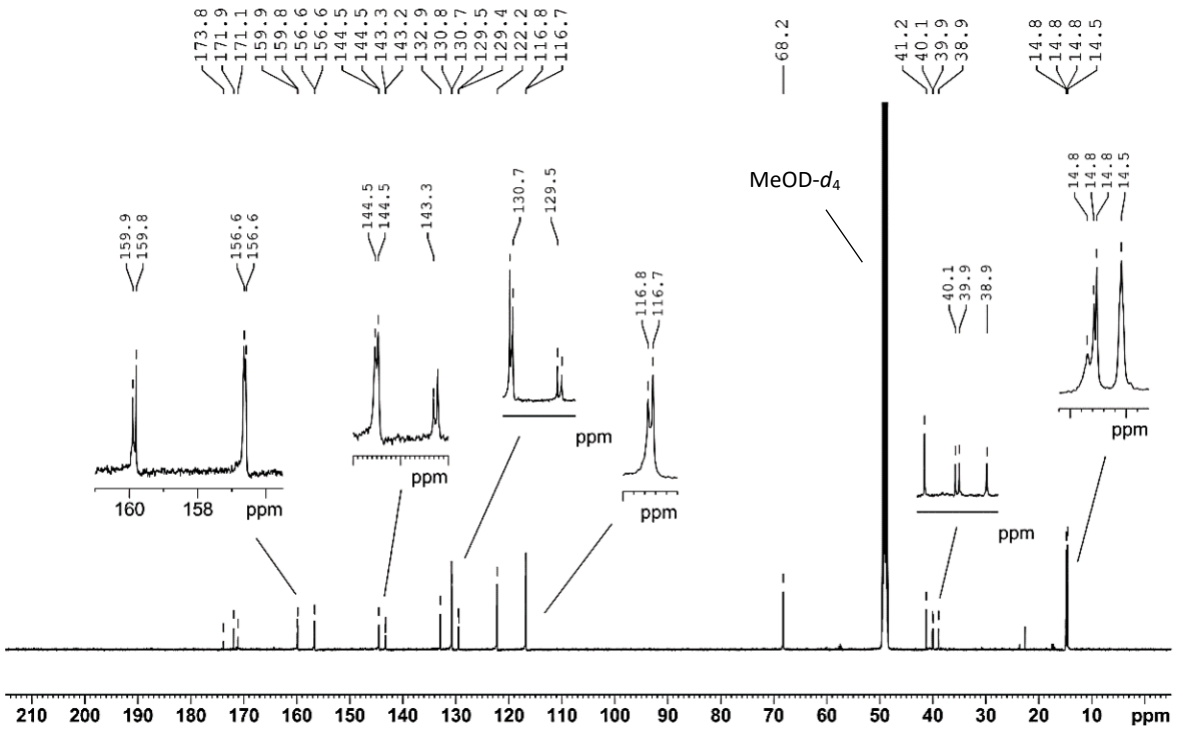

Figure S88: ^{13}C-NMR (125 MHz) spectrum of compound **15** in MeOD-d_4.

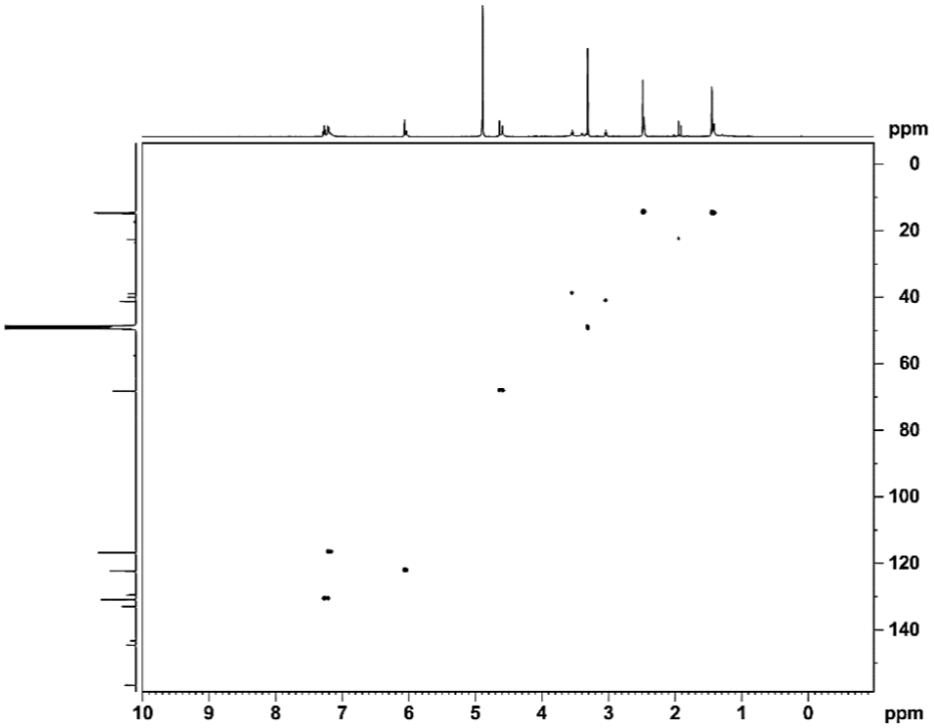

Figure S89: HSQC spectrum of compound **15** (^{1}H-NMR: 300 MHz, ^{13}C-NMR: 125 MHz, MeOD-d_4).

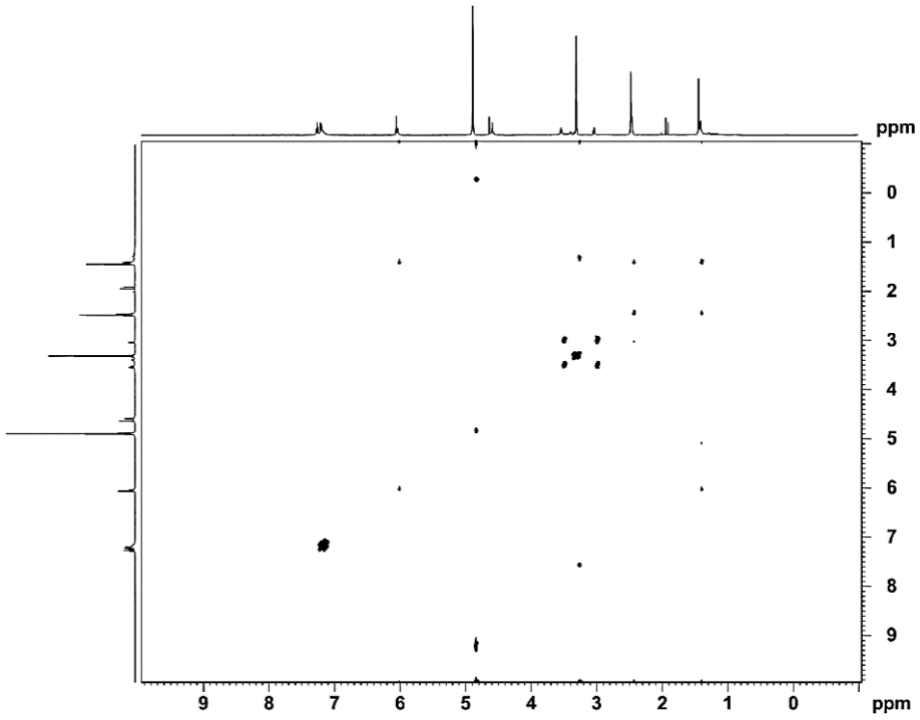

Figure S90: COSY spectrum of compound **15** (^{1}H-NMR: 300 MHz, MeOD-d_4).

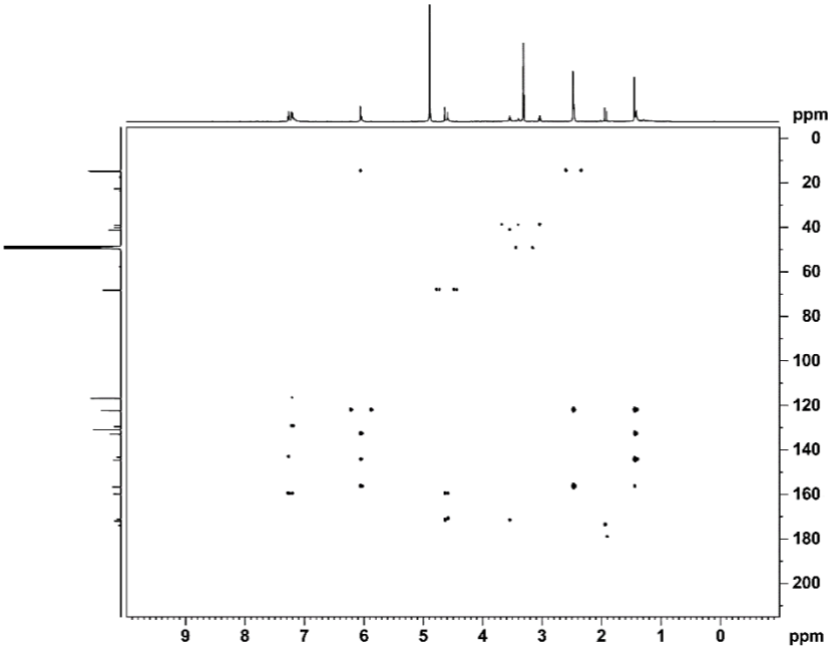

Figure S91: HMBC spectrum of compound **15** (^{1}H-NMR: 300 MHz, ^{13}C-NMR: 125 MHz, MeOD-d_4).

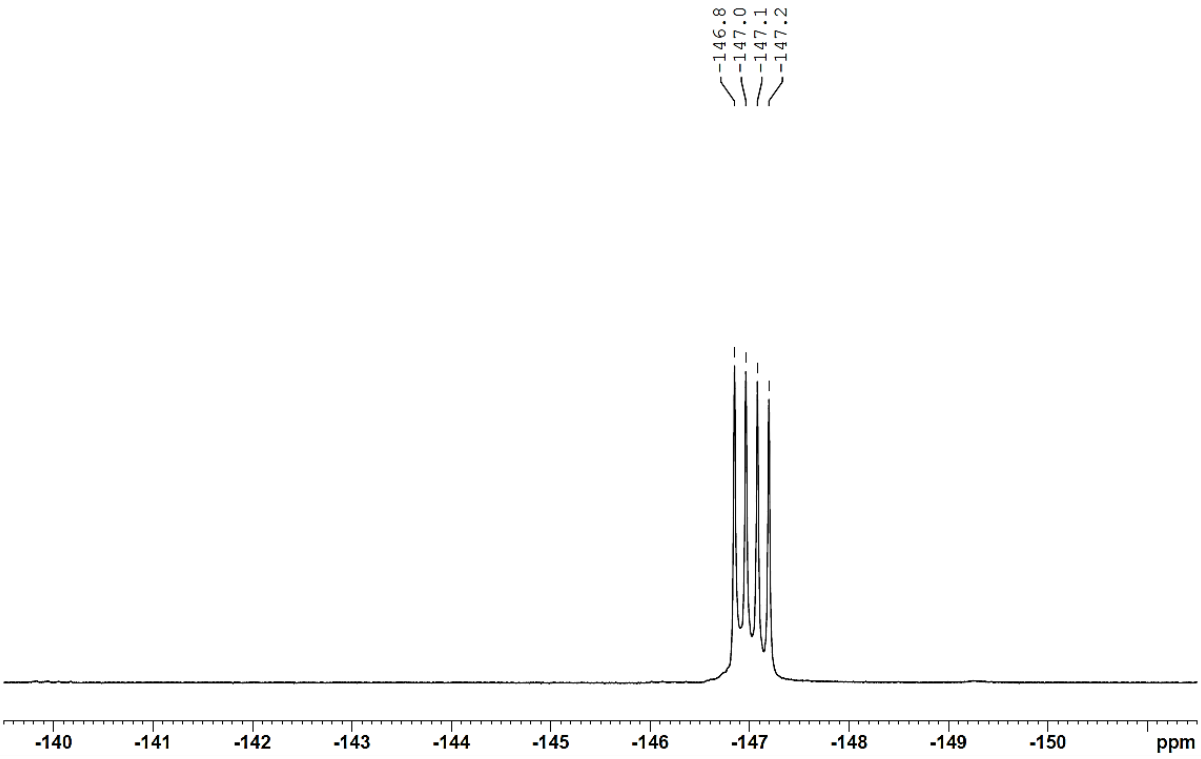

Figure S92: ^{19}F-NMR (282 MHz) spectrum of compound **15** in MeOD-d_4.

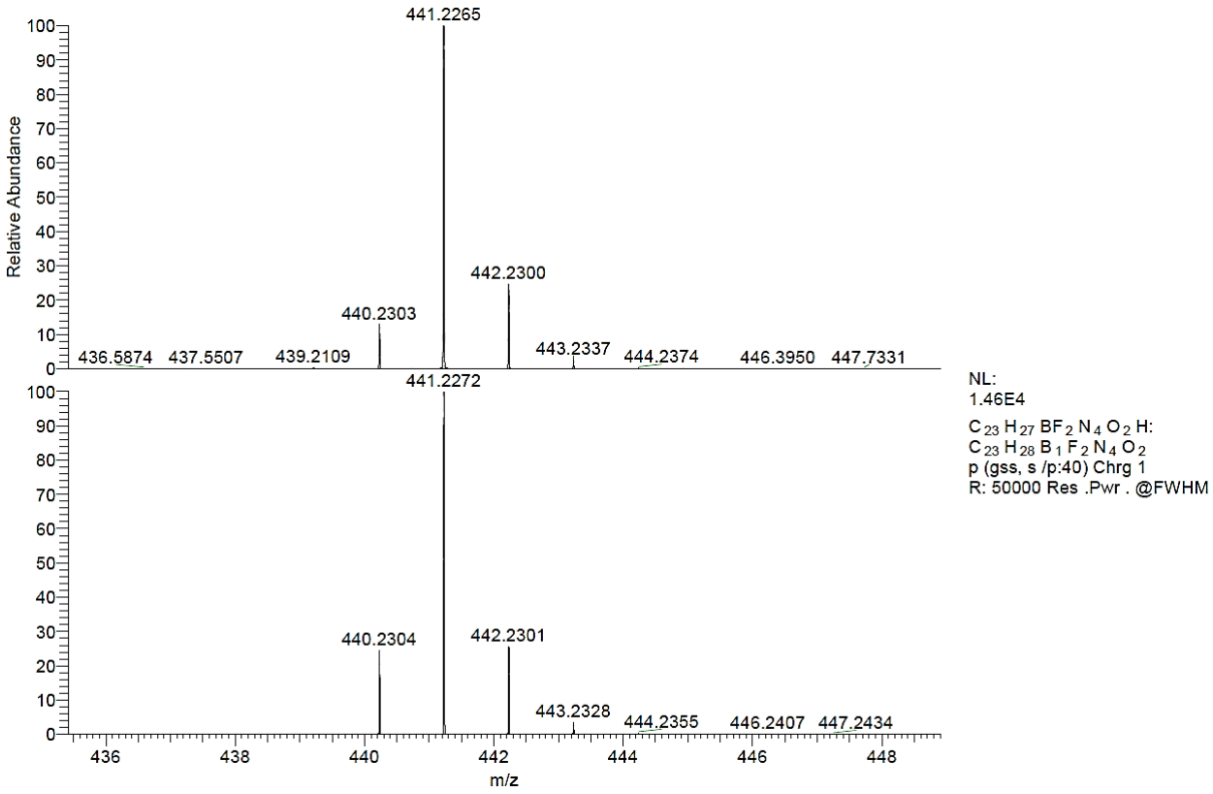

Figure S93: Measured (top) and calculated (bottom) HRMS-ESI spectrum of **15** in positive ion mode.

2I-BODIPY-CONH-NH_2 (16)

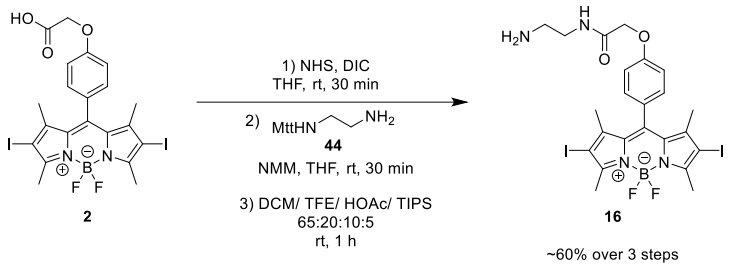

Scheme S18: Synthesis of 2I-BODIPY-CONH-NH_2 (**16**).

Based on synthetic procedures described by Akizawa *et al*.[33] and Bollhagen *et al*.[34], I_2-BODIPY **2** (160 mg, 0.25 mmol, 1.00 eq) and NHS (35.5 mg, 0.31 mmol, 1.25 eq) were dissolved in dry THF (640 µL). DIC (42.0 µL, 0.27 mmol, 1.10 eq) was added and the reaction mixture was shaken at rt for 30 min under nitrogen atmosphere. During this time, the coupling of the amine was prepared. For this, Mtt-protected ethylenediamine (**44**, 311 mg, 0.98 mmol, 4.00 eq) was dissolved in dry THF (930 µL) followed by addition of NMM (108 µL, 0.98 mmol, 4.00 eq). When NHS ester formation was completed, the prepared amine solution was added to the reaction mixture. The mixture was shaken for further 30 min at rt under nitrogen atmosphere. After complete conversion, the mixture was diluted with DCM (~50.0 mL) and washed with brine (~50.0 mL, 1×) acidified with citric acid. The aqueous phase was extracted with DCM (~50.0 mL, 3×). The combined organic phase was concentrated under reduced pressure. For the last step, the crude was dissolved in dry DCM/ TFE/ HOAc/ TIPS (65:20:10:5, 12.6 mL). The reaction mixture was stirred at rt under nitrogen atmosphere. After 1 h, complete conversion was confirmed by TLC ($UV_{254\ nm}$). The solvent was evaporated, and the remaining residue was purified by flash column chromatography (DCM·NH_3/ MeOH 9:1 (v/v)) to give compound **16** (~101 mg, ~0.15 mmol, ~60%) as pink solid.

TLC ($UV_{254\ nm}$): R_f = 0.13 (DCM/MeOH 9:1 + 0.2% DEA, v/v).

^{1}H-NMR (300 MHz, MeOD-d_4): δ = 7.28 (dd, ^3J(H,H) = 8.8 Hz, ^4J(H,H) = 1.9 Hz, 2H), 7.22 (dd, ^3J(H,H) = 8.8 Hz, ^4J(H,H) = 3.3 Hz, 2H), 4.65 (s, 1.2H), 4.62 (s, 0.8H), 3.53 (t, ^3J(H,H) = 6.1 Hz, 0.8H), 3.45-3.41 (m, 2H), 2.86 (t, ^3J(H,H) = 6.2 Hz, 1.2H), 2.58 (s, 6H), 1.47 (s, 6H) ppm.

^{13}C-NMR (125 MHz, MeOD-d_4): δ = 173.8 (*C*OO), 164.3 (C_q), 160.3 (C_q), 158.5 (C_q), 157.7 (C_q), 155.0 (C_q), 146.6 (C_q), 143.3 (C_q), 135.6 (C_q), 132.8 (C_q), 130.7 (2C; *C*H), 129.0 (C_q), 124.4 (C_q), 117.1 (2C; *C*H), 68.2 (*C*H_2), 45.7 (2C; *C*H_2), 20.0 (4C; *C*H_3) ppm.

^{19}F-NMR (282 MHz, $CDCl_3$): δ = -145.7 (dd, ^1J(B,F) = 32.2 Hz, 2F; BF_2) ppm.

HRMS-ESI (*m/z*): $[M + H]^+$ calcd for $C_{23}H_{26}BF_2I_2N_4O_2$: 693.0205; found: 693.0207.

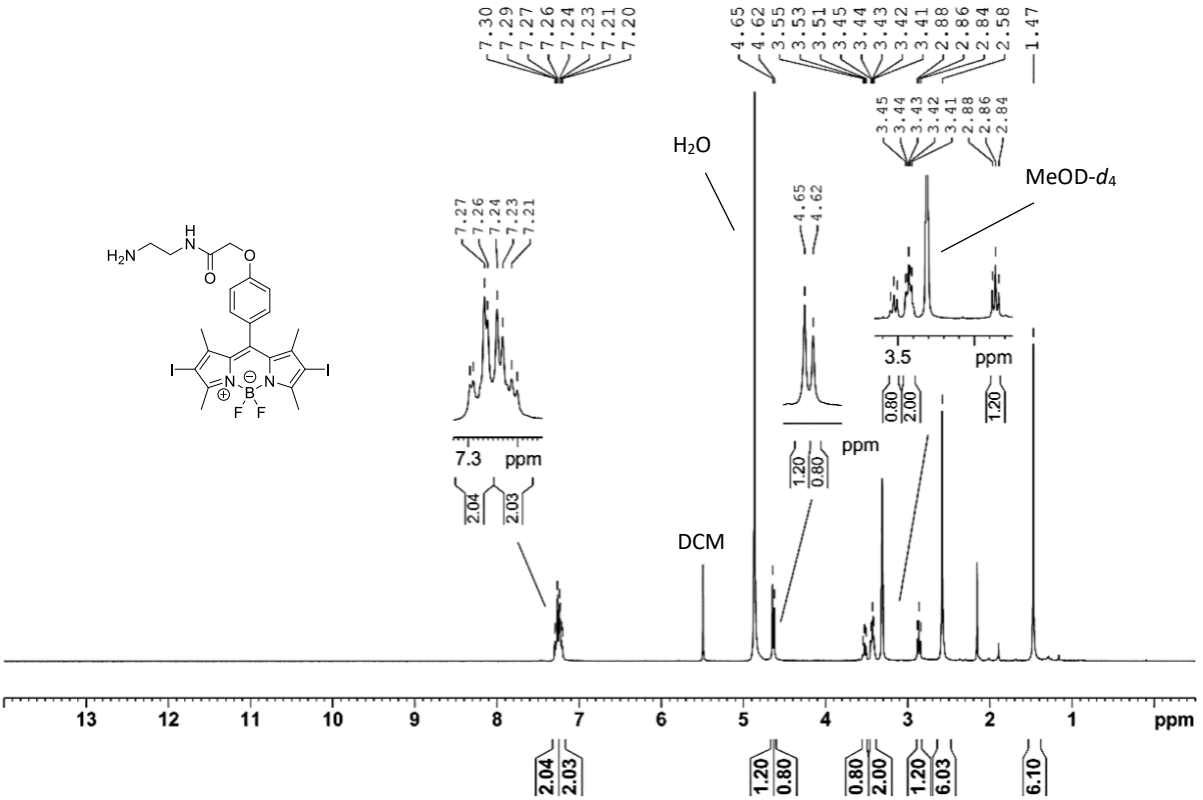

Figure S94: ^{1}H-NMR (300 MHz) spectrum of compound **16** in MeOD-d_4.

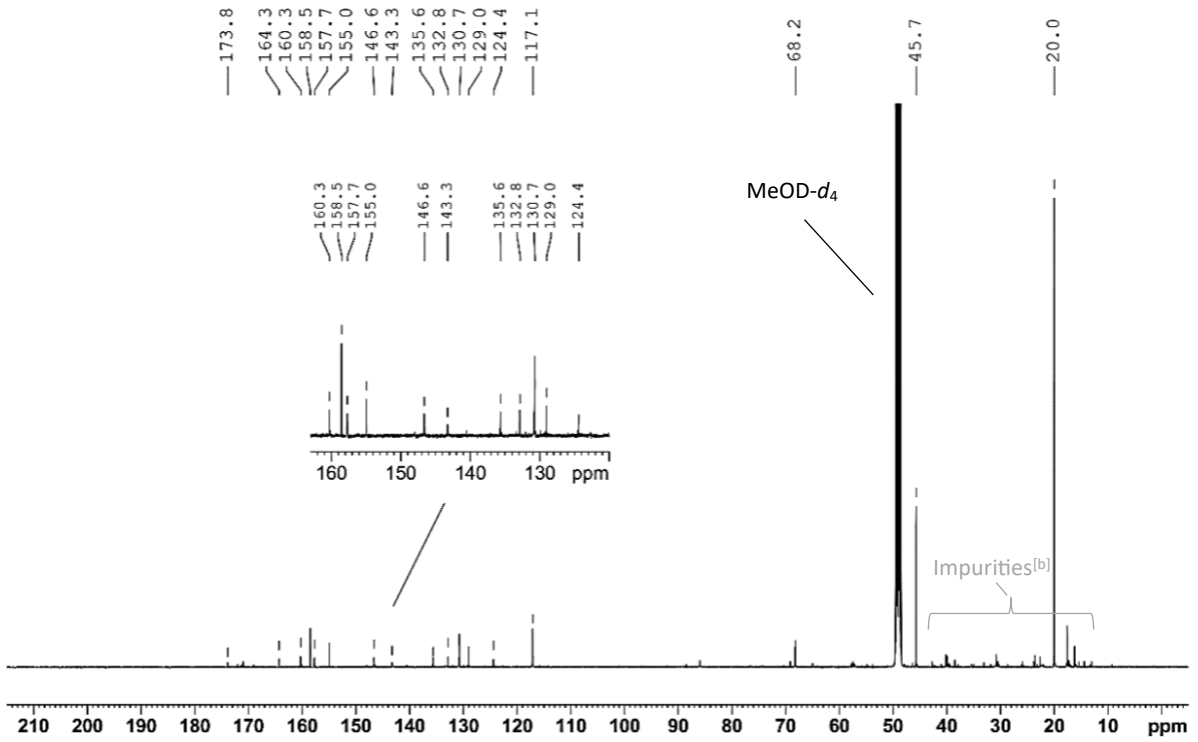

Figure S95: ^{13}C-NMR (125 MHz) spectrum of compound **16** in MeOD-d_4.

[b]The impurities visible in the ^{13}C-NMR spectra were not affecting the next synthesis step; however, they prevented informative 2D-NMR spectra.

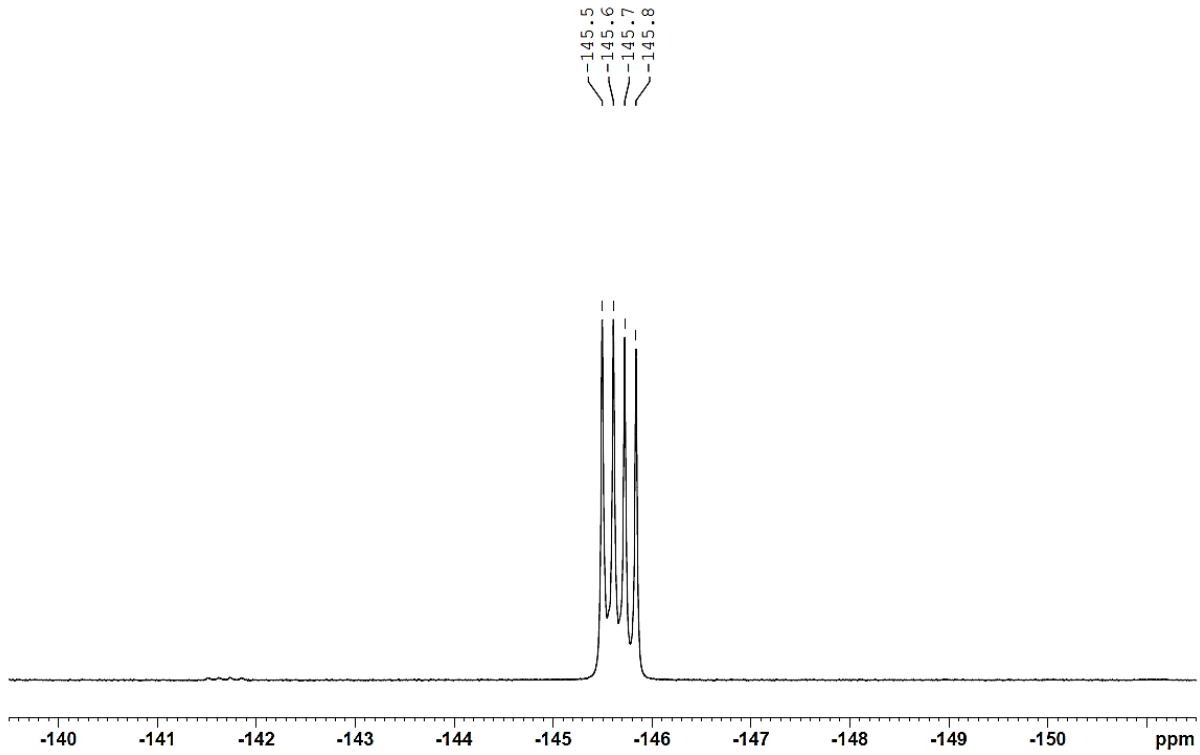

Figure S96: ^{19}F-NMR (282 MHz) spectrum of compound **16** in MeOD-d_4.

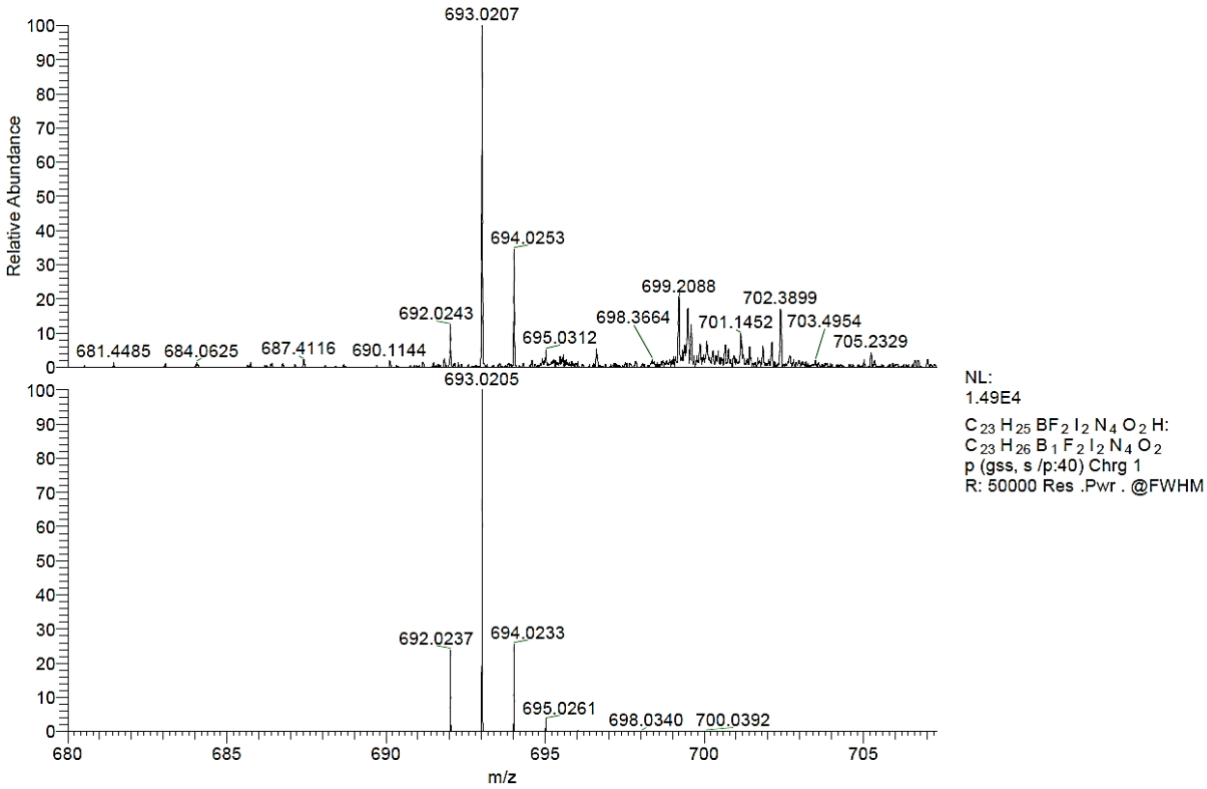

Figure S97: Measured (top) and calculated (bottom) HRMS-ESI spectrum of **16** in positive ion mode.

Long-linker BODIPY-CTZ Conjugate (5)

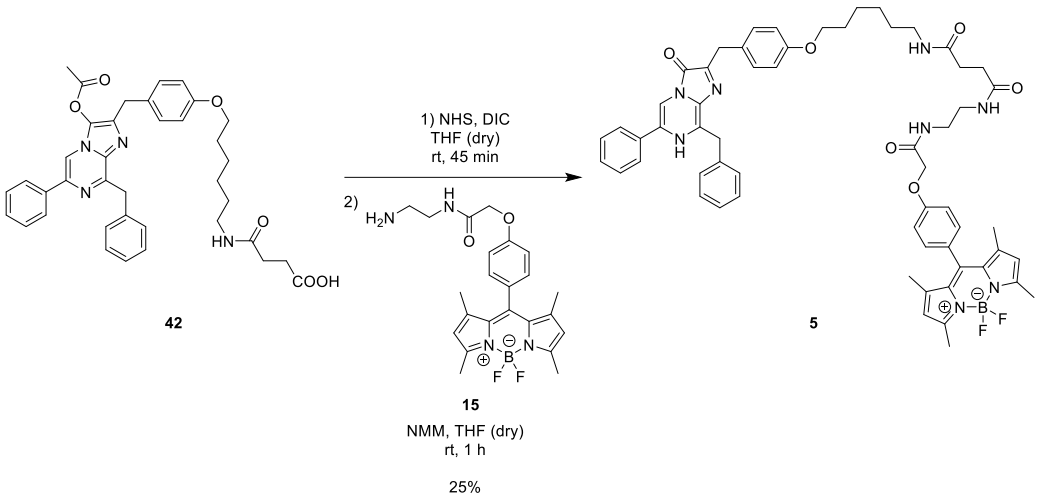

Scheme S19: Synthesis of long-linker BODIPY-CTZ conjugate **5**.

Coelenterazine **42** (50.0 mg, 77.0 µmol, 1.00 eq) was dissolved in dry THF (200 µL). NHS (11.1 mg, 96.0 µmol, 1.25 eq) and DIC (10.7 mg, 85.0 µmol, 1.10 eq) were added, and the mixture was shaken at rt in the dark under nitrogen atmosphere for 45 min. When successful NHS-ester formation was observed by TLC ($UV_{254\,nm}$), a solution of BODIPY **15** (33.9 mg, 77.0 µmol, 1.00 eq) and NMM (15.6 mg, 154 µmol, 2.00 eq) in dry THF (300 µL) was added to the reaction mixture. After 1 h, complete conversion was reached. The reaction mixture was diluted with DCM (~50.0 mL) and the organic phase was washed with distilled water (~50.0 mL, 2×). The organic phase was extracted with DCM (~50.0 mL, 1×) and the combined organic phases were washed with brine (~50.0 mL) and dried over $MgSO_4$. The solvent was removed under reduced pressure and the obtained crude was purified by flash column chromatography (DCM/MeOH, 0.5% → 1% → 2% → 3% → 4% → 5% → 10%, (v/v)) to yield the conjugate **5** (19.8 mg, 19.0 µmol, 25%) as an orange solid. Compound **5** was stored in the dark at -80 °C.

TLC ($UV_{254\,nm}$): R_f = 0.33 (DCM/MeOH 9:1, v/v).

^{1}H-NMR (500 MHz, MeOD-d_4): δ = 7.66 (s, 2H), 7.50 – 7.43 (m, 3H), 7.39 (d, ^3J(H,H) = 7.4 Hz, 2H), 7.29 (t, ^3J(H,H) = 7.6 Hz, 2H), 7.23 – 7.20 (m, 6H), 7.19 – 7.15 (m, 2H), 6.79 (d, ^3J(H,H) = 8.7 Hz, 2H), 6.01 (s, 2H), 4.56 (s, 2H), 4.40 (s, 2H), 4.10 (s, 2H), 3.90 (t, ^3J(H,H) = 6.3 Hz, 2H), 3.39 (t, ^3J(H,H) = 6.3 Hz, 2H), 3.15 (t, ^3J(H,H) = 6.3 Hz, 2H), 2.48 – 2.46 (m, 2H), 2.46 (s, 6H), 2.45 – 2.42 (m, 2H), 1.72 (quint, ^3J(H,H) = 7.1 Hz, 2H), 1.52 – 1.44 (m, 4H), 1.41 (s, 6H), 1.40 – 1.34 (m, 4H) ppm.

^{13}C-NMR (125 MHz, MeOD-d_4): δ = 175.3 (*C*ONH), 174.4 (*C*ONH), 171.1 (*C*ONH), 159.9 (2C; C_q), 159.9 (C_q), 159.2 (C_q), 156.5 (2C; C_q), 144.5 (2C; C_q), 143.3 (C_q), 132.9 (C_q), 132.9 (C_q), 130.8 (2C; *C*H), 130.8 (C_q), 130.7 (C_q), 130.7 (C_q), 130.7 (3C; *C*H), 130.5 (C_q), 130.1 (2C; *C*H), 129.8 (2C; *C*H), 129.7 (3C; *C*H), 129.3 (2C; C_q), 128.1 (C_q), 127.9 (*C*H), 126.4 (*C*H), 122.2 (*C*H), 122.2 (*C*H), 122.2 (*C*H), 116.8 (2C; *C*H), 115.5 (2C; *C*H), 68.8 (CH_2), 68.2 (CH_2), 40.4 (CH_2), 40.1 (CH_2), 39.9 (CH_2), 32.3 (CH_2), 32.1 (CH_2), 30.4 (CH_2), 30.3 (CH_2), 27.7 (CH_2), 26.9 (CH_2), 17.3 (CH_2), 17.1 (CH_2), 14.8 (2C; CH_3), 14.6 (2C; CH_3) ppm.

^{19}F-NMR (282 MHz, MeOD-d_4): δ = -147.0 (dd, ^1J(B,F) = 31.7 Hz, 2F; BF_2) ppm.

HRMS-ESI (*m/z*): $[M + H]^+$ calcd for $C_{59}H_{64}BF_2N_8O_6$: 1029.5014; found: 1029.5001.

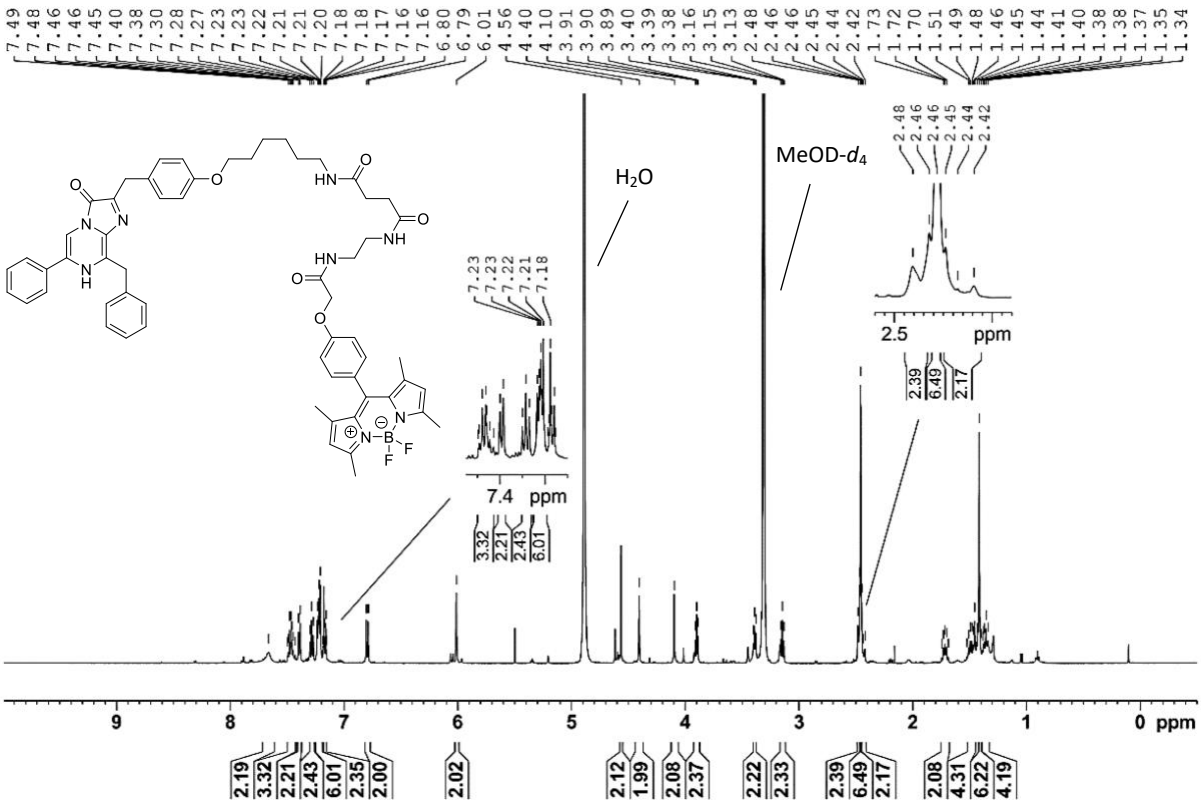

Figure S98: ^{1}H-NMR (500 MHz) spectrum of compound **5** in MeOD-d_4.

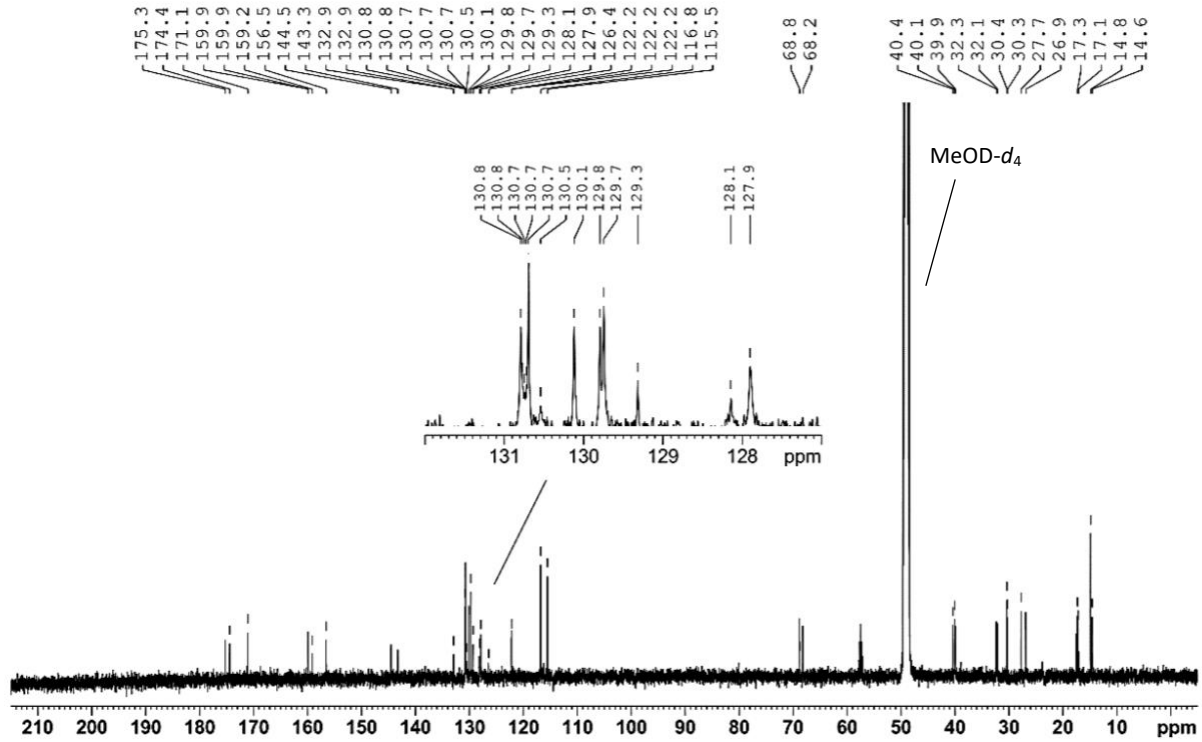

Figure S99: ^{13}C-NMR (125 MHz) spectrum of compound **5** in MeOD-d_4.

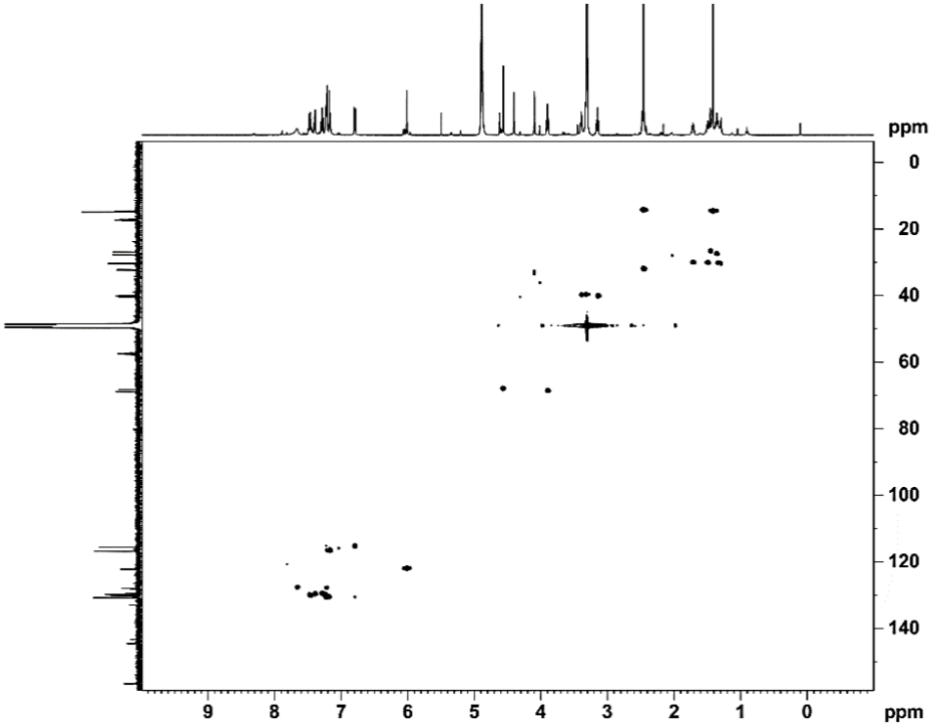

Figure S100: HSQC spectrum of compound **5** (^{1}H-NMR: 500 MHz, ^{13}C-NMR: 125 MHz, MeOD-d_4).

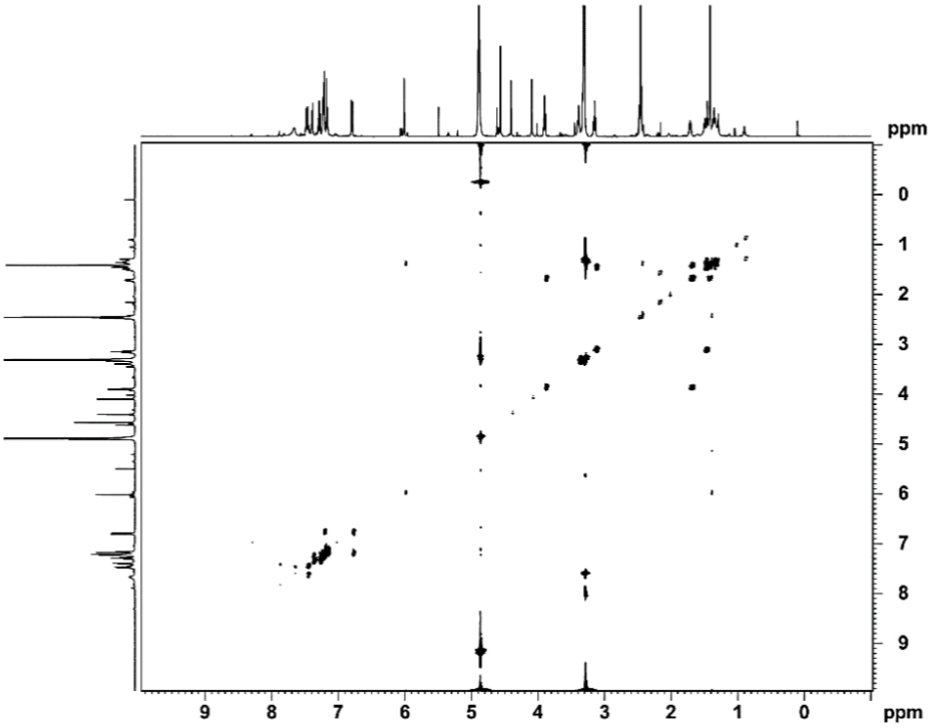

Figure S101: COSY spectrum of compound **5** (^{1}H-NMR: 500 MHz, MeOD-d_4).

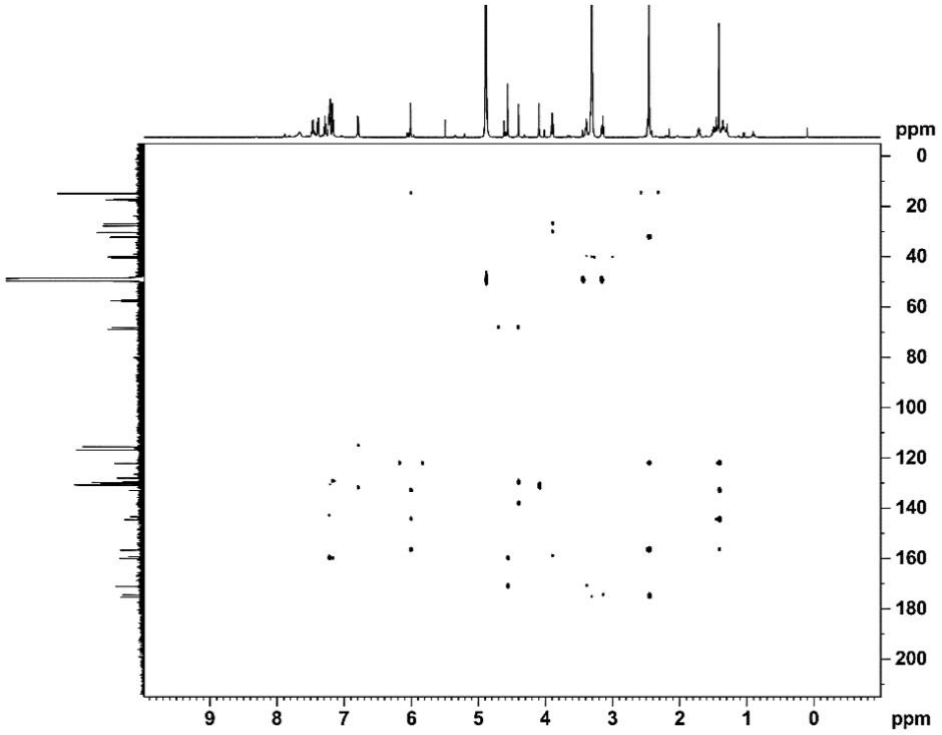

Figure S102: HMBC spectrum of compound **5** (^{1}H-NMR: 500 MHz, ^{13}C-NMR: 125 MHz, MeOD-d_4).

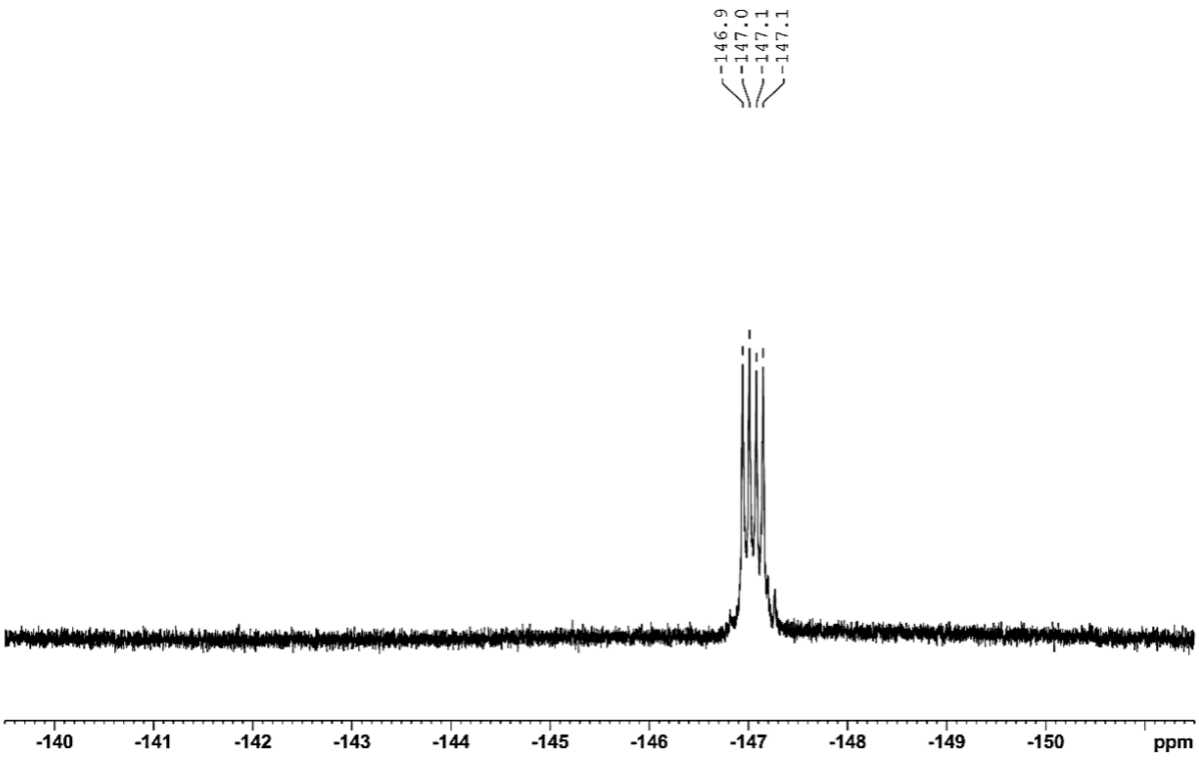

Figure S103: ^{19}F-NMR spectrum of compound **5** in MeOD-d_4 (282 MHz).

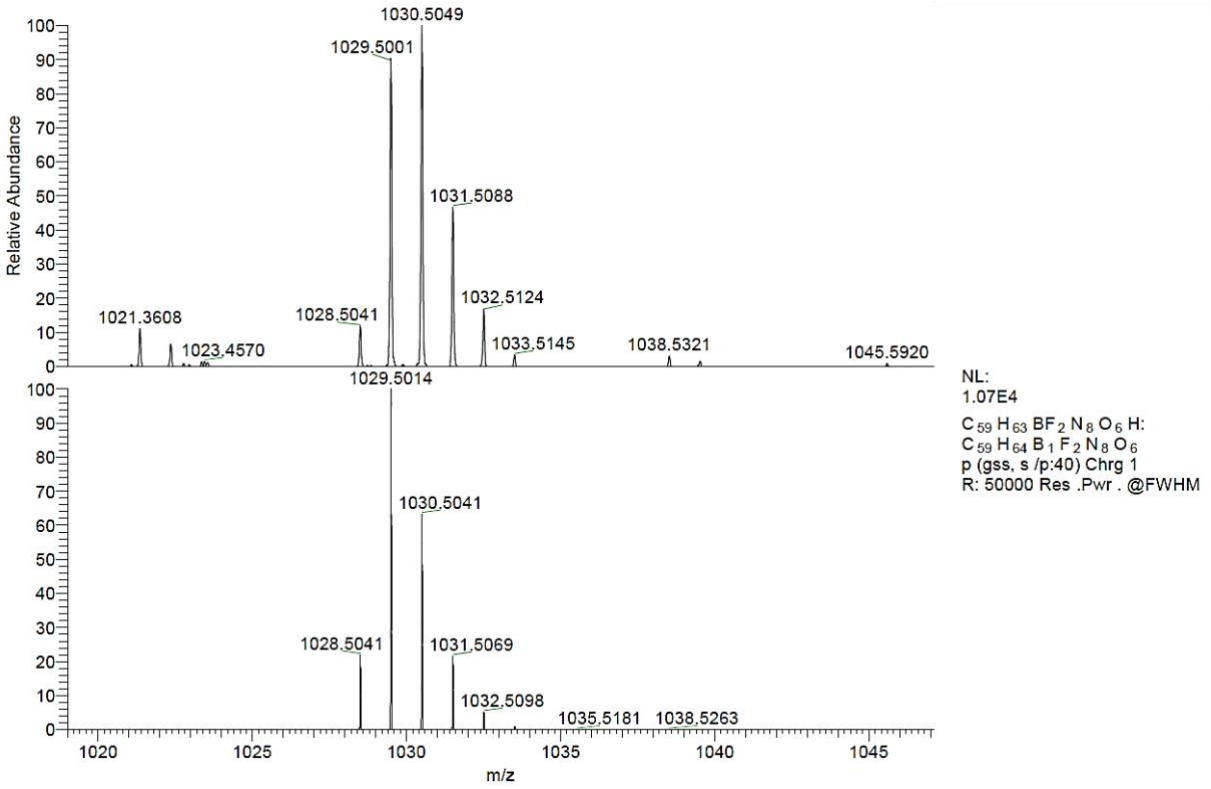

Figure S104: Measured (top) and calculated (bottom) HRMS-ESI spectrum of **5** in positive ion mode.

Long-linker 2I-BODIPY-CTZ Conjugate (6)

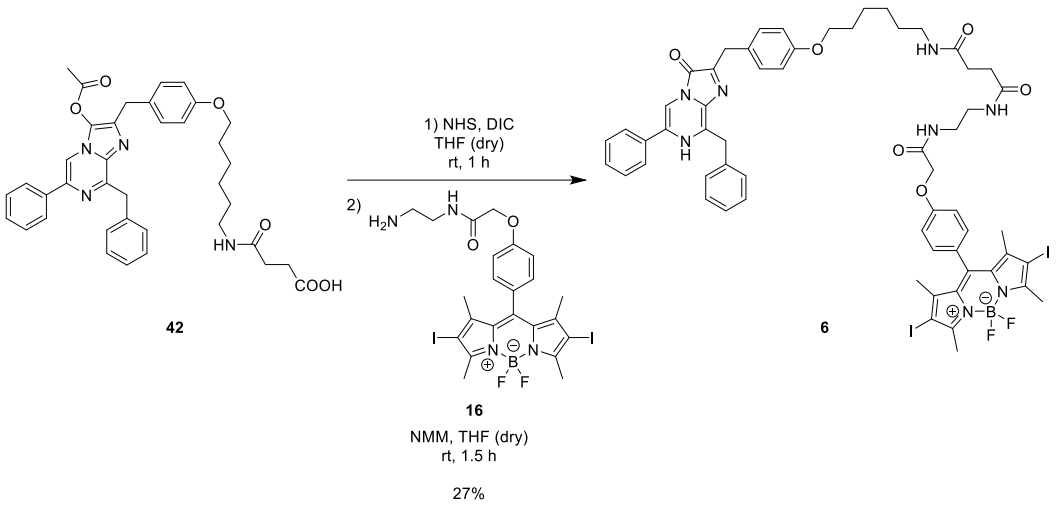

Scheme S20: Synthesis of long-linker 2I-BODIPY-CTZ conjugate **6**.

Coelenterazine **42** (50.0 mg, 77.0 µmol, 1.00 eq) was dissolved in dry THF (200 µL). NHS (17.7 mg, 154 µmol, 2.00 eq) and DIC (10.7 mg, 85.0 µmol, 1.10 eq) were added and the mixture was shaken at rt in the dark under nitrogen atmosphere for 1 h. When successful NHS-ester formation was observed by TLC ($UV_{254\ nm}$), a solution of BODIPY **16** (53.3 mg, 77.0 µmol, 1.00 eq) and NMM (15.6 mg, 154 µmol, 2.00 eq) in dry THF (300 µL) was added to the reaction mixture. After 1 h, complete conversion was reached. The reaction mixture was diluted with DCM (~50.0 mL), and the organic phase was washed with distilled water (~50.0 mL, 2×). The organic phase was extracted with DCM (~50.0 mL, 1×) and the combined organic phases were dried over $MgSO_4$. The solvent was removed under reduced pressure and the obtained crude was purified by flash column chromatography (DCM/MeOH, 0.5% ⟶ 1% ⟶ 2% ⟶ 3% ⟶ 4% ⟶ 10%, (v/v)) to yield the conjugate **6** (26.2 mg, 21.0 µmol, 27%) as pink solid. Compound **6** was stored in the dark at -80 °C.

TLC ($UV_{254\ nm}$): R_f = 0.49 (DCM/MeOH 9:1, v/v).

^{1}H-NMR (500 MHz, MeOD-d_4): δ = 7.64 (s, 2H), 7.49 – 7.45 (m, 3H), 7.39 (d, ^3J(H,H) = 7.4 Hz, 2H), 7.28 (t, ^3J(H,H) = 7.7 Hz, 2H), 7.24 – 7.19 (m, 8H), 6.79 (dt, ^3J(H,H) = 8.7 Hz, , ^4J(H,H) = 2.4 Hz, 2H), 4.59 (s, 2H), 4.40 (s, 2H), 4.09 (s, 2H), 3.89 (t, ^3J(H,H) = 6.4 Hz, 2H), 3.40 (t, ^3J(H,H) = 5.3 Hz, 2H), 3.14 (t, ^3J(H,H) = 7.0 Hz, 2H), 2.55 – 2.53 (m, 6H), 2.47 – 2.45 (m, 4H), 1.72 (quint, ^3J(H,H) = 7.1 Hz, 2H), 1.52 – 1.44 (m, 4H), 1.43 (s, 6H), 1.38 – 1.29 (m, 4H) ppm.

^{13}C-NMR (125 MHz, MeOD-d_4): δ = 175.3 (*C*ONH), 174.4 (*C*ONH), 171.0 (*C*ONH), 160.3 (2C; C_q), 159.1 (2C; C_q), 157.7 (2C; C_q), 146.6 (2C; C_q), 143.2 (C_q), 138.0 (2C; C_q), 132.8 (2C; C_q), 131.7 (C_q), 130.8 (2C; *C*H), 130.7 (3C; *C*H), 130.2 (3C; *C*H), 129.8 (4C; *C*H), 128.9 (2C; C_q), 128.2 (2C; C_q), 127.9 (3C; *C*H), 117.1 (2C; *C*H), 115.5 (2C; *C*H), 85.9 (2C; C_q), 68.8 (CH_2), 68.2 (CH_2), 40.4 (CH_2), 40.1 (CH_2), 39.9 (CH_2), 32.3 (CH_2), 32.1 (2C; CH_2), 30.4 (CH_2), 30.3 (2C; CH_2), 27.7 (CH_2), 26.9 (CH_2), 17.6 (2C; CH_3), 16.2 (2C; CH_3) ppm.

^{19}F-NMR (282 MHz, MeOD-d_4): δ = -146.5 (dd, ^1J(B,F) = 31.7 Hz, 2F; BF_2) ppm.

HRMS-ESI (*m/z*): $[M + H]^+$ calcd for $C_{59}H_{62}BF_2I_2N_8O_6$: 1281.2947; found: 1281.2979.

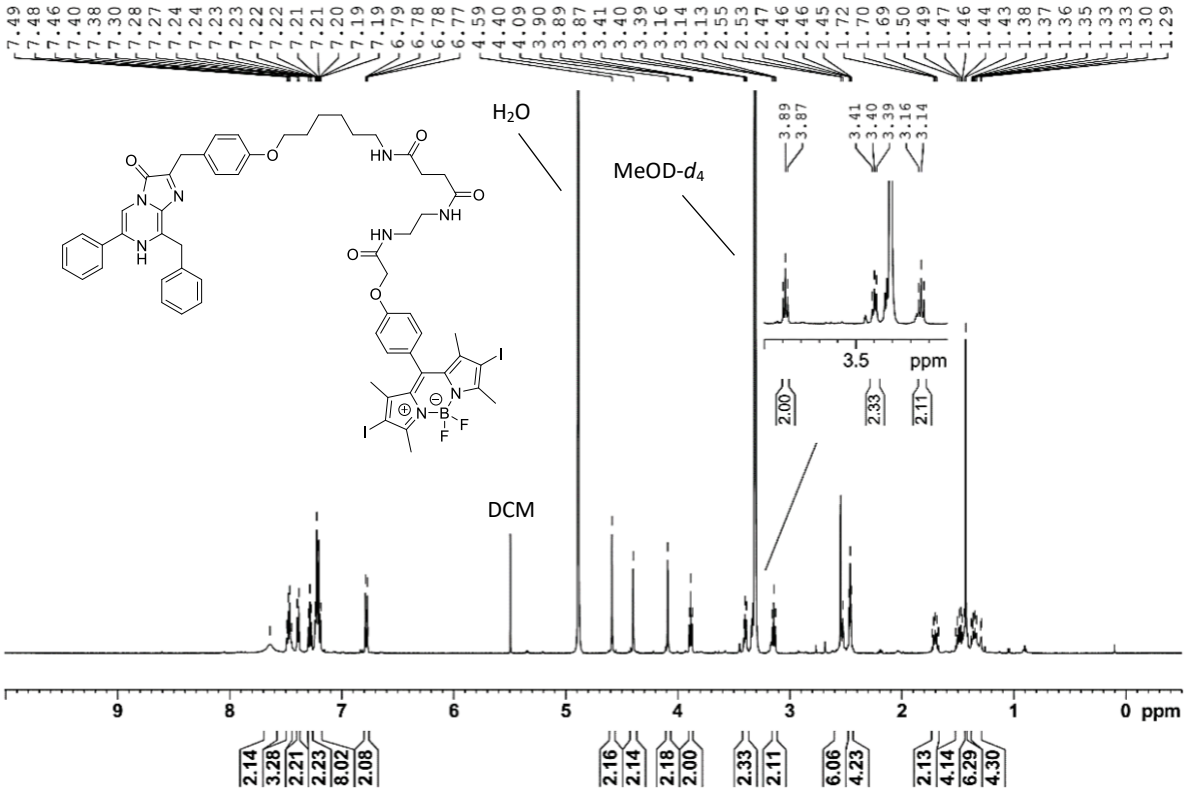

Figure S105: ^{1}H-NMR (500 MHz) spectrum of compound **6** in MeOD-d_4.

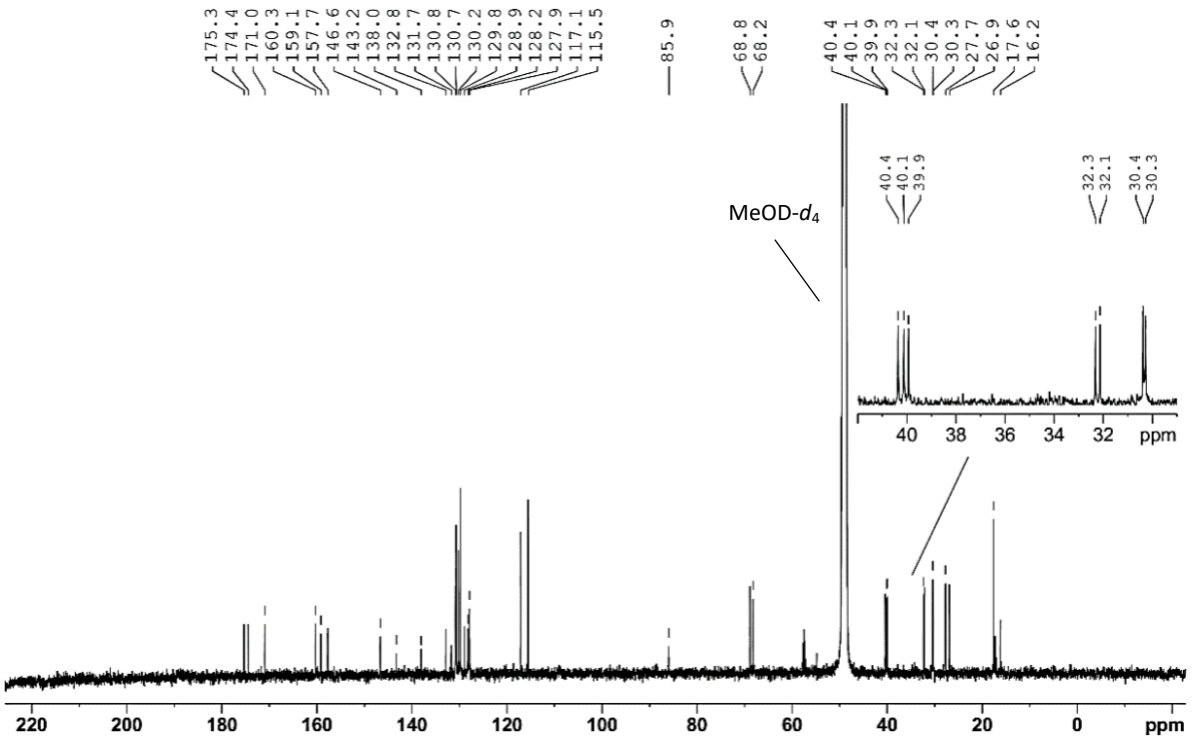

Figure S106: ^{13}C-NMR (125 MHz) spectrum of compound **6** in MeOD-d_4.

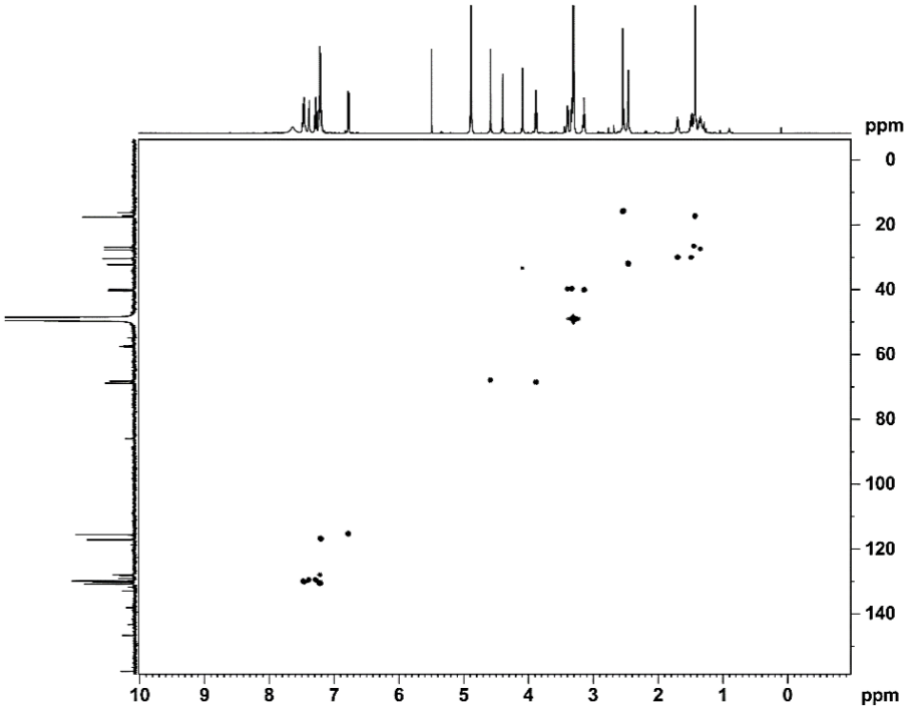

Figure S107: HSQC spectrum of compound **6** (^{1}H-NMR: 500 MHz, ^{13}C-NMR: 125 MHz, MeOD-d_4).

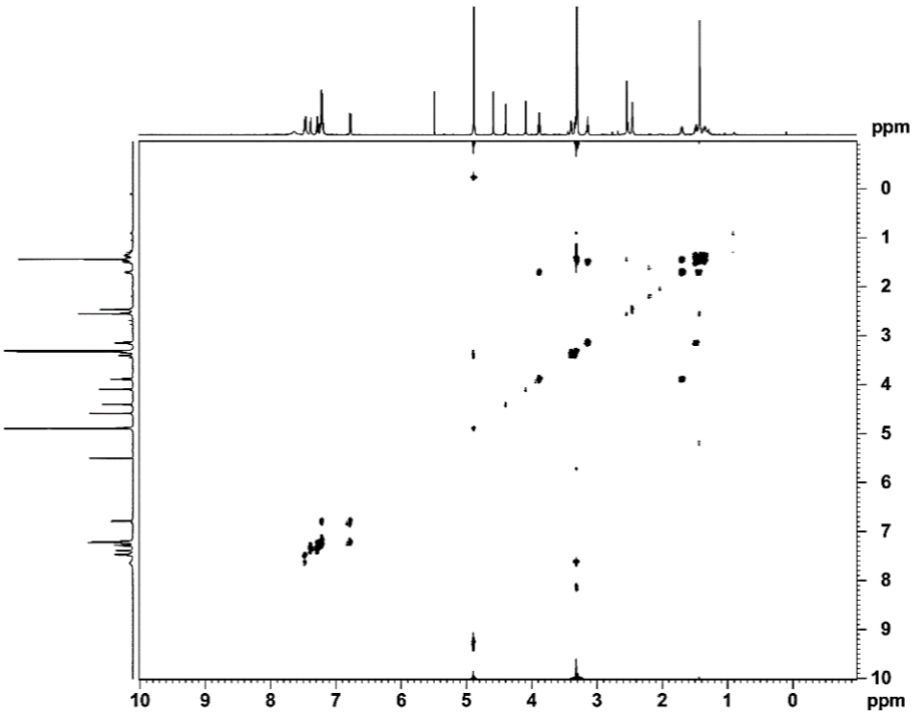

Figure S108: COSY spectrum of compound **6** (^{1}H-NMR: 500 MHz, MeOD-d_4).

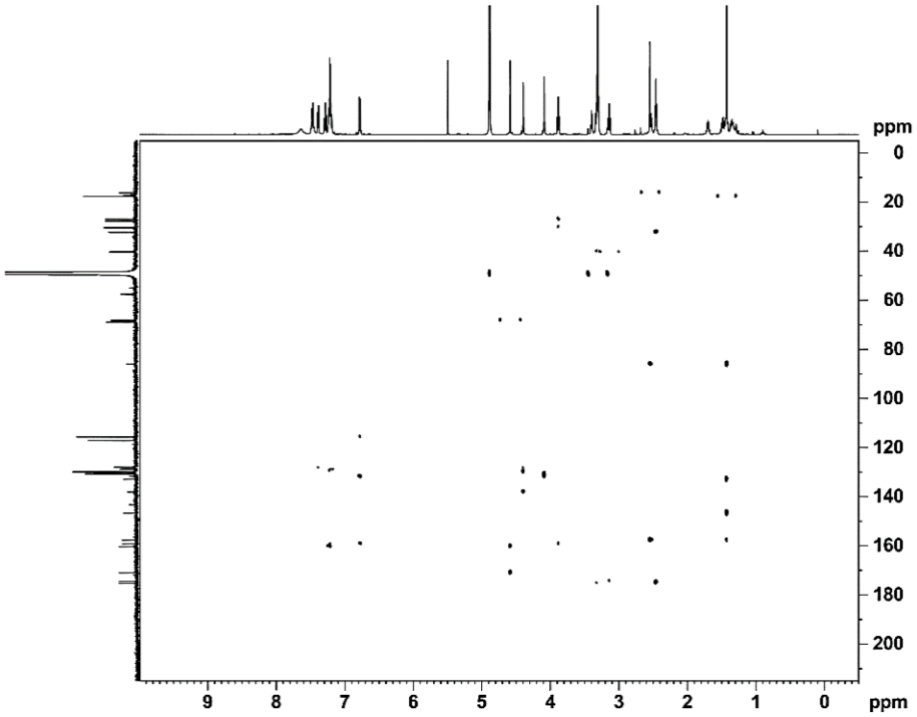

Figure S109: HMBC spectrum of compound **6** (^{1}H-NMR: 500 MHz, ^{13}C-NMR: 125 MHz, MeOD-d_4).

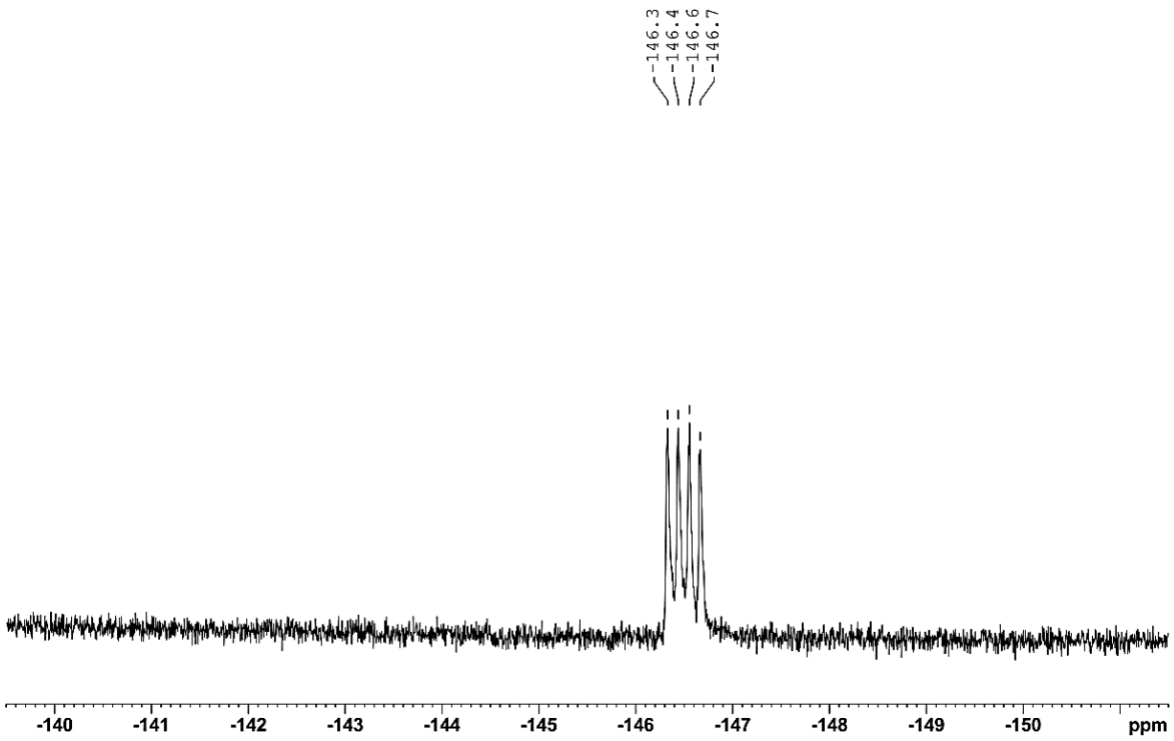

Figure S110: ^{19}F-NMR spectrum of compound **6** in MeOD-d_4 (282 MHz).

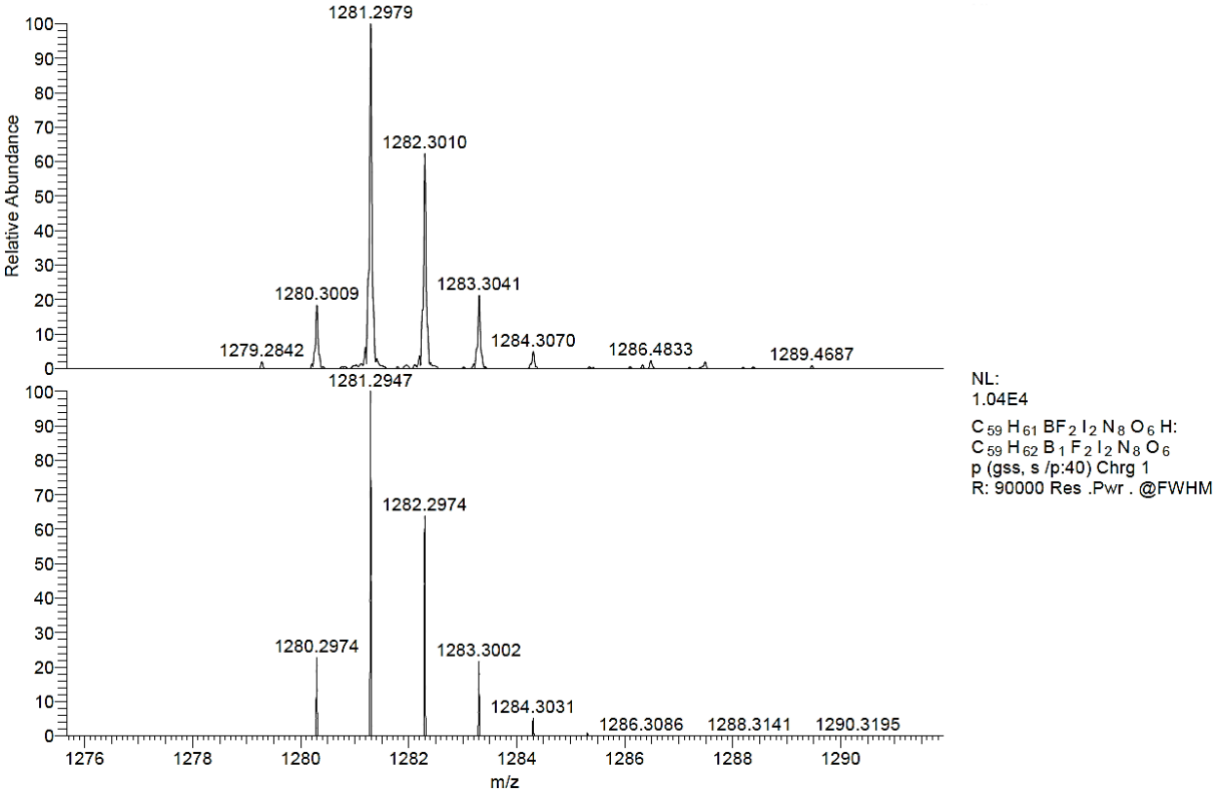

Figure S111: Measured (top) and calculated (bottom) HRMS-ESI spectrum of **6** in positive ion mode.

L-Tyrosine ethyl ester (49)

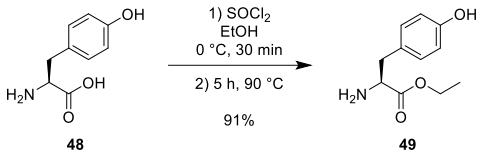

Scheme S21: Synthesis of *L*-tyrosine ethyl ester (**49**).

Adapted from the procedure of Moshikur *et al*.[36], *L*-tyrosine (**48**, 400 mg, 2.21 mmol, 1.00 eq) was suspended in absolute EtOH (4.50 mL). The suspension was cooled to 0 °C and thionyl chloride (400 µL, 5.53 mmol, 2.50 eq) was added over 30 min at 0 °C, leading to a clear solution. The reaction mixture was allowed to warm to rt and then heated to 90 °C to further react for 5 h. The reaction mixture was poured in distilled water/ EtOAc (1:1, ~100 mL) and the aqueous phase was extracted with EtOAc (~50.0 mL, 3×). The organic phase was washed with brine (50.0 mL, 1×), dried over $MgSO_4$ and concentrated under reduced pressure. The crude was purified by flash column chromatography (10% MeOH in DCM) to yield **49** (421 mg, 2.01 mmol, 91%) as colourless solid. The characterization is in agreement with the literature.[36]

TLC ($UV_{254\ nm}$): R_f = 0.39 (DCM/MeOH 9:1, v/v).

^{1}H-NMR (500 MHz, $CDCl_3$): δ = 6.99 (dt, ^3J(H,H) = 8.4 Hz, ^4J(H,H) = 2.4 Hz, 2H), 6.67 (dt, ^3J(H,H) = 8.4 Hz, ^4J(H,H) = 2.4 Hz, 2H), 4.18 (q, ^3J(H,H) = 7.0 Hz, 2H), 3.70 (dd, ^3J(H,H) = 7.7 Hz, ^3J(H,H) = 5.2 Hz, 1H), 3.46 (s (br), 2H), 3.03 (dd, ^2J(H,H) = 13.8 Hz, ^3J(H,H) = 5.2 Hz, 1H), 2.82 (dd, ^2J(H,H) = 13.8 Hz, ^3J(H,H) = 7.7 Hz, 1H), 1.26 (s, 3H) ppm.

^{13}C-NMR (125 MHz, $CDCl_3$): δ = 175.0 (*C*OO), 155.5 (C_qOH), 130.5 (2C; *C*H), 128.0 (C_q), 115.9 (2C; *C*H), 61.3 (CH_2), 55.7 (*C*H), 39.9 (*C*H), 14.3 (CH_3) ppm.

HRMS-ESI (*m/z*): $[M + H]^+$ calcd for $C_{11}H_{16}NO_3$: 210.1125; found: 210.1120.

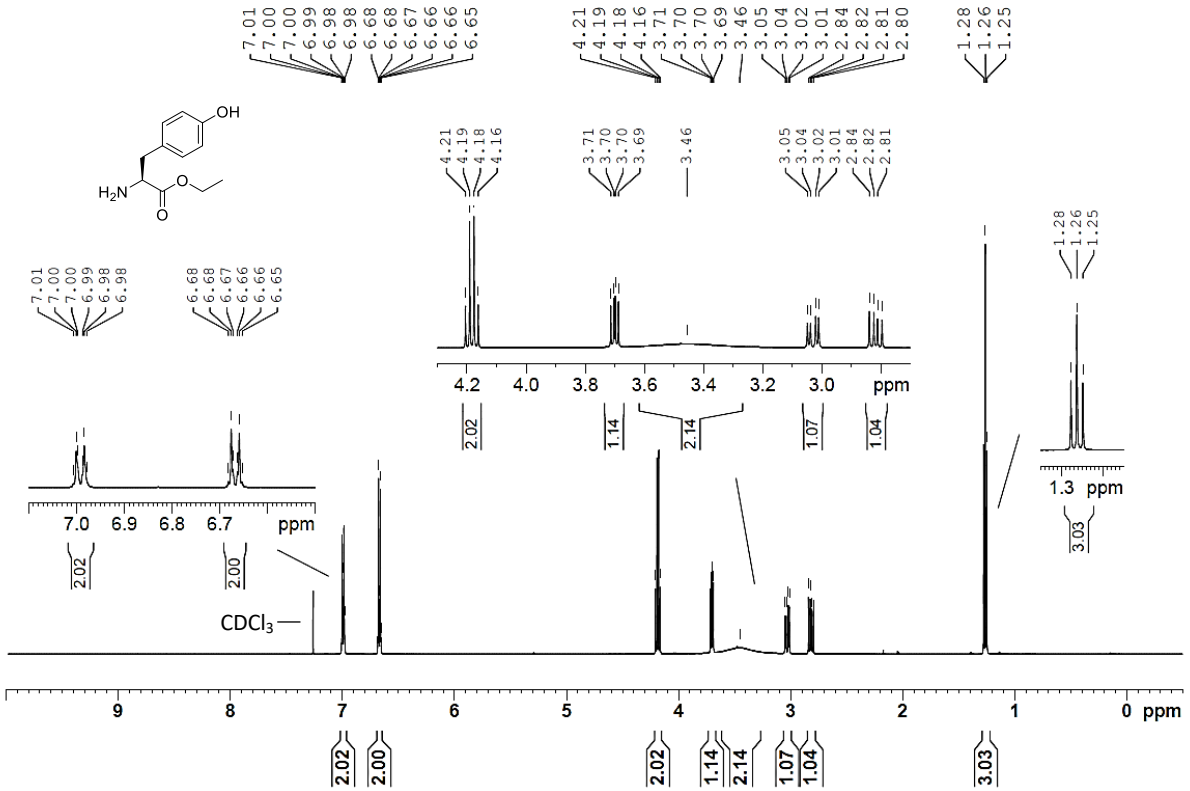

Figure S112: ^{1}H-NMR (500 MHz) spectrum of compound **49** in $CDCl_3$.

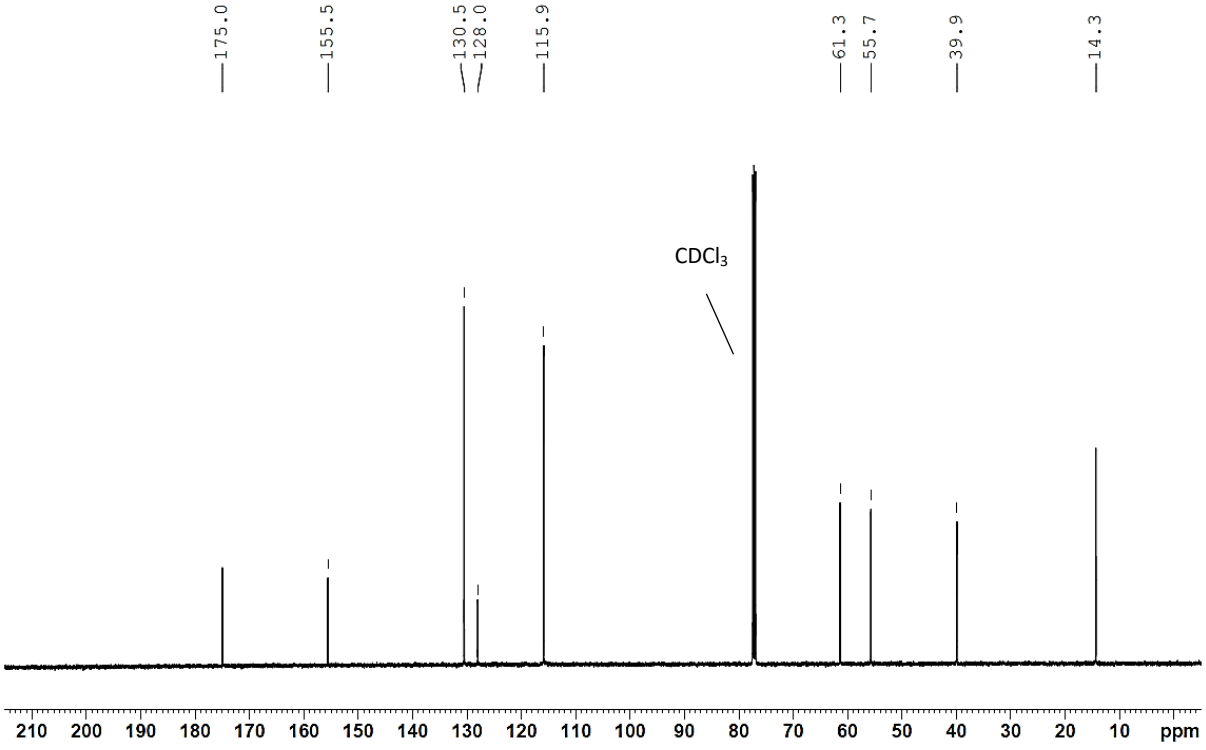

Figure S113: ^{13}C-NMR (125 MHz) spectrum of compound **49** in $CDCl_3$.

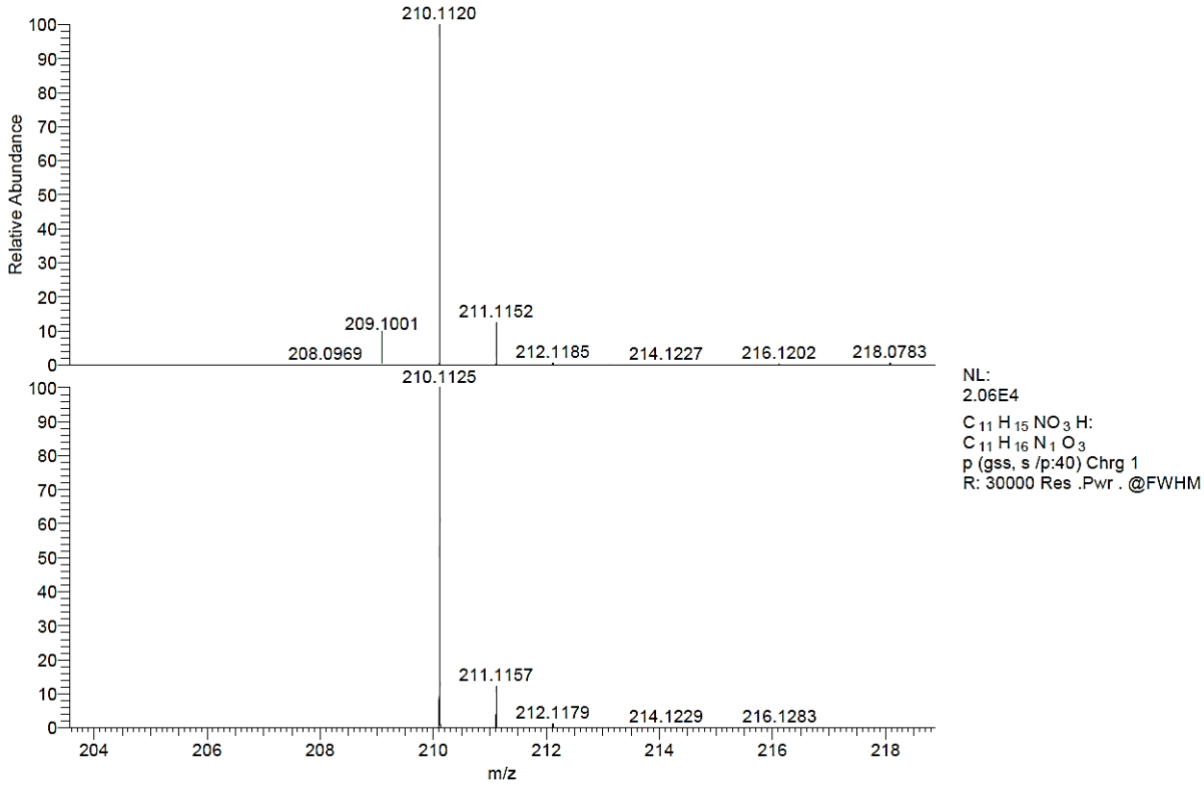

Figure S114: Measured (top) and calculated (bottom) HRMS-ESI spectrum of **49** in positive ion mode.

Ethyl (*tert*-butoxycarbonyl)-*L*-tyrosinate (50)

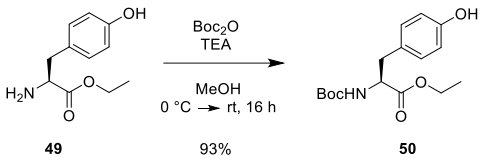

Scheme S22: Synthesis of ethyl (*tert*-butoxycarbonyl)-*L*-tyrosinate (**50**).

Based on a procedure of Bae *et al.*[37], *L*-tyrosine ethyl ester (**49**, 2.00 g, 9.56 mmol, 1.00 eq) was dissolved in MeOH (18.0 mL), the solution was cooled to 0°C and TEA (1.34 mL, 9.56 mmol, 1.00 eq) was added followed by the dropwise addition of a solution of Boc_2O (2,29 g, 10.5 mmol, 1.10 eq) in MeOH (4.00 mL). The reaction mixture was allowed to warm to rt and stirred for 16 h. After full conversion of the starting material, the reaction mixture was evaporated to dryness and the residue was dissolved in distilled water/ EtOAc (~200 mL, 1:1). The aqueous phase was extracted with EtOAc (~200 mL, 3×). Afterwards, the organic phase was washed with distilled water (~200 mL, 2×), brine (~200 mL, 1 ×) and dried over Na_2SO_4. The solvent was removed under reduced pressure and the crude was purified by flash column chromatography (*n*-pentane/EtOAc 4:1 → 2:1 (v/v)) to give the desired product **50** (2.76 g, 8.92 mmol, 93%) as white solid.

TLC (cerium molybdate developer): R_f = 0.38 (*n*-pentane/EtOAc 2:1, v/v).

^{1}H-NMR (300 MHz, $CDCl_3$): δ = 6.97 (d, ^3J(H,H) = 8.29 Hz, 2H), 6.72 (d, ^3J(H,H) = 8.29 Hz, 2H), 5.01 (d, ^3J(H,H) = 7.67 Hz, 1H), 4.51 (m, 1H), 4.16 (q, ^3J(H,H) = 6.92 Hz, 2H), 3.00 (m, 2H), 1.42 (s, 9H), 1.25 (t, ^3J(H,H) = 6.92 Hz 3H) ppm.

^{13}C-NMR (125 MHz, $CDCl_3$): δ = 172.3 (O-*C*=O), 155.4 (O-*C*=O), 155.2 (*C*-OH), 130.6 (2C; *C*H), 127.8 (C_q), 115.6 (2C; *C*H), 80.2 (C_q), 61.6 (CH_2), 54.8 (*C*H), 37.8 (CH_2), 28.4 (3C; CH_3), 14.3 (CH_3) ppm.

HRMS-ESI (*m/z*): $[M - H]^-$ calcd for $C_{16}H_{22}NO_5$: 308.1503; found: 308.1500.

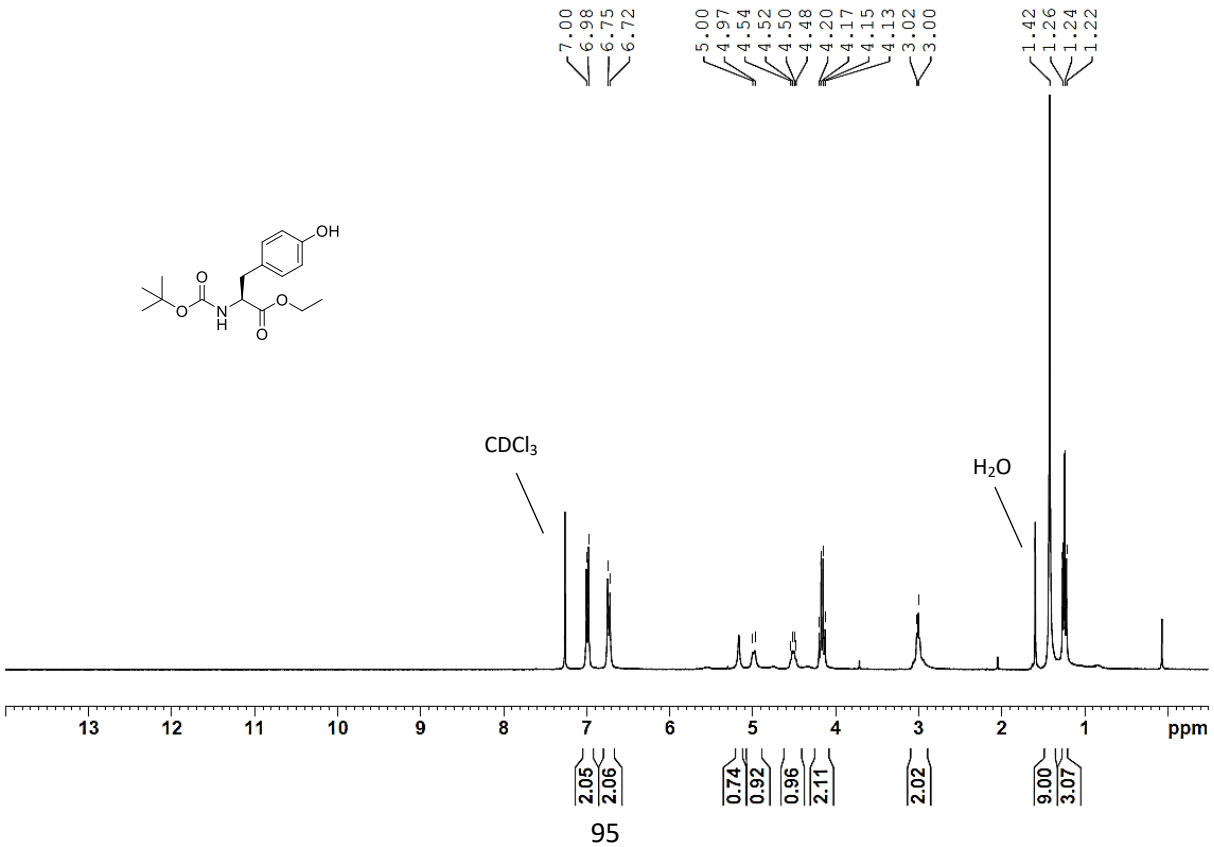

Figure S115: ^{1}H-NMR (300 MHz) spectrum of compound **50** in $CDCl_3$.

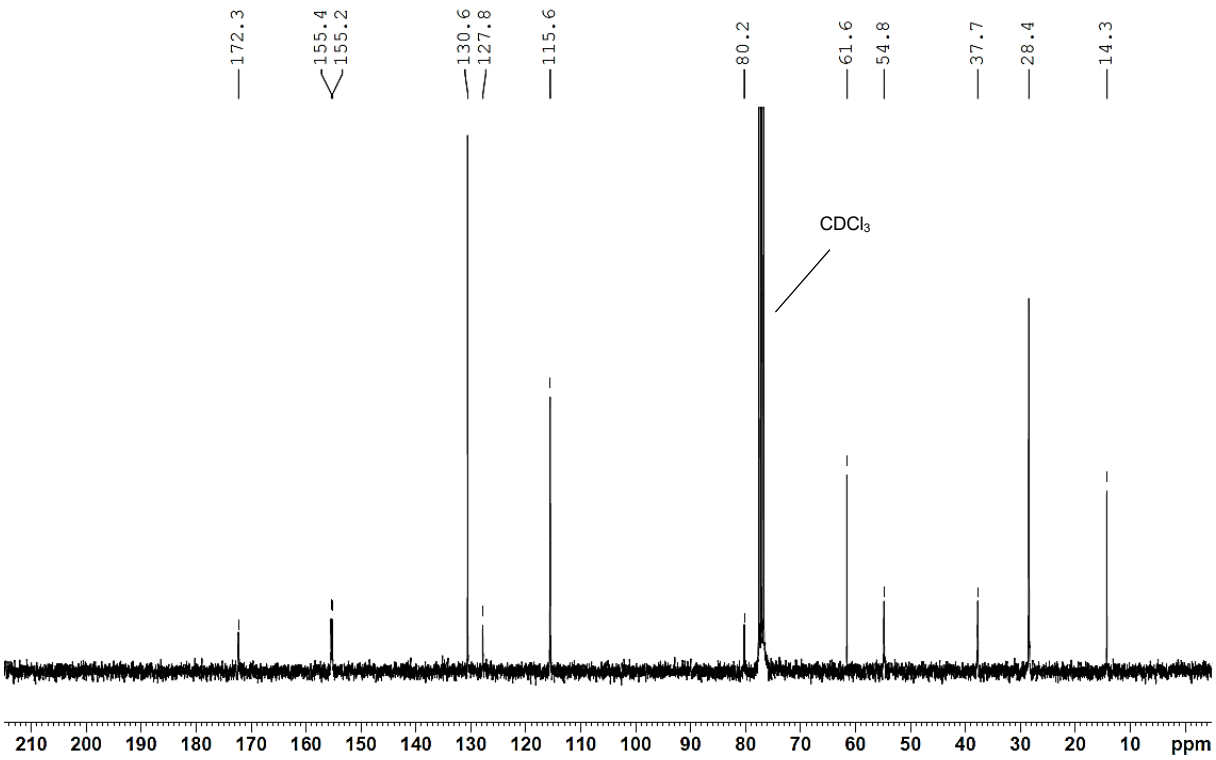

Figure S116: ^{13}C-NMR (125 MHz) spectrum of compound **50** in $CDCl_3$.

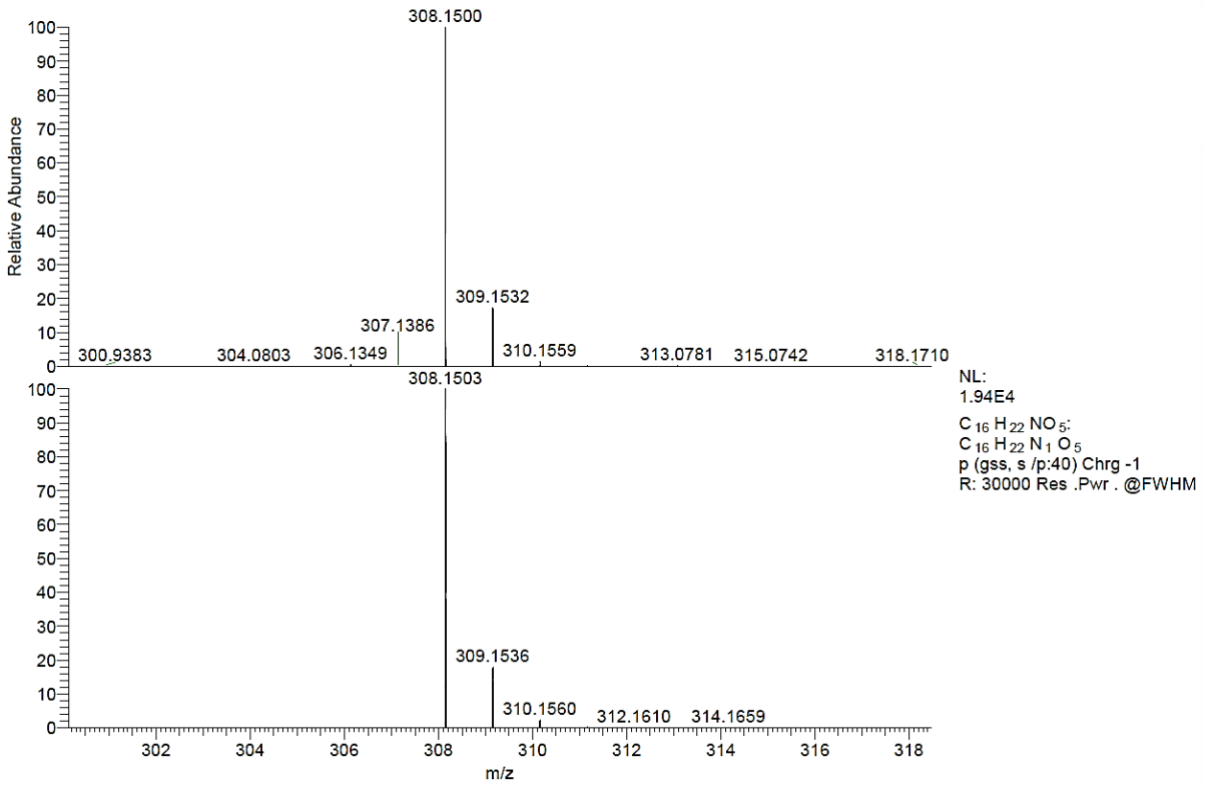

Figure S117: Measured (top) and calculated (bottom) HRMS-ESI spectrum of **50** in negative ion mode.

Benzyl 6-bromohexanoate (53)

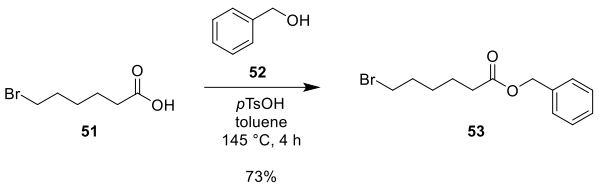

Scheme S23: Synthesis of benzyl 6-bromohexanoate (**53**).

Following the procedure of Li *et al.*[38], 6-bromohexanoic acid (**51**, 709 µL, 5.13 mmol, 1.00 eq), benzyl alcohol (**52**, 587 µL, 5.64 mmol, 1.10 eq), *p*-toluenesulfonic acid (*p*TsOH, 97.6 mg, 0.51 mmol, 0.10 eq) and toluene (5.50 mL) were added in a flask. A Dean-Stark apparatus was connected to the flask and the mixture was heated to 145 °C to reflux for 4 h. The reaction mixture was cooled to rt and concentrated under reduced pressure. The obtained crude was purified by flash column chromatography (*n*-pentane/ EtOAc 50:1 → 25:1) to yield the product **53** (1.07 g, 3.75 mmol, 73%) as a colourless liquid. The characterization is in agreement with the literature.[39]

TLC (permanganate developer): R_f = 0.17 (*n*-pentane/ EtOAc 50:1, v/v).

^{1}H-NMR (300 MHz, $CDCl_3$): δ = 7.40-7.30 (m, 5H), 5.12 (s, 2H), 3.39 (t, ^3J(H,H) = 6.7 Hz, 2H), 2.38 (t, ^3J(H,H) = 7.5 Hz, 2H), 1.87 (qi, ^3J(H,H) = 7.7 Hz, 2H), 1.68 (qi, ^3J(H,H) = 7.9 Hz, 2H), 1.52-1.42 (m, 2H) ppm.

^{13}C-NMR (75 MHz, $CDCl_3$): δ = 173.4 (*C*OO), 136.2 (C_q), 128.7 (2C; *C*H), 128.4 (3C; *C*H), 66.3 (CH_2), 34.2 (CH_2), 33.6 (CH_2), 32.5 (CH_2), 27.8 (CH_2), 24.2 (CH_2) ppm.

HRMS-EI (*m/z*): [M] calcd for $C_{13}H_{17}BrO_2$: 284.04119; found: 284.04059.

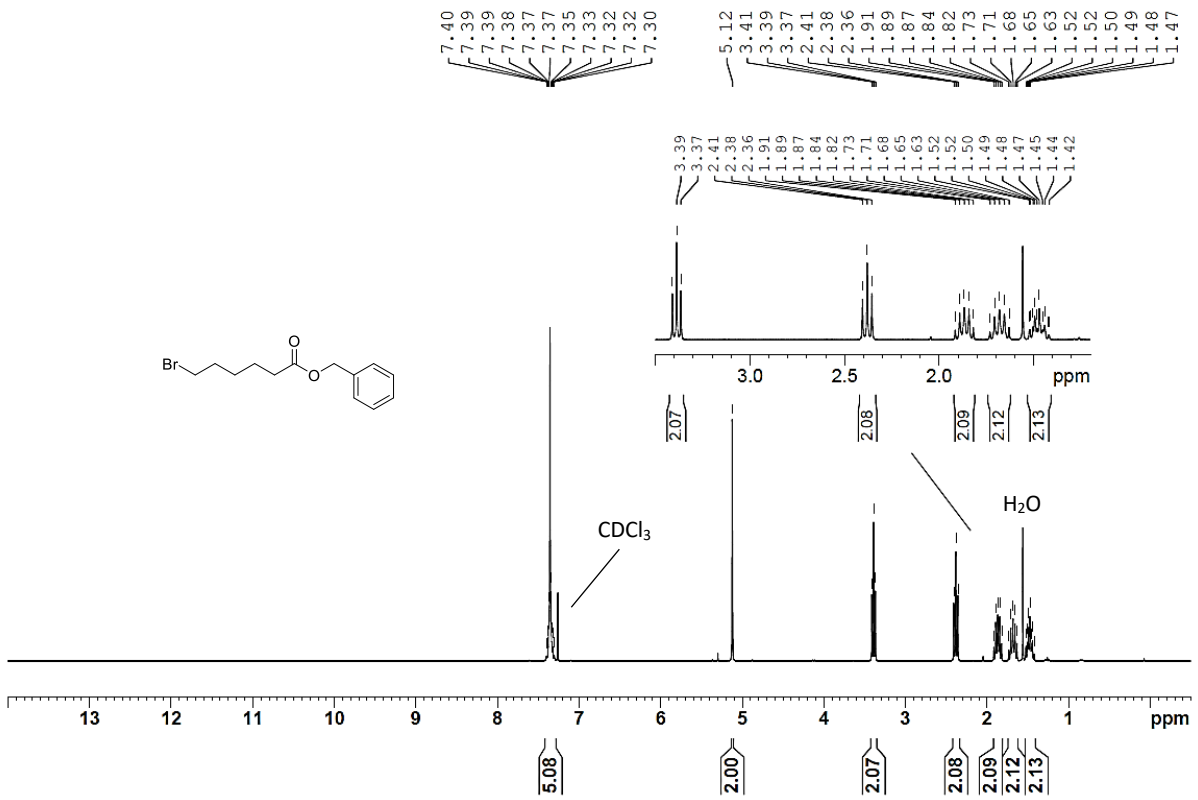

Figure S118: ^{1}H-NMR (300 MHz) spectrum of compound **53** in $CDCl_3$.

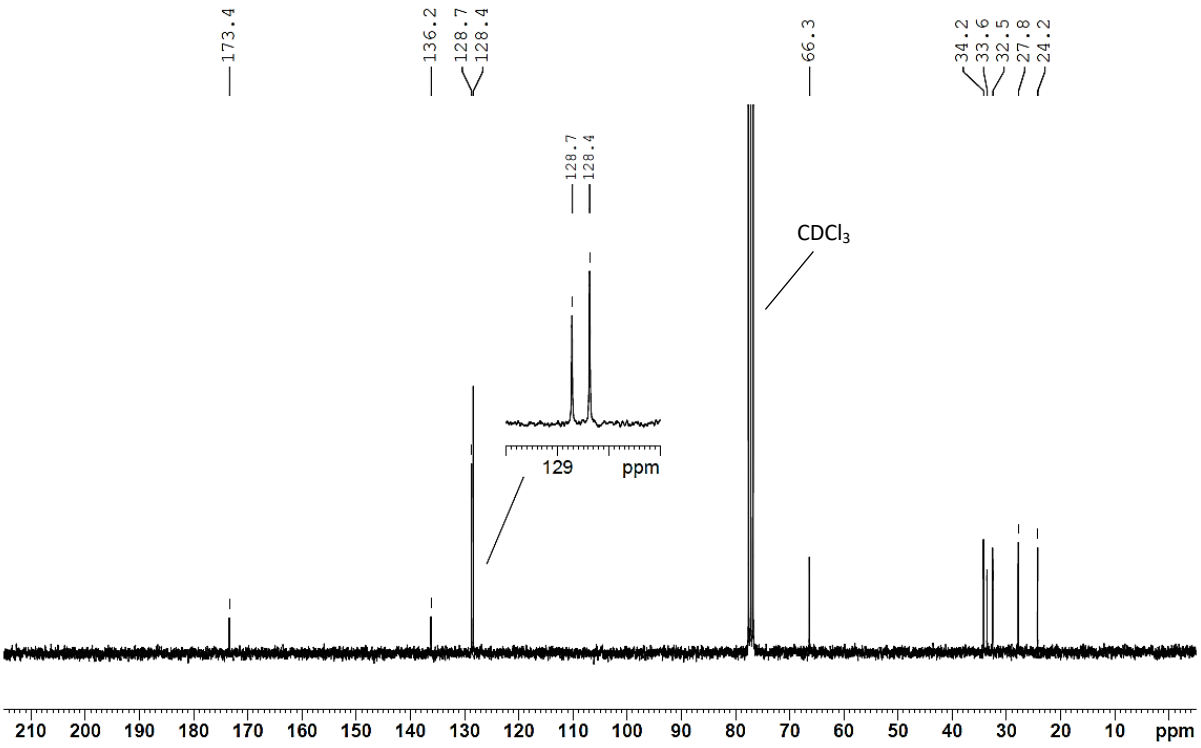

Figure S119: ^{13}C-NMR (75 MHz) spectrum of compound **53** in $CDCl_3$.

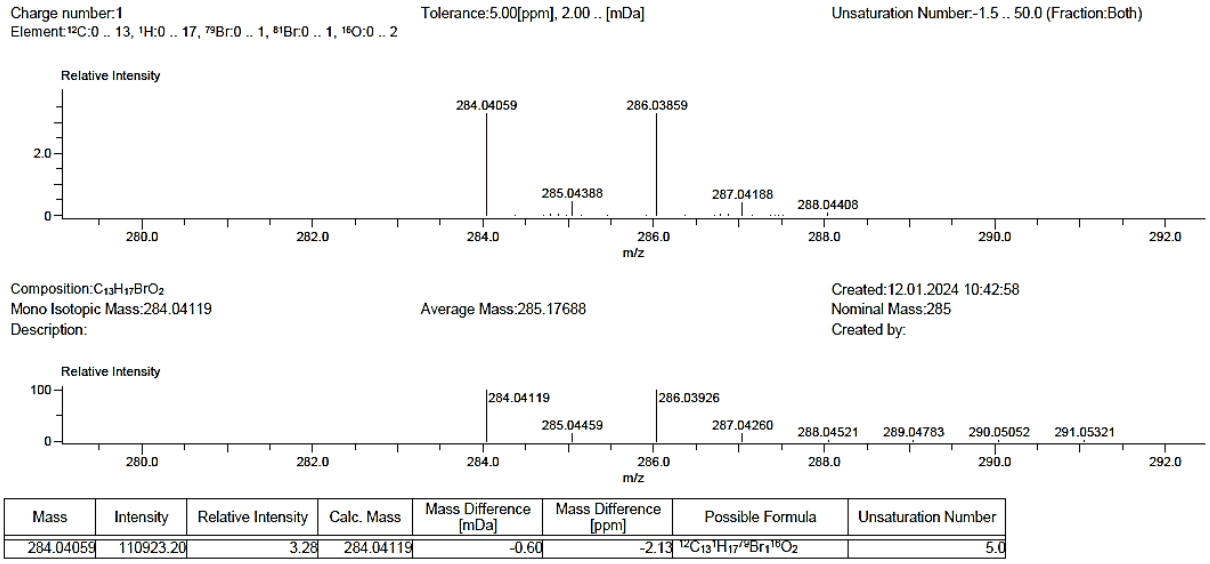

Mass	Intensity	Relative Intensity	Calc. Mass	Mass Difference [mDa]	Mass Difference [ppm]	Possible Formula	Unsaturation Number
284.04059	110923.20	3.28	284.04119	-0.60	-2.13	$^{12}C_{13}{}^{1}H_{17}{}^{79}Br_{1}{}^{16}O_{2}$	5.0

Figure S120: Measured (top) and calculated (bottom) HRMS-EI spectrum of **53**.

Compound 54

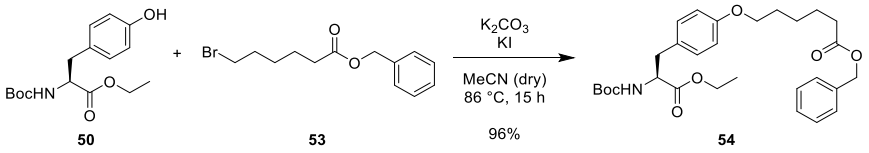

Scheme S24: Synthesis of compound **54**.

Ethyl (*tert*-butoxycarbonyl)-*L*-tyrosinate (**50**, 2.90 g, 9.37 mmol, 1.00 eq), potassium iodine (156 mg, 0.94 mmol, 0.10 eq) and potassium carbonate (3.11 g, 22.5 mmol, 2.40 eq) were suspended in dry MeCN (33.8 mL) under nitrogen atmosphere. Then, benzyl 6-bromohexanoate (**53**, 3.21 g, 11.2 mmol, 1.20 eq) was added. The reaction mixture was heated to 86 °C and refluxed for 15 h. Afterwards, the suspension was filtered over celite and rinsed with DCM (~200 mL). The solvent was removed under reduced pressure, and the crude was purified by flash column chromatography (*n*-pentane/EtOAc 9:1 ⟶ 1:1) to give the product **54** (4.60 g, 8.95 mmol, 96%) as a colourless oil.

TLC (permanganate developer): R_f = 0.30 (*n*-pentane/EtOAc 6:1, v/v).

^{1}H-NMR (500 MHz, $CDCl_3$): δ = 7.36-7.30 (m, 5H), 7.02 (d, ^3J(H,H) = 8.6 Hz, 2H), 6.79 (d, ^3J(H,H) = 8.6 Hz, 2H), 5.12 (s, 2H), 4.95 (d, ^3J(H,H) = 7.9 Hz, 1H), 4.50 (d, ^3J(H,H) = 6.6 Hz, 1H), 4.16 (q, ^3J(H,H) = 7.2 Hz, 2H), 3.91 (t, ^3J(H,H) = 6.5 Hz, 2H), 3.06-2.98 (m, 2H), 2.40 (t, ^3J(H,H) = 7.6 Hz, 2H), 1.80-1.75 (m, 2H), 1.75-1.69 (m, 2H), 1.52-1.46 (m, 2H), 1.42 (s, 9H), 1.24 (t, ^3J(H,H) = 7.1 Hz, 3H) ppm.

^{13}C-NMR (125 MHz, $CDCl_3$): δ = 173.6 (C_q), 172.1 (C_q), 158.3 (C_q), 155.3 (C_q), 136.2 (C_q), 130.5 (2C; *C*H), 128.7 (2C; *C*H), 128.3 (3C; *C*H), 128.1 (C_q), 114.7 (2C; *C*H), 79.9 (C_q), 67.8 (CH_2), 66.3 (CH_2), 61.4 (CH_2), 54.7 (*C*H), 37.6 (CH_2), 34.4 (CH_2), 29.1 (CH_2), 28.5 (3C; CH_3), 25.8 (CH_2), 24.8 (CH_2), 14.3 (CH_3) ppm.

HRMS-ESI (*m/z*): $[M + Na]^+$ calcd for $C_{29}H_{39}NO_7Na$: 536.2619; found: 536.2618.

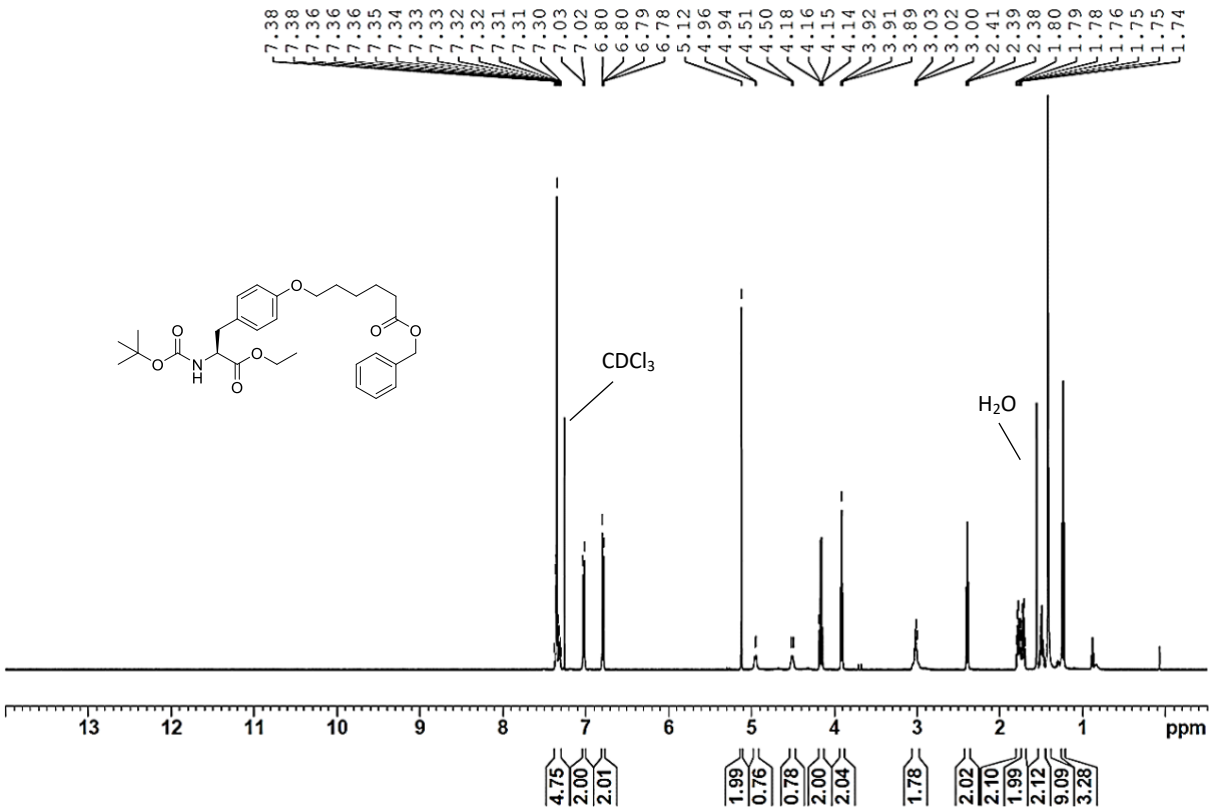

Figure S121: ^{1}H-NMR (500 MHz) spectrum of compound **54** in $CDCl_3$.

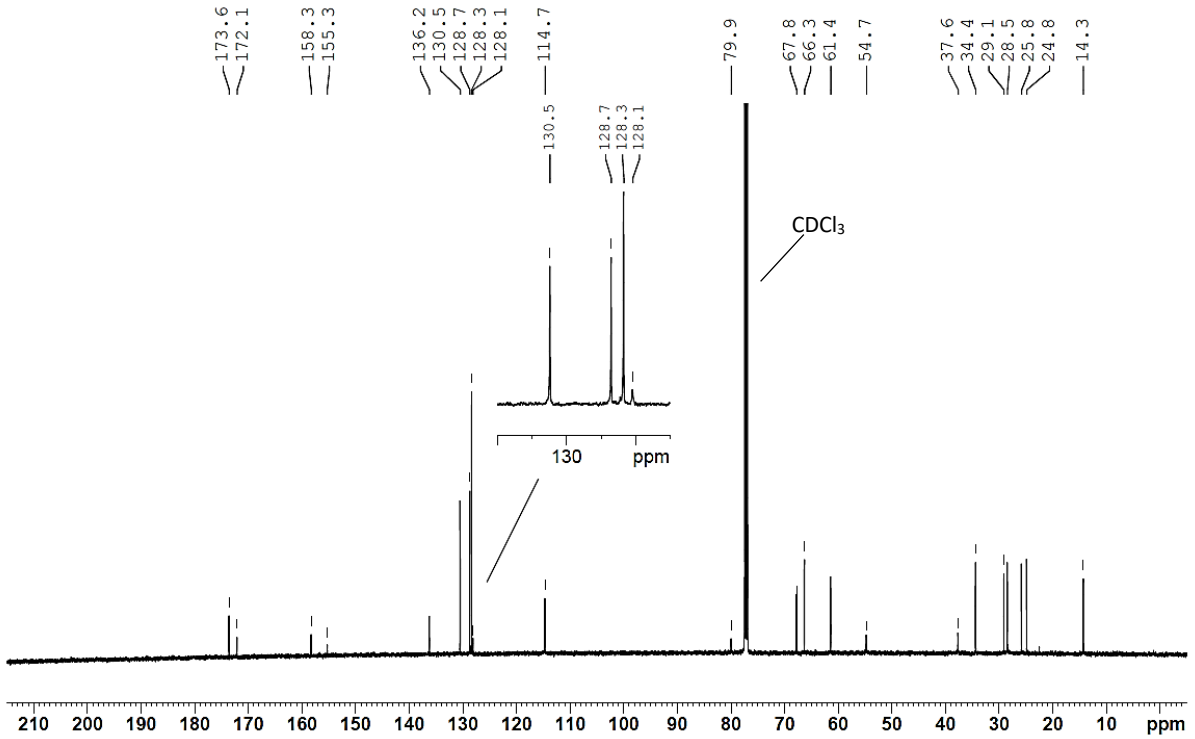

Figure S122: ^{13}C-NMR (125 MHz) spectrum of compound **54** in $CDCl_3$.

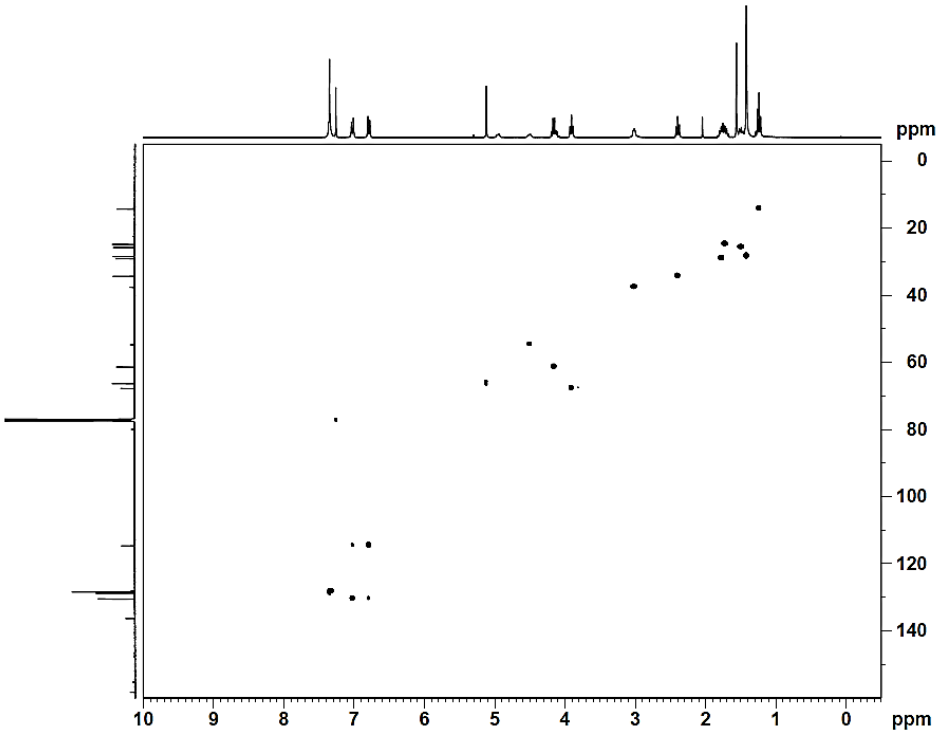

Figure S123: HSQC spectrum of compound **54** (^{1}H-NMR: 500 MHz, ^{13}C-NMR: 125 MHz, $CDCl_3$).

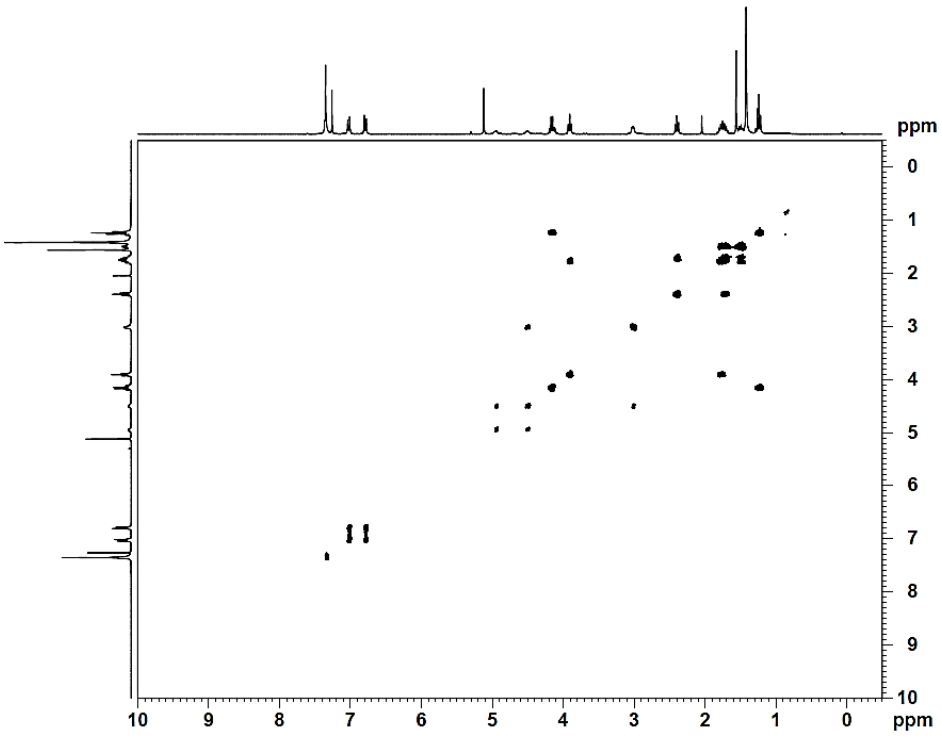

Figure S124: COSY spectrum of compound **54** (^{1}H-NMR: 500 MHz, $CDCl_3$).

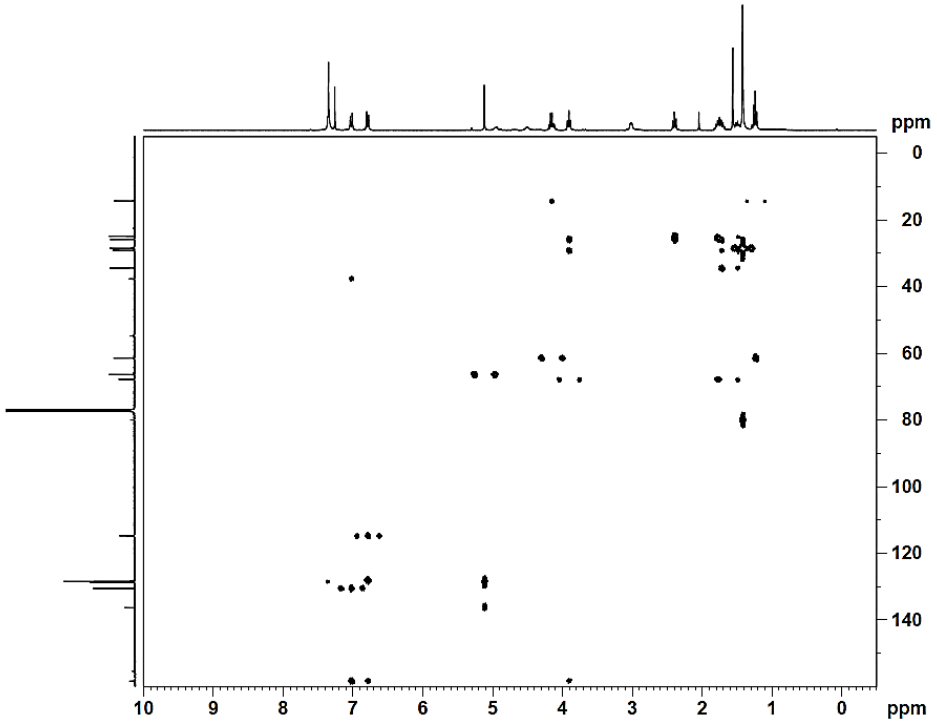

Figure S125: HMBC spectrum of compound **54** (^{1}H-NMR: 500 MHz, ^{13}C-NMR: 125 MHz, $CDCl_3$).

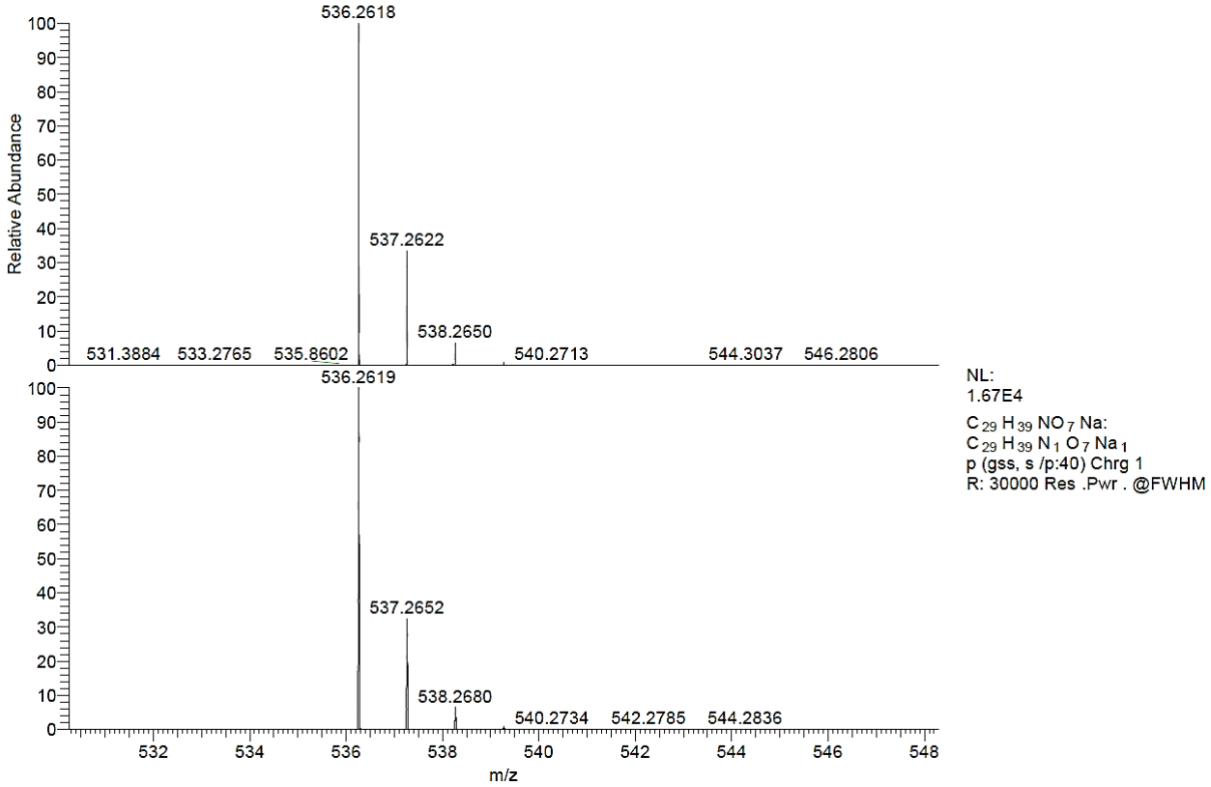

Figure S126: Measured (top) and calculated (bottom) HRMS-ESI spectrum of **54** in positive ion mode.

Compound 11

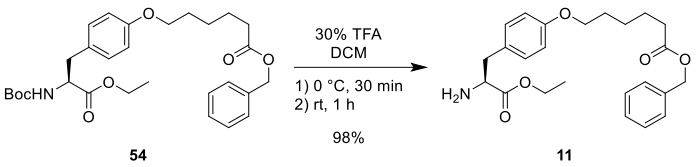

Scheme S25: Synthesis of compound (**11**).

Compound **54** (300 mg, 0.58 mmol, 1.00 eq) was dissolved in DCM (2.10 mL). The solution was cooled to 0 °C and a solution of TFA (1.80 mL) in DCM (2.10 mL) was added dropwise. After 30 minutes, the reaction mixture was left warm until rt, and it was continuously stirred for 1 h. When complete conversion of the starting material was confirmed by TLC (ninhydrin developer), the solvent was evaporated under reduced pressure. TFA was removed by co-evaporation with toluene (~10.0 mL, 3×). to give the product **11** as a yellow oil (301 mg, 0.57 mmol, 98%).

TLC (ninhydrin developer): R_f = 0.44 (DCM/MeOH 19:1 + 0.1% TEA, v/v).

^{1}H-NMR (300 MHz, $CDCl_3$): δ = 7.39-7.31 (m, 5H), 7.09 (d, ^3J(H,H) = 8.6 Hz, 2H), 6.84 (d, ^3J(H,H) = 8.6 Hz, 2H), 5.11 (s, 2H), 4.25 (q, ^3J(H,H) = 7.1 Hz, 3H), 3.91 (t, ^3J(H,H) = 6.4 Hz, 2H), 3.27 (dd, ^3J(H,H) = 6.8 Hz, ^2J(H,H) = 14.6 Hz, 1H), 3.15 (dd, ^3J(H,H) = 6.8 Hz, ^2J(H,H) = 14.6 Hz, 1H), 2.39 (t, ^3J(H,H) = 7.5 Hz, 2H), 1.82-1.66 (m, 4H), 1.53-1.43 (m, 2H), 1.24 (t, ^3J(H,H) = 7.1 Hz, 3H) ppm.

^{13}C-NMR (125 MHz, $CDCl_3$): δ = 175.2 (C_q), 173.6 (C_q), 158.1 (C_q), 136.2 (C_q), 130.4 (2C; *C*H), 129.2 (2C; *C*H), 128.7 (3C; *C*H), 128.3 (C_q), 114.7 (2C; *C*H), 67.8 (CH_2), 66.3 (CH_2), 61.1 (CH_2), 56.1 (*C*H), 40.3 (CH_2), 34.4 (CH_2), 29.1 (CH_2), 25.8 (CH_2), 24.8 (CH_2), 14.4 (CH_3) ppm.

HRMS-ESI (*m/z*): $[M + Na]^+$ calcd for $C_{24}H_{32}NO_5$: 414.2275; found: 414.2270.

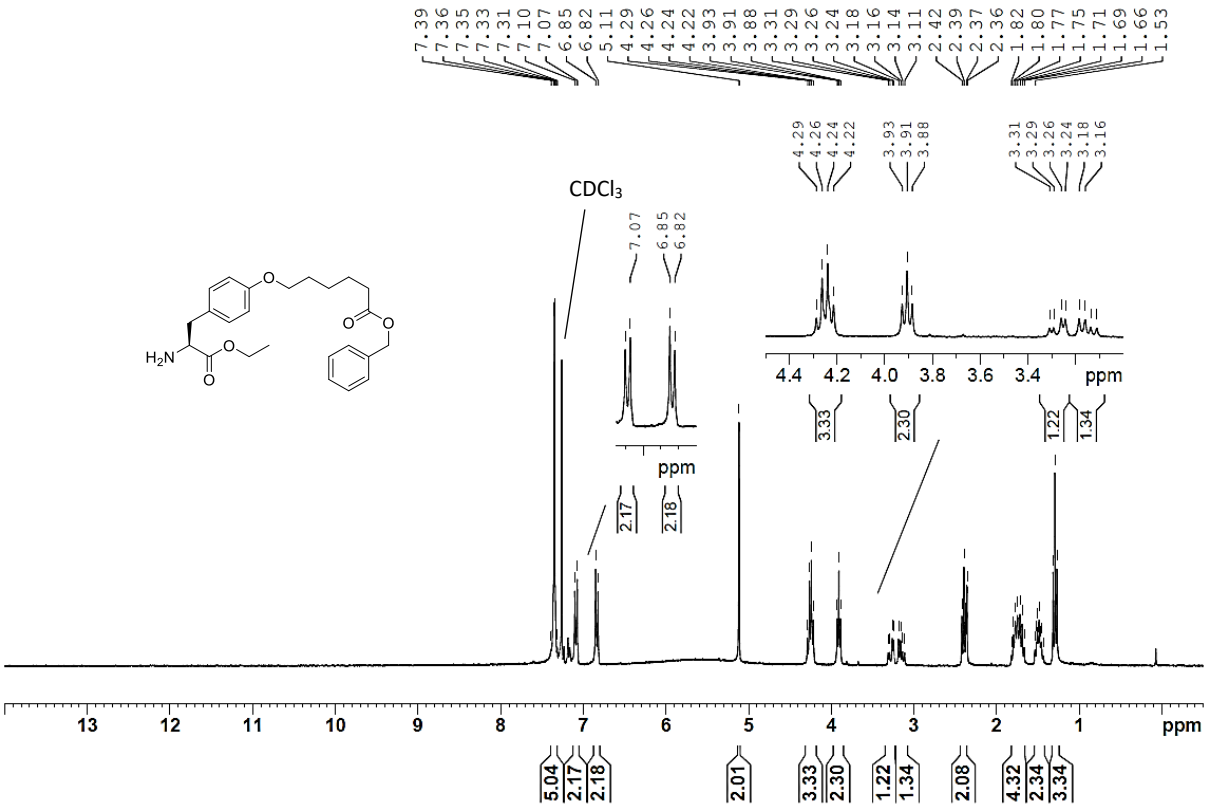

Figure S127: ^{1}H-NMR (300 MHz) spectrum of compound **11** in $CDCl_3$.

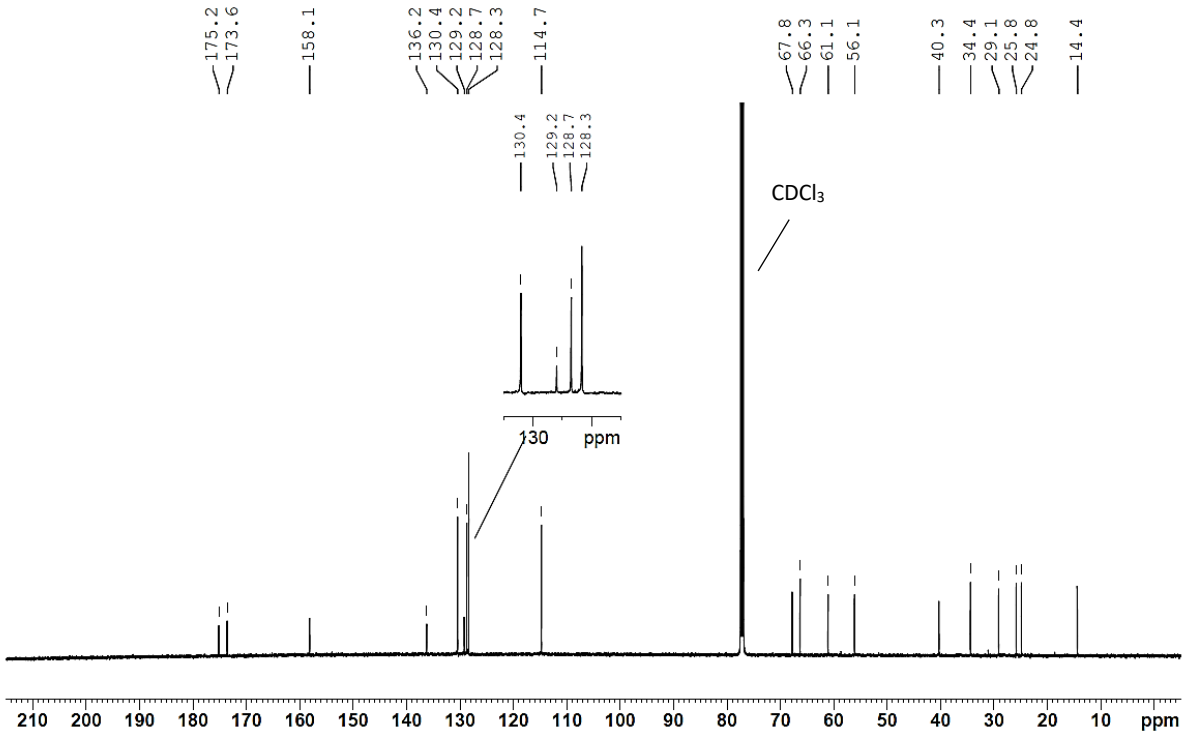

Figure S128: ^{13}C-NMR (125 MHz) spectrum of compound **11** in $CDCl_3$.

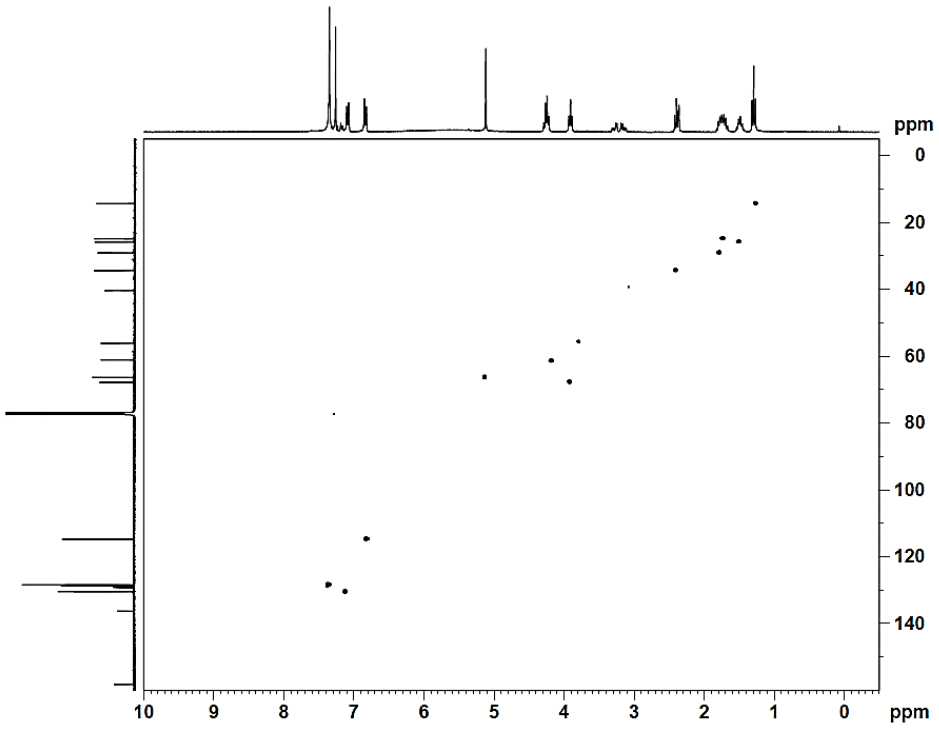

Figure S129: HSQC spectrum of compound **11** (^{1}H-NMR: 300 MHz, ^{13}C-NMR: 125 MHz, $CDCl_3$).

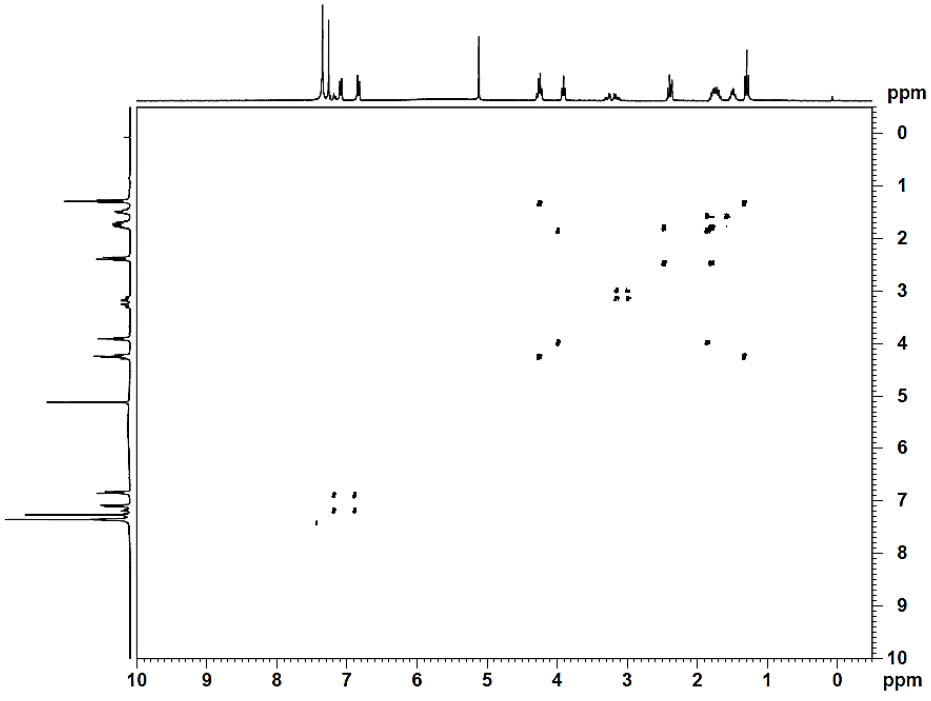

Figure S130: COSY spectrum of compound **11** (^{1}H-NMR: 300 MHz, $CDCl_3$).

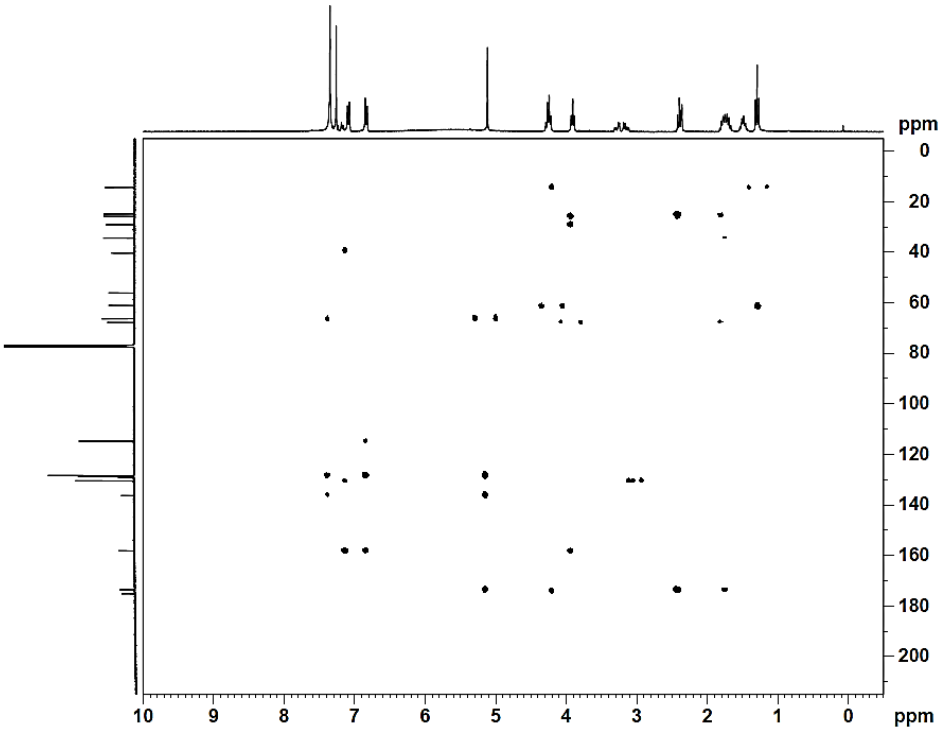

Figure S131: HMBC spectrum of compound **11** (^{1}H-NMR: 300 MHz, ^{13}C-NMR: 125 MHz, $CDCl_3$).

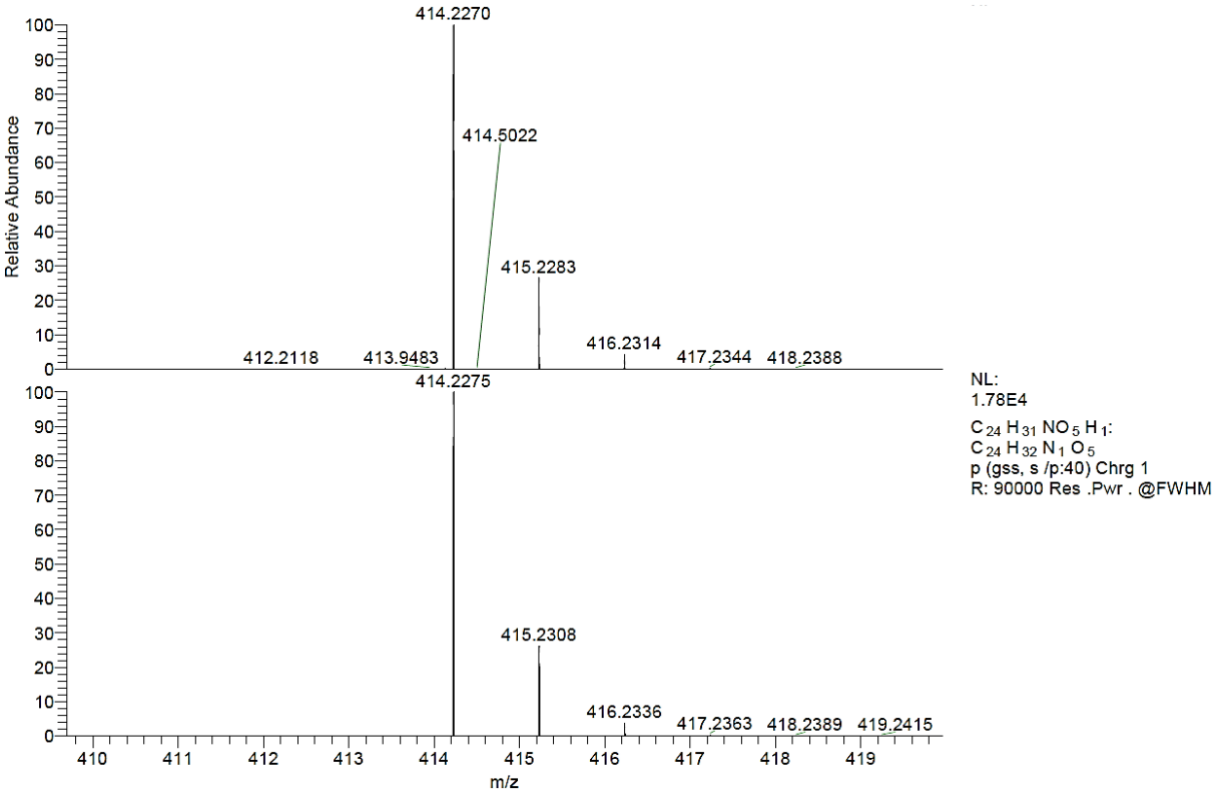

Figure S132: Measured (top) and calculated (bottom) HRMS-ESI spectrum of **11** in positive ion mode.

2-Nitrovinylbenzene (57)

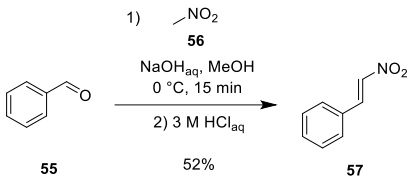

Scheme S26: Synthesis of 2-nitrovinylbenzene (**57**).

Based on the procedure of Worrall[40], nitromethane (**56**, 5.00 mL, 94.2 mmol, 1.00 eq) and benzaldehyde (**55**, 9.60 mL, 94.2 mmol, 1.00 eq) were dissolved in MeOH (19.0 mL). The reaction mixture was cooled to 0 °C. A solution of NaOH (3.96 g, 98.9 mmol, 1.05 eq) in distilled water (5.00 mL) was cooled to 4 °C by the addition of crushed ice and then added to the reaction mixture portion wise. Additional, MeOH (10.0 mL) was added, and the mixture was stirred for 15 min at 0 °C. After that, distilled water and crushed ice were added to the flask until the solution became clear. For the second step, the reaction mixture of the first step was added dropwise to 3 M HCl (aq), and a yellow solid formed immediately. The cloudy mixture was decanted and then filtrated to get a light yellow solid. The solid was washed with distilled water (~100 mL, 3×) and then melted by heating. After cooling to rt, yellow crystals formed, and the upper layer of water was removed. EtOH (~20.0 mL) was added to the solid and the suspension was heated until full dissolution. Then, a hot filtration was performed, and the filtrate was allowed to cool to room temperature to give the desired product **57** (7.30 g, 49.0 mmol, 52%) as a yellow solid. The characterization is in agreement with the literature.[41]

TLC (permanganate developer): R_f = 0.64 (*n*-pentane/EtOAc 9:1, v:v).

^{1}H-NMR (500 MHz, $CDCl_3$): δ = 8.00 (d, ^3J=13.6 Hz, 1H), 7.59 (d, ^3J=13.6 Hz, 1H), 7.57-7.54 (m, 2H), 7.52-7.49 (m, 1H), 7.47-7.44 (m, 2H) ppm.

^{13}C-NMR (125 MHz, $CDCl_3$): δ = 139.2 (*C*H), 137.3 (*C*H), 132.3 (*C*H), 130.2 (C_q), 129.5 (2 × *C*H), 129.3 (2 × *C*H) ppm.

HRMS-EI (*m/z*): $[M]^+$ calcd for $C_8H_7NO_2$: 149.04768; found: 149.04810.

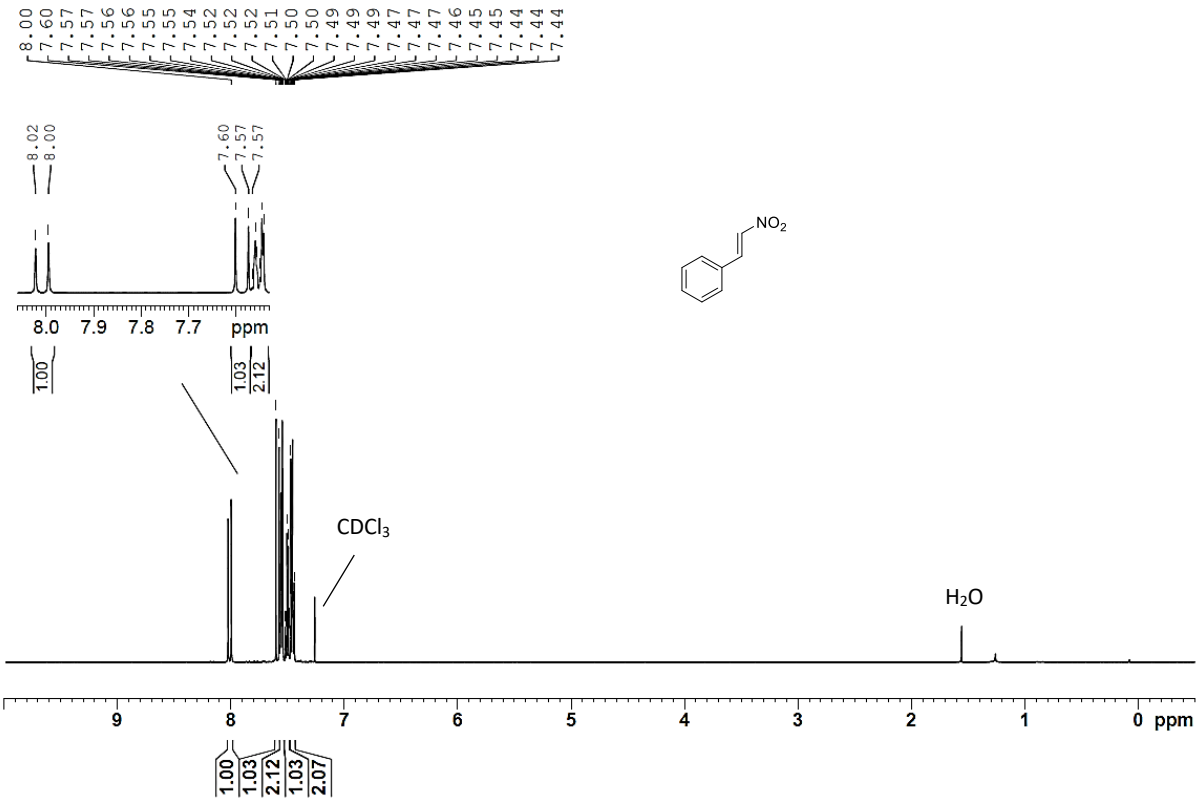

Figure S133: ^{1}H-NMR (500 MHz) spectrum of compound **57** in $CDCl_3$.

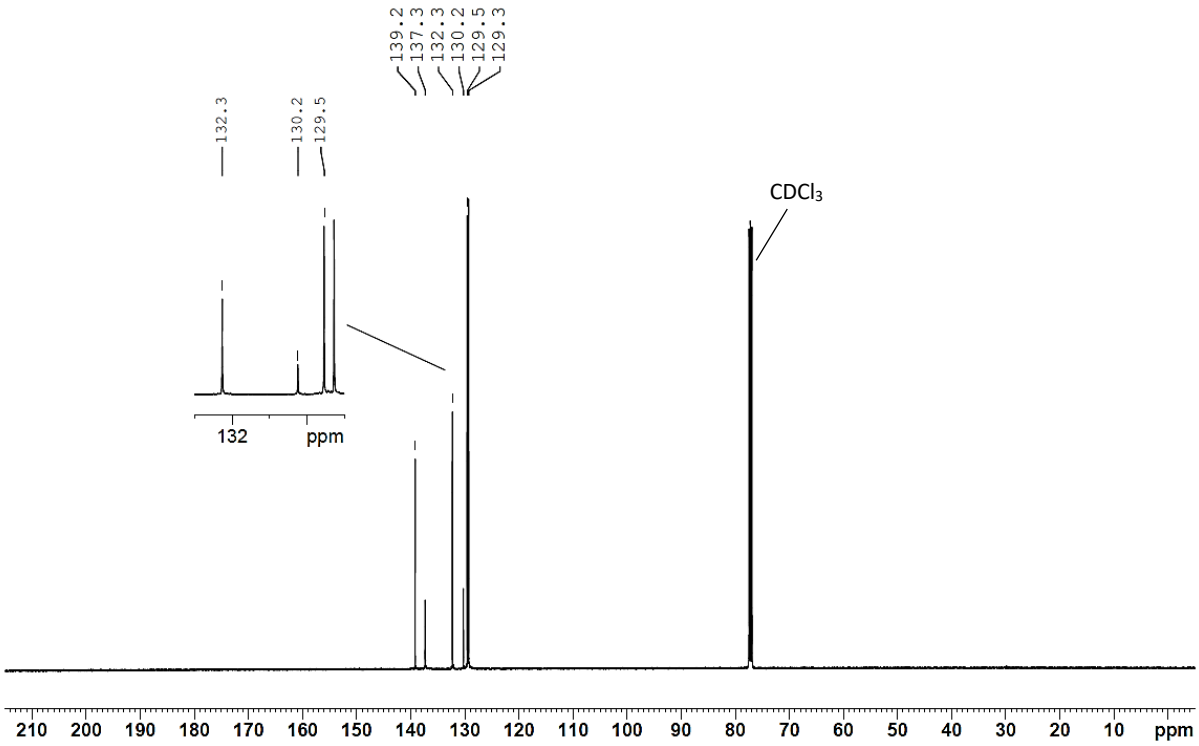

Figure S134: ^{13}C-NMR (125 MHz) spectrum of compound **57** in $CDCl_3$.

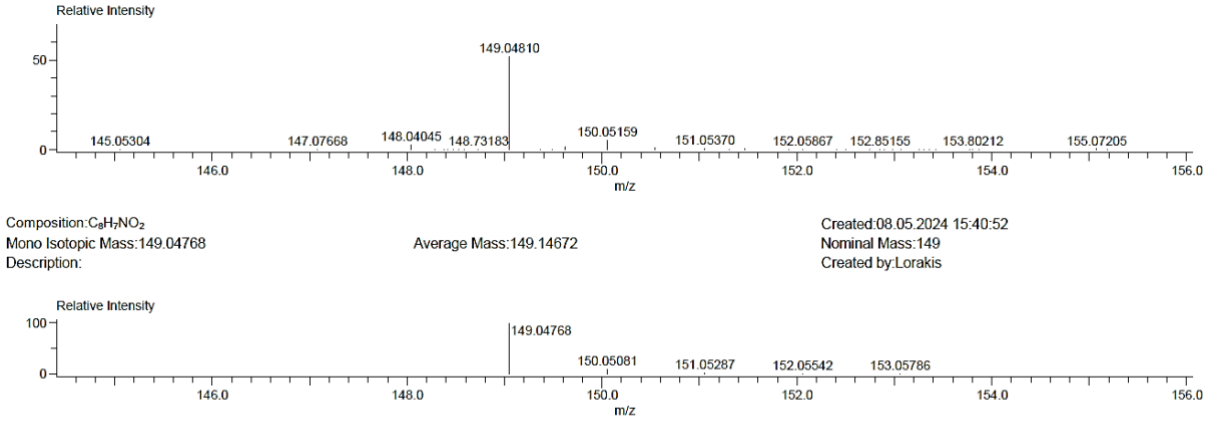

Mass	Intensity	Relative Intensity	Calc. Mass	Mass Difference [mDa]	Mass Difference [ppm]	Possible Formula	Unsaturation Number
149.04810	1323800.22	51.79	149.04768	0.42	2.81	$^{12}C_8{}^{1}H_7{}^{14}N_1{}^{16}O_2$	6.0

Figure S135: Measured (top) and calculated (bottom) HRMS-EI spectrum of **57**.

L-Phenylalanine ethyl ester (25)

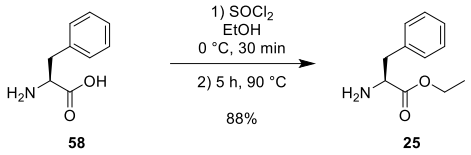

Scheme S27: Synthesis of ethyl *L*-phenylalanine ethyl ester (**25**).

Based on the procedure of Moshikur *et al*.[36], a suspension of *L*-phenylalanine (**58**, 4.82 g, 29.2 mmol, 1.00 eq) in EtOH (32.0 mL) was cooled to 0°C. Thionyl chloride (7.32 mL, 101 mmol, 3.46 eq) was added dropwise and the resulting solution was then refluxed for 5 h at 90 °C. After full conversion of the starting material, the reaction mixture was evaporated to dryness to give a white solid, which was treated with saturated aqueous Na_2CO_3 until pH 9 was reached. The mixture was extracted with EtOAc (~200 mL, 2×) and the combined organic phase was dried over Na_2SO_4 and evaporated under reduced pressure, which gave the pure *L*-phenylalanine ethyl ester (**25**, 4.97 g, 25.7 mmol, 88%).

TLC (ninydrin developer): R_f = 0.67 (DCM/MeOH 9:1 + 0.1% TEA, v/v).

^{1}H-NMR (500 MHz, $CDCl_3$): δ = 7.31-7.19 (m, 5H), 4.16 (q, ^3J(H,H) = 7.2 Hz, 2H), 3.71 (t, ^3J(H,H) = 6.5 Hz 1H), 3.08 (dd, ^2J(H,H) = 13.6 Hz, ^3J(H,H)= 5.4 Hz, 1H), 2.86 (dd, ^2J(H,H) = 13.5 Hz, ^3J(H,H) = 8.0 Hz, 1H), 1.24 (t, ^3J(H,H) = 7.2 Hz, 3H) ppm.

^{13}C-NMR (125 MHz, $CDCl_3$): δ = 175.2 (*C*OO), 137.5 (C_q), 129.4 (2C; *CH*), 128.7 (2C; *CH*), 126.9 (*CH*), 61.0 (CH_2), 56.0 (*CH*), 41.3 (CH_2), 14.3 (CH_3) ppm.

HRMS-ESI (*m/z*): $[M]^+$ calcd for $C_{11}H_{16}NO_2$: 194.1176; found: 194.1168.

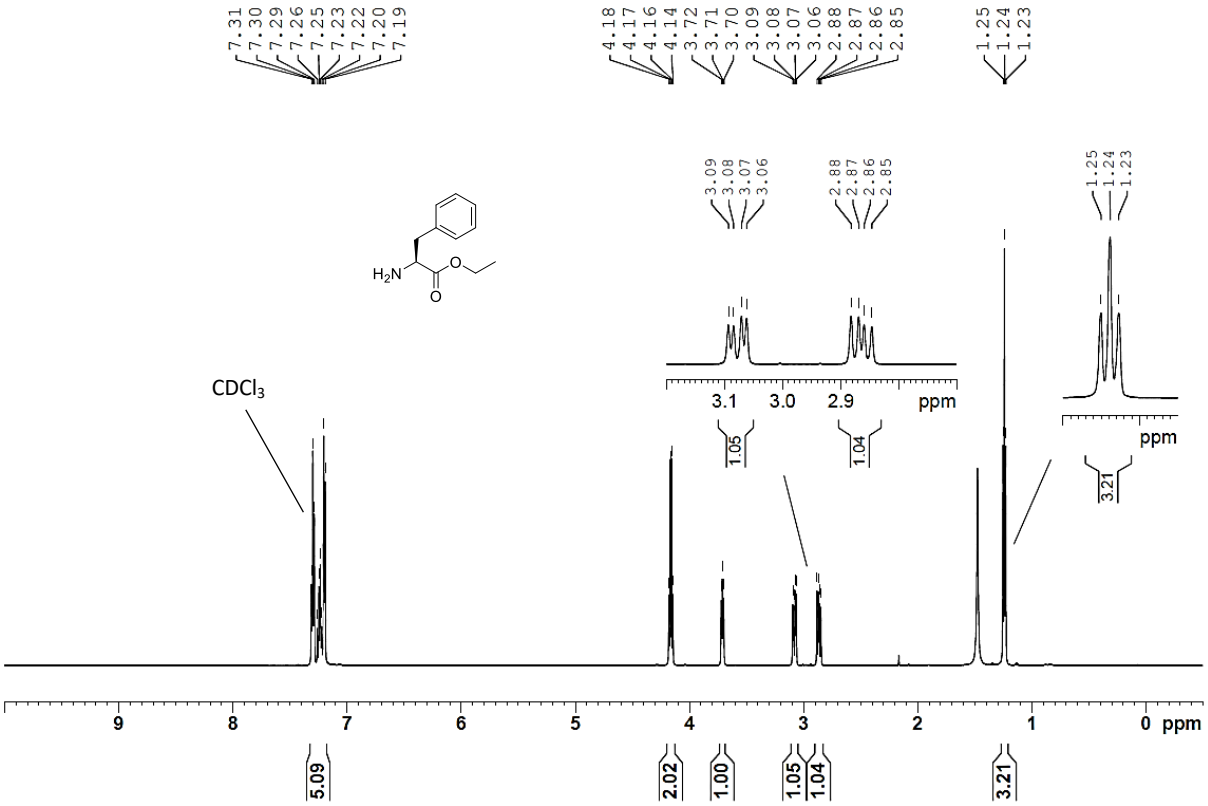

Figure S136: ^{1}H-NMR (500 MHz) spectrum of compound **25** in $CDCl_3$.

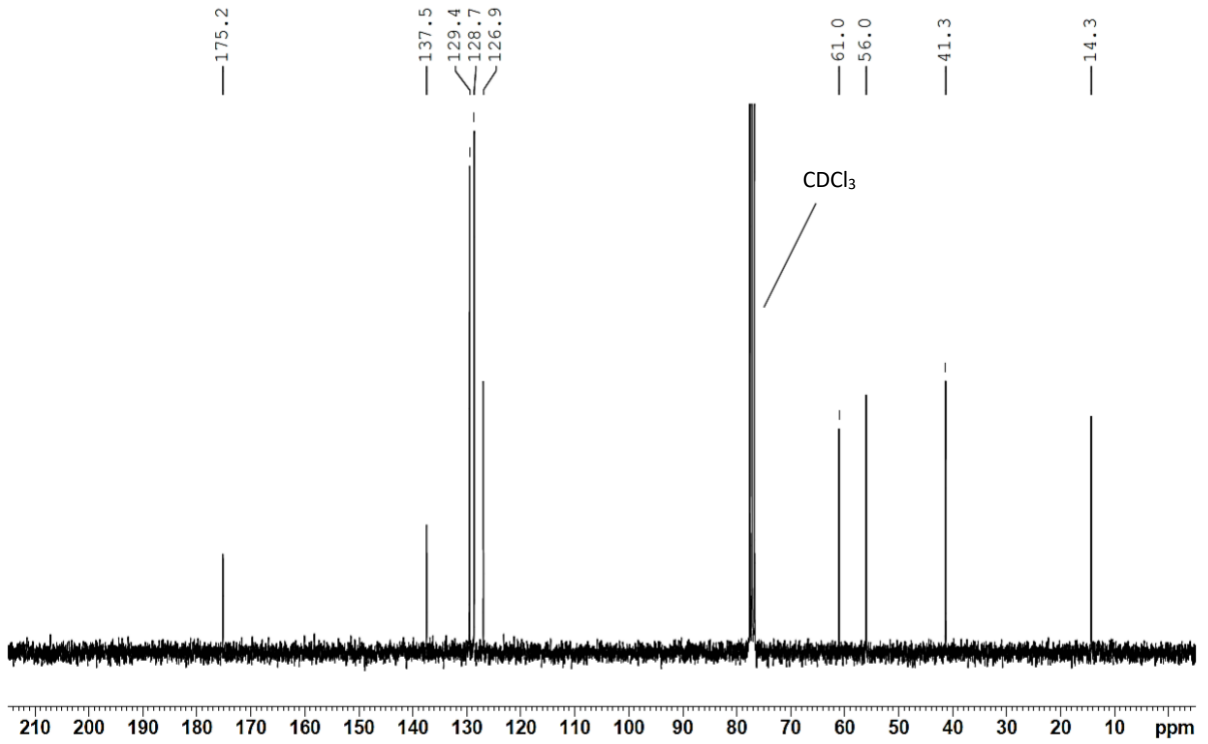

Figure S137: ^{13}C-NMR (125 MHz) spectrum of compound **25** in $CDCl_3$.

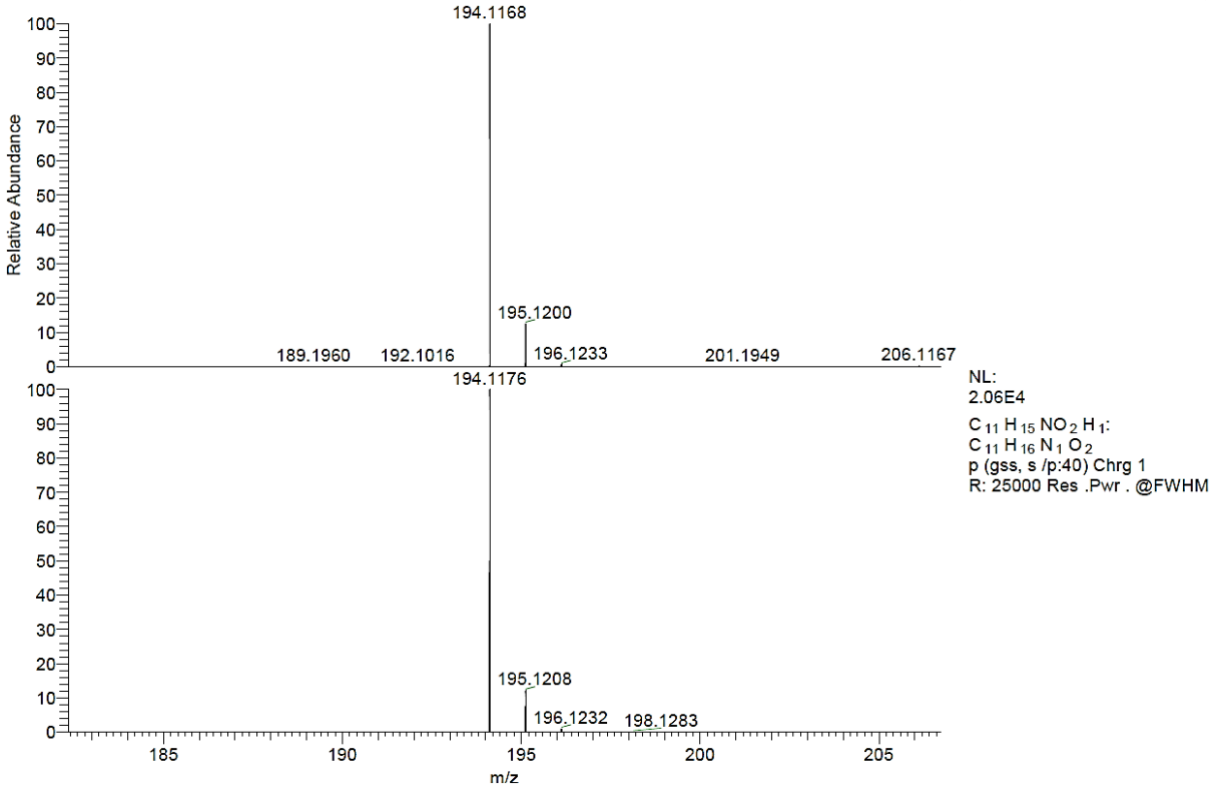

Figure S138: Measured (top) and calculated (bottom) HRMS-ESI spectrum of **25** in positive ion mode.

3-Benzyl-5-phenylpiperazin-2-one (23)

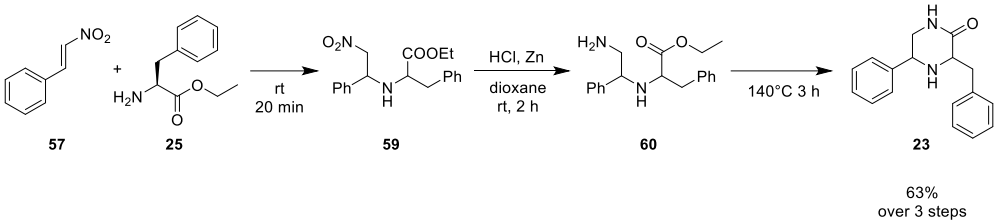

Scheme S28: Synthesis of 3-benzyl-5-phenylpiperazin-2-one (**23**).

Based on the procedure of Coutant *et al.*[20], 2-nitrovinylbenzene (**57**, 6.96 g, 47.0 mmol, 1.00 eq) and *L*-phenylalanine ethyl ester (**25**, 9.00 g, 47.0 mmol, 1.00 eq) were dissolved in a small amount of DCM and the solution was stirred for 20 min at rt. After that time, the solvent was removed under reduced pressure to give a thick yellow oil. The formation of the 1,4-adduct was confirmed via ^{1}H NMR. Next, the obtained oil was added to a cold (4 °C) mixture of dioxane (200 mL) and 37% HCl (77.3 mL). The reaction mixture was cooled to 0 °C and zinc dust (22.2 g, 0.35 mol, 7.40 eq) was added portion-wise over 10 min while stirring rapidly. The suspension was allowed to warm to rt and stirring was continued at rt. After 2h, the mixture was diluted in water, brought to pH 11 using an excess of 25% aqueous ammonia and extracted with EtOAc (~150 mL, 3×). The organic layer was washed with a small amount of 25% aqueous ammonia (~20 mL, 1×) water (~150 mL, 1×), brine (~150 mL, 1×), dried over Na_2SO_4 and concentrated to dryness to give the crude amino ester **60** as a dark yellow oil. The oil was heated at 140 °C for 3 h under reduced pressure to allow the removal of the EtOH formed. Finally, the obtained mixture of crystalline solid and yellow oil was dispersed in boiling cyclohexane followed by the removal of unreacted *L*-phenylalanine ethyl ester by filtration yielding the desired compound **23** (7.86 g, 29.4 mmol, 63%) as white solid. The characterization is in agreement with the literature.[20]

TLC (ninhydrin developer): R_f = 0.67 (DCM/MeOH 9:1 + 1% TEA, v/v).

^{1}H NMR (300 MHz, $CDCl_3$): δ = 7.29-7.16 (m, 10H), 6.72 (s, 1H), 4.00-3.95 (m, 1H), 3.76 (dd, ^{3}J(H,H) = 10.1 Hz, ^{2}J(H,H) = 2.5 Hz; 1H), 3.60 (dd, ^{3}J(H,H) = 13.6, ^{2}J(H,H) = 2.5 Hz, 1H), 3.27 (m, 2H), 2.84 (dd, ^{3}J(H,H) = 13.6 Hz, ^{3}J(H,H) = 10.1 Hz, 1H), 1.87 (s, 1H) ppm.

^{13}C NMR (75 MHz, $CDCl_3$): δ = 171.4 (N-*C*=O), 140.3 (C_q), 138.4 (C_q), 129.5 (2C; *C*H), 128.8 (2C; *C*H), 128.8 (2C; *C*H), 128.3 (*C*H), 126.9 (2C; *C*H), 126.8 (*C*H), 60.9 (*C*H), 57.8 (*C*H), 50.0 (CH_2), 38.6 (CH_2) ppm.

HRMS-ESI (m/z): $[M+H]^+$ calcd for $C_{17}H_{19}N_2O$: 267.1492; found: 267.1484.

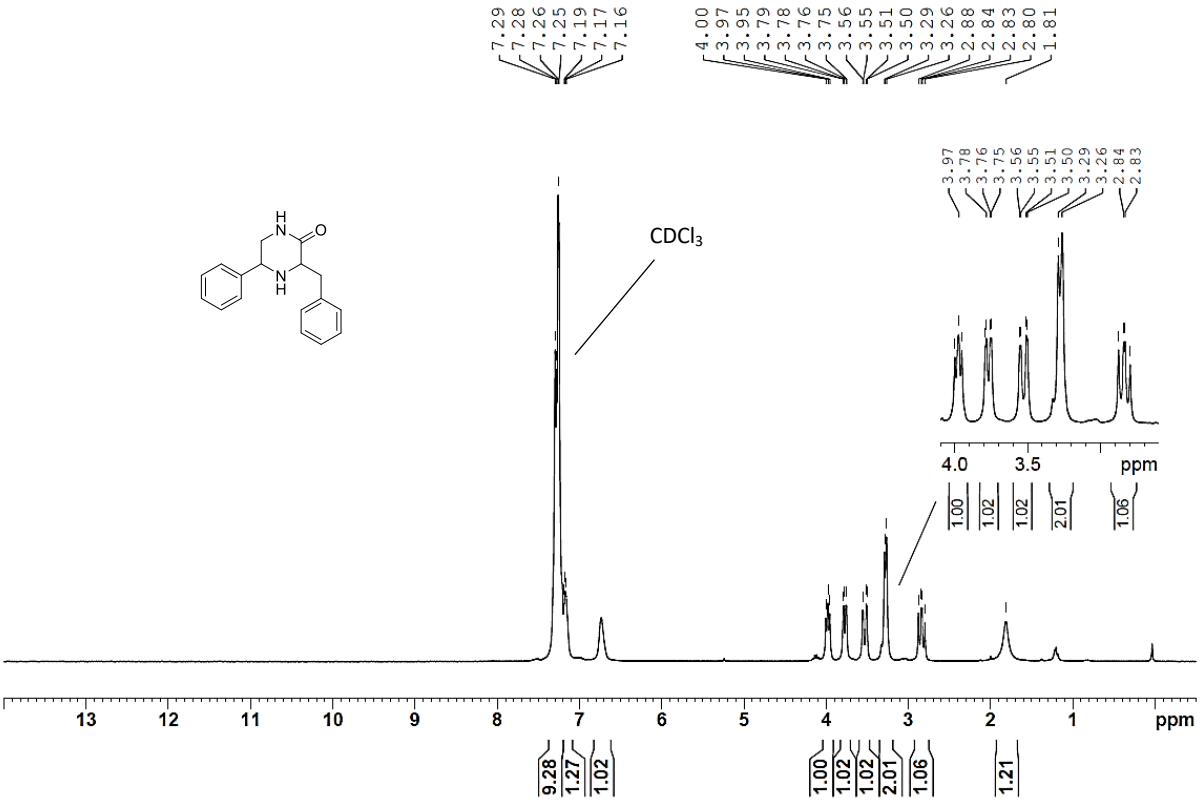

Figure S139: ^{1}H-NMR (300 MHz) spectrum of compound **23** in $CDCl_3$.

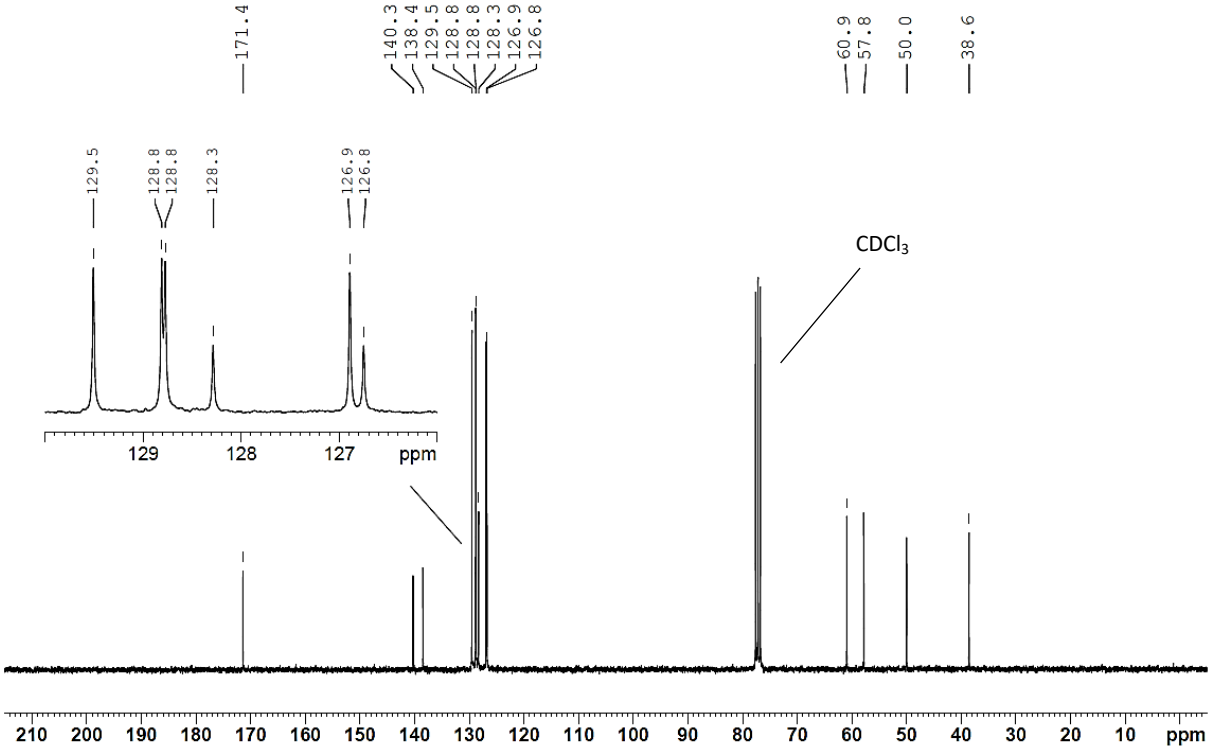

Figure S140: ^{13}C-NMR (75 MHz) spectrum of compound **23** in $CDCl_3$.

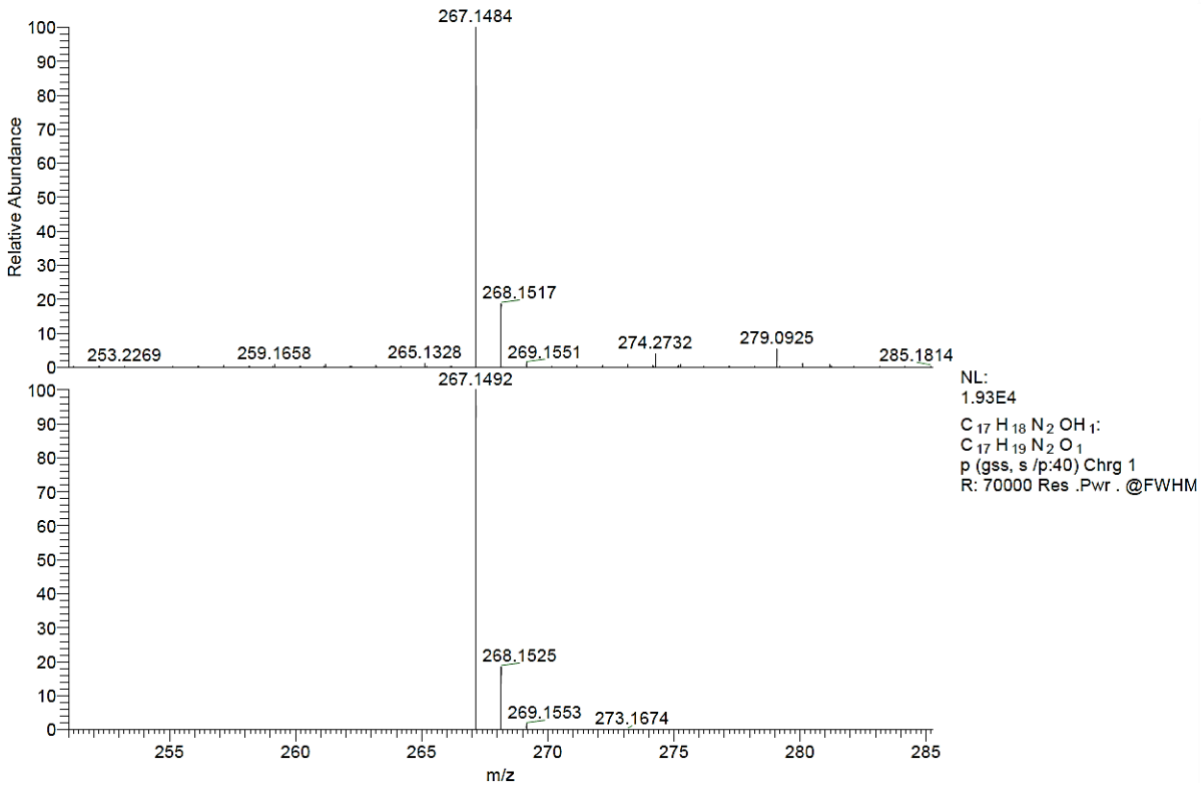

Figure S141: Measured (top) and calculated (bottom) HRMS-ESI spectrum of **23** in positive ion mode.

3-Benzyl-5-phenylpyrazin-2-ol (24)

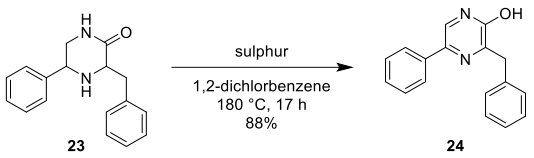

Scheme S29: Synthesis of 3-benzyl-5-phenylpyrazin-2-ol (**24**).

Based on the procedure of Coutant *et al*.[20] 3-benzyl-5-phenylpiperazin-2-one (**23**, 1.50 g, 29.2 mmol, 1.00 eq) and sulphur (1.92 g, 59.9 mmol, 2.00 eq) were heated to reflux in 1,2- dichlorobenzene (107 mL) for 17 h. The reaction mixture was concentrated to dryness and the crude was purified by flash column chromatography (*n*-pentane/EtOAc 3:1 (v/v) → EtOAc → DCM/MeOH 4:1 (v/v)) to give the desired product **24** (6.90 g, 26.2 mmol, 88%) as a brown solid. The characterization is in agreement with the literature.

TLC (UV_{254nm}): R_f = 0.67 (EtOAc/*n*-pentane 4:1, v/v).

^{1}H NMR (300 MHz, DMSO-d_6): δ = 12.43 (s, 1H), 7.88 (s, 1H), 7.84 (d, 2H, ^3J=7.4 Hz), 7.39-7.28 (m, 7H), 7.30 (m, 3H), 4.06 (s, 2H) ppm.

^{13}C NMR (75 MHz, DMSO-d_6): 154.9 (C_q), 137.9 (C_q), 135.9 (C_q), 129.1 (*C*H), 129.0 (*C*H), 128.8 (*C*H), 128.6 (*C*H), 128.4 (*C*H), 128.3 (*C*H), 128.2 (*C*H), 128.2 (*C*H), 127.2 (*C*H), 126.7 (C_q), 126.4 (*C*H), 124.4 (*C*H), 124.0 (C_q), 33.9 (CH_2) ppm.

HRMS-ESI (m/z): $[M-H]^-$ calcd for $C_{17}H_{13}N_2O$: 261.1033; found, 261.1035.

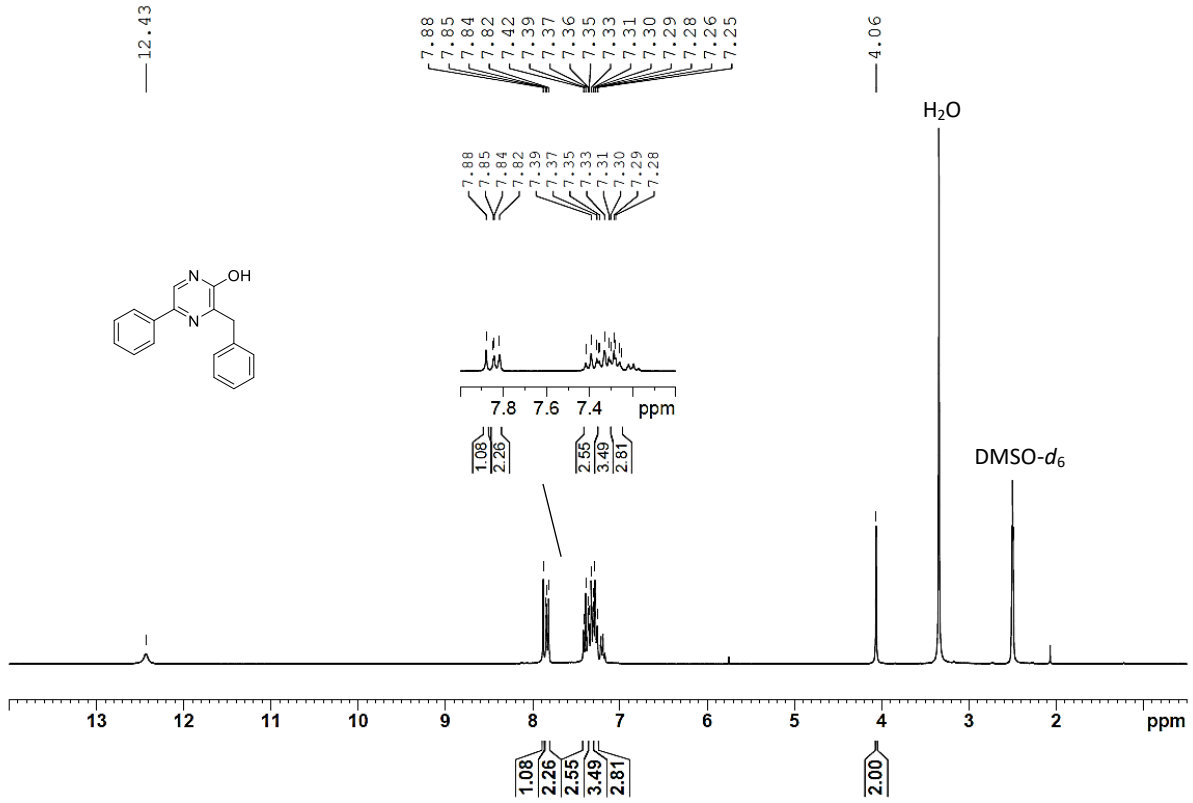

Figure S142: ^{1}H-NMR (300 MHz) spectrum of compound **24** in DMSO-d_6.

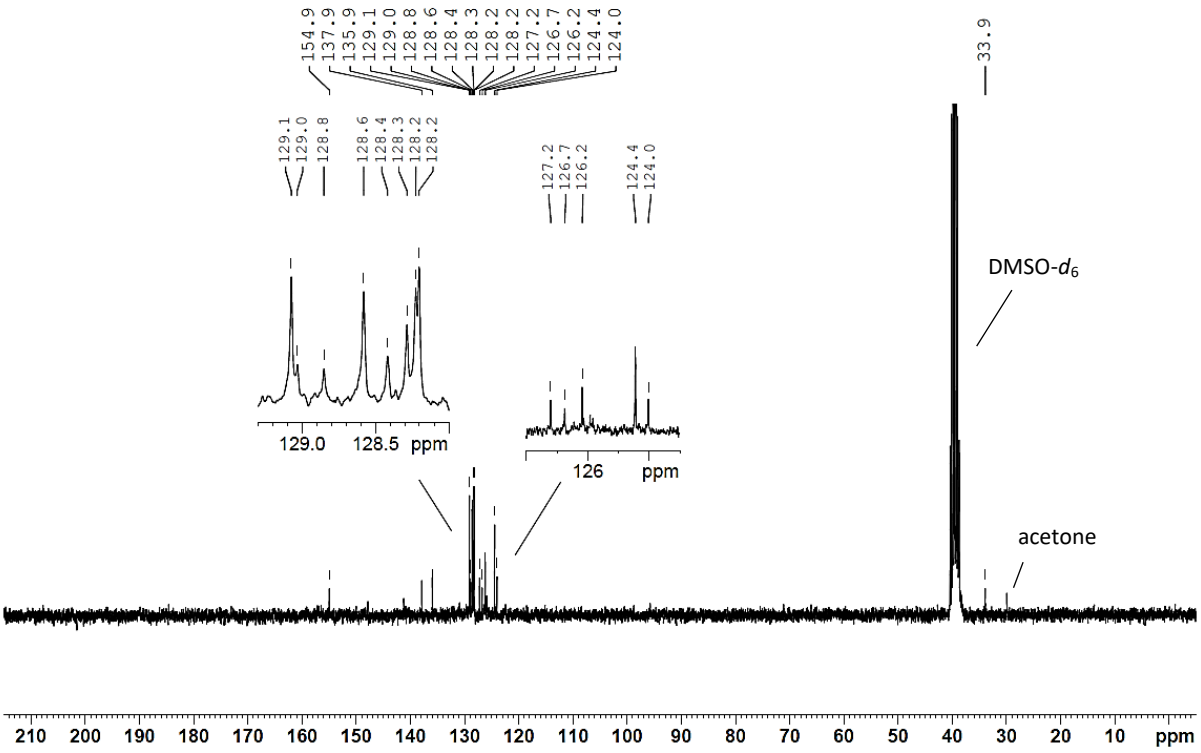

Figure S143: ^{13}C-NMR (75 MHz) spectrum of compound **24** in DMSO-d_6.

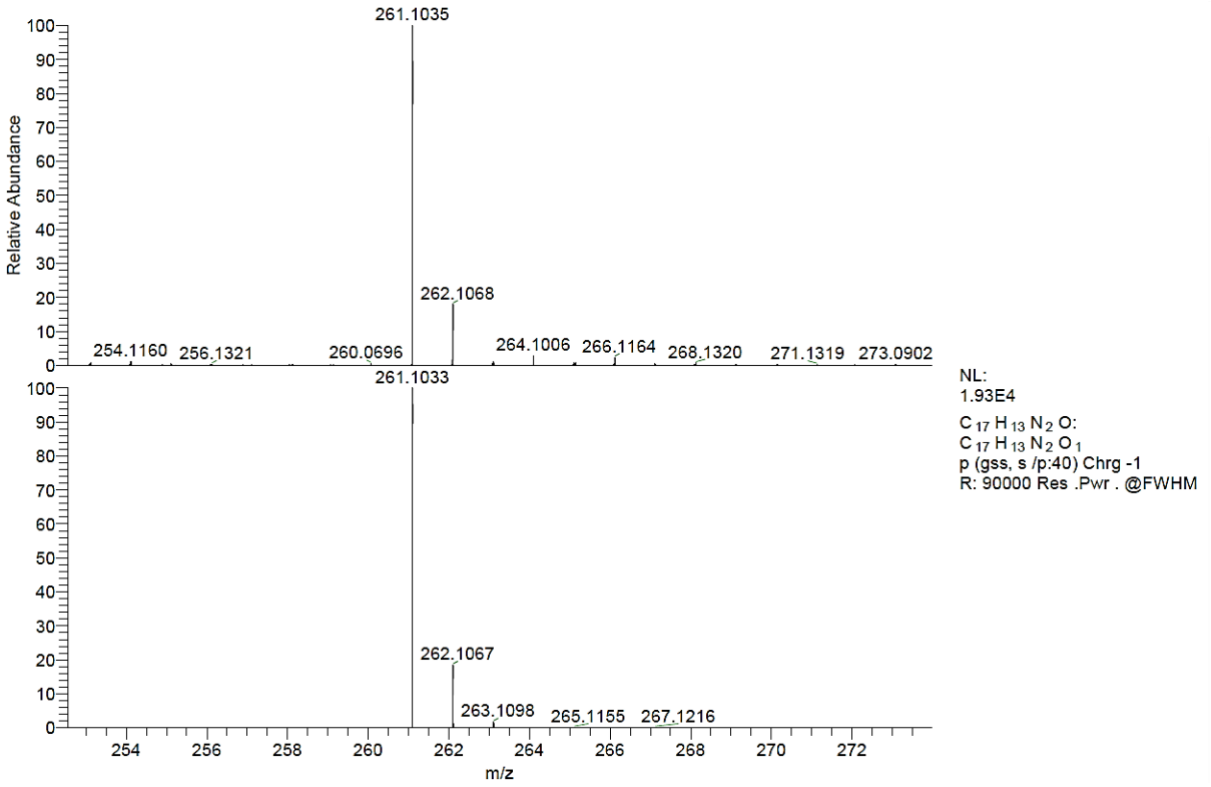

Figure S144: Measured (top) and calculated (bottom) HRMS-ESI spectrum of **24** in negative ion mode.

3-Benzyl-2-chloro-5-phenylpyrazine (10)

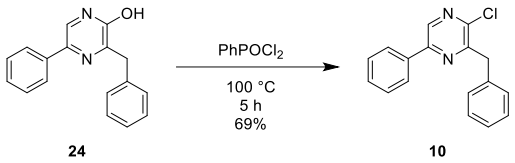

24 **10**

Scheme S30: Synthesis of 3-benzyl-2-chloro-5-phenylpyrazine (**10**).

Based on the procedure of Coutant *et al.*[20] 3-benzyl-5-phenylpyrazin-2-ol (**24**, 0.026 mol) was dispersed in phenyl phosphonic dichloride (13.0 mL) and the suspension was stirred at 100 °C for 5 h. The resulting solution was poured onto water and stirred for 15 min. This was basified with 25% ammonia (aq) and extracted with EtOAc (~200 mL, 3×). The combined organic phases were washed with water (~200 mL), brine (~200 mL) and dried over Na_2SO_4. The solvent was removed under reduced pressure and the crude was purified by flash column chromatography (*n*-pentane/EtOAc 1:1) to give the desired product **10** (5.08 g, 18.1 mmol, 69%) as a brown solid.

TLC (UV_{254nm}): R_f = 0.61 (EtOAc/*n*-pentane 4:1, v/v).

^{1}H NMR (300 MHz, $CDCl_3$): δ = 8.66 (s, 1H), 8.01 (m, 2H), 7.49 (m, 3H), 7.36 (m, 2H), 7.29 (m, 2H), 7.25 (m, 1H), 4.38 (s, 2H) ppm.

^{13}C NMR (75 MHz, $CDCl_3$): δ = 153.8 (C_q), 150.5 (C_q), 147.0 (C_q), 138.7 (*C*H), 137.2 (C_q), 135.5 (C_q), 130.2 (*C*H), 129.3 (*C*H), 129.2 (*C*H), 128.7 (*C*H), 127.0 (*C*H), 126.9 (*C*H), 41.4 (CH_2) ppm.

HRMS (m/z): $[M+H]^+$ calcd for $C_{17}H_{14}ClN_2$: 281.0840, found: 281.0836.

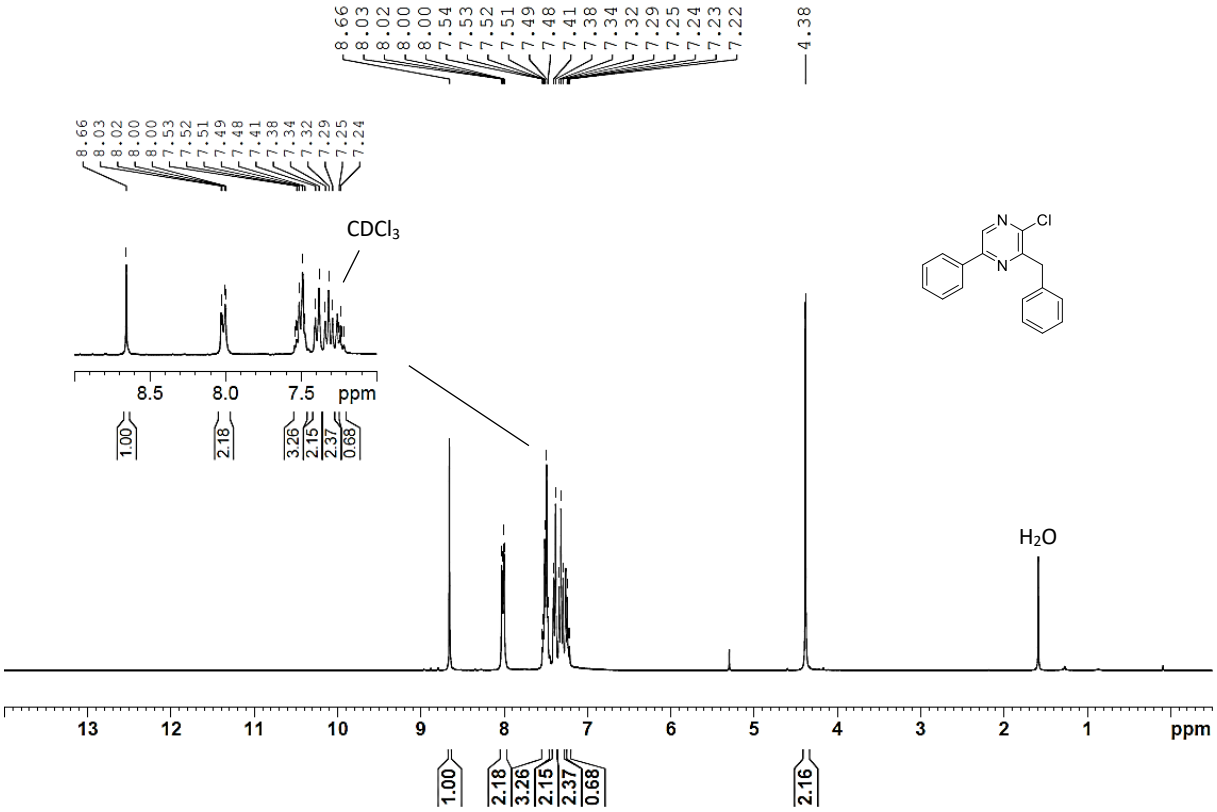

Figure S145: ^{1}H-NMR (300 MHz) spectrum of compound **10** in $CDCl_3$.

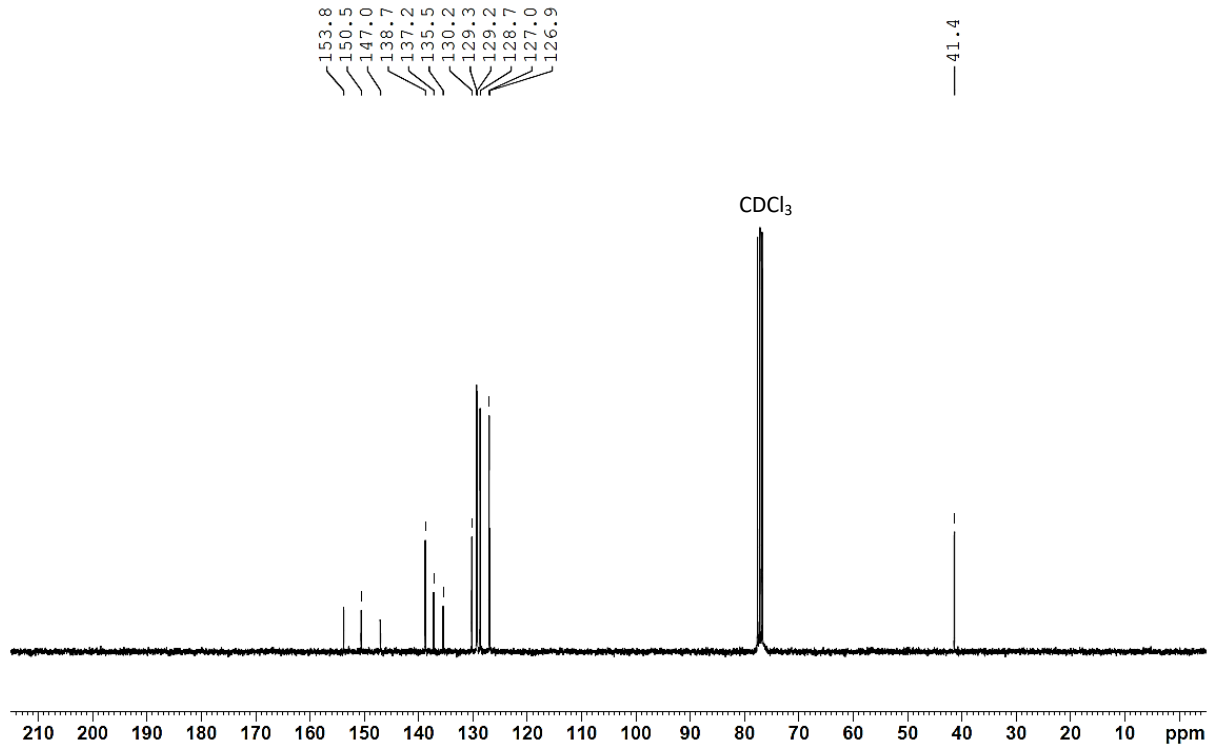

Figure S146: ^{13}C-NMR (75 MHz) spectrum of compound **10** in $CDCl_3$.

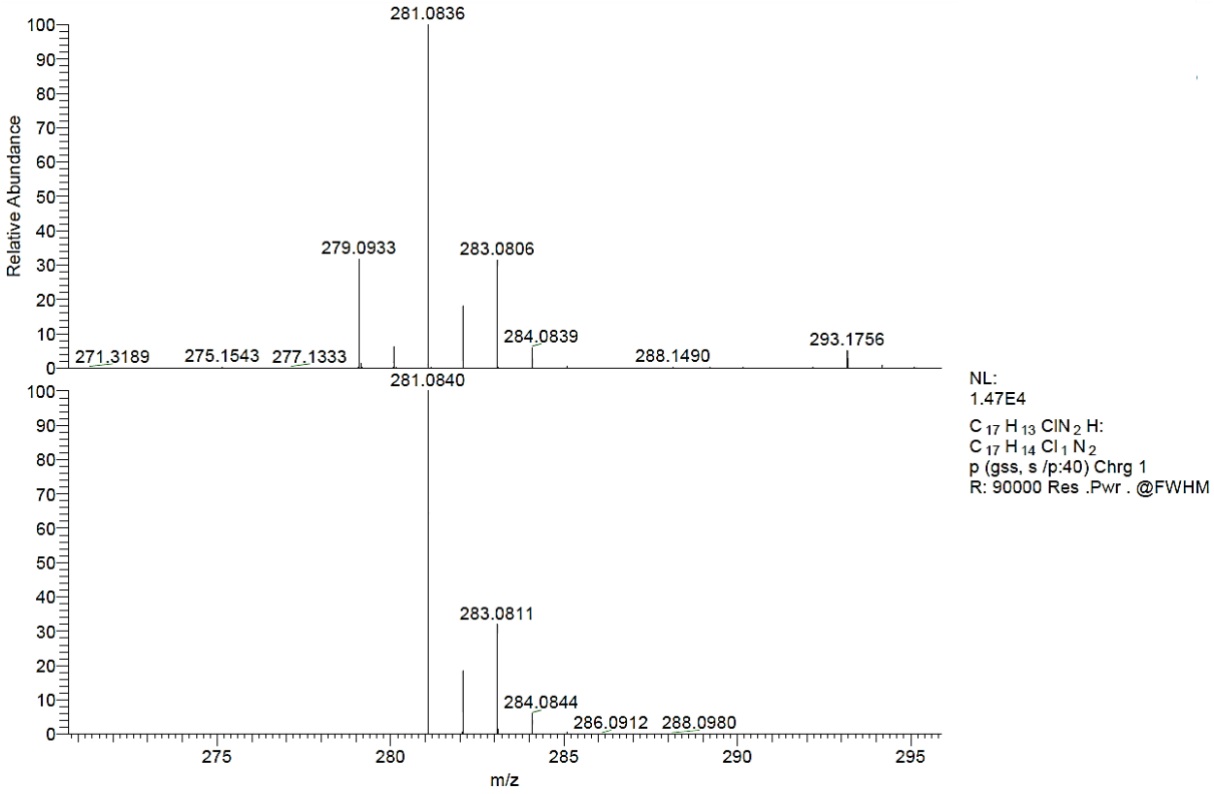

Figure S147: Measured (top) and calculated (bottom) HRMS-ESI spectrum of **10** in positive ion mode.

Compound 12

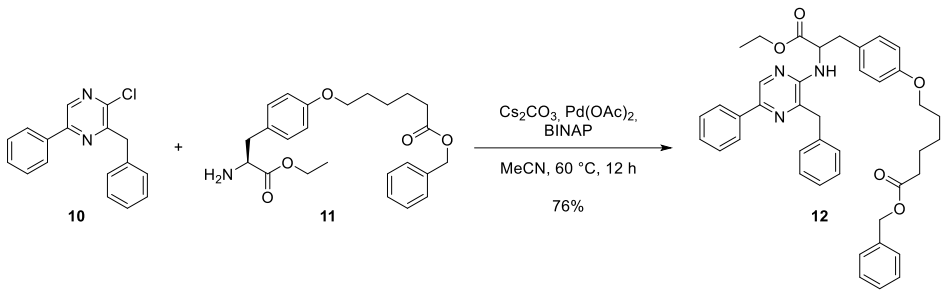

Scheme S31: Synthesis of compound **12**.

Based on the procedure of Coutant *et al*.[20], 3-benzyl-2-chloro-5-phenylpyrazine (**10**, 100 mg, 356 µmol, 1.00 eq), Cs_2CO_3 (371 mg, 1.14 mmol, 3.20 eq), $Pd(OAc)_2$ (4.04 mg, 17.8 µmol, 0.05 eq) and BINAP (16.6 mg, 26.7 µmol, 0.075 eq.) were weight in a flask and connected to high vacuum for 1 h. Compound **11** (162 mg, 392 µmol, 1.10 eq) was dissolved in dry MeCN (1.42 mL) and added under inert atmosphere. The reaction mixture was heated to 60 °C and stirred for 12 h. The resulting brown suspension was dispersed in DCM, the solution was filtered over celite, rinsed with DCM (~200 mL) and the filtrate was concentrated to dryness. The crude was purified by flash column chromatography (*n*-pentane/EtOAc 9:1 → 4:1, v/v) to give the pure product (**12**, 179 mg, 272 µmol, 76%) as yellow oil.

TLC (ninydrin developer): R_f = 0.53 (*n*-pentane/EtOAc 4:1 + 0.1% TEA, v/v).

^{1}H NMR (500 MHz, $CDCl_3$): δ = 8.39 (s, 1H), 7.93-7.91 (m, 2H), 7.45 (t, ^3J(H,H) = 7.9 Hz, 2H), 7.36-7.32 (m, 7H), 7.27-7.26 (m, 1H), 7.26-7.22 (m, 2H), 7.20-7.18 (m, 2H), 6.84 (d, ^3J(H,H) = 8.6 Hz, 2H), 6.70 (d, ^3J(H,H) = 8.6 Hz, 2H), 5.12 (s, 2H), 4.89-4.87 (m, 2H), 4.13-4.09 (m, 4H), 3.91 (t, ^3J(H,H) = 6.5 Hz, 2H), 3.11-3.07 (m, 1H), 3.01-2.97 (m, 1H), 2.41 (t, ^3J(H,H) = 7.5 Hz, 2H), 1.82-1.77 (m, 2H), 1.75-1.71 (m, 2H), 1.54-1.48 (m, 2H), 1.18 (t, ^3J(H,H) = 7.1 Hz, 3H) ppm.

^{13}C NMR (125 MHz, $CDCl_3$): δ = 173.6 (C_q), 172.7 (C_q), 158.9 (C_q), 150.5 (C_q), 141.3 (C_q), 141.1 (C_q), 137.6 (C_q), 137.0 (*C*H), 136.6 (C_q), 136.2 (C_q), 130.3 (2C; *C*H), 128.9 (3C; *C*H), 128.9 (2C; *C*H), 128.8 (2C; *C*H), 128.7 (3C; *C*H), 128.4 (3C; *C*H), 128.1 (C_q), 127.9 (*C*H), 127.0 (*C*H), 125.8 (2C; *C*H), 114.6 (2C; *C*H), 67.7 (CH_2), 66.3 (CH_2), 61.3 (CH_2), 55.1 (*C*H), 41.0 (CH_2), 37.0 (CH_2), 34.4 (CH_2), 29.1 (CH_2), 25.8 (CH_2), 24.8 (CH_2), 14.3 (CH_3) ppm.

HRMS (m/z): $[M+H]^+$ calcd for $C_{41}H_{44}N_3O_5$: 658.3275; found: 658.3256.

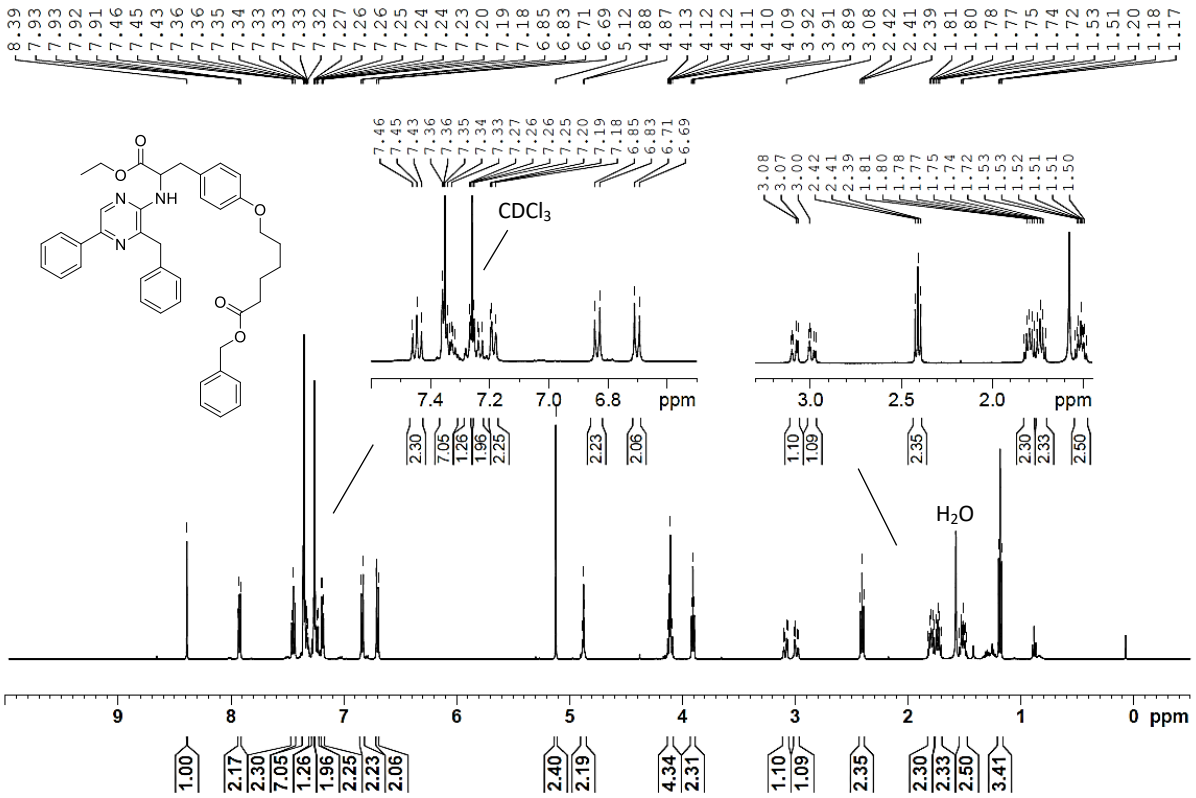

Figure S148: ^{1}H-NMR (500 MHz) spectrum of compound **12** in $CDCl_3$.

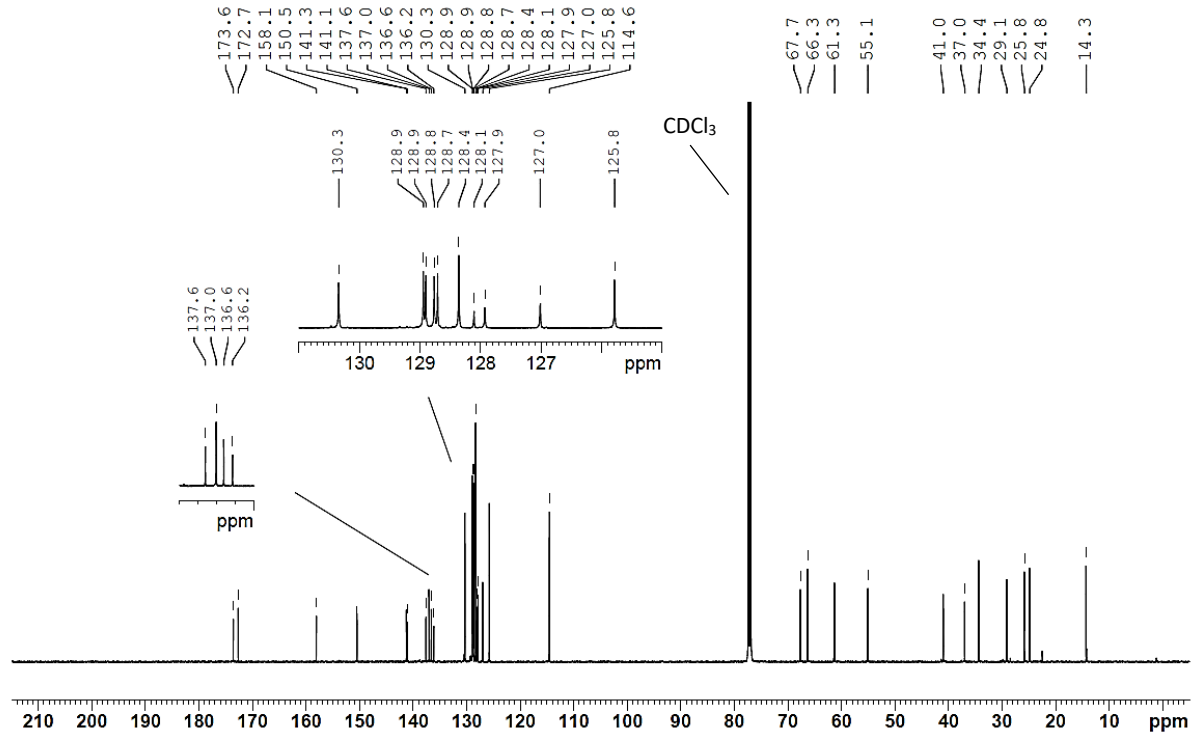

Figure S149: ^{13}C-NMR (125 MHz) spectrum of compound **12** in $CDCl_3$.

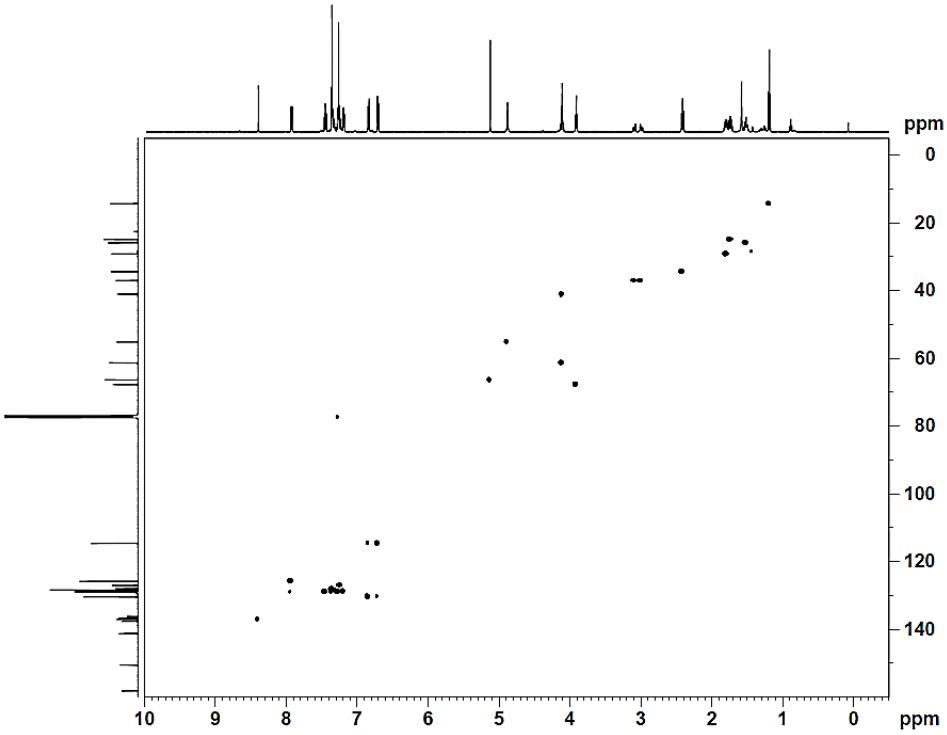

Figure S150: HSQC spectrum of compound **12** (^{1}H-NMR: 500 MHz, ^{13}C-NMR: 125 MHz, $CDCl_3$).

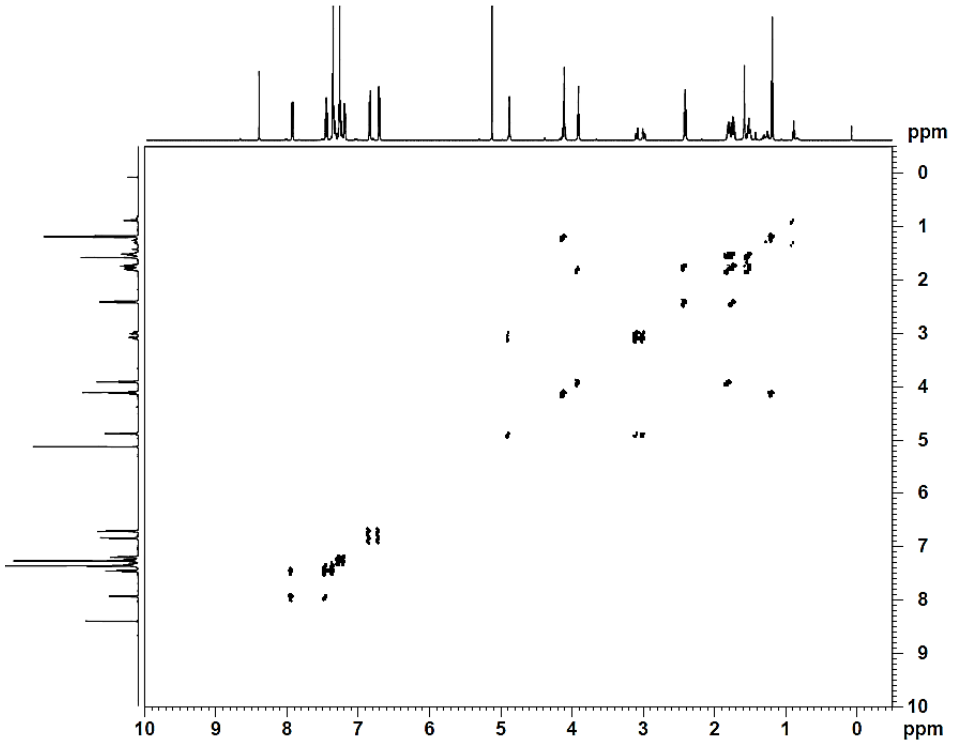

Figure S151: COSY spectrum of compound **12** (^{1}H-NMR: 500 MHz, $CDCl_3$).

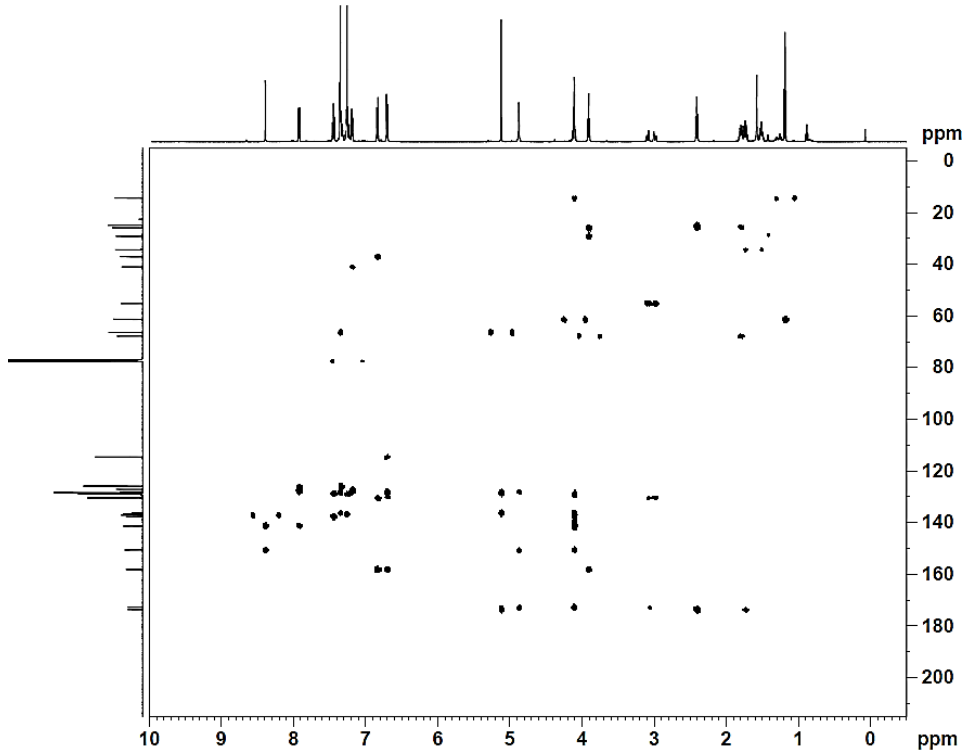

Figure S152: HMBC spectrum of compound **12** (^{1}H-NMR: 500 MHz, ^{13}C-NMR: 125 MHz, $CDCl_3$.

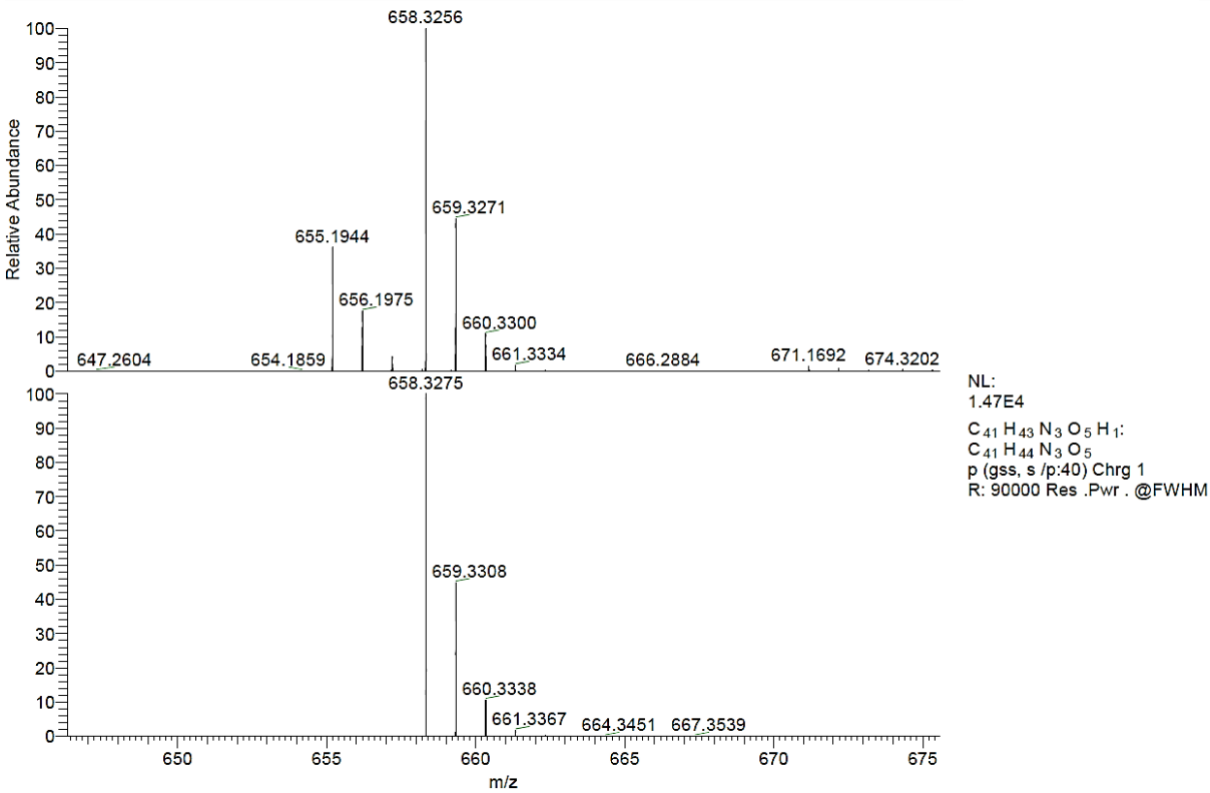

Figure S153: Measured (top) and calculated (bottom) HRMS-ESI spectrum of **12** in positive ion mode.

Compound 14

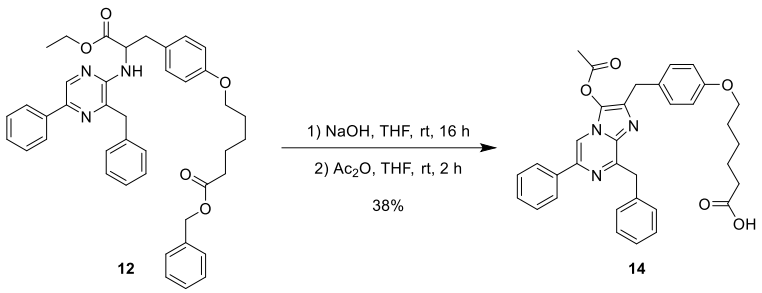

Scheme S32: Synthesis of compound **14**.

Based on the adapted procedure of Coutant *et al.*[20], the pyrazine **12** (275 mg, 0.42 mmol, 1.00 eq) and NaOH (66.9 mg, 1.67 mmol, 4.00 eq) were dissolved in dry THF (2.10 mL) under inert atmosphere. The solution was stirred in the dark for 16 h at rt. After such time, a solution of acetic anhydride (79.0 µL, 0.84 mmol, 2.00 eq) in dry THF (1.00 mL) was added, and continuously stirred in the dark for 2 h at rt. After the second step, the reaction mixture was diluted with EtOAc (~50 mL) and washed with distilled water (~ 100 mL, 2×), brine (~ 100 mL) and dried over $MgSO_4$. The crude was purified by flash column chromatography (*n*-pentane/EtOAc 4:1 → 2:1 → 1:1 + 0.1% HOAc (v/v)) to give the desired product **14** (124 mg, 0.22 mmol, 38%) as an orange oil.

TLC ($UV_{254\ nm}$): R_f = 0.45 (EtOAc/*n*-pentane 1:1 + 1% HOAc, v/v).

^{1}H NMR (500 MHz, $CDCl_3$): δ = 7.88-7.85 (m, 2H), 7.79-7.75 (m, 1H), 7.60 (d, ^3J(H,H) = 7.5 Hz, 2H), 7.46-7.36 (m, 3H), 7.30 (t, ^3J(H,H) = 7.8 Hz, 2H), 7.23-7.15 (m, 3H), 6.83-8.81 (m, 2H), 4.61 (s, 2H), 4.13 (s, 2H), 3.93 (t, ^3J(H,H) = 6.6 Hz, 2H), 2.39 (t, ^3J(H,H) = 7.5 Hz, 2H), 2.19 (s, 3H), 1.82-1.77 (m, 2H), 1.74-1.68 (m, 2H), 1.55-1.49 (m, 2H) ppm.

^{13}C NMR (125 MHz, $CDCl_3$): δ = 178.3 (C_q), 167.3 (C_q), 157.8 (C_q), 152.9 (C_q), 139.3 (C_q), 137.9 (C_q), 136.9 (C_q), 135.7 (C_q), 133.6 (C_q), 130.1 (*C*H), 130.1 (C_q), 130.0 (*C*H), 129.9 (2C; *C*H), 129.8 (C_q), 128.9 (2C; *C*H), 128.7 (*C*H), 128.4 (2C; *C*H), 126.6 (*C*H), 126.6 (2C; *C*H), 114.6 (2C; *C*H), 109.0 (*C*H), 67.8 (CH_2), 39.5 (CH_2), 33.9 (CH_2), 33.3 (CH_2), 29.1 (CH_2), 25.7 (CH_2), 24.6 (CH_2), 20.1 (CH_3) ppm.

HRMS-ESI (m/z): $[M-H]^-$ calcd for $C_{34}H_{32}N_3O_5$: 562.2347; found: 562.2350.

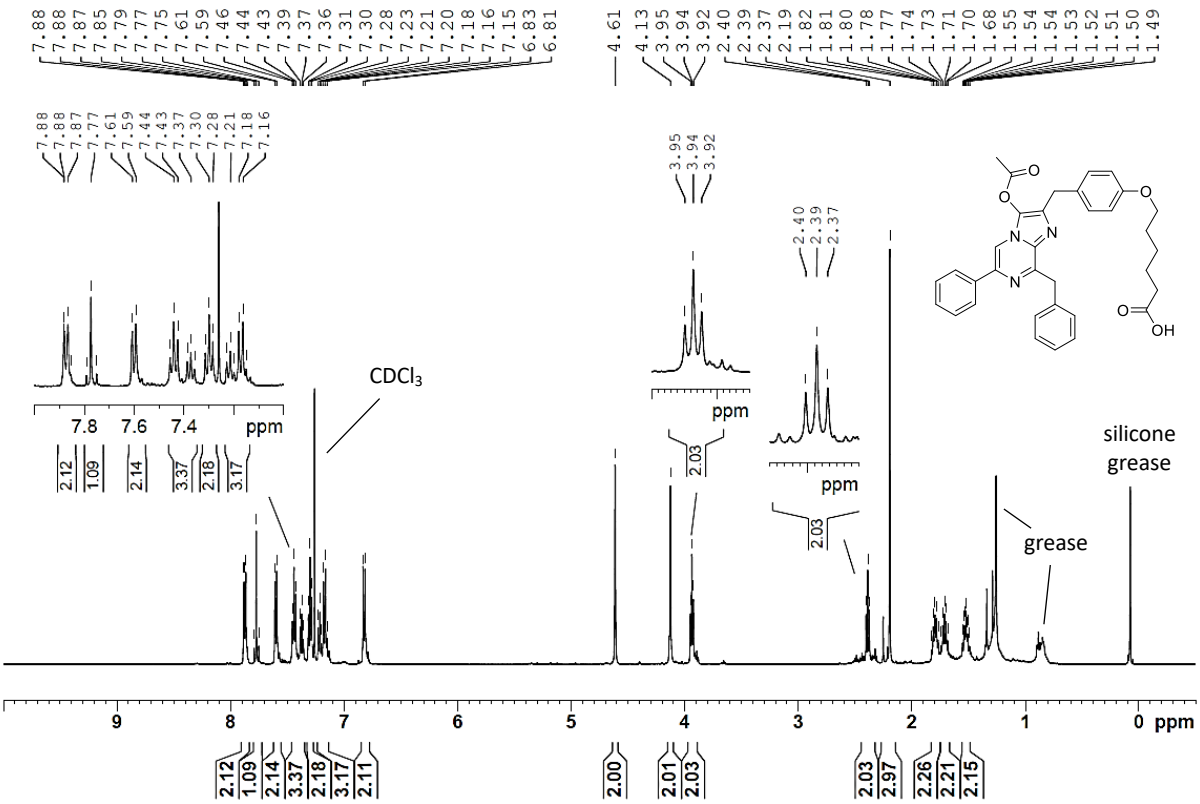

Figure S154: ^{1}H-NMR (500 MHz) spectrum of compound **14** in $CDCl_3$.

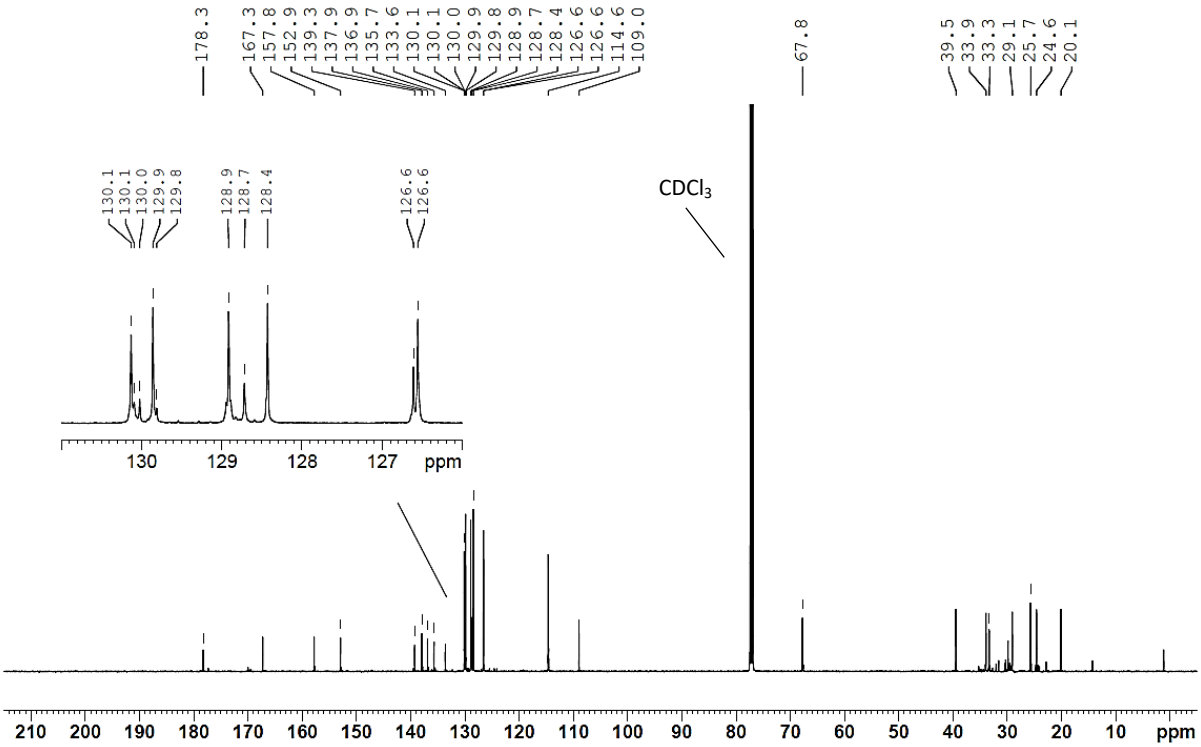

Figure S155: ^{13}C-NMR (125 MHz) spectrum of compound **14** in $CDCl_3$.

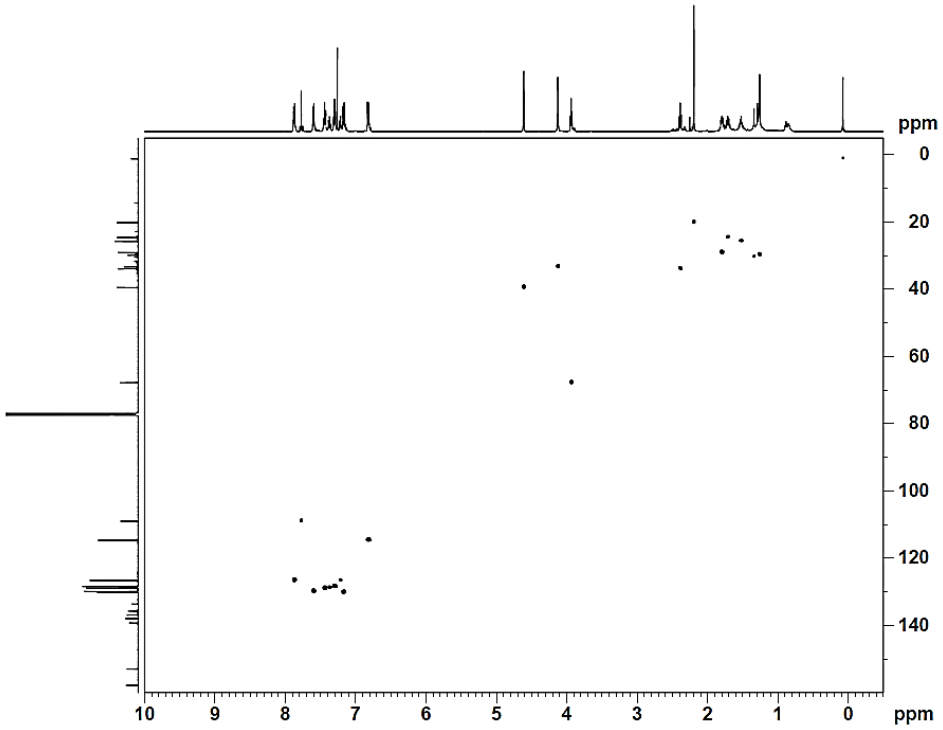

Figure S156: HSQC spectrum of compound **14** (^{1}H-NMR: 500 MHz, ^{13}C-NMR: 125 MHz, $CDCl_3$).

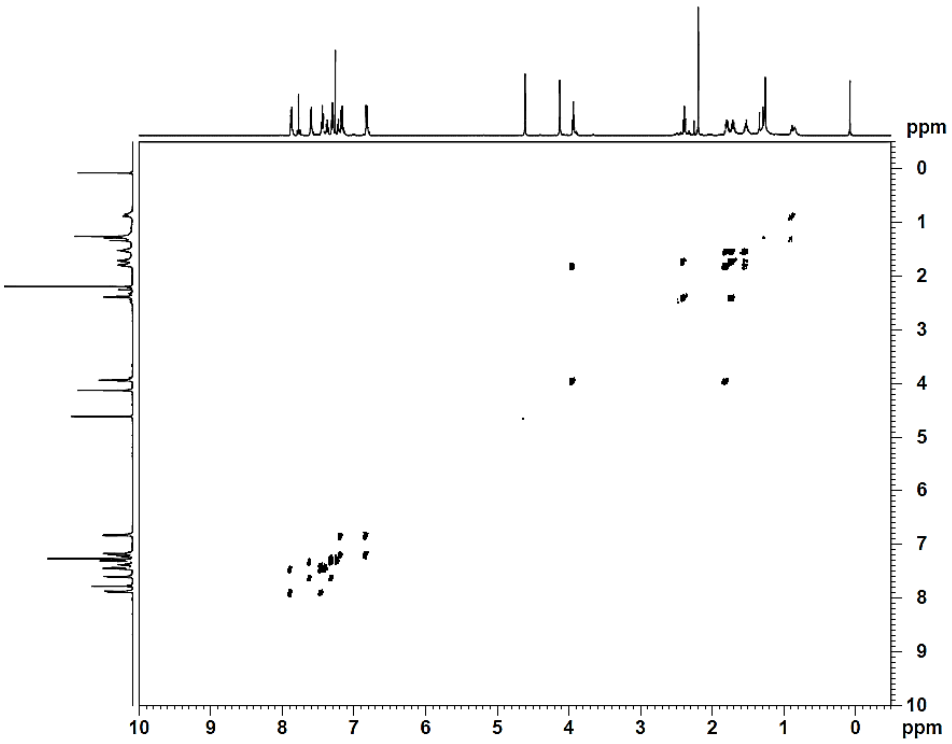

Figure S157: COSY spectrum of compound **14** (^{1}H-NMR: 500 MHz, $CDCl_3$).

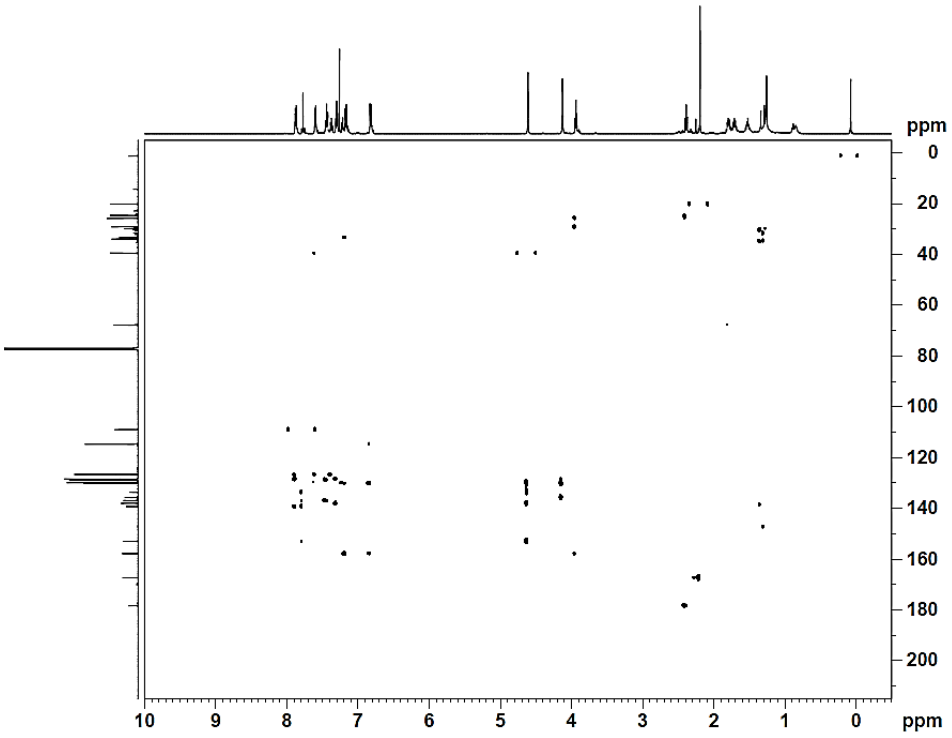

Figure S158: HMBC spectrum of compound **14** (^{1}H-NMR: 500 MHz, ^{13}C-NMR: 125 MHz, $CDCl_3$.

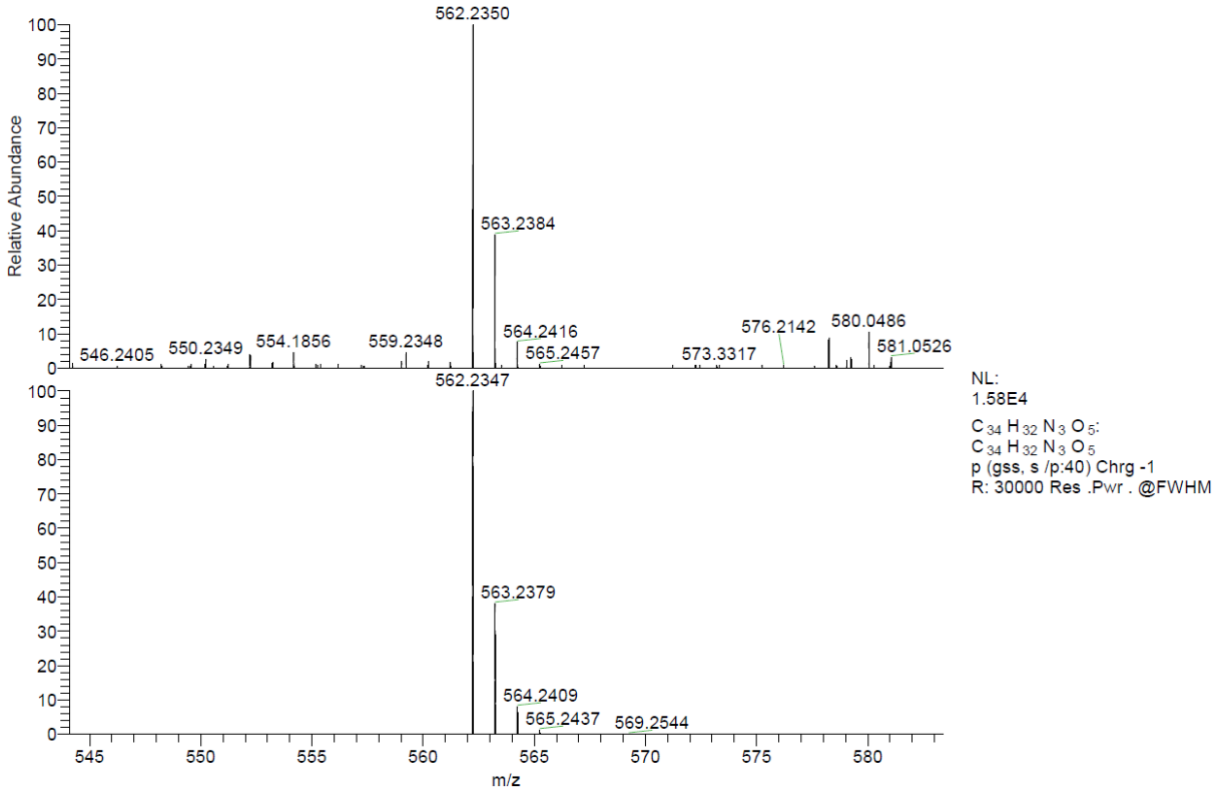

Figure S159: Measured (top) and calculated (bottom) HRMS-ESI spectrum of **14** in negative ion mode.

Synthesis of BODIPY-N_3 (64) and 2I-BODIPY-N_3 (65)

BODIPY-N_3 (**64**) and I_2-BODIPY-N_3 (**65**) were synthesized following the procedure that was previously reported by the Vázquez lab (Linden *et al.* [11]).

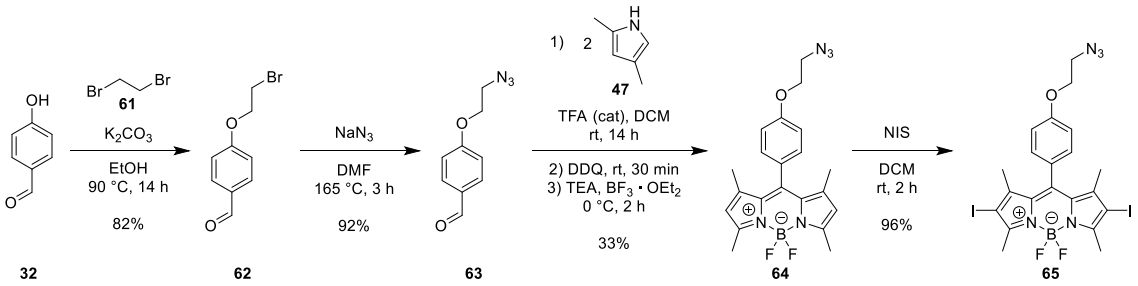

Scheme S33: Synthesis of BODIPY-N_3 (**64**) and I_2-BODIPY-N_3 (**65**) reported by Linden *et al.*[11] following an altered literature procedure of the Huang lab.[42] The halogenation step was performed according to Li *et al.*[43]

BODIPY-NH_2 (17)

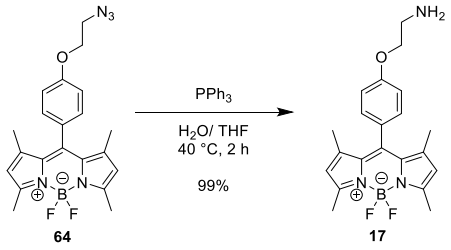

Scheme S34: Synthesis of BODIPY-NH_2 (**17**).

Triphenylphosphine (64.1 mg, 240 µmol, 2.00 eq) was suspended in degassed, distilled water (140 µL) under nitrogen atmosphere. Azide **64** (50.0 mg, 130 µmol, 1.00 eq) was dissolved in degassed THF (557 µL) and added to the suspension. The reaction mixture was heated to 40 °C and stirred for 2 h. The solvent was evaporated, and the obtained crude was purified by flash column chromatography (DCM/MeOH 98:2 → 95:5 → 90:10, (v/v) + 1% TEA) to yield compound **17** (49.4 mg, 129 µmol, 99%) as an orange solid.

TLC ($UV_{254\ nm}$): R_f = 0.41 (DCM/MeOH 19:1 + 1% TEA, v/v).

^{1}H-NMR (500 MHz, $CDCl_3$): δ = 7.17 (dt, ^3J(H,H) = 8.7 Hz, ^4J(H,H) = 2.2 Hz, 2H), 7.02 (dt, ^3J(H,H) = 8.7 Hz, ^4J(H,H) = 2.2 Hz, 2H), 5.97 (s, 2H), 4.10 (t, ^3J(H,H) = 5.1 Hz, 2H), 3.20 (t, ^3J(H,H) = 5.1 Hz, 2H), 2.55 (s, 6H), 1.42 (s, 6H) ppm.

^{13}C-NMR (125 MHz, $CDCl_3$): δ = 159.3 (2C; C_q), 155.5 (2C; C_q), 143.2 (C_q), 141.8 (C_q), 131.9 (C_q), 129.4 (2C; *C*H), 127.6 (2C; C_q), 121.3 (2C; *C*H), 115.2 (2C; *C*H), 69.1 (CH_2), 41.2 (CH_2), 14.8 (2C; CH_3), 14.7 (2C; CH_3) ppm.

^{19}F-NMR (282 MHz, $CDCl_3$): δ = -146.3 ppm (dd, ^1J(B,F) = 33.6 Hz, 2F, BF_2) ppm.

HRMS-ESI (*m/z*): $[M + H]^+$ calcd for $C_{21}H_{25}BF_2N_3O$: 384.2057; found: 384.2044.

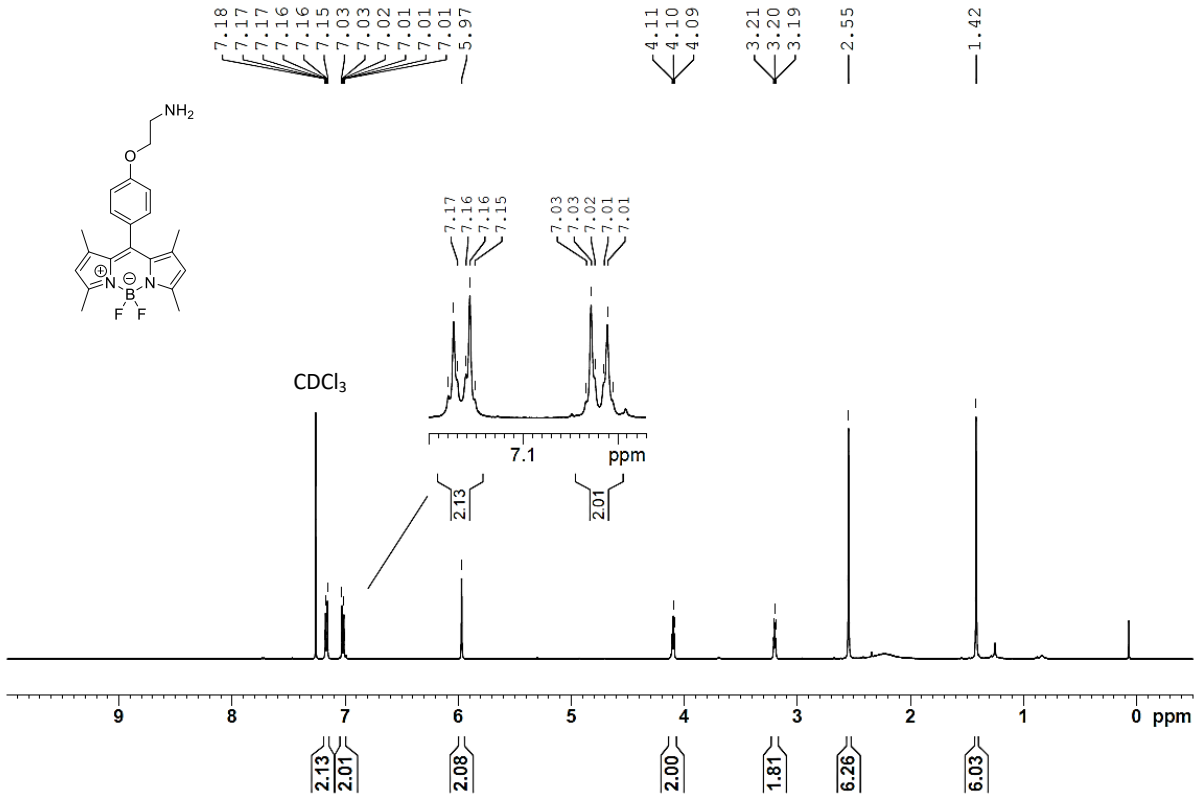

Figure S160: ^{1}H-NMR (500 MHz) spectrum of compound **17** in $CDCl_3$.

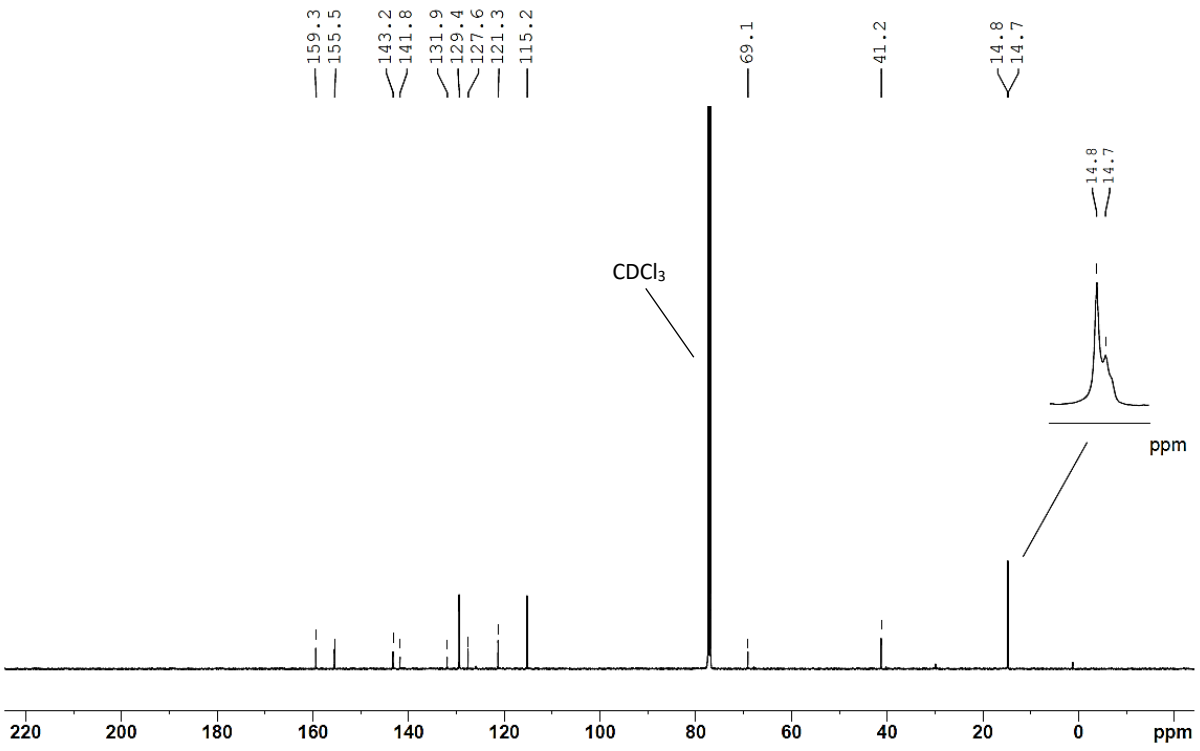

Figure S161: ^{13}C-NMR (125 MHz) spectrum of compound **17** in $CDCl_3$.

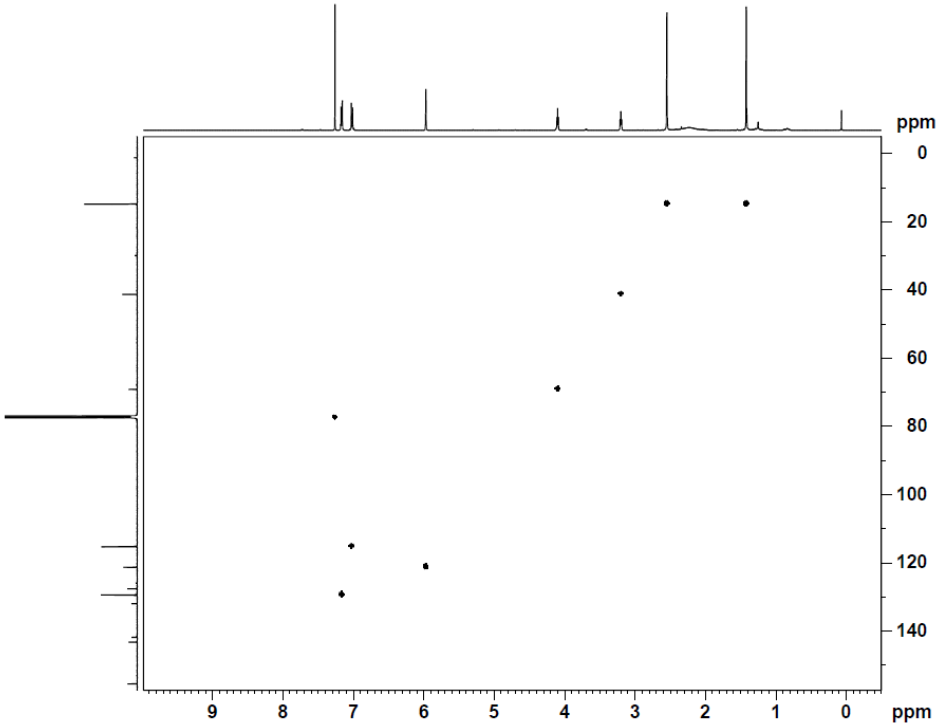

Figure S162: HSQC spectrum of compound **17** (^{1}H-NMR: 500 MHz, ^{13}C-NMR: 125 MHz, $CDCl_3$).

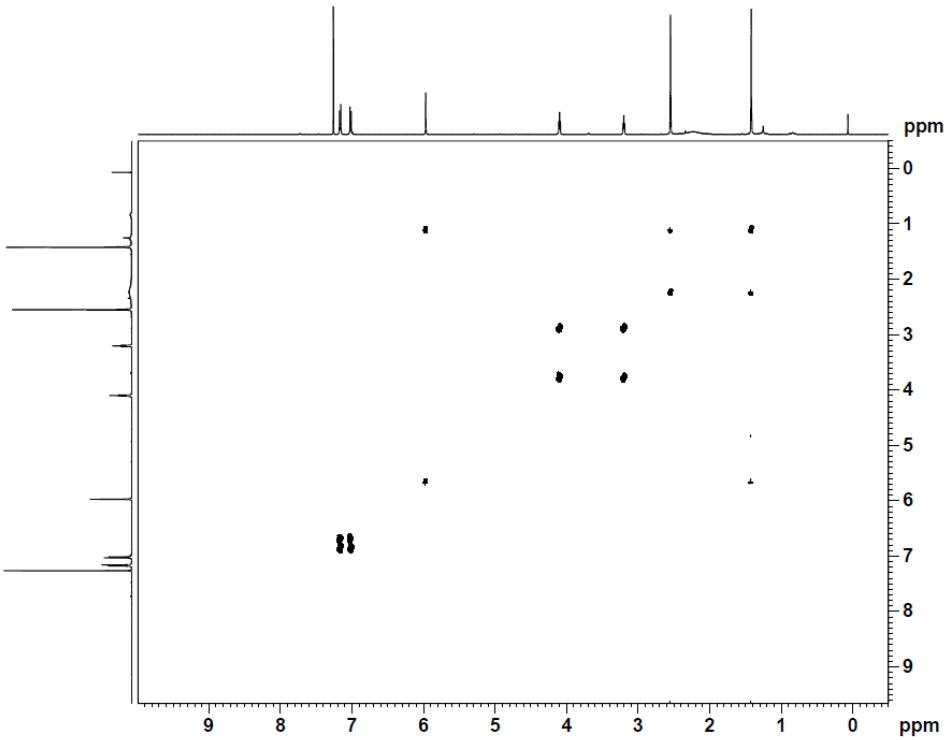

Figure S163: COSY spectrum of compound **17** (^{1}H-NMR: 500 MHz, $CDCl_3$).

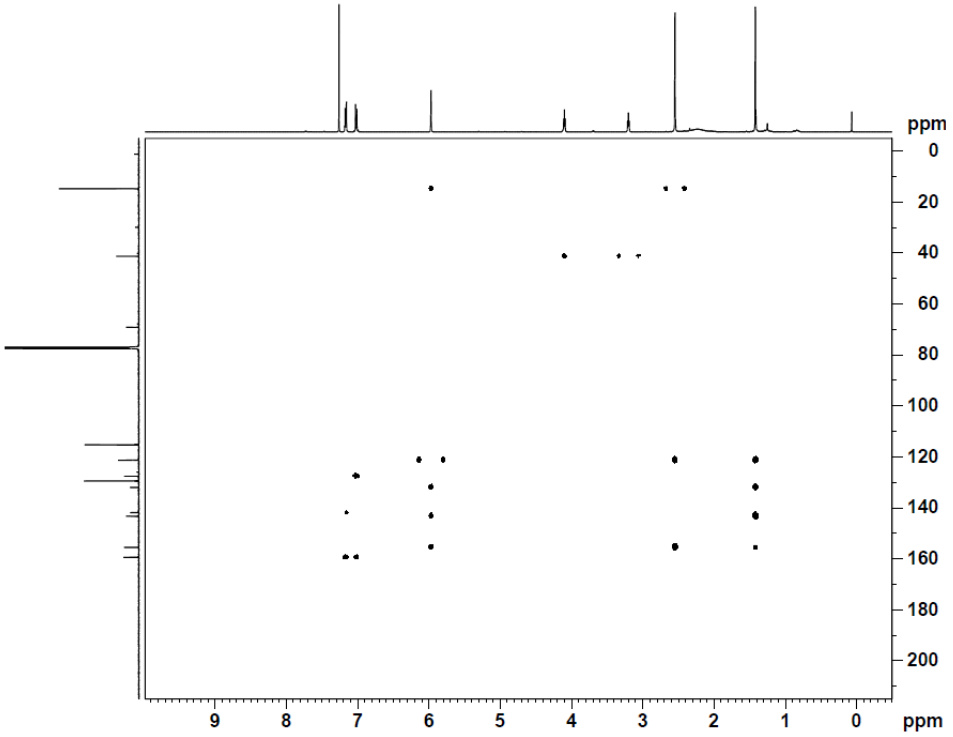

Figure S164: HMBC spectrum of compound **17** (^{1}H-NMR: 500 MHz, ^{13}C-NMR: 125 MHz, $CDCl_3$).

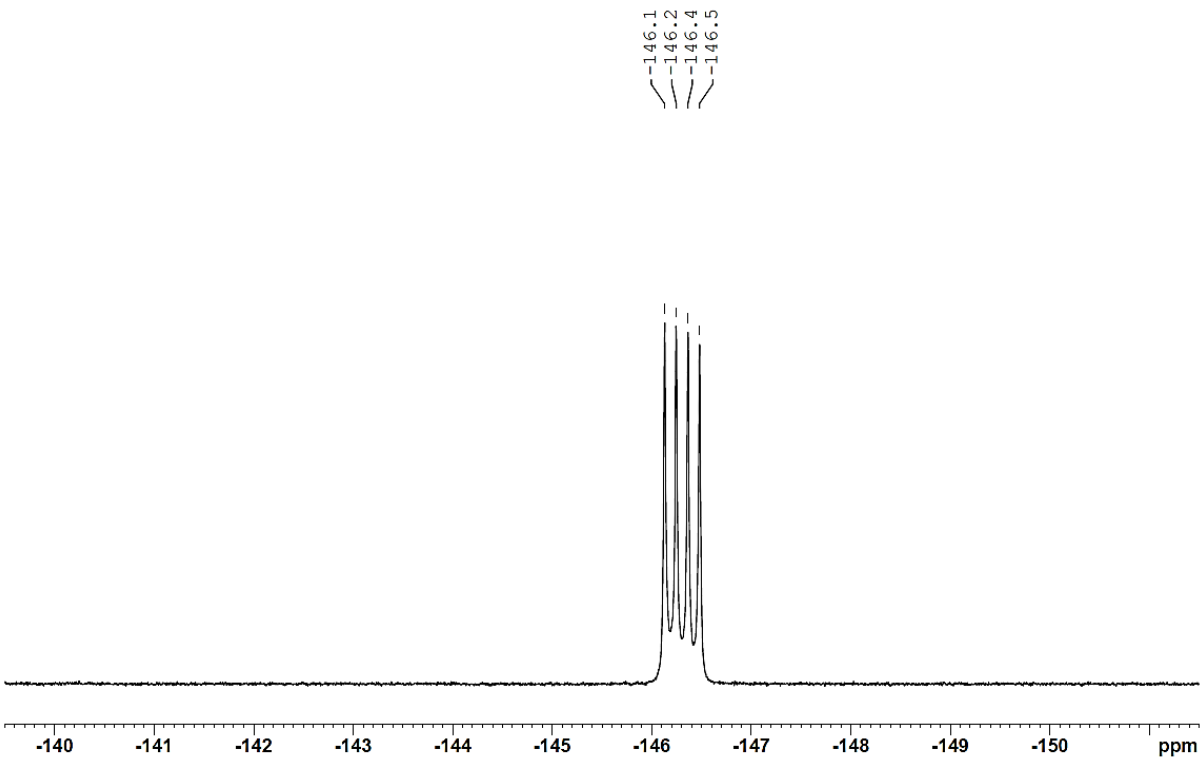

Figure S165: ^{19}F-NMR (282 MHz) spectrum of compound **17** in $CDCl_3$.

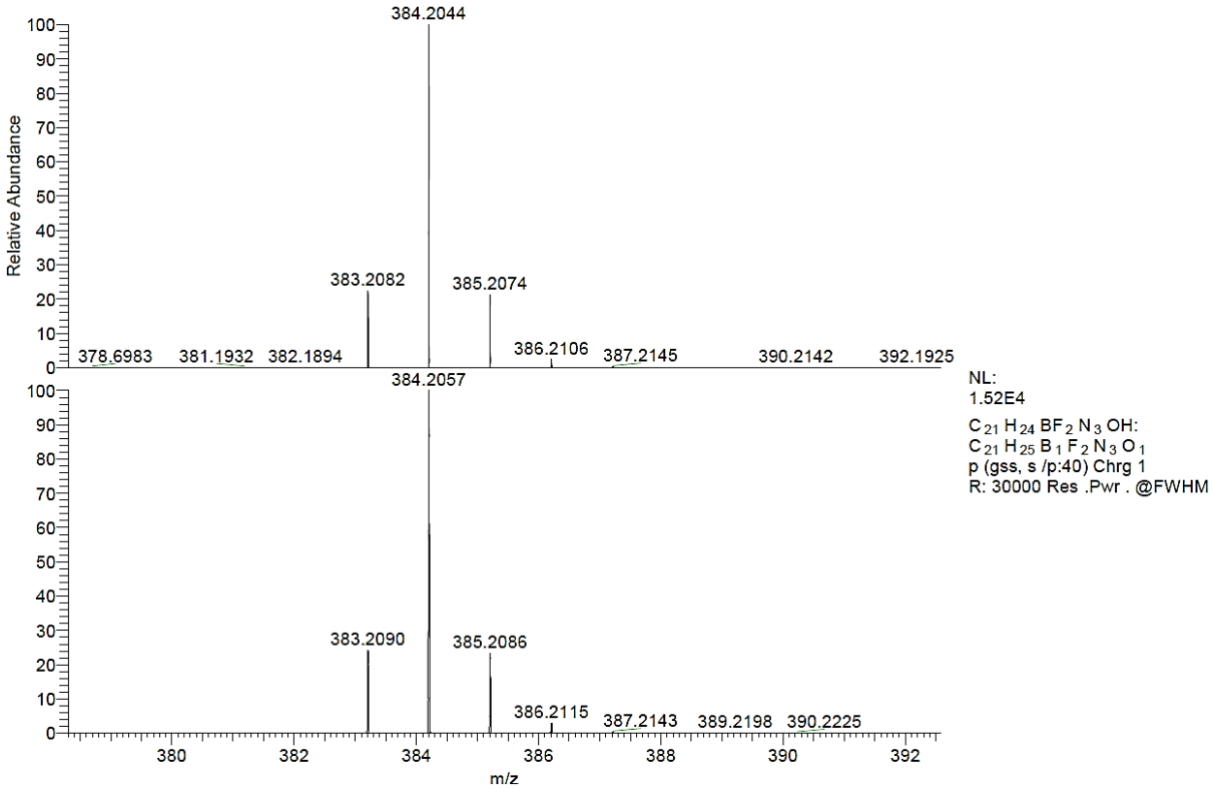

Figure S166: Measured (top) and calculated (bottom) HRMS-ESI spectrum of **17** in positive ion mode.

2I-BODIPY-NH_2 (18)

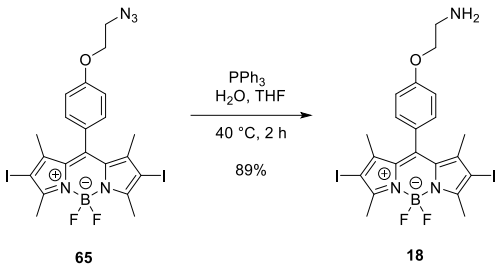

Scheme S35: Synthesis of compound 2I-BODIPY-NH_2 (**18**).

Triphenylphosphine (32.3 mg, 123 µmol, 2.00 eq) was suspended in degassed, distilled water (70.0 µL) under nitrogen atmosphere. Azide **65** (40.6 mg, 61.4 µmol, 1.00 eq) was dissolved in degassed THF (285 µL) and added to the suspension. The reaction mixture was heated to 40 °C and stirred for 2 h. The solvent was evaporated, and the obtained crude was purified by flash column chromatography (DCM/MeOH 10:1, (v/v) + 1% TEA) to yield the compound **18** (34.7 mg, 54.6 µmol, 89%) as a pink solid.

TLC ($UV_{254\ nm}$): R_f = 0.25 (DCM/MeOH 10:1 + 0.1 % TFA, v/v).

^{1}H NMR (500 MHz, $CDCl_3$): δ = 7.14 (d, ^3J(H,H) = 8.2 Hz, 2H), 7.07 (d, ^3J(H,H) = 8.2 Hz, 2H), 4.17 (s, 2H), 3.28 (s, 2H), 2.63 (s, 6H), 1.43 (s, 6H) ppm.

^{13}C NMR (125 MHz, $CDCl_3$): δ = 159.5 (C_q), 156.8 (2C; C_q), 145.4 (2C; C_q), 141.4 (C_q), 131.8 (C_q), 129.3 (2C; *C*H), 127.4 (2C; C_q), 115.6 (2C; *C*H), 85.8 (2C; C_q), 68.2 (CH_2), 40.9 (CH_2), 17.4 (2C; CH_3), 16.2 (2C; CH_3) ppm.

^{19}F-NMR (282 MHz, $CDCl_3$): δ = -145.7 (dd, ^1J(B, F) = 32.5 Hz, 2F, BF_2) ppm.

HRMS-ESI (m/z): calcd for $[M+H]^+$ $C_{21}H_{23}BF_2I_2N_3O$: 635.9990; found: 635.9975.

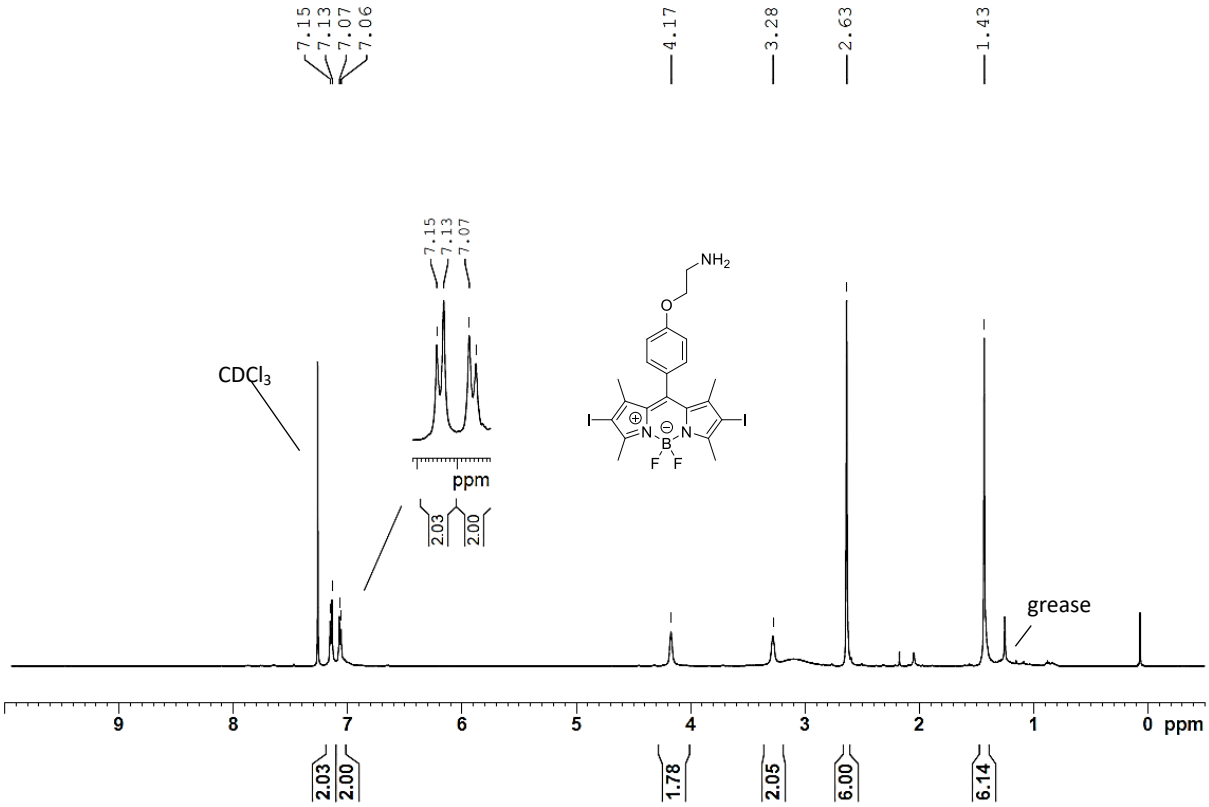

Figure S167: ^{1}H-NMR (500 MHz) spectrum of compound **18** in $CDCl_3$.

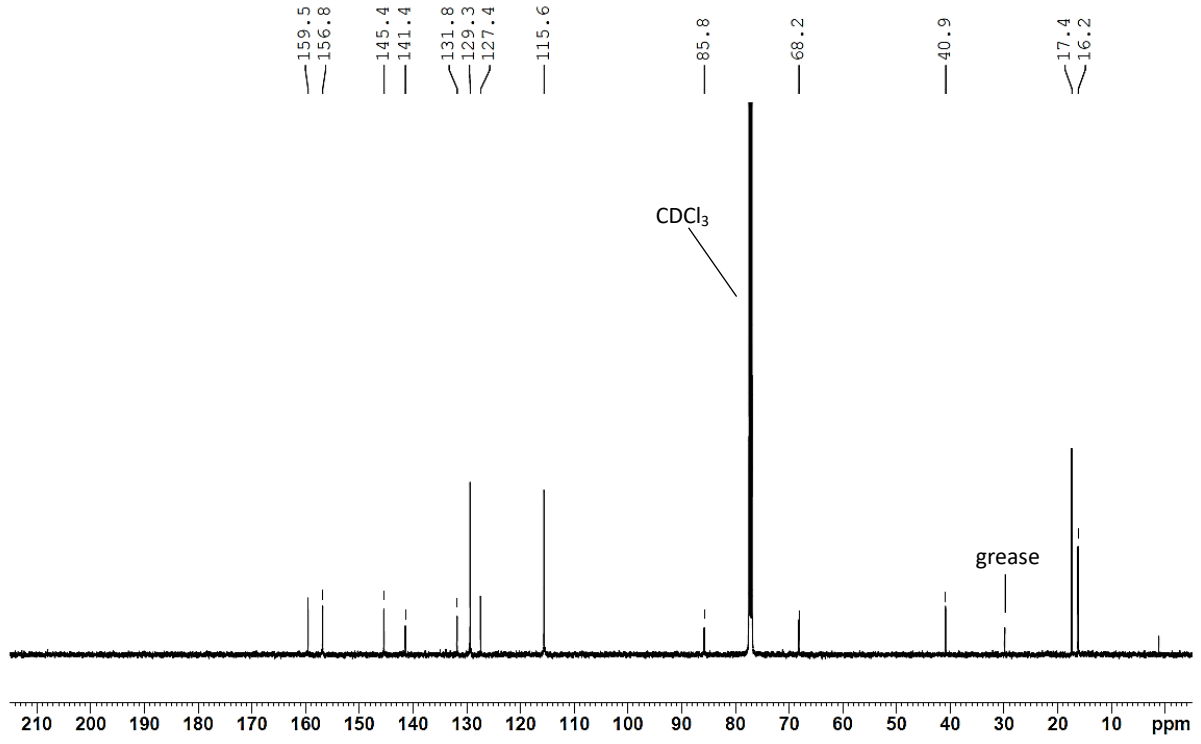

Figure S168: ^{13}C-NMR (125 MHz) spectrum of compound **18** in $CDCl_3$.

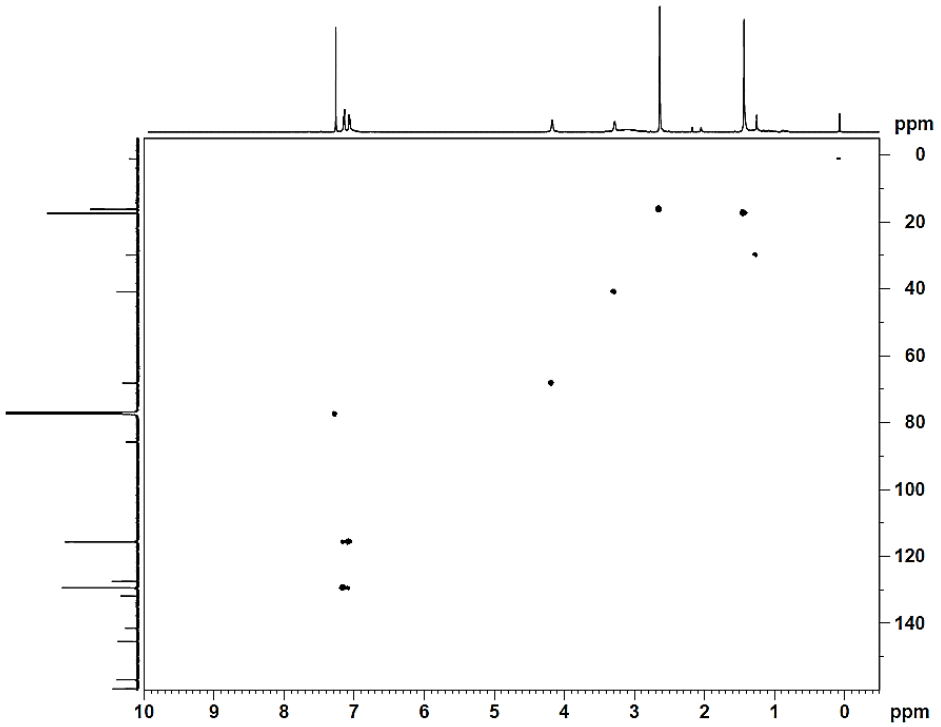

Figure S169: HSQC spectrum of compound **18** (^{1}H-NMR: 500 MHz, ^{13}C-NMR: 125 MHz, $CDCl_3$).

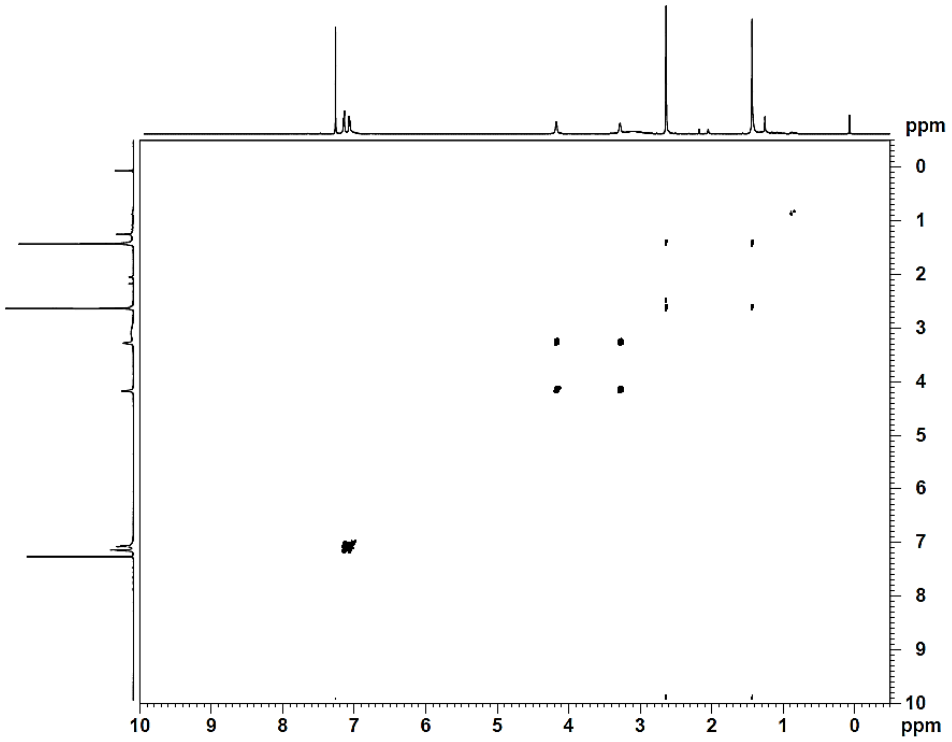

Figure S170: COSY spectrum of compound **18** (^{1}H-NMR: 500 MHz, $CDCl_3$).

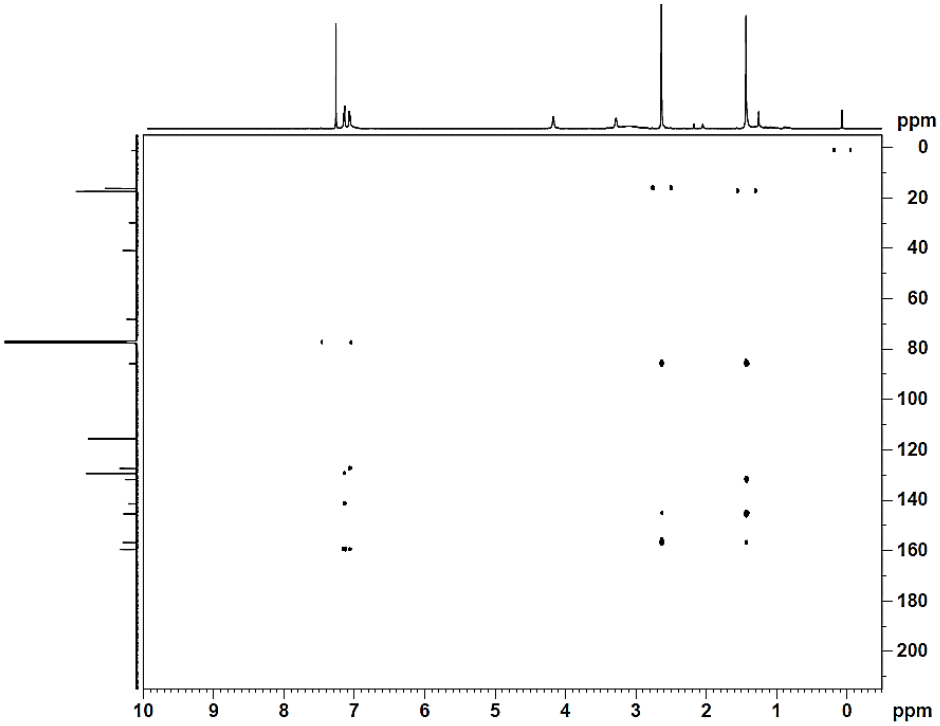

Figure S171: HMBC spectrum of compound **18** (^{1}H-NMR: 500 MHz, ^{13}C-NMR: 125 MHz, $CDCl_3$).

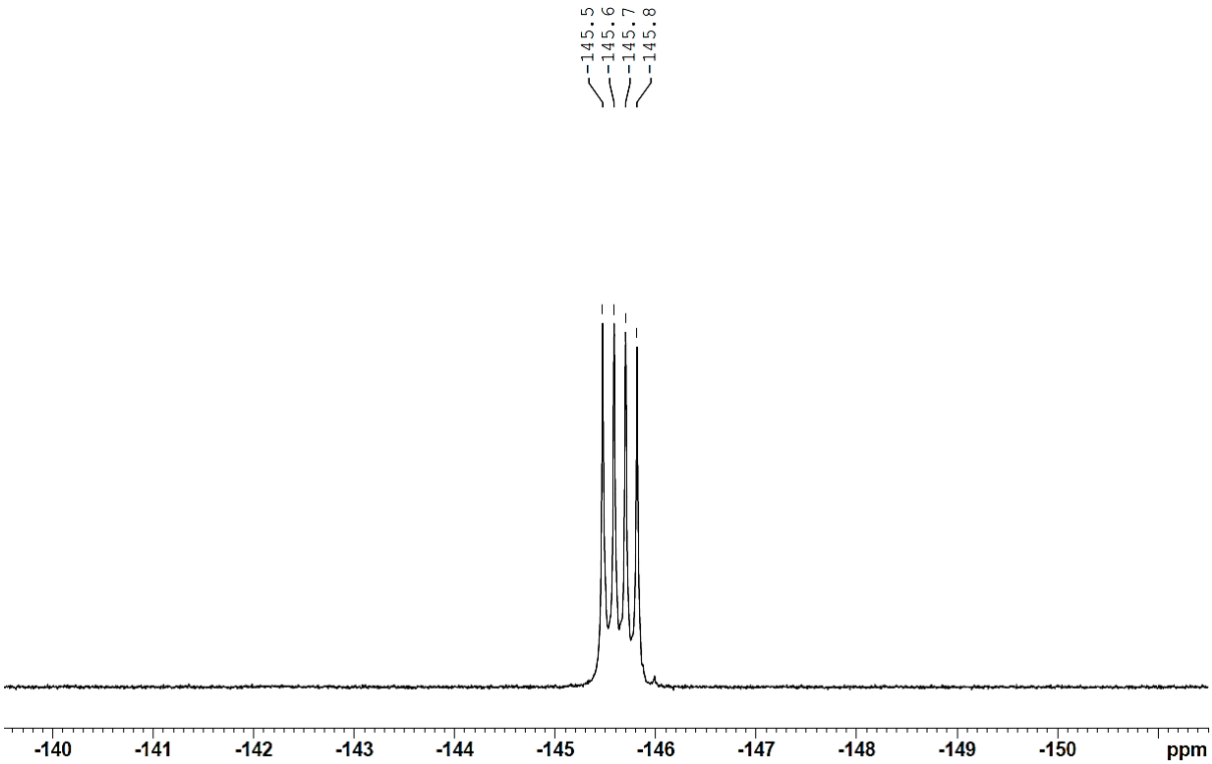

Figure S172: ^{19}F-NMR (282 MHz) spectrum of compound **18** in $CDCl_3$.

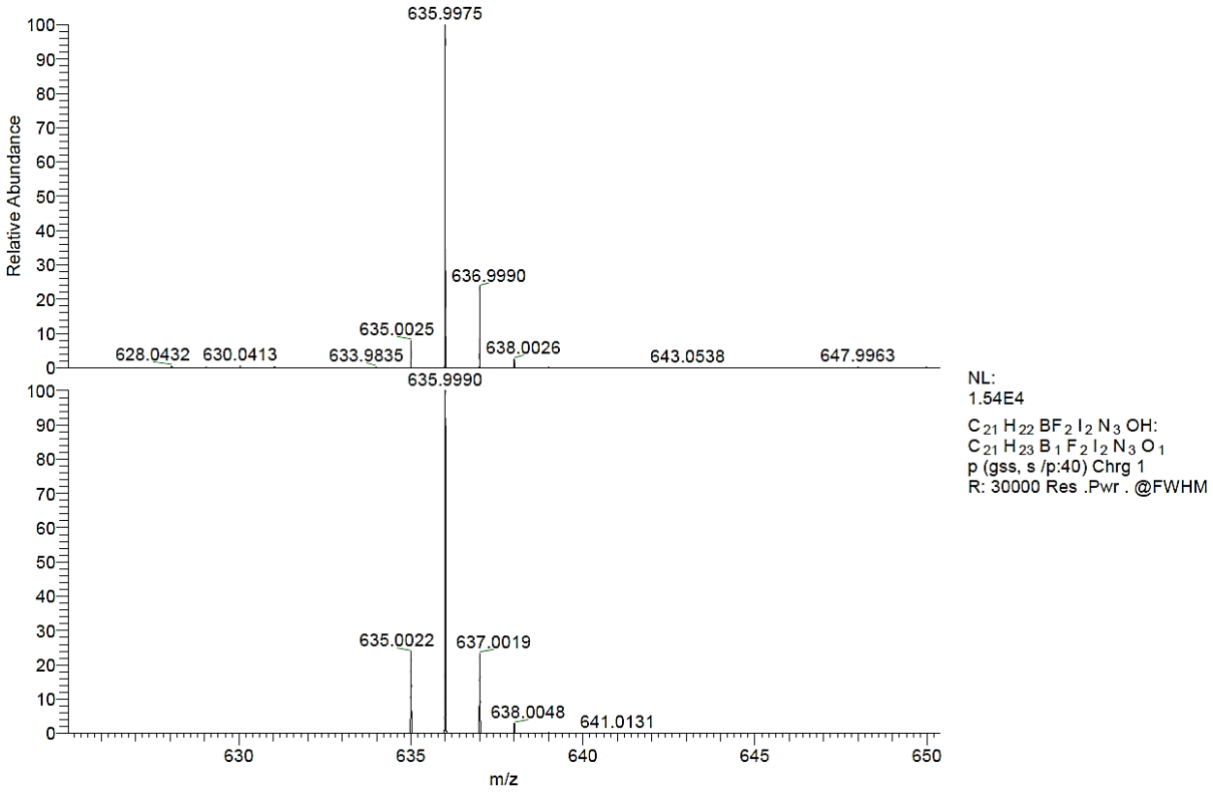

Figure S173: Measured (top) and calculated (bottom) HRMS-ESI spectrum of **18** in positive ion mode.

Short-linker BODIPY-CTZ Conjugate (3)

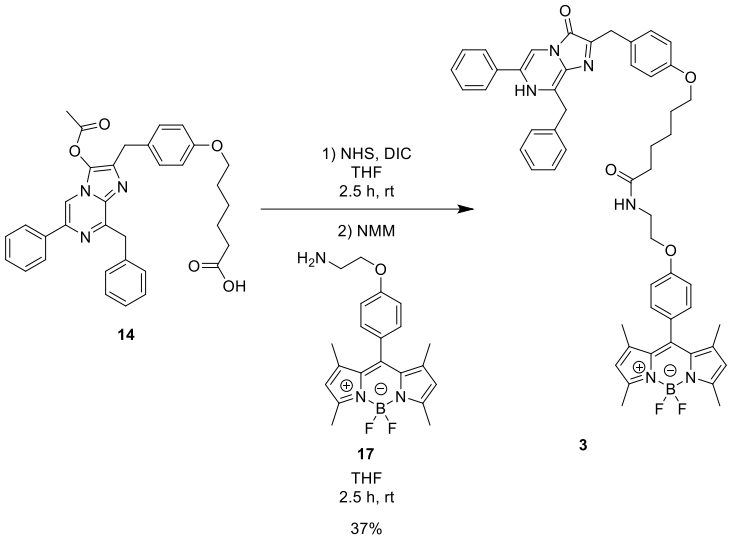

Scheme S36: Synthesis of short-linker BODIPY-CTZ conjugate **3**.

Under an inert atmosphere, coelenterazine **14** (47.9 mg, 85.0 µmol, 1.00 eq) was dissolved in dry THF (424 µL). NHS (19.5 mg, 170 µmol, 2.00 eq) and DIC (26.3 µL, 170 µmol, 2.00 eq) were added, and the reaction mixture was shaken at rt for 2.5 h. The solvent was removed under reduced pressure, and the remaining residue was purified using a Pure C-810 Flash system (Büchi, column: FP ECOFLEX C18 12 g, 0% → 100% MeOH for 16 min, 0.1% formic acid) to give the coelenterazine NHS ester as an orange solid with quantitative yield. The coelenterazine-NHS ester (56.2, 85.0 µmol, 1.00 eq) was dissolved in dry THF (213 µL) under inert atmosphere, and BODIPY-NH_2 (**17**, 32.6 mg, 85.0 µmol, 1.00 eq) was added. NMM (18.7 µL, 170 µmol, 2.00 eq) was added to the reaction mixture, which was shaken at rt for 2.5 h. The solvent was diluted with DCM (~50 mL) and washed with distilled water (~50 mL, 1×). The aqueous phase was extracted with DCM (~50 mL, 3×) and the combined organic phase was washed with brine (~50 mL, 2×) and dried over $MgSO_4$. The crude was purified by flash column chromatography (DCM/MeOH 97:3, (v/v)). After removing the solvent under reduced pressure, the short-linker BODIPY-CTZ conjugate (**3**, 27.8 mg, 31.3 µmol, 37%) was obtained as an orange solid.

TLC ($UV_{254\ nm}$): R_f = 0.64 (DCM/MeOH 9:1, v/v).

^{1}H NMR (500 MHz, MeOD-d_4): δ = 7.86 (s, 1H), 7.72-7.70 (m, 2H), 7.47-7.42 (m, 2H), 7.40-7.37 (m, 3H), 7.26-7.11 (m, 9H), 7.09-7.07 (m, 2H), 6.78 (d, ^3J(H,H) = 8.8 Hz, 2H), 6.01 (s, 2H), 4.38 (s, 2H), 4.13-4.09 (m, 2H), 4.08-4.07 (m, 2H), 3.90 (t, ^3J(H,H) = 6.6 Hz, 2H), 2.46 (s, 6H), 2.25 (t, ^3J(H,H) = 7.7 Hz, 2H), 1.77-1.71 (m, 2H), 1.69-1.65 (m, 2H), 1.51-147 (m, 2H), 1.40 (s, 6 H) ppm.

^{13}C NMR (125 MHz, MeOD-d_4): δ = 176.5 (2C; C_q), 173.4 (C_q), 161.1 (2C; C_q), 159.1 (2C; C_q), 156.4 (2C; C_q), 144.5 (2C; C_q), 143.6 (C_q), 138.1 (C_q), 133.0 (C_q), 131.7 (C_q), 130.8 (*C*H), 130.6 (C_q), 130.5 (3C; *C*H), 130.1 (3C; *C*H), 129.8 (6C; *C*H), 128.4 (2C; C_q), 128.2 (C_q), 127.9 (2C; *C*H), 122.1 (2C; *C*H), 116.4 (2C; *C*H), 115.5 (2C; *C*H), 68.7 (*C*H_2), 67.7 (*C*H_2), 40.1 (*C*H_2), 38.4 (*C*H_2), 36.9 (*C*H_2), 35.5 (*C*H_2), 30.1 (*C*H_2), 26.7 (*C*H_2), 26.7 (*C*H_2), 21.3 (2C; *C*H_3), 14.8 (2C; *C*H_3) ppm.

^{19}F NMR (282 MHz, MeOD-d_4): δ = -147.1 (dd, ^1J(B, F) = 32.6 Hz, 2F, BF_2) ppm.

HRMS-ESI (m/z): $[M + H]^+$ calcd for $C_{53}H_{54}BF_2N_6O_4$: 887.4271; found: 887.4259.

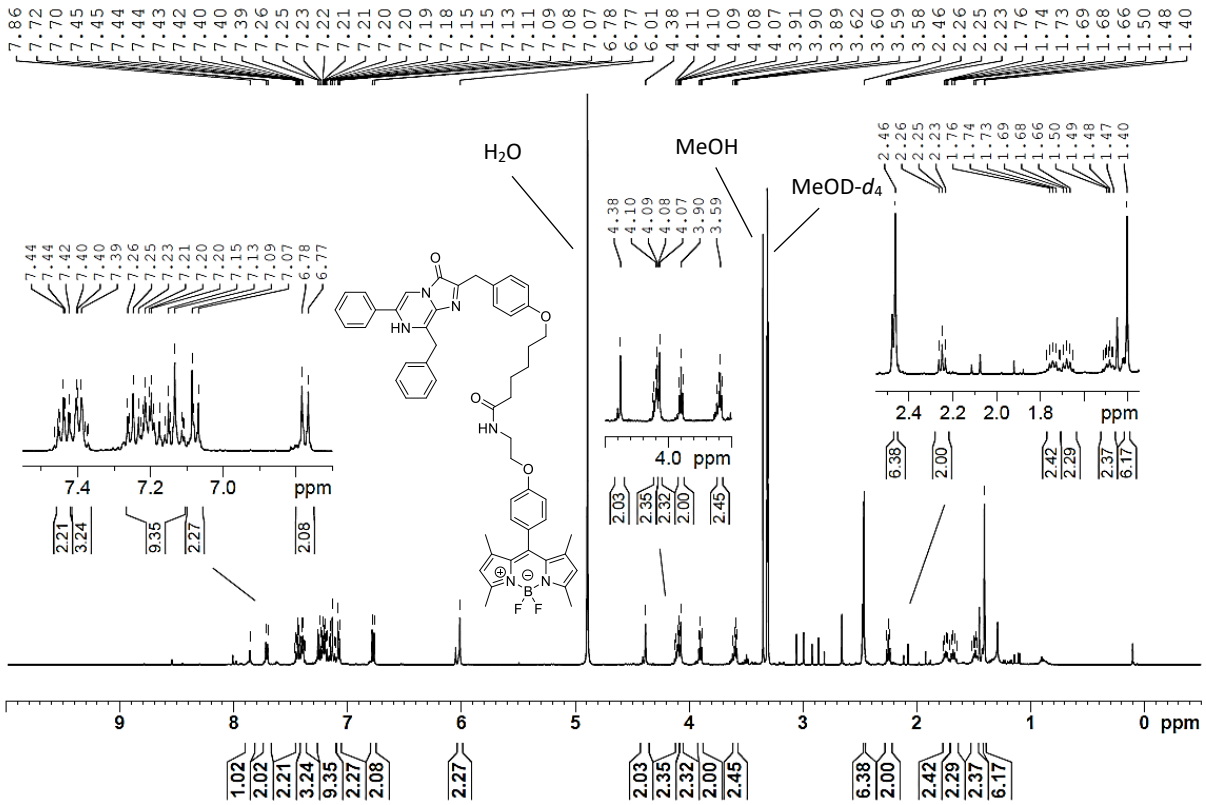

Figure S174: ^{1}H-NMR (500 MHz) spectrum of compound **3** in MeOD-d_4.

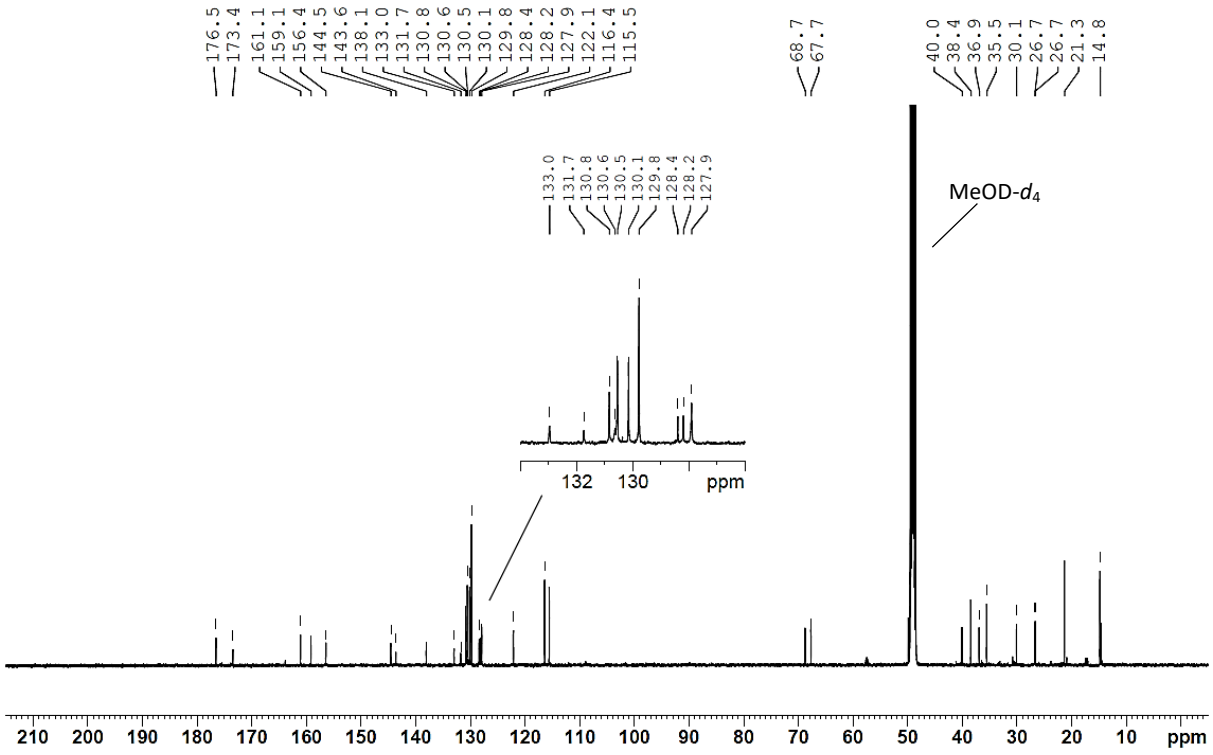

Figure S175: ^{13}C-NMR (125 MHz) spectrum of compound **3** in MeOD-d_4.

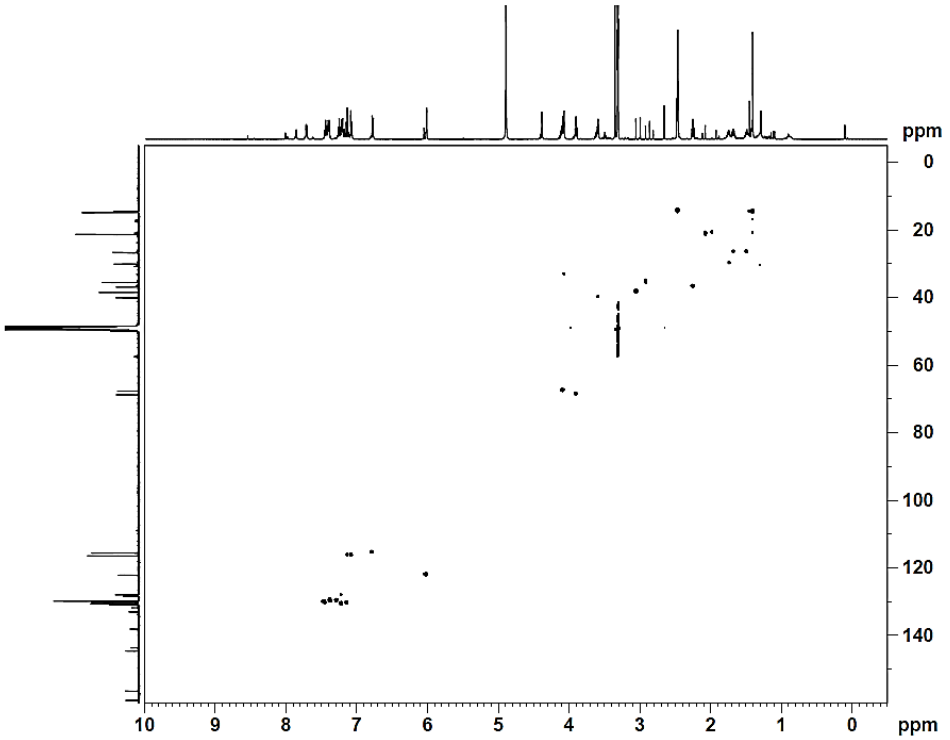

Figure S176: HSQC spectrum of compound **3** (^{1}H-NMR: 500 MHz, ^{13}C-NMR: 125 MHz, MeOD-d_4).

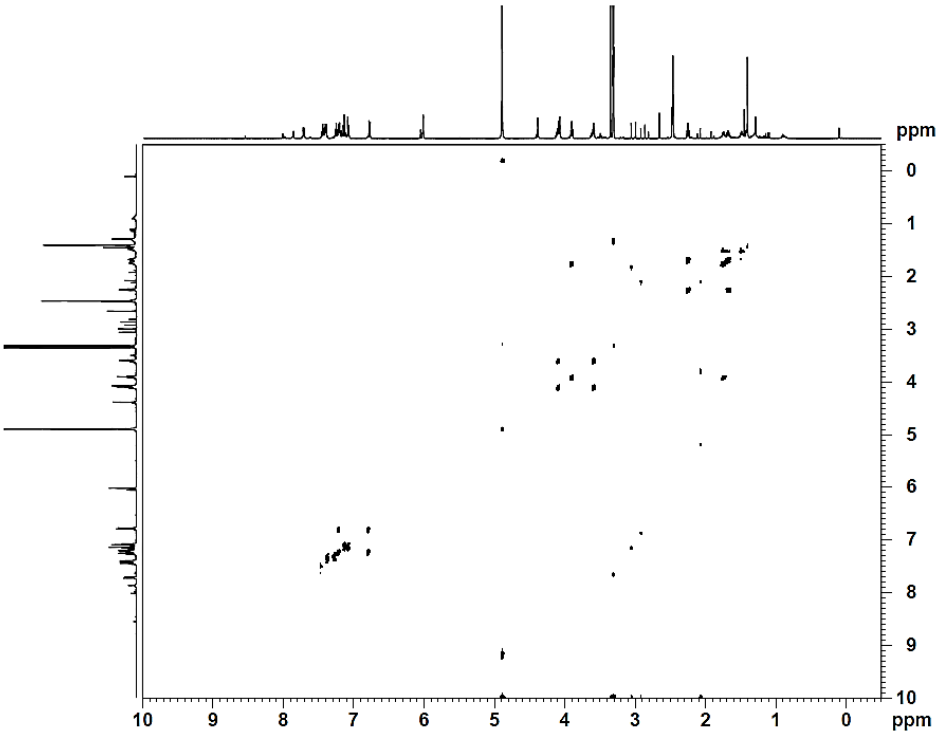

Figure S177: COSY spectrum of compound **3** (^{1}H-NMR: 500 MHz, MeOD-d_4).

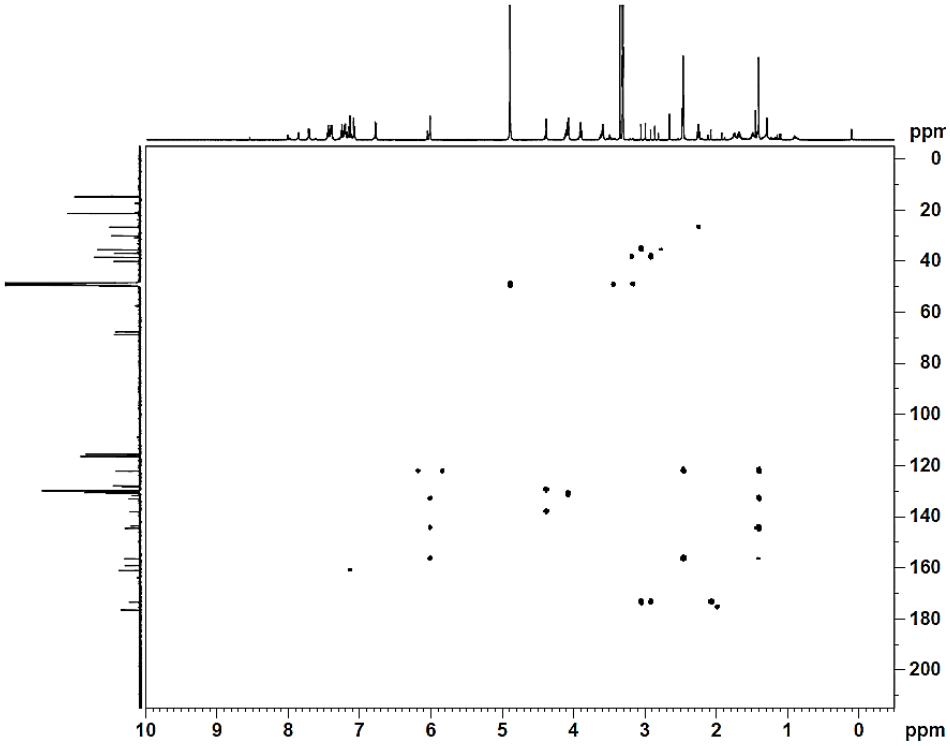

Figure S178: HMBC spectrum of compound **3** (^{1}H-NMR: 500 MHz, ^{13}C-NMR: 125 MHz, MeOD-d_4).

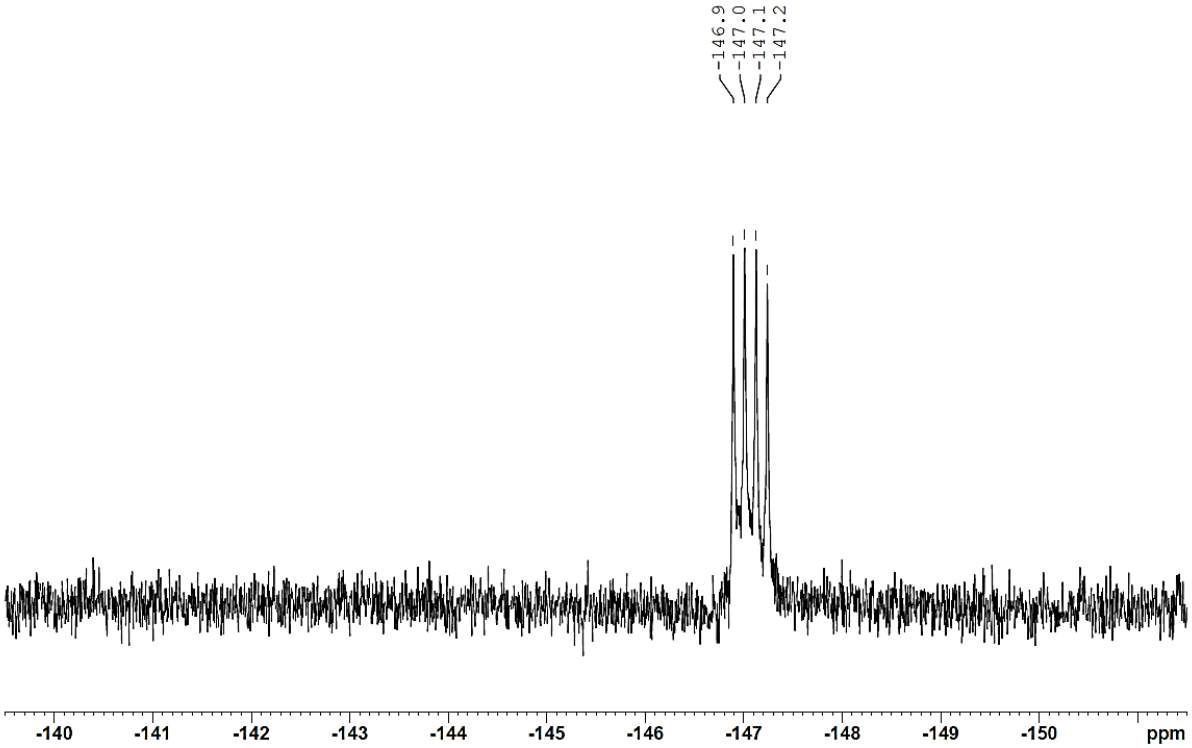

Figure S179: ^{19}F-NMR (282 MHz) spectrum of compound **3** in MeOD-d_4.

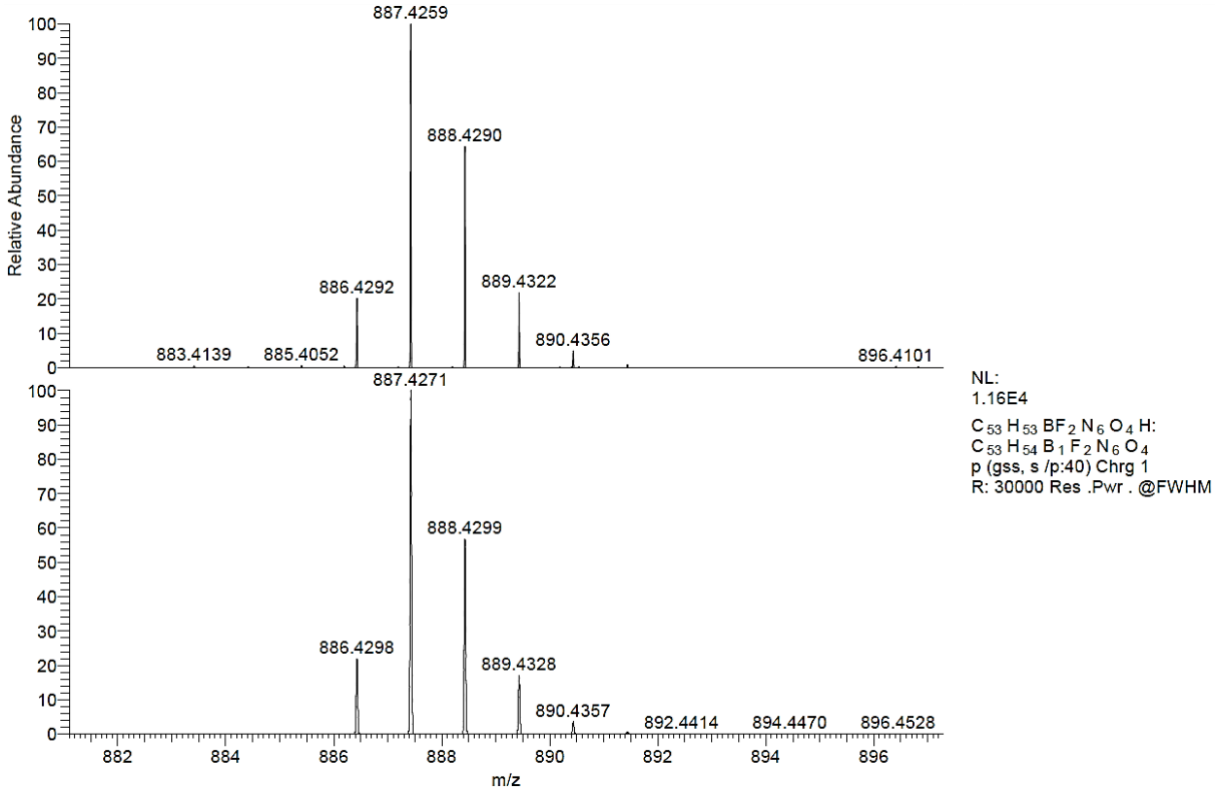

Figure S180: Measured (top) and calculated (bottom) HRMS-ESI spectrum of **3** in positive ion mode.

Short-linker 2I-BODIPY-CTZ Conjugate (4)

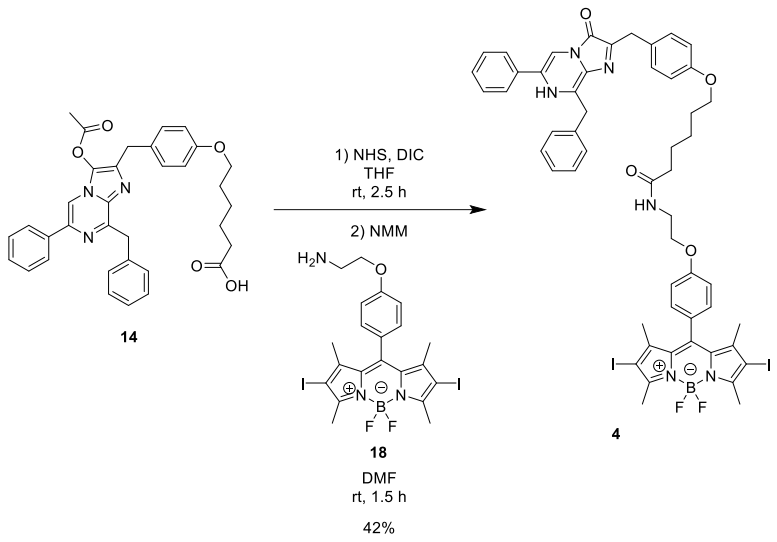

Scheme S37: Synthesis of short-linker 2I-BODIPY-CTZ conjugate **4**.

Under an inert atmosphere, coelenterazine **14** (34.1 mg, 60.5 µmol, 1.00 eq) was dissolved in dry THF (302 µL). NHS (13.9 mg, 121 µmol, 2.00 eq) and DIC (18.7 µL, 121 µmol, 2.00 eq) were added, and the reaction mixture was shaken at rt for 2.5 h. The solvent was removed under reduced pressure and the remaining residue was purified using a Pure C-810 Flash system (Büchi, column: FP ECOFLEX C18 12 g, 0% → 100% MeOH for 16 min, 0.1% formic acid) to give the coelenterazine-NHS ester as an orange solid with quantitative yield. The obtained NHS ester (40.0 mg, 60.5 µmol, 1.00 eq) was dissolved in dry, degassed DMF (303 µL) under inert atmosphere. 2I-BODIPY-NH_2 (**18**, 38.4 mg, 60.5 µmol, 1.00 eq) and NMM (13.3 µL, 121 µmol, 2.00 eq) were added and the reaction mixture was shaken at rt in the dark for 1.5 h. The mixture was diluted with DCM (~50 mL) and washed with distilled water (~50 mL, 1×). The aqueous phase was extracted with DCM (~50 mL, 3×) and the combined organic phase was washed with brine (~50 mL, 2×) and dried over $MgSO_4$. The crude was purified by flash column chromatography (DCM/MeOH 97:3, (v/v)). After removing the solvent under reduced pressure, the short-linker 2I-BODIPY-CTZ conjugate (**4**, 28.9 mg, 25.4 µmol, 42%) was obtained as a pink solid.

TLC ($UV_{254\ nm}$): R_f = 0.58 (DCM/MeOH 9:1, v/v).

^{1}H NMR (500 MHz, MeOD-*d*$_4$): δ = 7.64 (s, 2H), 7.50-7.47 (m, 3H), 7.38 (m, 3H), 7.29-7.26 (m, 2H), 7.23-7.21 (m, 3H), 7.17-7.15 (m, 2H), 7.13-7.11 (m, 2H), 6.79 (d, ^3J(H,H) = 8.6 Hz, 2H), 4.38 (s, 2H), 4.13 (t, ^3J(H,H) = 5.4 Hz, 2H), 4.06 (s, 2H), 3.91 (t, ^3J(H,H) = 6.3 Hz, 2H), 3.63-3.60 (m, 2H), 2.55 (s, 6H), 2.28-2.25 (m, 2H), 1.79-1.73 (m, 2H), 1.71-1.67 (m, 2H), 1.53-1.47 (m, 2H), 1.42 (s, 6H) ppm.

^{13}C NMR (125 MHz, MeOD-*d*$_4$): δ = 176.6 (2C; C_q), 174.9 (C_q), 167.7 (C_q), 161.5 (2C; C_q), 159.0 (C_q), 157.6 (2C; C_q), 146.6 (2C; C_q), 143.6 (C_q), 141.6 (C_q), 132.9 (2C; C_q), 132.4 (C_q), 130.8 (2C; *C*H), 130.7 (C_q), 130.5 (2C; *C*H), 130.0 (2C; *C*H), 129.9 (2C; *C*H), 129.7 (2C; C_q), 129.6 (2C; *C*H), 128.0 (2C; C_q), 128.0 (*C*H), 127.8 (2C; *C*H), 122.1 (2C; *C*H), 116.7 (2C; *C*H), 115.5 (2C; *C*H), 68.8 (CH_2), 67.7 (CH_2), 58.3 (CH_2), 40.0 (CH_2), 38.9 (CH_2), 31.1 (CH_2), 30.8 (CH_2), 30.1 (CH_2), 26.7 (CH_2), 18.4 (2C; CH_3), 17.5 (2C; CH_3) ppm.

^{19}F-NMR (282 MHz, MeOD-*d*$_4$): δ = -146.5 (dd, ^1J(B, F) = 31.6 Hz, 2F, BF_2) ppm.

HRMS-ESI (m/z): $[M + H]^+$ calcd for $C_{53}H_{52}BF_2I_2N_6O_4$: 1139.2204; found: 1139.2206.

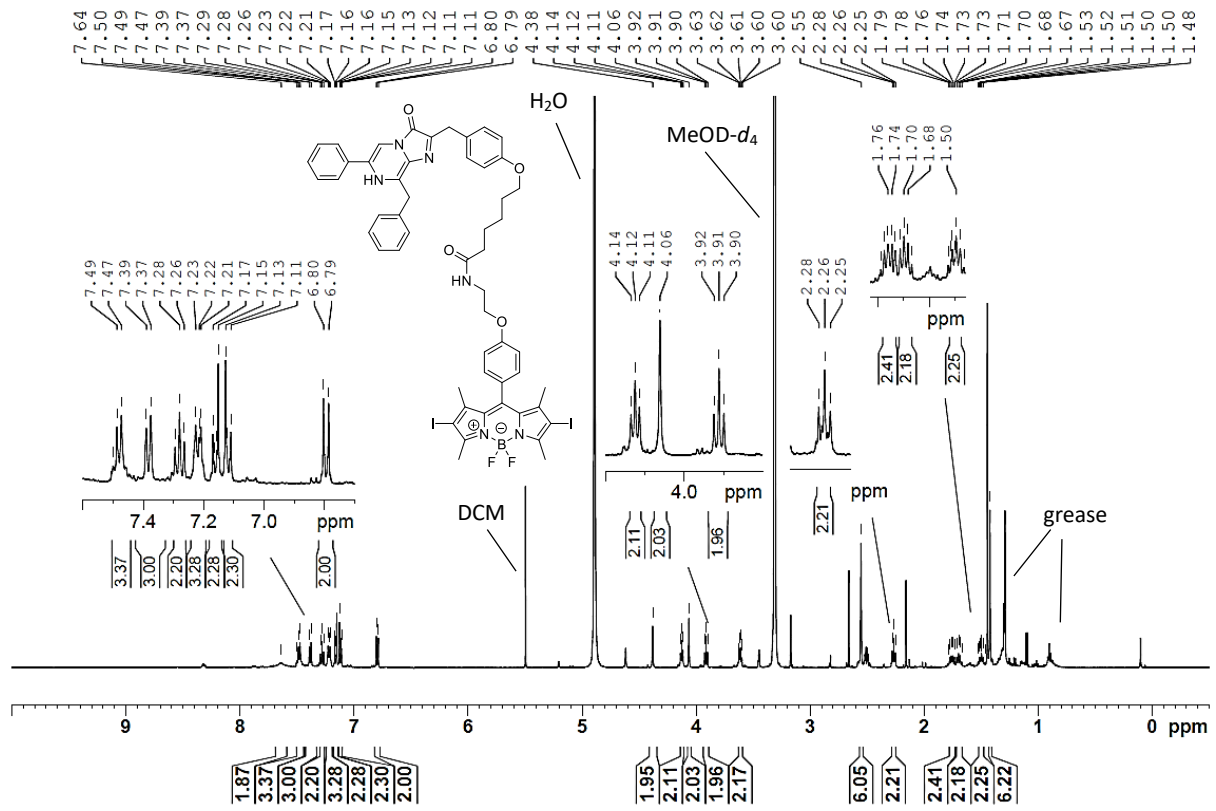

Figure S181: ^{1}H-NMR (500 MHz) spectrum of compound **4** in MeOD-d_4.

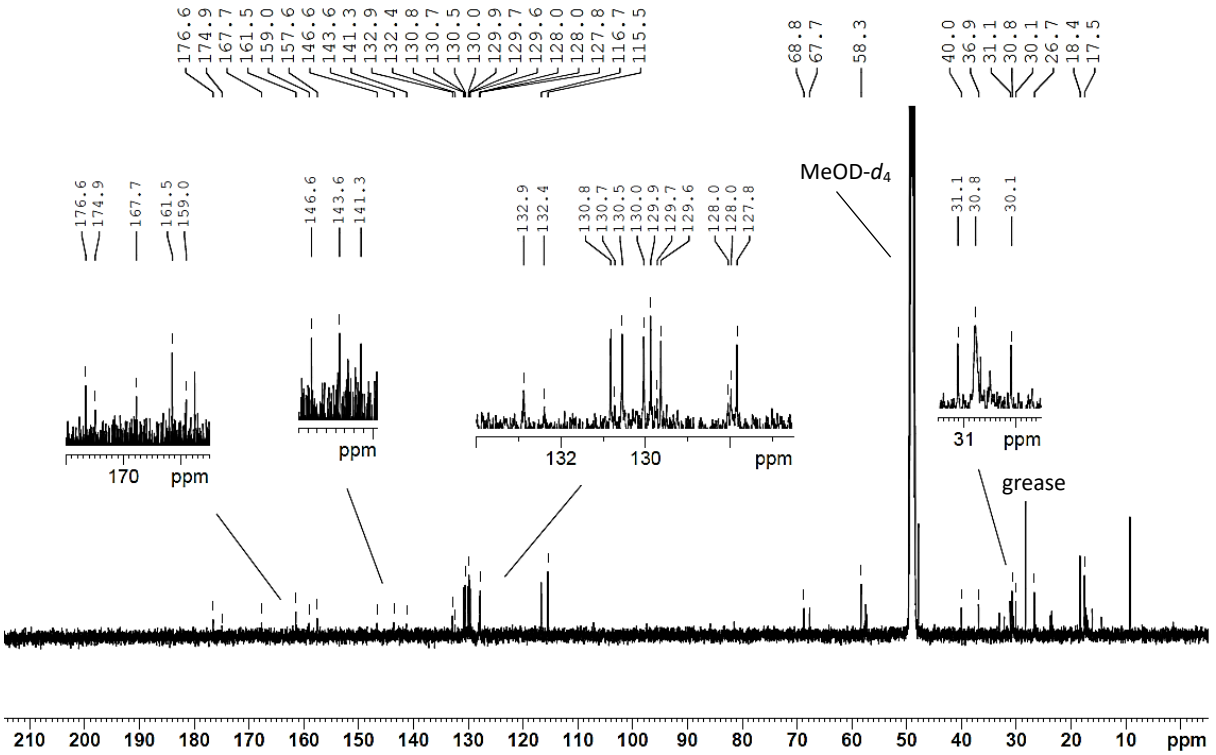

Figure S182: ^{13}C-NMR (125 MHz) spectrum of compound **4** in MeOD-d_4.

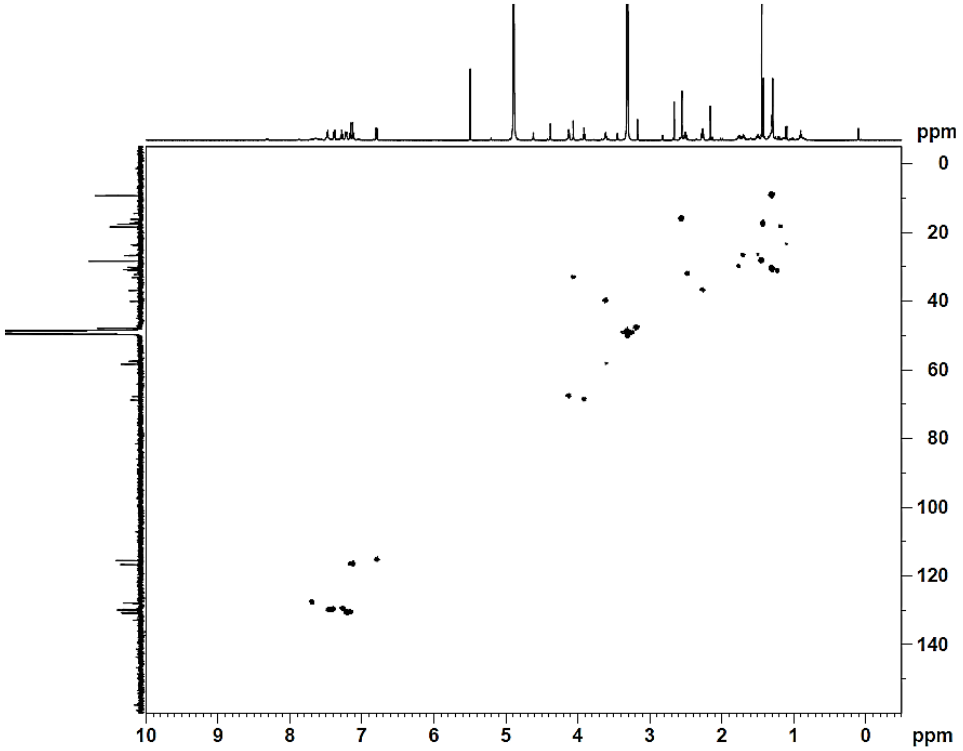

Figure S183: HSQC spectrum of compound **4** (^{1}H-NMR: 500 MHz, ^{13}C-NMR: 125 MHz, MeOD-d_4).

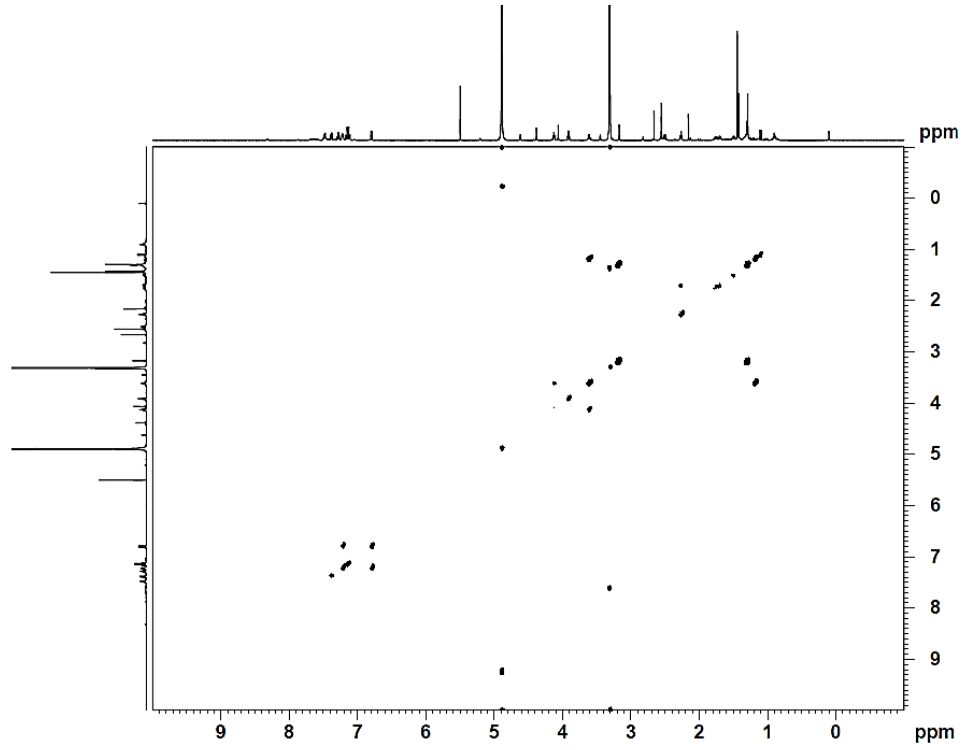

Figure S184: COSY spectrum of compound **4** (^{1}H-NMR: 500 MHz, MeOD-d_4).

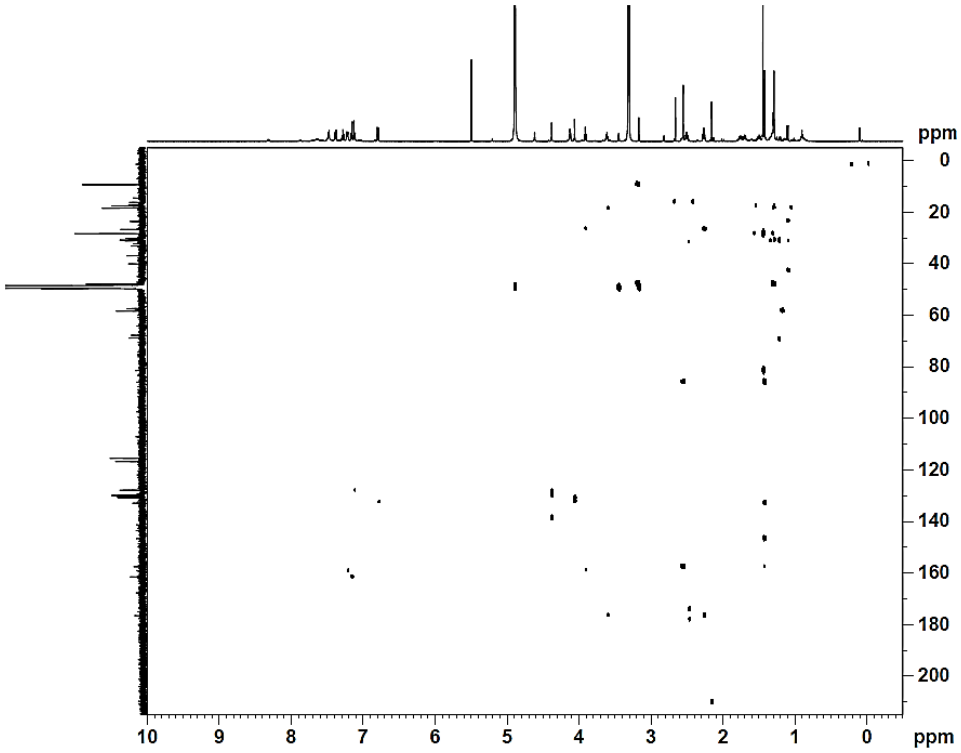

Figure S185: HMBC spectrum of compound **4** (^{1}H-NMR: 500 MHz, ^{13}C-NMR: 125 MHz, MeOD-d_4).

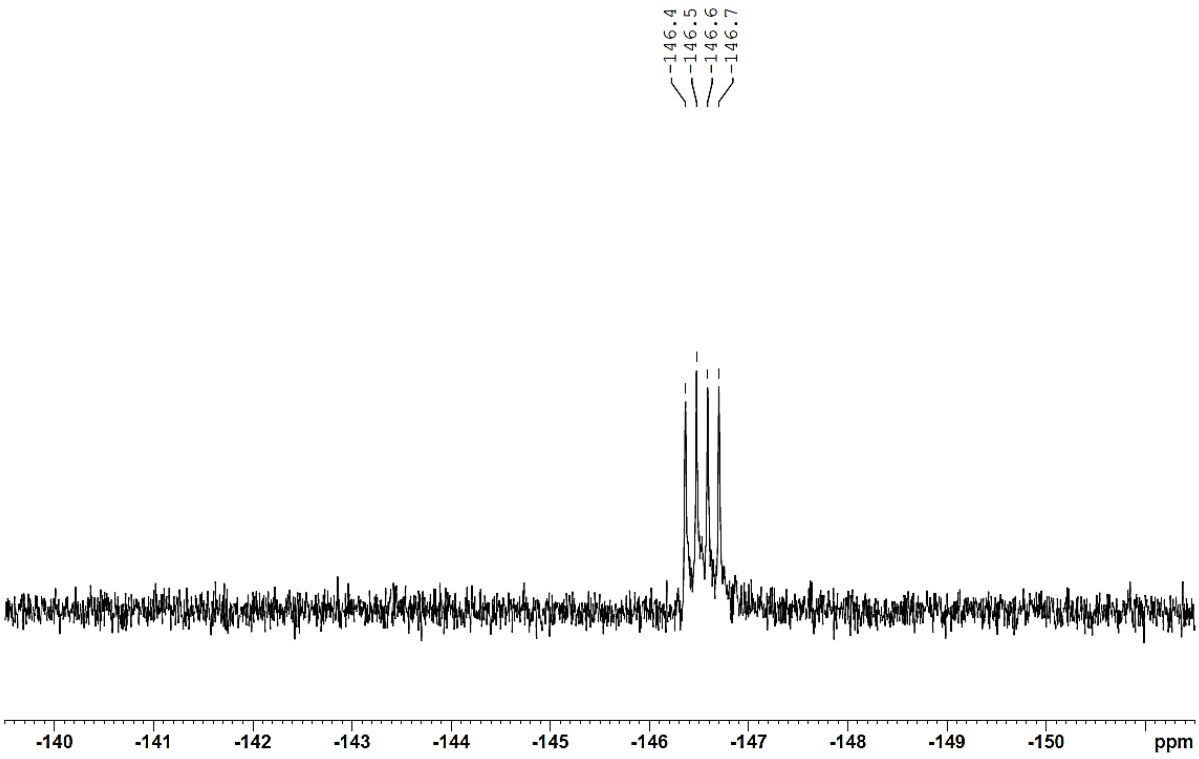

Figure S186: ^{19}F-NMR (282 MHz) spectrum of compound **4** in MeOD-d_4.

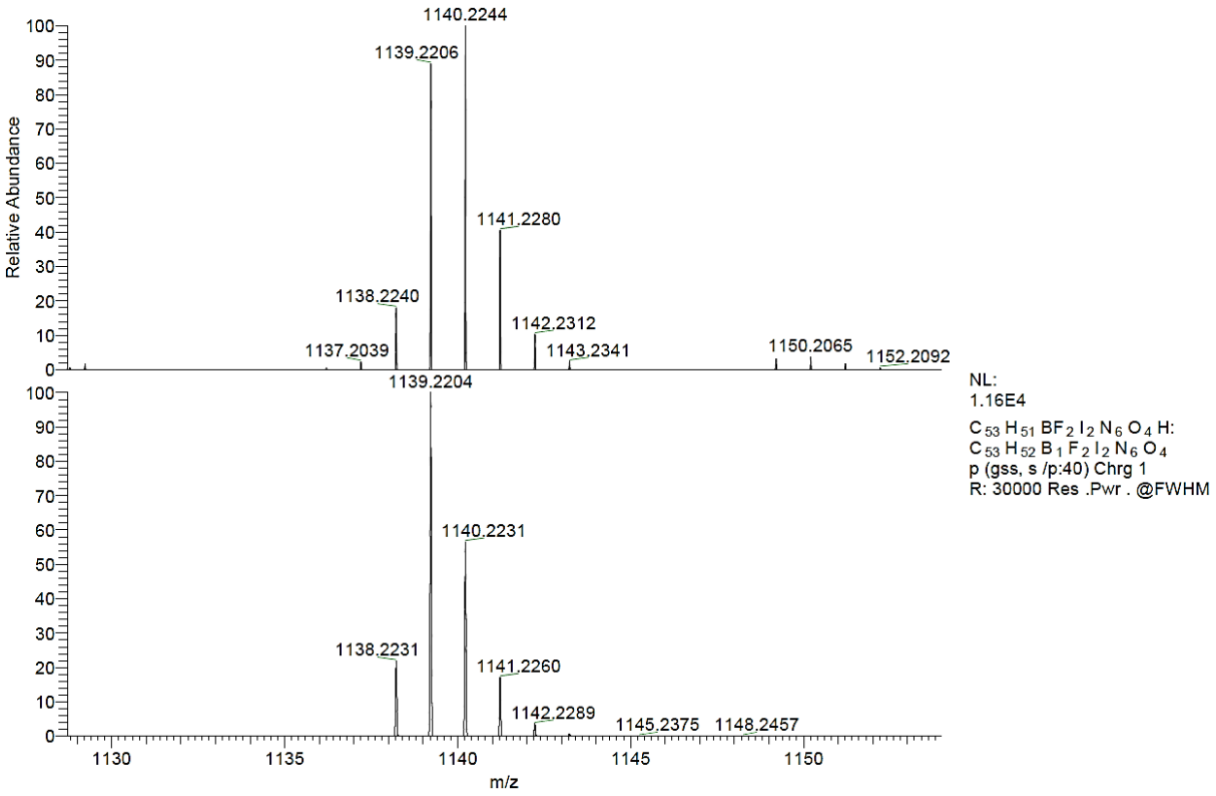

Figure S187: Measured (top) and calculated (bottom) HRMS-ESI spectrum of **4** in positive ion mode.

Solid Phase Peptide Synthesis (SPPS)

For peptide synthesis, the amino acids were coupled automatically by a ResPep SLi Synthesizer (Intavis) in microscale colums (Intavis, 1-5 µmol, 35.101). TentaGel® S RAM resin (loading = 0.22 mmol/g) was used as solid support. The amounts of reagents of the following synthesis protocol correspond to 5 µmol scale of the peptide.

Swelling: 22.7 mg of resin (5 µmol) were swollen in DMF (500 µL) for 30 min.

Deprotection of the Fmoc-protecting group: Piperidine (150 µL, 20% in DMF, vol %) was added to the resin. After 5 min, the solution was removed, and the procedure was repeated once. Afterwards the solution was removed, and the resin was washed with DMF (1× 300 µL, 3× 225 µL).

Coupling of the amino acids: Amino acids were coupled by charging the reactor with a solution of the corresponding Fmoc-amino acid (0.5 M solution in DMF, 4.00 eq), Oxyma (2 M solution in DMF, 4.00 eq) and DIC (2 M solution in DMF, 4.00 eq) using a total volume of 100 µL. After 20 min, the solution was removed, and the coupling step was repeated once.

Capping: A solution of Ac_2O/2,6-lutidine/DMF (120 µL, 5:6:89, v/v/v) was added. The solution was removed after 8 min, and the resin was washed with DMF (3 × 225 µL).

After the last coupling cycle, the resin was washed with DMF (1× 300 µL, 3× 225 µL), EtOH (4× 150 µL) and DCM (5× 150 µL). Vacuum was applied to the reactor for 5 min. Finally, the resin was transferred to a 2 mL polypropylen reactor with plunger and frit (V020PE061, pore size 25 µm, Multisyntech GmbH, Germany) for the final coupling step and the cleavage step, which was carried out manually.

Cleavage Deprotection Step

The dried resin was treated with the TFA-based cleavage cocktail (2.0 mL for 22.7 mg of resin) and shaken for 2 h. As cleavage cocktail, TFA/DCM/H_2O/TIPS (90:5:2.5:2.5, v/v/v/v) was used. Then, the resin was filtered off, the filtrate was precipitated in -20 °C cold Et_2O (10.0 mL of Et_2O for 1.0 mL cleavage cocktail). Afterwards, the precipitated peptide was centrifuged (8000 rpm, 8 min, 4 °C), the supernatant was discarded, and the pellet was washed with Et_2O. This step was repeated once. Finally, the peptide pellet was dried in high vacuum for 10 min, dissolved in ultrapure H_2O, and purified.

Purification and Characterization

Purification: The synthesized peptide was purified at 25 °C by an Agilent 1260 Series preparative HPLC-system (Agilent Technologies) equipped with column 3, 5 µm, 10 mL/min.

The detection was carried out by measuring the absorption at 220 nm and 260 nm. Ultrapure water (A) and MeCN (B) were employed as eluents with an addition of 0.1 % of TFA for both solvents. The fractions which were containing the desired peptide were combined and lyophilized and stored at -20 °C.

Characterization: The freeze-dried peptide was characterized by analytical HPLC-MS using an Agilent 1260 Series analytical HPLC-system (Agilent Technologies) equipped with column 2, 1 mL/min at 55 °C. For analytical purposes, ultrapure water containing 0,05% TFA (A) and MeCN containing 0.03% TFA (B) were used as eluents. Detection of the signal was achieved with a UV detector at 220 nm and the measurement of the corresponding mass signal was performed with an LTQ-FT Ultra coupled to an Agilent 1260 Infinity II HPLC (Agilent Technologies).

A high-resolution electrospray ionization (ESI) mass spectra of the peptide was measured with an LTQ-FT Ultra mass spectrometer (Thermo Fischer Scientific) by the employees of the Marburg University mass department.

Analytical Data

HiBiT (19): H_2N-GGGGS-VSGWRLFKKIS-$CONH_2$: For the final cleavage step, 45.5 mg of resin (loading = 0.22 mmol/g, peptide: 16.3 mg, 10 µmol) were treated with 4 mL of cleavage cocktail. After purification using 5% - 75% of solvent B in 24 min, column 3), the desired peptide (7.74 mg, 3.70 µmol, 37%) was obtained as white 4× TFA salt solid. t_R = 12.14 min (5 – 75% of solvent B in 25 min, column 2), Purity ≥ 98%. Formula: $C_{74}H_{119}N_{23}O_{19}$. HRMS-ESI (m/z): $[M+3H]^{3+}$ cald.: 545.6424; found: 545.6442.

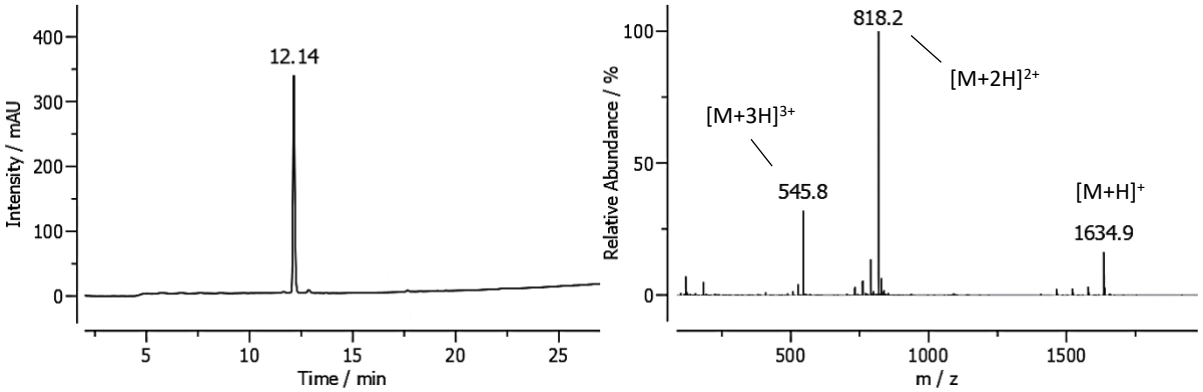

Figure S188: HPLC chromatogram (220 nm, 5 – 75% of solvent B in 25 min) of purified peptide **19** and corresponding ESI^+ spectra.

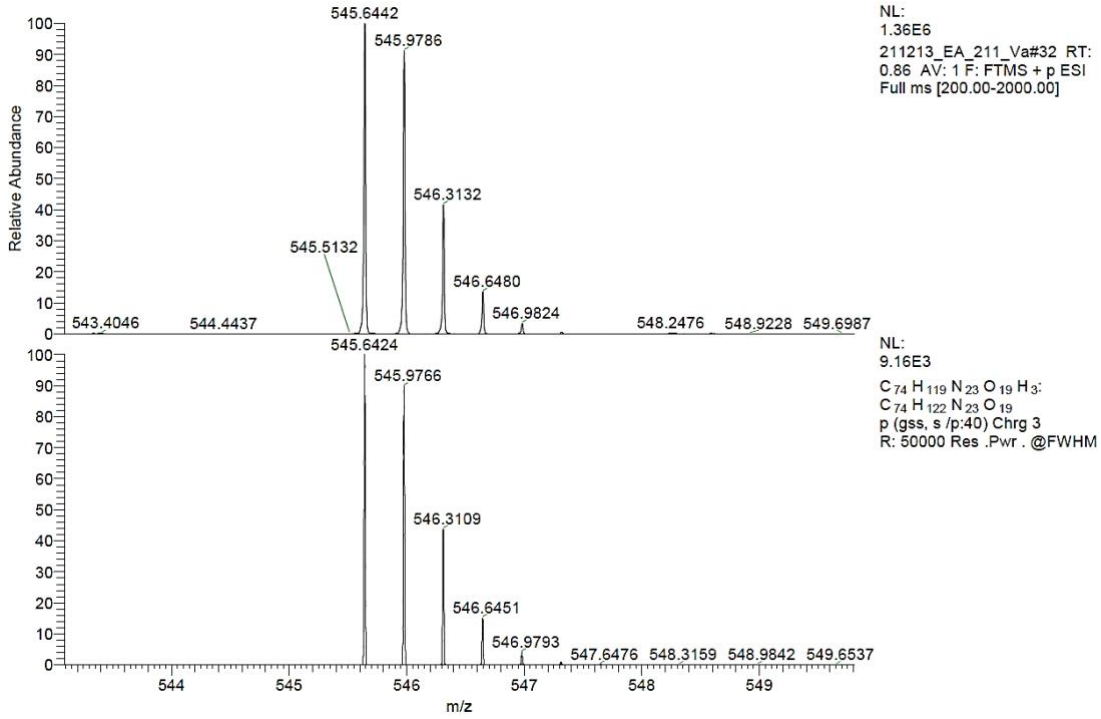

Figure S189: Measured (top) and calculated (bottom) HRMS-ESI spectrum of H_2N-GGGGS-VSGWRLFKKIS-$CONH_2$ (**19**) in positive ion mode.

Molecular and FRET Modelling

Computational Details

Molecular structures were optimized using the CAM-B3LYP/def2-SVP level of theory, incorporating Grimme's D3 dispersion term with Becke-Johnson damping[44] in the CPCM acetonitrile solvent model. Local minima geometry was verified with computing vibrational frequencies. Excited states were calculated using the TD-DFT method at the TD-DFT CAM-B3LYP/def2-TZVPP level, applying the same empirical dispersion and solvent models. All electronic structure calculations were performed using the *Gaussian16* software.[45] Coordinates of the optimized molecular structures are provided in table S7 below.

FRET modelling was performed using the PyFREC software as detailed elsewhere.[46] Briefly, we considered the lowest excited states with non-zero transition dipole moments of the donor and acceptor groups, along with the spectral overlap calculated from empirical donor fluorescence and acceptor absorption spectra. Donor-acceptor distances were determined based on the ground-state charge centres of the donor and acceptor moieties. Mutual orientation factors were calculated according to FRET theory, based on the relative orientation of the transition dipole moments and the donor-acceptor distance vector. Parameters of the excited states and results of the FRET calculations are summarized in tables SR4 and SR5.

Optimized Molecular Geometries

Table S7: Optimized Molecular Geometries of the Molecules.

Short BODIPY-CTZ (3)

```
TITLE     BPY_CTZ_REDC_Short_opt_1
REMARK   1 BPY_CTZ_REDC_Short_opt_1
HETATM    1  O   LNK     1      -4.566  -3.950   1.008                O
HETATM    2  C   LNK     1      -3.591  -3.795  -0.004                C
HETATM    3  H   LNK     1      -3.760  -4.533  -0.809                H
HETATM    4  H   LNK     1      -3.670  -2.790  -0.456                H
HETATM    5  C   LNK     1      -2.227  -3.992   0.620                C
HETATM    6  H   LNK     1      -2.196  -4.990   1.087                H
HETATM    7  H   LNK     1      -2.102  -3.259   1.434                H
HETATM    8  C   LNK     1      -1.094  -3.851  -0.388                C
HETATM    9  H   LNK     1      -1.230  -4.584  -1.201                H
HETATM   10  H   LNK     1      -1.145  -2.856  -0.864                H
HETATM   11  C   LNK     1       0.281  -4.037   0.241                C
HETATM   12  H   LNK     1       0.335  -5.028   0.723                H
HETATM   13  H   LNK     1       0.432  -3.299   1.043                H
HETATM   14  C   LNK     1       1.418  -3.901  -0.762                C
HETATM   15  H   LNK     1       1.347  -4.670  -1.546                H
HETATM   16  H   LNK     1       1.344  -2.926  -1.275                H
HETATM   17  C   LNK     1       2.782  -3.944  -0.105                C
HETATM   18  O   LNK     1       2.988  -3.487   1.011                O
HETATM   19  N   LNK     1       3.771  -4.506  -0.841                N
HETATM   20  H   LNK     1       3.559  -4.850  -1.769                H
HETATM   21  C   LNK     1       5.133  -4.560  -0.367                C
HETATM   22  H   LNK     1       5.131  -4.797   0.706                H
HETATM   23  H   LNK     1       5.666  -5.363  -0.894                H
HETATM   24  C   BPY     2       5.860  -3.242  -0.572                C
HETATM   25  H   BPY     2       5.890  -2.979  -1.643                H
HETATM   26  H   BPY     2       5.330  -2.440  -0.031                H
HETATM   27  O   BPY     2       7.167  -3.406  -0.063                O
HETATM   28  C   BPY     2       8.023  -2.364  -0.082                C
```

```
HETATM  29  C   BPY   2       7.711  -1.102  -0.593           C
HETATM  30  C   BPY   2       9.297  -2.598   0.452           C
HETATM  31  C   BPY   2       8.670  -0.091  -0.563           C
HETATM  32  H   BPY   2       6.730  -0.892  -1.015           H
HETATM  33  C   BPY   2      10.241  -1.584   0.475           C
HETATM  34  H   BPY   2       9.523  -3.589   0.847           H
HETATM  35  C   BPY   2       9.937  -0.316  -0.033           C
HETATM  36  H   BPY   2       8.419   0.894  -0.963           H
HETATM  37  H   BPY   2      11.231  -1.776   0.895           H
HETATM  38  C   BPY   2      10.952   0.771  -0.002           C
HETATM  39  C   BPY   2      11.013   1.629   1.101           C
HETATM  40  C   BPY   2      11.836   0.923  -1.076           C
HETATM  41  N   BPY   2      11.959   2.654   1.153           N
HETATM  42  C   BPY   2      10.241   1.685   2.301           C
HETATM  43  C   BPY   2      11.975   0.197  -2.298           C
HETATM  44  N   BPY   2      12.800   1.933  -1.066           N
HETATM  45  B   BPY   2      13.010   2.959   0.066           B
HETATM  46  C   BPY   2      11.808   3.325   2.305           C
HETATM  47  C   BPY   2      10.753   2.749   3.036           C
HETATM  48  C   BPY   2       9.107   0.812   2.732           C
HETATM  49  C   BPY   2      13.024   0.800  -2.984           C
HETATM  50  C   BPY   2      11.187  -0.972  -2.793           C
HETATM  51  C   BPY   2      13.511   1.864  -2.201           C
HETATM  52  F   BPY   2      14.298   2.839   0.593           F
HETATM  53  F   BPY   2      12.839   4.257  -0.421           F
HETATM  54  C   BPY   2      12.662   4.485   2.681           C
HETATM  55  H   BPY   2      10.406   3.087   4.011           H
HETATM  56  H   BPY   2       9.403  -0.245   2.785           H
HETATM  57  H   BPY   2       8.752   1.122   3.724           H
HETATM  58  H   BPY   2       8.263   0.866   2.031           H
HETATM  59  H   BPY   2      13.411   0.509  -3.959           H
HETATM  60  H   BPY   2      11.554  -1.280  -3.780           H
HETATM  61  H   BPY   2      11.262  -1.831  -2.112           H
HETATM  62  H   BPY   2      10.118  -0.734  -2.880           H
HETATM  63  C   BPY   2      14.624   2.801  -2.514           C
HETATM  64  H   BPY   2      12.577   5.284   1.932           H
HETATM  65  H   BPY   2      12.368   4.877   3.662           H
HETATM  66  H   BPY   2      13.720   4.189   2.712           H
HETATM  67  H   BPY   2      14.261   3.838  -2.532           H
HETATM  68  H   BPY   2      15.401   2.749  -1.737           H
HETATM  69  H   BPY   2      15.071   2.558  -3.486           H
HETATM  70  H   CTZ   3      -8.102  -3.190  -1.798           H
HETATM  71  C   CTZ   3      -7.730  -3.428  -0.799           C
HETATM  72  C   CTZ   3      -8.646  -3.592   0.241           C
HETATM  73  C   CTZ   3      -6.357  -3.540  -0.585           C
HETATM  74  C   CTZ   3     -10.133  -3.427  -0.002           C
HETATM  75  C   CTZ   3      -8.148  -3.865   1.519           C
HETATM  76  C   CTZ   3      -5.875  -3.820   0.697           C
HETATM  77  H   CTZ   3      -5.675  -3.406  -1.424           H
HETATM  78  C   CTZ   3     -10.503  -1.995  -0.215           C
HETATM  79  H   CTZ   3     -10.429  -3.999  -0.894           H
HETATM  80  H   CTZ   3     -10.698  -3.815   0.856           H
HETATM  81  H   CTZ   3      -8.843  -3.992   2.353           H
HETATM  82  C   CTZ   3     -10.372  -1.321  -1.519           C
HETATM  83  N   CTZ   3     -10.919  -1.185   0.729           N
HETATM  84  N   CTZ   3     -10.754  -0.039  -1.220           N
HETATM  85  O   CTZ   3     -10.013  -1.744  -2.619           O
```

```
HETATM  86 C  CTZ    3    -11.085   0.033   0.154              C
HETATM  87 C  CTZ    3    -10.840   1.087  -2.025              C
HETATM  88 C  CTZ    3    -11.472   1.219   0.697              C
HETATM  89 C  CTZ    3    -11.220   2.262  -1.478              C
HETATM  90 H  CTZ    3    -10.615   0.953  -3.080              H
HETATM  91 C  CTZ    3    -11.766   1.385   2.155              C
HETATM  92 N  CTZ    3    -11.535   2.309  -0.117              N
HETATM  93 C  CTZ    3    -11.358   3.516  -2.245              C
HETATM  94 H  CTZ    3    -12.745   1.872   2.272              H
HETATM  95 H  CTZ    3    -11.831   0.383   2.595              H
HETATM  96 C  CTZ    3    -10.693   2.202   2.845              C
HETATM  97 H  CTZ    3    -11.700   3.216   0.307              H
HETATM  98 C  CTZ    3    -10.498   3.796  -3.315              C
HETATM  99 C  CTZ    3    -12.357   4.443  -1.921              C
HETATM 100 C  CTZ    3    -10.953   3.492   3.308              C
HETATM 101 C  CTZ    3     -9.408   1.671   2.999              C
HETATM 102 C  CTZ    3    -10.643   4.968  -4.049              C
HETATM 103 H  CTZ    3     -9.696   3.099  -3.561              H
HETATM 104 C  CTZ    3    -12.494   5.620  -2.651              C
HETATM 105 H  CTZ    3    -13.054   4.237  -1.106              H
HETATM 106 C  CTZ    3     -9.947   4.243   3.916              C
HETATM 107 H  CTZ    3    -11.955   3.915   3.198              H
HETATM 108 C  CTZ    3     -8.404   2.418   3.606              C
HETATM 109 H  CTZ    3     -9.198   0.661   2.638              H
HETATM 110 C  CTZ    3    -11.640   5.886  -3.719              C
HETATM 111 H  CTZ    3     -9.963   5.173  -4.878              H
HETATM 112 H  CTZ    3    -13.281   6.329  -2.388              H
HETATM 113 C  CTZ    3     -8.671   3.708   4.065              C
HETATM 114 H  CTZ    3    -10.164   5.251   4.274              H
HETATM 115 H  CTZ    3     -7.405   1.991   3.724              H
HETATM 116 H  CTZ    3    -11.747   6.809  -4.291              H
HETATM 117 H  CTZ    3     -7.882   4.294   4.542              H
HETATM 118 C  CTZ    3     -6.784  -3.980   1.749              C
HETATM 119 H  CTZ    3     -6.395  -4.198   2.745              H
END
```

Short 2I-BODIPY-CTZ (4)

```
TITLE     I2BPY_CTZ_REDC_Short_opt_1
REMARK   1 I2BPY_CTZ_REDC_Short_opt_1
HETATM   1 O   LNK    1      6.945  -2.821  -3.055              O
HETATM   2 C   LNK    1      5.937  -3.310  -2.193              C
HETATM   3 H   LNK    1      6.108  -4.380  -1.979              H
HETATM   4 H   LNK    1      5.967  -2.772  -1.229              H
HETATM   5 C   LNK    1      4.599  -3.111  -2.870              C
HETATM   6 H   LNK    1      4.614  -3.632  -3.841              H
HETATM   7 H   LNK    1      4.472  -2.038  -3.091              H
HETATM   8 C   LNK    1      3.433  -3.610  -2.027              C
HETATM   9 H   LNK    1      3.568  -4.684  -1.811              H
HETATM  10 H   LNK    1      3.440  -3.100  -1.048              H
HETATM  11 C   LNK    1      2.083  -3.392  -2.698              C
HETATM  12 H   LNK    1      2.074  -3.894  -3.680              H
HETATM  13 H   LNK    1      1.933  -2.321  -2.902              H
HETATM  14 C   LNK    1      0.914  -3.893  -1.863              C
HETATM  15 H   LNK    1      0.985  -4.979  -1.695              H
HETATM  16 H   LNK    1      0.943  -3.423  -0.864              H
HETATM  17 C   LNK    1     -0.429  -3.542  -2.471              C
HETATM  18 O   LNK    1     -0.613  -2.508  -3.097              O
HETATM  19 N   LNK    1     -1.422  -4.438  -2.260              N
```

```
HETATM  20 H   LNK   1      -1.230  -5.268  -1.714                H
HETATM  21 C   LNK   1      -2.768  -4.202  -2.725                C
HETATM  22 H   LNK   1      -2.725  -3.739  -3.721                H
HETATM  23 H   LNK   1      -3.293  -5.162  -2.816                H
HETATM  24 C   BPY   2      -3.539  -3.281  -1.795                C
HETATM  25 H   BPY   2      -3.608  -3.722  -0.785                H
HETATM  26 H   BPY   2      -3.019  -2.313  -1.718                H
HETATM  27 O   BPY   2      -4.826  -3.112  -2.352                O
HETATM  28 C   BPY   2      -5.716  -2.308  -1.738                C
HETATM  29 C   BPY   2      -5.458  -1.613  -0.553                C
HETATM  30 C   BPY   2      -6.968  -2.183  -2.354                C
HETATM  31 C   BPY   2      -6.451  -0.809   0.003                C
HETATM  32 H   BPY   2      -4.494  -1.689  -0.054                H
HETATM  33 C   BPY   2      -7.943  -1.373  -1.797                C
HETATM  34 H   BPY   2      -7.151  -2.734  -3.278                H
HETATM  35 C   BPY   2      -7.695  -0.678  -0.608                C
HETATM  36 H   BPY   2      -6.245  -0.272   0.931                H
HETATM  37 H   BPY   2      -8.914  -1.280  -2.287                H
HETATM  38 C   BPY   2      -8.744   0.186  -0.009                C
HETATM  39 C   BPY   2      -8.934   1.486  -0.496                C
HETATM  40 C   BPY   2      -9.534  -0.308   1.038                C
HETATM  41 N   BPY   2      -9.926   2.307   0.037                N
HETATM  42 C   BPY   2      -8.248   2.217  -1.513                C
HETATM  43 C   BPY   2      -9.558  -1.586   1.675                C
HETATM  44 N   BPY   2     -10.511   0.492   1.629                N
HETATM  45 B   BPY   2     -10.868   1.936   1.206                B
HETATM  46 C   BPY   2      -9.905   3.492  -0.586                C
HETATM  47 C   BPY   2      -8.874   3.462  -1.553                C
HETATM  48 C   BPY   2      -7.102   1.779  -2.363                C
HETATM  49 C   BPY   2     -10.558  -1.493   2.642                C
HETATM  50 C   BPY   2      -8.716  -2.784   1.390                C
HETATM  51 C   BPY   2     -11.131  -0.201   2.591                C
HETATM  52 F   BPY   2     -12.198   1.994   0.795                F
HETATM  53 F   BPY   2     -10.672   2.815   2.269                F
HETATM  54 C   BPY   2     -10.832   4.599  -0.234                C
HETATM  55 I   BPY   2      -8.394   5.053  -2.816                I
HETATM  56 H   BPY   2      -7.417   1.030  -3.104                H
HETATM  57 H   BPY   2      -6.684   2.636  -2.905                H
HETATM  58 H   BPY   2      -6.305   1.320  -1.765                H
HETATM  59 I   BPY   2     -11.149  -2.996   3.965                I
HETATM  60 H   BPY   2      -9.116  -3.661   1.915                H
HETATM  61 H   BPY   2      -8.675  -3.007   0.317                H
HETATM  62 H   BPY   2      -7.680  -2.633   1.725                H
HETATM  63 C   BPY   2     -12.240   0.367   3.402                C
HETATM  64 H   BPY   2     -10.567   5.020   0.747                H
HETATM  65 H   BPY   2     -10.787   5.398  -0.983                H
HETATM  66 H   BPY   2     -11.861   4.223  -0.160                H
HETATM  67 H   BPY   2     -11.969   1.368   3.764                H
HETATM  68 H   BPY   2     -13.144   0.477   2.786                H
HETATM  69 H   BPY   2     -12.471  -0.280   4.255                H
HETATM  70 H   CTZ   3      10.364  -3.801  -0.175                H
HETATM  71 C   CTZ   3      10.032  -3.411  -1.139                C
HETATM  72 C   CTZ   3      10.983  -2.910  -2.029                C
HETATM  73 C   CTZ   3       8.671  -3.401  -1.444                C
HETATM  74 C   CTZ   3      12.452  -2.883  -1.661                C
HETATM  75 C   CTZ   3      10.533  -2.383  -3.244                C
HETATM  76 C   CTZ   3       8.238  -2.876  -2.665                C
```

```
HETATM   77 H   CTZ    3       7.962  -3.803  -0.722                H
HETATM   78 C   CTZ    3      12.747  -1.801  -0.674                C
HETATM   79 H   CTZ    3      12.743  -3.847  -1.218                H
HETATM   80 H   CTZ    3      13.062  -2.720  -2.560                H
HETATM   81 H   CTZ    3      11.255  -1.979  -3.958                H
HETATM   82 C   CTZ    3      12.537  -1.963   0.775                C
HETATM   83 N   CTZ    3      13.149  -0.592  -0.991                N
HETATM   84 N   CTZ    3      12.858  -0.719   1.253                N
HETATM   85 O   CTZ    3      12.167  -2.933   1.438                O
HETATM   86 C   CTZ    3      13.229   0.109   0.168                C
HETATM   87 C   CTZ    3      12.851  -0.222   2.548                C
HETATM   88 C   CTZ    3      13.560   1.410   0.390                C
HETATM   89 C   CTZ    3      13.177   1.072   2.760                C
HETATM   90 H   CTZ    3      12.598  -0.923   3.340                H
HETATM   91 C   CTZ    3      13.882   2.362  -0.720                C
HETATM   92 N   CTZ    3      13.533   1.872   1.670                N
HETATM   93 C   CTZ    3      13.213   1.698   4.097                C
HETATM   94 H   CTZ    3      14.805   2.906  -0.474                H
HETATM   95 H   CTZ    3      14.068   1.768  -1.622                H
HETATM   96 C   CTZ    3      12.748   3.340  -0.954                C
HETATM   97 H   CTZ    3      13.661   2.865   1.827                H
HETATM   98 C   CTZ    3      12.300   1.317   5.088                C
HETATM   99 C   CTZ    3      14.167   2.679   4.398                C
HETATM  100 C   CTZ    3      12.883   4.692  -0.637                C
HETATM  101 C   CTZ    3      11.532   2.882  -1.473                C
HETATM  102 C   CTZ    3      12.349   1.894   6.352                C
HETATM  103 H   CTZ    3      11.531   0.577   4.860                H
HETATM  104 C   CTZ    3      14.208   3.261   5.661                C
HETATM  105 H   CTZ    3      14.903   2.977   3.649                H
HETATM  106 C   CTZ    3      11.821   5.574  -0.834                C
HETATM  107 H   CTZ    3      13.830   5.062  -0.236                H
HETATM  108 C   CTZ    3      10.473   3.761  -1.671                C
HETATM  109 H   CTZ    3      11.421   1.823  -1.723                H
HETATM  110 C   CTZ    3      13.302   2.870   6.643                C
HETATM  111 H   CTZ    3      11.629   1.589   7.113                H
HETATM  112 H   CTZ    3      14.961   4.021   5.880                H
HETATM  113 C   CTZ    3      10.614   5.111  -1.350                C
HETATM  114 H   CTZ    3      11.940   6.630  -0.582                H
HETATM  115 H   CTZ    3       9.530   3.391  -2.079                H
HETATM  116 H   CTZ    3      13.335   3.327   7.634                H
HETATM  117 H   CTZ    3       9.782   5.801  -1.505                H
HETATM  118 C   CTZ    3       9.182  -2.367  -3.564                C
HETATM  119 H   CTZ    3       8.830  -1.961  -4.513                H
END
```

Short BODIPY-CTZ (oxidized form)

```
TITLE     BPY_CTZ_Short_opt_ox
REMARK   1 BPY_CTZ_Short_opt_ox
HETATM    1 C   CTZ    1      10.469   0.812   0.344                C
HETATM    2 C   CTZ    1       9.644   1.617  -0.471                C
HETATM    3 N   CTZ    1      11.383   1.348   1.135                N
HETATM    4 N   CTZ    1      10.298  -0.576   0.340                N
HETATM    5 N   CTZ    1       9.782   2.933  -0.448                N
HETATM    6 C   CTZ    1       8.600   1.026  -1.377                C
HETATM    7 C   CTZ    1      11.516   2.668   1.129                C
HETATM    8 C   CTZ    1      11.299  -1.515   0.385                C
HETATM    9 H   CTZ    1       9.353  -0.926   0.214                H
HETATM   10 C   CTZ    1      10.715   3.490   0.331                C
```

```
HETATM  11 H   CTZ   1      8.349   1.797  -2.119                H
HETATM  12 H   CTZ   1      9.032   0.179  -1.932                H
HETATM  13 C   CTZ   1      7.323   0.570  -0.693                C
HETATM  14 H   CTZ   1     12.266   3.089   1.802                H
HETATM  15 C   CTZ   1     10.818  -2.963   0.427                C
HETATM  16 O   CTZ   1     12.480  -1.244   0.401                O
HETATM  17 C   CTZ   1     10.838   4.969   0.318                C
HETATM  18 C   CTZ   1      6.367  -0.124  -1.443                C
HETATM  19 C   CTZ   1      7.044   0.852   0.646                C
HETATM  20 H   CTZ   1     11.047  -3.320   1.443                H
HETATM  21 H   CTZ   1     11.486  -3.514  -0.250                H
HETATM  22 C   CTZ   1      9.371  -3.207   0.095                C
HETATM  23 C   CTZ   1      9.781   5.745  -0.174                C
HETATM  24 C   CTZ   1     11.989   5.617   0.783                C
HETATM  25 C   CTZ   1      5.156  -0.506  -0.879                C
HETATM  26 H   CTZ   1      6.576  -0.361  -2.489                H
HETATM  27 C   CTZ   1      5.834   0.457   1.219                C
HETATM  28 H   CTZ   1      7.767   1.397   1.255                H
HETATM  29 C   CTZ   1      8.406  -3.300   1.096                C
HETATM  30 C   CTZ   1      8.945  -3.306  -1.238                C
HETATM  31 C   CTZ   1      9.868   7.133  -0.190                C
HETATM  32 H   CTZ   1      8.888   5.239  -0.541                H
HETATM  33 C   CTZ   1     12.076   7.006   0.764                C
HETATM  34 H   CTZ   1     12.840   5.039   1.147                H
HETATM  35 C   CTZ   1      4.884  -0.215   0.458                C
HETATM  36 H   CTZ   1      4.424  -1.045  -1.483                H
HETATM  37 H   CTZ   1      5.634   0.687   2.267                H
HETATM  38 C   CTZ   1      7.057  -3.490   0.800                C
HETATM  39 H   CTZ   1      8.710  -3.226   2.144                H
HETATM  40 C   CTZ   1      7.609  -3.492  -1.551                C
HETATM  41 H   CTZ   1      9.678  -3.237  -2.045                H
HETATM  42 C   CTZ   1     11.016   7.769   0.280                C
HETATM  43 H   CTZ   1      9.033   7.723  -0.572                H
HETATM  44 H   CTZ   1     12.983   7.495   1.126                H
HETATM  45 H   CTZ   1      3.933  -0.513   0.903                H
HETATM  46 C   CTZ   1      6.650  -3.584  -0.533                C
HETATM  47 H   CTZ   1      6.337  -3.559   1.613                H
HETATM  48 H   CTZ   1      7.274  -3.566  -2.586                H
HETATM  49 H   CTZ   1     11.085   8.859   0.267                H
HETATM  50 O   LNK   2      5.372  -3.756  -0.927                O
HETATM  51 C   LNK   2      4.355  -3.878   0.050                C
HETATM  52 H   LNK   2      4.539  -4.770   0.675                H
HETATM  53 H   LNK   2      4.365  -2.998   0.714                H
HETATM  54 C   LNK   2      3.026  -3.986  -0.663                C
HETATM  55 H   LNK   2      3.049  -4.863  -1.331                H
HETATM  56 H   LNK   2      2.900  -3.102  -1.310                H
HETATM  57 C   LNK   2      1.852  -4.089   0.302                C
HETATM  58 H   LNK   2      1.982  -4.973   0.950                H
HETATM  59 H   LNK   2      1.854  -3.215   0.976                H
HETATM  60 C   LNK   2      0.509  -4.171  -0.411                C
HETATM  61 H   LNK   2      0.498  -5.047  -1.081                H
HETATM  62 H   LNK   2      0.373  -3.292  -1.059                H
HETATM  63 C   LNK   2     -0.670  -4.253   0.547                C
HETATM  64 H   LNK   2     -0.612  -5.159   1.171                H
HETATM  65 H   LNK   2     -0.643  -3.398   1.245                H
HETATM  66 C   LNK   2     -2.009  -4.196  -0.161                C
HETATM  67 O   LNK   2     -2.165  -3.620  -1.229                O
```

```
HETATM   68 N   LNK     2      -3.035  -4.805   0.479              N
HETATM   69 H   LNK     2      -2.866  -5.247   1.374              H
HETATM   70 C   LNK     2      -4.381  -4.771  -0.040              C
HETATM   71 H   LNK     2      -4.349  -4.901  -1.131              H
HETATM   72 H   LNK     2      -4.954  -5.605   0.387              H
HETATM   73 C   BPY     3      -5.080  -3.458   0.272              C
HETATM   74 H   BPY     3      -5.134  -3.298   1.362              H
HETATM   75 H   BPY     3      -4.513  -2.624  -0.175              H
HETATM   76 O   BPY     3      -6.375  -3.535  -0.285              O
HETATM   77 C   BPY     3      -7.206  -2.479  -0.184              C
HETATM   78 C   BPY     3      -6.874  -1.277   0.447              C
HETATM   79 C   BPY     3      -8.474  -2.628  -0.760              C
HETATM   80 C   BPY     3      -7.808  -0.244   0.495              C
HETATM   81 H   BPY     3      -5.896  -1.133   0.903              H
HETATM   82 C   BPY     3      -9.393  -1.593  -0.705              C
HETATM   83 H   BPY     3      -8.716  -3.573  -1.249              H
HETATM   84 C   BPY     3      -9.069  -0.386  -0.076              C
HETATM   85 H   BPY     3      -7.542   0.692   0.990              H
HETATM   86 H   BPY     3     -10.379  -1.720  -1.158              H
HETATM   87 C   BPY     3     -10.058   0.723  -0.019              C
HETATM   88 C   BPY     3     -10.098   1.668  -1.050              C
HETATM   89 C   BPY     3     -10.942   0.809   1.063              C
HETATM   90 N   BPY     3     -11.021   2.714  -1.022              N
HETATM   91 C   BPY     3      -9.319   1.805  -2.240              C
HETATM   92 C   BPY     3     -11.103  -0.011   2.221              C
HETATM   93 N   BPY     3     -11.881   1.838   1.134              N
HETATM   94 B   BPY     3     -12.068   2.954   0.085              B
HETATM   95 C   BPY     3     -10.851   3.472  -2.115              C
HETATM   96 C   BPY     3      -9.805   2.936  -2.888              C
HETATM   97 C   BPY     3      -8.201   0.946  -2.736              C
HETATM   98 C   BPY     3     -12.140   0.558   2.952              C
HETATM   99 C   BPY     3     -10.345  -1.236   2.619              C
HETATM  100 C   BPY     3     -12.598   1.694   2.258              C
HETATM  101 F   BPY     3     -13.358   2.902  -0.450              F
HETATM  102 F   BPY     3     -11.872   4.207   0.673              F
HETATM  103 C   BPY     3     -11.678   4.677  -2.398              C
HETATM  104 H   BPY     3      -8.524  -0.092  -2.896              H
HETATM  105 H   BPY     3      -7.821   1.340  -3.688              H
HETATM  106 H   BPY     3      -7.368   0.908  -2.020              H
HETATM  107 H   BPY     3     -10.738  -1.628   3.567              H
HETATM  108 H   BPY     3     -10.421  -2.028   1.860              H
HETATM  109 H   BPY     3      -9.274  -1.029   2.748              H
HETATM  110 C   BPY     3     -13.692   2.627   2.643              C
HETATM  111 H   BPY     3     -11.579   5.412  -1.585              H
HETATM  112 H   BPY     3     -11.373   5.141  -3.343              H
HETATM  113 H   BPY     3     -12.743   4.408  -2.455              H
HETATM  114 H   BPY     3     -13.308   3.653   2.736              H
HETATM  115 H   BPY     3     -14.470   2.648   1.866              H
HETATM  116 H   BPY     3     -14.142   2.322   3.595              H
HETATM  117 H   BPY     3      -9.446   3.345  -3.830              H
HETATM  118 H   BPY     3     -12.538   0.197   3.899              H
END
```

Long BODIPY-CTZ (5)

```
TITLE     BPY_CTZ_REDC_Long_opt_1
REMARK   1 BPY_CTZ_REDC_Long_opt_1
HETATM    1 O   LNK     1       9.307   3.837   0.404              O
HETATM    2 C   LNK     1       7.953   3.571   0.712              C
```

```
HETATM    3 H   LNK     1       7.759   2.484   0.657                H
HETATM    4 H   LNK     1       7.727   3.894   1.744                H
HETATM    5 C   LNK     1       7.086   4.316  -0.280                C
HETATM    6 H   LNK     1       7.358   3.992  -1.298                H
HETATM    7 H   LNK     1       7.324   5.390  -0.217                H
HETATM    8 C   LNK     1       5.598   4.094  -0.040                C
HETATM    9 H   LNK     1       5.373   3.015  -0.095                H
HETATM   10 H   LNK     1       5.341   4.406   0.988                H
HETATM   11 C   LNK     1       4.712   4.843  -1.028                C
HETATM   12 H   LNK     1       4.971   4.533  -2.056                H
HETATM   13 H   LNK     1       4.936   5.922  -0.972                H
HETATM   14 C   LNK     1       3.225   4.620  -0.791                C
HETATM   15 H   LNK     1       2.992   3.545  -0.863                H
HETATM   16 H   LNK     1       2.957   4.933   0.232                H
HETATM   17 C   LNK     1       2.350   5.372  -1.789                C
HETATM   18 H   LNK     1       2.580   5.034  -2.809                H
HETATM   19 H   LNK     1       2.562   6.451  -1.742                H
HETATM   20 N   LNK     1       0.932   5.179  -1.569                N
HETATM   21 H   LNK     1       0.446   5.808  -0.943                H
HETATM   22 C   LNK     1       0.252   4.141  -2.102                C
HETATM   23 O   LNK     1       0.786   3.305  -2.820                O
HETATM   24 C   LNK     1      -1.232   4.104  -1.791                C
HETATM   25 H   LNK     1      -1.751   4.659  -2.588                H
HETATM   26 H   LNK     1      -1.446   4.632  -0.850                H
HETATM   27 C   LNK     1      -1.778   2.688  -1.768                C
HETATM   28 H   LNK     1      -1.347   2.141  -2.621                H
HETATM   29 H   LNK     1      -1.466   2.151  -0.860                H
HETATM   30 C   LNK     1      -3.285   2.652  -1.920                C
HETATM   31 O   LNK     1      -3.895   3.485  -2.578                O
HETATM   32 N   LNK     1      -3.910   1.618  -1.315                N
HETATM   33 H   LNK     1      -3.368   0.978  -0.749                H
HETATM   34 C   LNK     1      -5.340   1.430  -1.413                C
HETATM   35 H   LNK     1      -5.573   0.377  -1.205                H
HETATM   36 H   LNK     1      -5.659   1.659  -2.439                H
HETATM   37 C   LNK     1      -6.110   2.323  -0.437                C
HETATM   38 H   LNK     1      -5.867   3.374  -0.640                H
HETATM   39 H   LNK     1      -5.801   2.088   0.592                H
HETATM   40 N   LNK     1      -7.541   2.149  -0.543                N
HETATM   41 H   LNK     1      -8.065   2.775  -1.144                H
HETATM   42 C   LNK     1      -8.182   1.139   0.083                C
HETATM   43 O   LNK     1      -7.615   0.305   0.764                O
HETATM   44 C   BPY     2      -9.695   1.166  -0.090                C
HETATM   45 H   BPY     2     -10.103   1.952   0.572                H
HETATM   46 H   BPY     2      -9.954   1.437  -1.127                H
HETATM   47 O   BPY     2     -10.200  -0.094   0.250                O
HETATM   48 C   BPY     2     -11.536  -0.292   0.240                C
HETATM   49 C   BPY     2     -11.971  -1.566   0.627                C
HETATM   50 C   BPY     2     -12.473   0.676  -0.126                C
HETATM   51 C   BPY     2     -13.324  -1.863   0.650                C
HETATM   52 H   BPY     2     -11.223  -2.308   0.909                H
HETATM   53 C   BPY     2     -13.831   0.364  -0.098                C
HETATM   54 H   BPY     2     -12.165   1.674  -0.435                H
HETATM   55 C   BPY     2     -14.271  -0.899   0.287                C
HETATM   56 H   BPY     2     -13.653  -2.858   0.954                H
HETATM   57 H   BPY     2     -14.559   1.126  -0.384                H
HETATM   58 C   BPY     2     -15.723  -1.219   0.316                C
HETATM   59 C   BPY     2     -16.462  -0.974   1.479                C
```

```
HETATM  60 C   BPY   2     -16.335  -1.762  -0.819           C
HETATM  61 N   BPY   2     -17.826  -1.265   1.529           N
HETATM  62 C   BPY   2     -16.082  -0.441   2.748           C
HETATM  63 C   BPY   2     -15.815  -2.099  -2.106           C
HETATM  64 N   BPY   2     -17.696  -2.072  -0.814           N
HETATM  65 B   BPY   2     -18.658  -1.862   0.374           B
HETATM  66 C   BPY   2     -18.294  -0.942   2.743           C
HETATM  67 C   BPY   2     -17.238  -0.429   3.520           C
HETATM  68 C   BPY   2     -14.738   0.023   3.209           C
HETATM  69 C   BPY   2     -16.888  -2.604  -2.833           C
HETATM  70 C   BPY   2     -14.419  -1.960  -2.622           C
HETATM  71 C   BPY   2     -18.031  -2.574  -2.011           C
HETATM  72 F   BPY   2     -19.684  -0.985   0.014           F
HETATM  73 F   BPY   2     -19.219  -3.081   0.763           F
HETATM  74 C   BPY   2     -19.718  -1.125   3.134           C
HETATM  75 H   BPY   2     -17.325  -0.086   4.549           H
HETATM  76 H   BPY   2     -14.365   0.858   2.600           H
HETATM  77 H   BPY   2     -14.796   0.357   4.254           H
HETATM  78 H   BPY   2     -13.986  -0.775   3.143           H
HETATM  79 H   BPY   2     -16.862  -2.962  -3.860           H
HETATM  80 H   BPY   2     -14.369  -2.306  -3.663           H
HETATM  81 H   BPY   2     -14.074  -0.918  -2.587           H
HETATM  82 H   BPY   2     -13.705  -2.547  -2.029           H
HETATM  83 C   BPY   2     -19.414  -3.010  -2.345           C
HETATM  84 H   BPY   2     -20.008  -2.182   3.049           H
HETATM  85 H   BPY   2     -19.881  -0.789   4.165           H
HETATM  86 H   BPY   2     -20.378  -0.559   2.461           H
HETATM  87 H   BPY   2     -19.745  -3.801  -1.657           H
HETATM  88 H   BPY   2     -20.119  -2.173  -2.231           H
HETATM  89 H   BPY   2     -19.463  -3.383  -3.375           H
HETATM  90 H   CTZ   3      13.690   3.251   1.185           H
HETATM  91 C   CTZ   3      12.664   3.032   1.491           C
HETATM  92 C   CTZ   3      12.448   2.190   2.592           C
HETATM  93 C   CTZ   3      11.600   3.566   0.782           C
HETATM  94 C   CTZ   3      13.616   1.578   3.337           C
HETATM  95 C   CTZ   3      11.133   1.901   2.946           C
HETATM  96 C   CTZ   3      10.281   3.272   1.152           C
HETATM  97 H   CTZ   3      11.764   4.223  -0.075           H
HETATM  98 C   CTZ   3      14.296   0.521   2.529           C
HETATM  99 H   CTZ   3      14.353   2.359   3.577           H
HETATM 100 H   CTZ   3      13.268   1.134   4.279           H
HETATM 101 C   CTZ   3      10.050   2.432   2.243           C
HETATM 102 H   CTZ   3      10.938   1.243   3.797           H
HETATM 103 C   CTZ   3      15.309   0.825   1.502           C
HETATM 104 N   CTZ   3      14.029  -0.761   2.605           N
HETATM 105 H   CTZ   3       9.037   2.182   2.557           H
HETATM 106 N   CTZ   3      15.589  -0.418   0.997           N
HETATM 107 O   CTZ   3      15.805   1.894   1.142           O
HETATM 108 C   CTZ   3      14.803  -1.378   1.677           C
HETATM 109 C   CTZ   3      16.461  -0.806  -0.009           C
HETATM 110 C   CTZ   3      14.890  -2.691   1.333           C
HETATM 111 C   CTZ   3      16.537  -2.111  -0.349           C
HETATM 112 H   CTZ   3      17.066  -0.024  -0.462           H
HETATM 113 C   CTZ   3      14.040  -3.752   1.960           C
HETATM 114 N   CTZ   3      15.749  -3.040   0.336           N
HETATM 115 C   CTZ   3      17.440  -2.634  -1.394           C
HETATM 116 H   CTZ   3      14.689  -4.562   2.326           H
```

```
HETATM  117  H   CTZ     3      13.537  -3.304   2.825                H
HETATM  118  C   CTZ     3      13.028  -4.302   0.977                C
HETATM  119  H   CTZ     3      15.721  -3.993  -0.009                H
HETATM  120  C   CTZ     3      17.713  -1.881  -2.543                C
HETATM  121  C   CTZ     3      18.043  -3.890  -1.251                C
HETATM  122  C   CTZ     3      13.143  -5.598   0.472                C
HETATM  123  C   CTZ     3      11.974  -3.493   0.540                C
HETATM  124  C   CTZ     3      18.579  -2.367  -3.516                C
HETATM  125  H   CTZ     3      17.227  -0.914  -2.684                H
HETATM  126  C   CTZ     3      18.903  -4.378  -2.231                C
HETATM  127  H   CTZ     3      17.863  -4.487  -0.354                H
HETATM  128  C   CTZ     3      12.220  -6.080  -0.456                C
HETATM  129  H   CTZ     3      13.959  -6.240   0.812                H
HETATM  130  C   CTZ     3      11.052  -3.974  -0.384                C
HETATM  131  H   CTZ     3      11.880  -2.477   0.930                H
HETATM  132  C   CTZ     3      19.175  -3.618  -3.365                C
HETATM  133  H   CTZ     3      18.780  -1.768  -4.407                H
HETATM  134  H   CTZ     3      19.368  -5.357  -2.101                H
HETATM  135  C   CTZ     3      11.174  -5.270  -0.886                C
HETATM  136  H   CTZ     3      12.321  -7.097  -0.842                H
HETATM  137  H   CTZ     3      10.232  -3.334  -0.716                H
HETATM  138  H   CTZ     3      19.849  -4.001  -4.134                H
HETATM  139  H   CTZ     3      10.450  -5.647  -1.612                H
END
```

Long 2I-BODIPY-CTZ (6)

```
TITLE     I2BPY_CTZ_REDC_Long_opt_1
REMARK   1 I2BPY_CTZ_REDC_Long_opt_1
HETATM    1  O   LNK     1      12.121  -3.555   1.655                O
HETATM    2  C   LNK     1      10.764  -3.533   1.258                C
HETATM    3  H   LNK     1      10.537  -2.587   0.734                H
HETATM    4  H   LNK     1      10.562  -4.358   0.552                H
HETATM    5  C   LNK     1       9.908  -3.673   2.498                C
HETATM    6  H   LNK     1      10.159  -2.854   3.192                H
HETATM    7  H   LNK     1      10.179  -4.612   3.008                H
HETATM    8  C   LNK     1       8.417  -3.657   2.188                C
HETATM    9  H   LNK     1       8.159  -2.719   1.666                H
HETATM   10  H   LNK     1       8.178  -4.472   1.484                H
HETATM   11  C   LNK     1       7.546  -3.795   3.431                C
HETATM   12  H   LNK     1       7.791  -2.982   4.138                H
HETATM   13  H   LNK     1       7.801  -4.734   3.952                H
HETATM   14  C   LNK     1       6.054  -3.769   3.130                C
HETATM   15  H   LNK     1       5.792  -2.827   2.621                H
HETATM   16  H   LNK     1       5.797  -4.586   2.434                H
HETATM   17  C   LNK     1       5.199  -3.893   4.387                C
HETATM   18  H   LNK     1       5.427  -3.061   5.069                H
HETATM   19  H   LNK     1       5.435  -4.829   4.916                H
HETATM   20  N   LNK     1       3.776  -3.869   4.121                N
HETATM   21  H   LNK     1       3.298  -4.744   3.942                H
HETATM   22  C   LNK     1       3.078  -2.717   4.030                C
HETATM   23  O   LNK     1       3.600  -1.619   4.176                O
HETATM   24  C   LNK     1       1.590  -2.873   3.783                C
HETATM   25  H   LNK     1       1.096  -2.922   4.766                H
HETATM   26  H   LNK     1       1.377  -3.826   3.277                H
HETATM   27  C   LNK     1       1.008  -1.698   3.020                C
HETATM   28  H   LNK     1       1.442  -0.773   3.433                H
HETATM   29  H   LNK     1       1.290  -1.728   1.957                H
HETATM   30  C   LNK     1      -0.496  -1.601   3.173                C
```

```
HETATM  31  O   LNK   1      -1.073  -1.954   4.194                O
HETATM  32  N   LNK   1      -1.158  -1.062   2.125                N
HETATM  33  H   LNK   1      -0.642  -0.824   1.288                H
HETATM  34  C   LNK   1      -2.589  -0.863   2.147                C
HETATM  35  H   LNK   1      -2.848  -0.085   1.417                H
HETATM  36  H   LNK   1      -2.884  -0.512   3.146                H
HETATM  37  C   LNK   1      -3.358  -2.144   1.816                C
HETATM  38  H   LNK   1      -3.100  -2.922   2.547                H
HETATM  39  H   LNK   1      -3.064  -2.496   0.817                H
HETATM  40  N   LNK   1      -4.791  -1.948   1.836                N
HETATM  41  H   LNK   1      -5.302  -2.166   2.683                H
HETATM  42  C   LNK   1      -5.448  -1.425   0.778                C
HETATM  43  O   LNK   1      -4.894  -1.072  -0.247                O
HETATM  44  C   BPY   2      -6.959  -1.368   0.950                C
HETATM  45  H   BPY   2      -7.364  -2.379   0.763                H
HETATM  46  H   BPY   2      -7.218  -1.092   1.986                H
HETATM  47  O   BPY   2      -7.469  -0.440   0.034                O
HETATM  48  C   BPY   2      -8.803  -0.255  -0.045                C
HETATM  49  C   BPY   2      -9.239   0.680  -0.992                C
HETATM  50  C   BPY   2      -9.739  -0.926   0.746                C
HETATM  51  C   BPY   2     -10.590   0.943  -1.142                C
HETATM  52  H   BPY   2      -8.492   1.192  -1.599                H
HETATM  53  C   BPY   2     -11.097  -0.660   0.578                C
HETATM  54  H   BPY   2      -9.431  -1.656   1.493                H
HETATM  55  C   BPY   2     -11.535   0.271  -0.359                C
HETATM  56  H   BPY   2     -10.919   1.676  -1.880                H
HETATM  57  H   BPY   2     -11.824  -1.191   1.195                H
HETATM  58  C   BPY   2     -12.985   0.550  -0.526                C
HETATM  59  C   BPY   2     -13.769  -0.307  -1.310                C
HETATM  60  C   BPY   2     -13.553   1.667   0.100                C
HETATM  61  N   BPY   2     -15.134  -0.075  -1.466                N
HETATM  62  C   BPY   2     -13.424  -1.470  -2.063                C
HETATM  63  C   BPY   2     -12.982   2.653   0.962                C
HETATM  64  N   BPY   2     -14.906   1.960  -0.060                N
HETATM  65  B   BPY   2     -15.918   1.117  -0.871                B
HETATM  66  C   BPY   2     -15.658  -1.018  -2.259                C
HETATM  67  C   BPY   2     -14.619  -1.897  -2.642                C
HETATM  68  C   BPY   2     -12.087  -2.113  -2.225                C
HETATM  69  C   BPY   2     -14.033   3.513   1.279                C
HETATM  70  C   BPY   2     -11.574   2.766   1.444                C
HETATM  71  C   BPY   2     -15.209   3.062   0.637                C
HETATM  72  F   BPY   2     -16.933   0.661  -0.033                F
HETATM  73  F   BPY   2     -16.472   1.880  -1.897                F
HETATM  74  C   BPY   2     -17.096  -1.043  -2.635                C
HETATM  75  I   BPY   2     -14.872  -3.557  -3.881                I
HETATM  76  H   BPY   2     -11.771  -2.615  -1.300                H
HETATM  77  H   BPY   2     -12.123  -2.865  -3.023                H
HETATM  78  H   BPY   2     -11.310  -1.379  -2.471                H
HETATM  79  I   BPY   2     -13.929   5.200   2.503                I
HETATM  80  H   BPY   2     -11.506   3.519   2.238                H
HETATM  81  H   BPY   2     -11.201   1.811   1.833                H
HETATM  82  H   BPY   2     -10.897   3.066   0.632                H
HETATM  83  C   BPY   2     -16.582   3.628   0.685                C
HETATM  84  H   BPY   2     -17.324  -0.209  -3.315                H
HETATM  85  H   BPY   2     -17.354  -1.984  -3.132                H
HETATM  86  H   BPY   2     -17.723  -0.915  -1.743                H
HETATM  87  H   BPY   2     -17.001   3.694  -0.328                H
```

```
HETATM   88 H   BPY    2    -17.244   2.971   1.268                H
HETATM   89 H   BPY    2    -16.579   4.622   1.145                H
HETATM   90 H   CTZ    3     16.496  -3.331   0.670                H
HETATM   91 C   CTZ    3     15.469  -3.337   0.298                C
HETATM   92 C   CTZ    3     15.245  -3.206  -1.081                C
HETATM   93 C   CTZ    3     14.411  -3.451   1.184                C
HETATM   94 C   CTZ    3     16.407  -3.045  -2.041                C
HETATM   95 C   CTZ    3     13.928  -3.186  -1.531                C
HETATM   96 C   CTZ    3     13.089  -3.436   0.718                C
HETATM   97 H   CTZ    3     14.580  -3.554   2.258                H
HETATM   98 C   CTZ    3     17.056  -1.706  -1.911                C
HETATM   99 H   CTZ    3     17.163  -3.819  -1.839                H
HETATM  100 H   CTZ    3     16.058  -3.169  -3.074                H
HETATM  101 C   CTZ    3     12.850  -3.302  -0.651                C
HETATM  102 H   CTZ    3     13.726  -3.080  -2.600                H
HETATM  103 C   CTZ    3     18.054  -1.395  -0.871                C
HETATM  104 N   CTZ    3     16.777  -0.667  -2.663                N
HETATM  105 H   CTZ    3     11.835  -3.286  -1.046                H
HETATM  106 N   CTZ    3     18.310  -0.069  -1.104                N
HETATM  107 O   CTZ    3     18.557  -2.098   0.007                O
HETATM  108 C   CTZ    3     17.527   0.364  -2.200                C
HETATM  109 C   CTZ    3     19.161   0.811  -0.453                C
HETATM  110 C   CTZ    3     17.600   1.658  -2.614                C
HETATM  111 C   CTZ    3     19.222   2.096  -0.865                C
HETATM  112 H   CTZ    3     19.763   0.403   0.356                H
HETATM  113 C   CTZ    3     16.765   2.202  -3.730                C
HETATM  114 N   CTZ    3     18.440   2.501  -1.950                N
HETATM  115 C   CTZ    3     20.100   3.112  -0.251                C
HETATM  116 H   CTZ    3     17.426   2.649  -4.488                H
HETATM  117 H   CTZ    3     16.243   1.357  -4.195                H
HETATM  118 C   CTZ    3     15.777   3.236  -3.232                C
HETATM  119 H   CTZ    3     18.401   3.489  -2.173                H
HETATM  120 C   CTZ    3     20.361   3.092   1.126                C
HETATM  121 C   CTZ    3     20.693   4.110  -1.036                C
HETATM  122 C   CTZ    3     15.922   4.586  -3.554                C
HETATM  123 C   CTZ    3     14.715   2.845  -2.410                C
HETATM  124 C   CTZ    3     21.204   4.038   1.698                C
HETATM  125 H   CTZ    3     19.883   2.340   1.755                H
HETATM  126 C   CTZ    3     21.528   5.061  -0.458                C
HETATM  127 H   CTZ    3     20.522   4.134  -2.114                H
HETATM  128 C   CTZ    3     15.022   5.532  -3.064                C
HETATM  129 H   CTZ    3     16.745   4.903  -4.200                H
HETATM  130 C   CTZ    3     13.816   3.787  -1.922                C
HETATM  131 H   CTZ    3     14.597   1.789  -2.153                H
HETATM  132 C   CTZ    3     21.789   5.027   0.910                C
HETATM  133 H   CTZ    3     21.394   4.010   2.773                H
HETATM  134 H   CTZ    3     21.986   5.829  -1.085                H
HETATM  135 C   CTZ    3     13.968   5.135  -2.247                C
HETATM  136 H   CTZ    3     15.147   6.585  -3.324                H
HETATM  137 H   CTZ    3     12.989   3.468  -1.284                H
HETATM  138 H   CTZ    3     22.444   5.773   1.362                H
HETATM  139 H   CTZ    3     13.262   5.874  -1.863                H
END
```

Long BODIPY-CTZ (oxidized form)

```
TITLE     BPY_CTZ_Long_opt_ox
REMARK   1 BPY_CTZ_Long_opt_ox
HETATM    1 C   CTZ    1    -14.037   1.940   1.278                C
```

```
HETATM    2 C   CTZ    1    -12.959   2.457   0.524                C
HETATM    3 N   CTZ    1    -15.182   2.594   1.374                N
HETATM    4 N   CTZ    1    -13.902   0.700   1.908                N
HETATM    5 N   CTZ    1    -13.092   3.617  -0.097                N
HETATM    6 C   CTZ    1    -11.647   1.733   0.406                C
HETATM    7 C   CTZ    1    -15.285   3.763   0.756                C
HETATM    8 C   CTZ    1    -14.423   0.340   3.126                C
HETATM    9 H   CTZ    1    -13.297   0.019   1.459                H
HETATM   10 C   CTZ    1    -14.235   4.303   0.007                C
HETATM   11 H   CTZ    1    -10.908   2.469   0.063                H
HETATM   12 H   CTZ    1    -11.323   1.400   1.405                H
HETATM   13 C   CTZ    1    -11.630   0.542  -0.536                C
HETATM   14 H   CTZ    1    -16.245   4.277   0.837                H
HETATM   15 C   CTZ    1    -14.167  -1.111   3.525                C
HETATM   16 O   CTZ    1    -15.050   1.089   3.842                O
HETATM   17 C   CTZ    1    -14.331   5.605  -0.697                C
HETATM   18 C   CTZ    1    -10.445  -0.194  -0.667                C
HETATM   19 C   CTZ    1    -12.736   0.162  -1.298                C
HETATM   20 H   CTZ    1    -15.131  -1.629   3.397                H
HETATM   21 H   CTZ    1    -13.971  -1.089   4.606                H
HETATM   22 C   CTZ    1    -13.077  -1.831   2.778                C
HETATM   23 C   CTZ    1    -13.407   5.915  -1.703                C
HETATM   24 C   CTZ    1    -15.321   6.545  -0.382                C
HETATM   25 C   CTZ    1    -10.368  -1.273  -1.538                C
HETATM   26 H   CTZ    1     -9.571   0.093  -0.078                H
HETATM   27 C   CTZ    1    -12.665  -0.931  -2.163                C
HETATM   28 H   CTZ    1    -13.670   0.724  -1.231                H
HETATM   29 C   CTZ    1    -13.370  -2.669   1.694                C
HETATM   30 C   CTZ    1    -11.736  -1.647   3.117                C
HETATM   31 C   CTZ    1    -13.477   7.126  -2.383                C
HETATM   32 H   CTZ    1    -12.633   5.186  -1.943                H
HETATM   33 C   CTZ    1    -15.390   7.757  -1.062                C
HETATM   34 H   CTZ    1    -16.039   6.345   0.414                H
HETATM   35 C   CTZ    1    -11.482  -1.650  -2.288                C
HETATM   36 H   CTZ    1     -9.433  -1.828  -1.633                H
HETATM   37 H   CTZ    1    -13.544  -1.215  -2.746                H
HETATM   38 C   CTZ    1    -12.361  -3.296   0.978                C
HETATM   39 H   CTZ    1    -14.411  -2.831   1.404                H
HETATM   40 C   CTZ    1    -10.710  -2.266   2.406                C
HETATM   41 H   CTZ    1    -11.477  -0.999   3.959                H
HETATM   42 C   CTZ    1    -14.470   8.051  -2.067                C
HETATM   43 H   CTZ    1    -12.751   7.349  -3.168                H
HETATM   44 H   CTZ    1    -16.165   8.479  -0.800                H
HETATM   45 H   CTZ    1    -11.424  -2.503  -2.967                H
HETATM   46 C   CTZ    1    -11.021  -3.095   1.326                C
HETATM   47 H   CTZ    1    -12.587  -3.943   0.130                H
HETATM   48 H   CTZ    1     -9.677  -2.092   2.703                H
HETATM   49 H   CTZ    1    -14.525   9.003  -2.599                H
HETATM   50 O   LNK    2    -10.104  -3.732   0.569                O
HETATM   51 C   LNK    2     -8.728  -3.514   0.815                C
HETATM   52 H   LNK    2     -8.503  -2.434   0.755                H
HETATM   53 H   LNK    2     -8.466  -3.851   1.833                H
HETATM   54 C   LNK    2     -7.934  -4.279  -0.220                C
HETATM   55 H   LNK    2     -8.244  -3.942  -1.223                H
HETATM   56 H   LNK    2     -8.201  -5.347  -0.153                H
HETATM   57 C   LNK    2     -6.431  -4.100  -0.051                C
HETATM   58 H   LNK    2     -6.183  -3.025  -0.088                H
```

```
HETATM  59 H   LNK   2     -6.129  -4.448   0.952                H
HETATM  60 C   LNK   2     -5.615  -4.836  -1.107                C
HETATM  61 H   LNK   2     -5.917  -4.484  -2.109                H
HETATM  62 H   LNK   2     -5.862  -5.912  -1.076                H
HETATM  63 C   LNK   2     -4.113  -4.652  -0.938                C
HETATM  64 H   LNK   2     -3.864  -3.579  -0.963                H
HETATM  65 H   LNK   2     -3.797  -5.028   0.049                H
HETATM  66 C   LNK   2     -3.305  -5.356  -2.024                C
HETATM  67 H   LNK   2     -3.592  -4.961  -3.009                H
HETATM  68 H   LNK   2     -3.523  -6.434  -2.025                H
HETATM  69 N   LNK   2     -1.874  -5.186  -1.874                N
HETATM  70 H   LNK   2     -1.351  -5.884  -1.360                H
HETATM  71 C   LNK   2     -1.231  -4.085  -2.316                C
HETATM  72 O   LNK   2     -1.812  -3.172  -2.890                O
HETATM  73 C   LNK   2      0.269  -4.064  -2.094                C
HETATM  74 H   LNK   2      0.744  -4.434  -3.016                H
HETATM  75 H   LNK   2      0.557  -4.756  -1.289                H
HETATM  76 C   LNK   2      0.783  -2.661  -1.827                C
HETATM  77 H   LNK   2      0.294  -1.977  -2.539                H
HETATM  78 H   LNK   2      0.509  -2.318  -0.819                H
HETATM  79 C   LNK   2      2.278  -2.548  -2.047                C
HETATM  80 O   LNK   2      2.857  -3.182  -2.920                O
HETATM  81 N   LNK   2      2.926  -1.676  -1.244                N
HETATM  82 H   LNK   2      2.411  -1.205  -0.511                H
HETATM  83 C   LNK   2      4.345  -1.430  -1.372                C
HETATM  84 H   LNK   2      4.576  -0.461  -0.910                H
HETATM  85 H   LNK   2      4.603  -1.373  -2.439                H
HETATM  86 C   LNK   2      5.186  -2.522  -0.708                C
HETATM  87 H   LNK   2      4.955  -3.490  -1.172                H
HETATM  88 H   LNK   2      4.931  -2.579   0.359                H
HETATM  89 N   LNK   2      6.605  -2.274  -0.831                N
HETATM  90 H   LNK   2      7.105  -2.680  -1.614                H
HETATM  91 C   LNK   2      7.259  -1.459   0.025                C
HETATM  92 O   LNK   2      6.713  -0.875   0.943                O
HETATM  93 C   BPY   3      8.760  -1.377  -0.219                C
HETATM  94 H   BPY   3      9.227  -2.279   0.217                H
HETATM  95 H   BPY   3      8.973  -1.382  -1.302                H
HETATM  96 O   BPY   3      9.239  -0.212   0.390                O
HETATM  97 C   BPY   3     10.564   0.047   0.366                C
HETATM  98 C   BPY   3     10.973   1.217   1.017                C
HETATM  99 C   BPY   3     11.515  -0.766  -0.256                C
HETATM 100 C   BPY   3     12.313   1.568   1.045                C
HETATM 101 H   BPY   3     10.216   1.838   1.497                H
HETATM 102 C   BPY   3     12.860  -0.402  -0.219                C
HETATM 103 H   BPY   3     11.227  -1.680  -0.772                H
HETATM 104 C   BPY   3     13.273   0.760   0.426                C
HETATM 105 H   BPY   3     12.622   2.482   1.555                H
HETATM 106 H   BPY   3     13.598  -1.041  -0.707                H
HETATM 107 C   BPY   3     14.711   1.140   0.457                C
HETATM 108 C   BPY   3     15.527   0.677   1.494                C
HETATM 109 C   BPY   3     15.231   1.960  -0.551                C
HETATM 110 N   BPY   3     16.878   1.024   1.545                N
HETATM 111 C   BPY   3     15.246  -0.153   2.622                C
HETATM 112 C   BPY   3     14.623   2.549  -1.701                C
HETATM 113 N   BPY   3     16.576   2.335  -0.539                N
HETATM 114 B   BPY   3     17.611   1.922   0.528                B
HETATM 115 C   BPY   3     17.430   0.457   2.628                C
```

```
HETATM 116 C   BPY   3     16.445 -0.278  3.315                C
HETATM 117 C   BPY   3     13.953 -0.785  3.026                C
HETATM 118 C   BPY   3     15.630  3.263 -2.343                C
HETATM 119 C   BPY   3     13.207  2.454 -2.170                C
HETATM 120 C   BPY   3     16.818  3.112 -1.605                C
HETATM 121 F   BPY   3     18.663  1.221 -0.066                F
HETATM 122 F   BPY   3     18.124  3.054  1.166                F
HETATM 123 C   BPY   3     18.866  0.626  2.984                C
HETATM 124 H   BPY   3     13.584 -1.481  2.259                H
HETATM 125 H   BPY   3     14.086 -1.343  3.962                H
HETATM 126 H   BPY   3     13.163 -0.038  3.177                H
HETATM 127 H   BPY   3     13.082  3.022 -3.100                H
HETATM 128 H   BPY   3     12.910  1.413 -2.358                H
HETATM 129 H   BPY   3     12.504  2.851 -1.425                H
HETATM 130 C   BPY   3     18.160  3.688 -1.895                C
HETATM 131 H   BPY   3     19.104  1.690  3.126                H
HETATM 132 H   BPY   3     19.101  0.078  3.904                H
HETATM 133 H   BPY   3     19.509  0.261  2.171                H
HETATM 134 H   BPY   3     18.498  4.317 -1.059                H
HETATM 135 H   BPY   3     18.904  2.887 -2.013                H
HETATM 136 H   BPY   3     18.130  4.290 -2.810                H
HETATM 137 H   BPY   3     15.528  3.841 -3.259                H
HETATM 138 H   BPY   3     16.607 -0.842  4.231                H
END
```

Supplementary Results

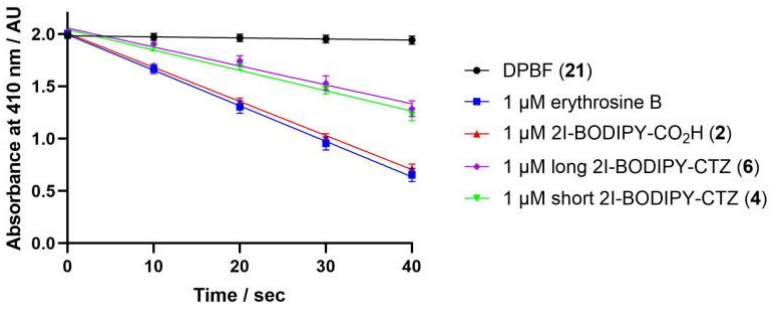

Figure SR1: Decrease in absorbance at 410 nm of a 200 µM DPBF (**21**) solution in MeOH containing 1 µM photosensitizer. All measurements were performed in three independent experiments.

Table SR1: Results of Φ_Δ determination in MeOH. Φ_Δ are mean values derived from three independent experiments. I_a values were determined of 10 µM stocks in MeOH at 517 nm.

Compound	$I_{a,\ 517\ nm}$ ± SD		k [$s^{-1}10^{-3}$] ± SD		Φ_Δ
erythrosine B (reference)	0.621 0.626 0.596	0.614 ± 0.0164	34.0 32.6 35.1	33.9 ± 1.17	0.62 (ref)[10]
2I-BODIPY-CO_2H (2)	0.464 0.464 0.499	0.476 ± 0.020	32.6 31.1 34.0	32.6 ± 1.48	0.719
long 2I-BODIPY-CTZ conjugate (6)	0.388 0.386 0.422	0.399 ± 0.020	15.8 18.0 20.5	18.1 ± 2.36	0.476
short 2I-BODIPY-CTZ conjugate (4)	0.406 0.404 0.443	0.418 ± 0.022	19.1 19.5 19.7	19.4 ± 0.32	0.490

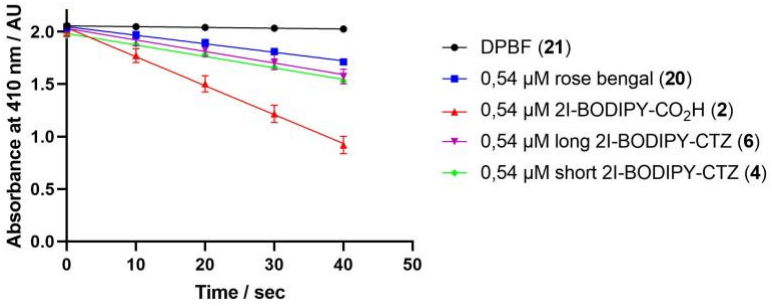

Figure SR2: Decrease in absorbance at 410 nm of a 200 µM DPBF (**21**) solution in MeCN containing 0.54 µM photosensitizer. All measurements were performed in three independent experiments.

Table SR2: Results of Φ_Δ determination in MeCN. Φ_Δ are mean values derived from three independent experiments. I_a values were determined of 5.4 µM stocks in MeCN at 517 nm. [a]The overestimation of 2I-BODIPY-CO_2H (Φ_Δ = 1.26) is because of using rose bengal as a standard.

Compound	$I_{a,\ 517\ nm}$ ± SD		k [$s^{-1}10^{-3}$] ± SD		Φ_Δ
rose bengal (20, reference)	0.153 0.153 0.161	0.156 ± 0.0047	7.8 8.0 8.5	8.1 ± 0.36	0.530 (ref)[9]
2I-BODIPY-CO_2H (2)	0.222 0.215 0.232	0.223 ± 0.0085	27.4 26.8 28.4	27.5 ± 0.80	1.261[a]
long 2I-BODIPY-CTZ conjugate (6)	0.234 0.224 0.238	0.232 ± 0.0072	11.1 10.4 11.4	11.0 ± 0.52	0.482
short 2I-BODIPY-CTZ conjugate (4)	0.232 0.225 0.226	0.228 ± 0.0039	11.3 10.9 10.6	10.9 ± 0.35	0.490

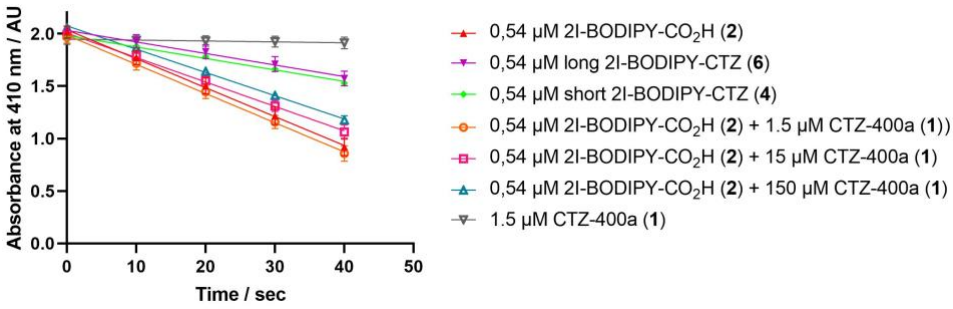

Figure SR3: Effect of the presence of CTZ-400a (**1**) towards the slope of 2I-BODIPY-CO_2H (**2**).

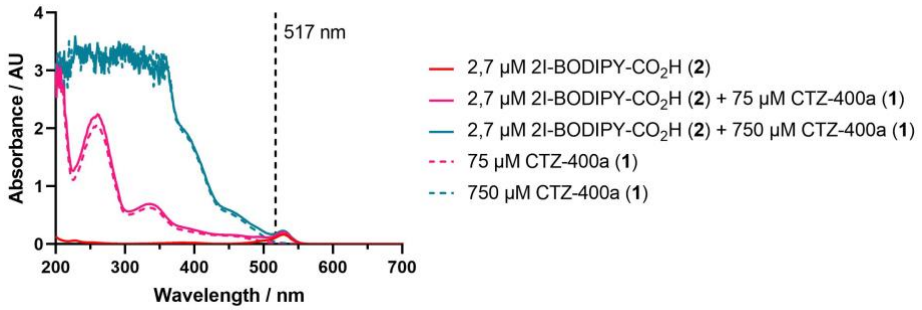

Figure SR4: Absorbance spectra of 2I-BODIPY-CO_2H (**2**) in the presence of various amounts of CTZ-400a (**1**) and corresponding absorbance spectra of CTZ-400a (**1**) in the absence of 2I-BODIPY-CO_2H (**2**).

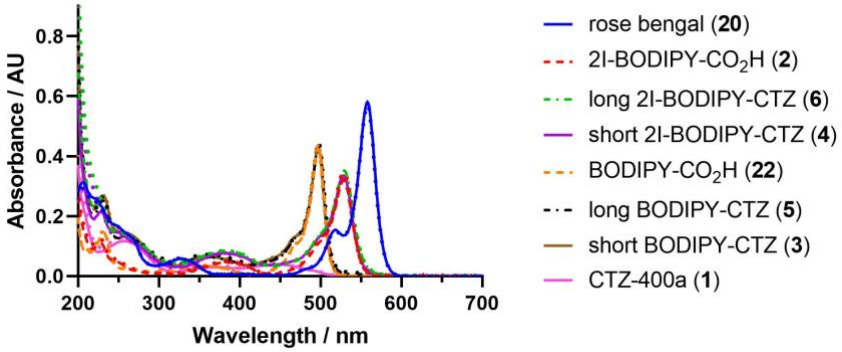

Figure SR5: Absorbance spectra recorded at 5.4 µM in MeCN measured in duplicate. Second replicate is shown as dotted line for all compounds.

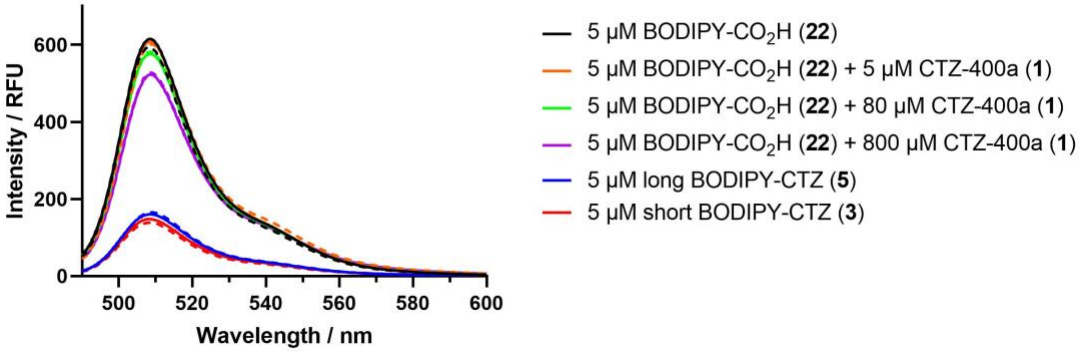

Figure SR6: Fluorescence spectra of not iodinated BODIPY derivative **22**, **3**, **5** in MeCN. Fluorescence of BODIPY-CO_2H (**22**) was also recorded in the presence of different amounts of CTZ-400a (**1**). Measurements were performed in duplicate (solid line: 1. replicate; dashed line: 2. replicate).

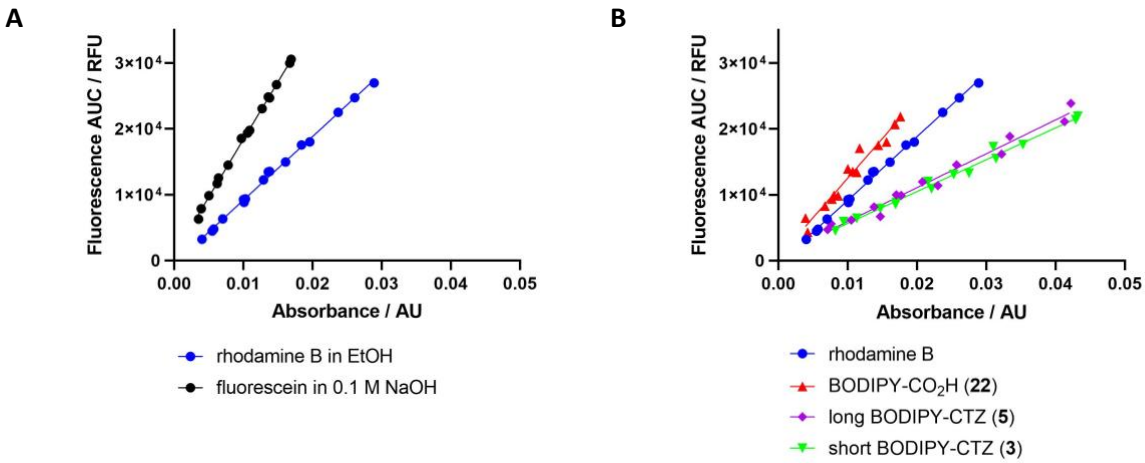

Figure SR7: Plots for fluorescence quantum yield determination. A) Cross calibration of fluorimeter using rhodamine B in EtOH and fluorescein in 0.1 M NaOH. B) Measurement of fluorescence quantum yields of samples 3, 5 and 22 in EtOH using rhodamine B as reference. All measurements were performed in three independent experiments.

Table SR3: Determined slopes and corresponding quantum yields for the two reference compounds fluorescein and rhodamine B as well as for sample compounds **22**, **5** and **3**.

Compound	**Grad ± SD**		**Reference**	**Φ_F**	**Φ_F (lit.)**
Fluorescein	1768762 1732467 1733020	1744750 ± 20797	Rhodamine B	0.827	0.790[4]
Rhodamine B	960884 973821 974618	969774 ± 7710	Fluorescein	0.460	0.490[6]
BODIPY-CO_2H (22)	1155927 1161697 1267601	1195075 ± 62875	Rhodamine B	0.604	-
long BODIPY-CTZ (5)	539182 530699 526678	532186 ± 6383	Rhodamine B	0.269	-
short BODIPY-CTZ (3)	480103 497246 465962	481103 ± 15666	Rhodamine B	0.243	-

Electronic Excited State Properties of Donor and Acceptor Moieties Used for FRET Modelling

Table SR4: Components of the transition dipole moments (x, y, z) in atomic units (a.u.), fluorescence quantum yield of the donor (Q), and fluorescence lifetime of the donor in the absence of the acceptor (τ, s) used in FRET modelling.

Molecule: **Short BODIPY-CTZ (3)**			
	x y z, a.u.	**Q[47]**	**τ, s[47]**
Donor moiety: BPY_EXP1S	0.0133 -3.0343 -0.0046	0.45	3.8E-9
Acceptor moiety: CTZ_EXP1S	-1.7421 -0.4623 -0.1225	-	-
Molecule: **Short 2I-BODIPY-CTZ (4)**			
Donor moiety: I2BPY_EXP2S	3.4761 0.0163 -0.0063	0.03	0.24E-9
Acceptor moiety: CTZ_EXP2S	-1.7226 -0.4956 -0.1218	-	-
*Molecule: BRET **Short BODIPY-CTZ (oxidized form)**		-	-
Donor moiety: CTZox_EXP3S	1.6981 0.2223 -0.0415	-	-
Acceptor moiety: BPY_EXP3S	-0.0020 3.0363 0.0016	-	-
Molecule: **Long BODIPY-CTZ (5)**			
Donor moiety: BPY_EXP1L	0.0158 3.0343 0.0062	0.45	3.8E-9
Acceptor moiety: CTZ_EXP1L	-1.7605 -0.4428 -0.1241	-	-
Molecule: **Long 2I-BODIPY-CTZ (6)**			
Donor moiety: I2BPY_EXP2L	3.4764 0.0189 -0.0069	0.03	0.24E-9
Acceptor moiety: CTZ_EXP2L	-1.7832 -0.3967 -0.1288	-	-
*Molecule: BRET **Long BODIPY-CTZ (oxidized form)**			
Donor moiety: CTZox_EXP3L	-1.8102 -0.2667 0.0528	-	-
Acceptor moiety: BPY_EXP3L.txt	0.0029 -3.0348 -0.0047	-	-
***Absolute energy transfer rates were not calculated for the BRET experiment.**			

FRET Modelling Results

Table SR5: Calculated absolut (k) and relative (k_{rel}) FRET rates based on donor-acceptor distance (d_{DA}), orientation factor magnitude (Θ), and spectral overlap (J) between donor emission and acceptor absorption spectra.

Molecules	**d_{DA}, Å**	**Θ, %**	**J, M^{-1} cm^{-1} nm^4**	**k, s^{-1}**	**k_{rel}**
Short BODIPY-CTZ (3)	20.966	5.083	1.55E+13	6.02E+06	1
Long BODIPY-CTZ (5)	30.140	32.570	1.55E+13	2.80E+07	4.65
Short 2I-BODIPY-CTZ (4)	21.210	7.608	2.29E+13	1.96E+07	1
Long 2I-BODIPY-CTZ (6)	30.640	32.909	2.29E+13	4.03E+07	2.06
***BRET Short BODIPY-CTZ (oxidized)**	19.251	7.730	-	-	1
***BRET Long BODIPY-CTZ (oxidized)**	27.911	37.179	-	-	2.48
***Absolute energy transfer rates were not calculated for the BRET experiment.**					

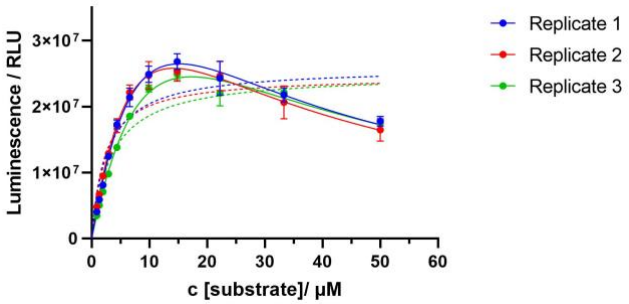

Figure SR8: Plots for K_m determination using CTZ-400a (**1**) as substrate of the LgBiT-HiBiT enzyme complex. Buffer: 50 mM Tris pH = 7.5, 150 mM NaCl, 0.005% Igepal CA-630 and 0.1 g/L BSA. All measurements were carried out in triplicate as three independent measurements, i.e. from different stock solutions.

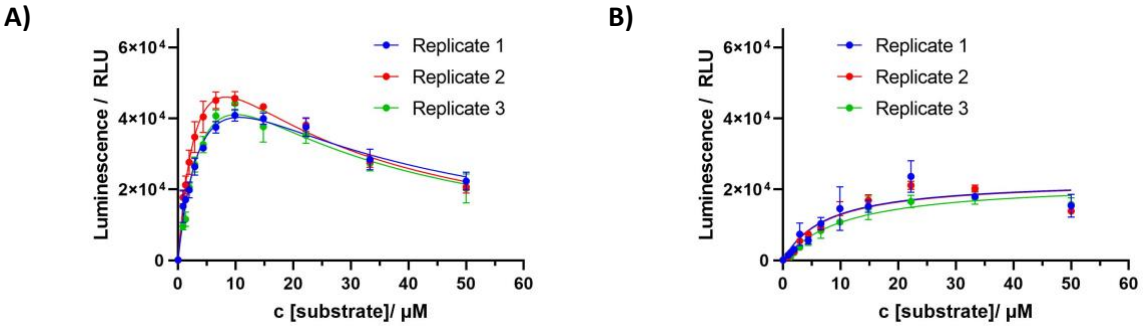

Figure SR9: Plots for K_m determination testing: **A)** long BODIPY-CTZ (**5**), **B)** short BODIPY-CTZ (**3**) as substrates of the LgBiT-HiBiT enzyme complex. Buffer: 50 mM Tris pH = 7.5, 150 mM NaCl, 0.005% Igepal CA-630 and 0.1 g/L BSA. All measurements were carried out in triplicate as three independent measurements, i.e. from different stock solutions.

Table SR6: Results of K_m determination of the LgBiT-HiBiT restored enzyme 5 min after substrate addition. Buffer: 50 mM Tris pH = 7.5, 150 mM NaCl, 0.005% Igepal CA-630 and 0.1 g/L BSA. [a]Equation for substrate inhibition used; [b]Michaelis Menten plot used.

Substrate	V_{max} [RLU/s] ± SD		K_m [µM] ± SD		K_i [µM] ± SD	
CTZ-400a (1)[a]	80.18×10^7	$75.70 \times 10^7 \pm 4.96 \times 10^7$	15.40	15.34 ± 3.04	14.97	15.90 ± 0.81
	70.37×10^7		12.27		16.44	
	76.53×10^7		18.34		16.28	
long BODIPY-CTZ conjugate (5)[a]	79.25×10^4	$90.54 \times 10^4 \pm 9.93 \times 10^4$	5.157	5.51 ± 1.34	22.09	17.48 ± 4.03
	94.45×10^4		4.380		15.76	
	97.92×10^4		7.000		14.60	
short BODIPY-CTZ conjugate (3)[b]	22.79×10^4	$22.57 \times 10^4 \pm 0.29 \times 10^4$	7.444	8.01 ± 1.88	-	-
	22.69×10^4		7.601		-	
	22.24×10^4		10.77		-	

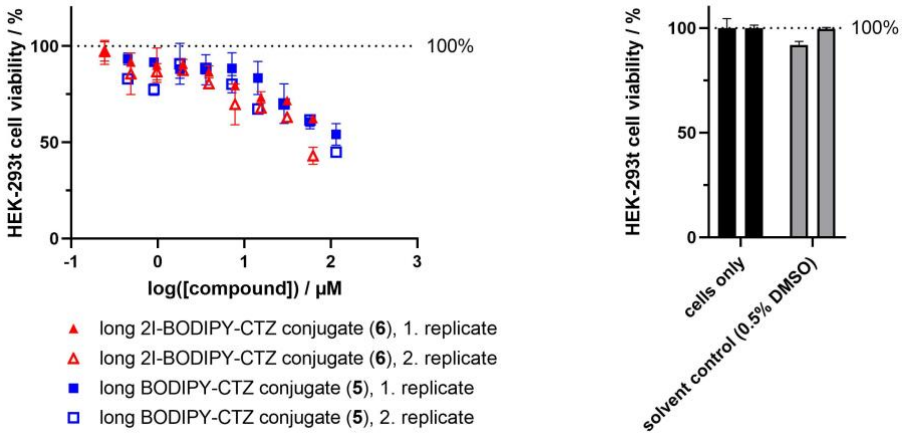

Figure SR10: Results of cell viability studies testing long 2I-BODIPY- and BODIPY-CTZ conjugates **6** and **5** performed in two independent experiments.

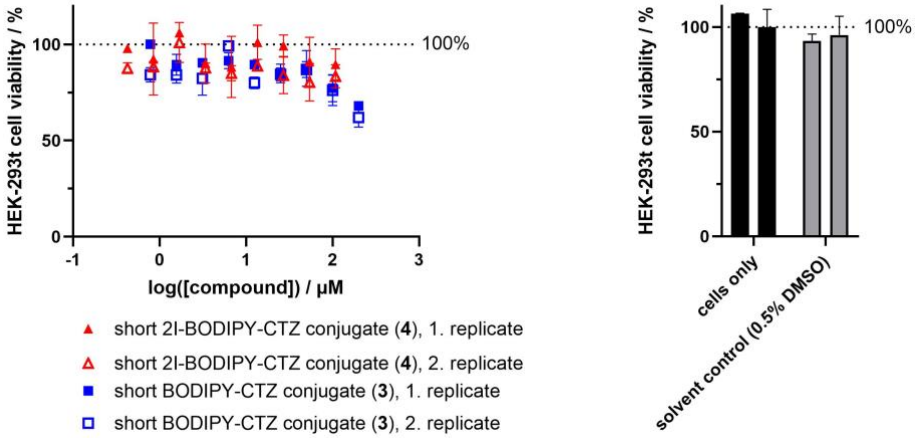

Figure SR11: Results of cell viability studies testing short 2I-BODIPY- and BODIPY-CTZ conjugates **4** and **3** performed in two independent experiments.

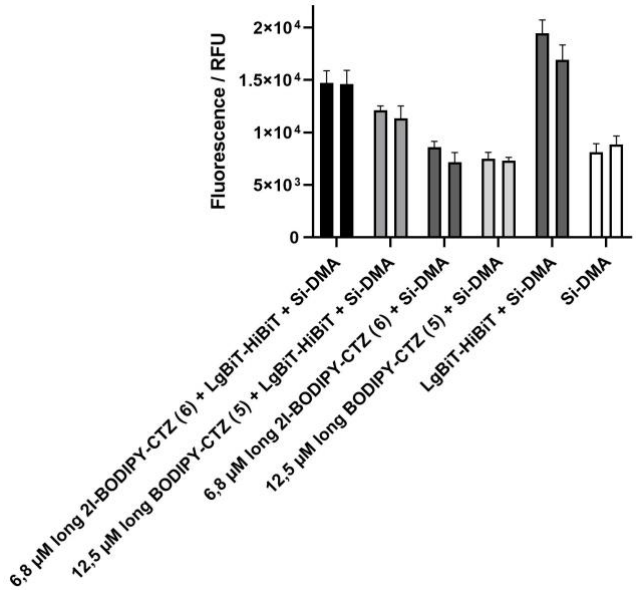

Figure SR12: Luminescence-based detection of $^1O_2$ using 25 µM Si-DMA as $^1O_2$ sensor performed in two independent experiments. All controls without Si-DMA showed hardly any fluorescence.

No fluorescence was detected for the samples: i) 6.8 µM long 2I-BODIPY-CTZ (**6**); ii) 12,5 µM long BODIPY-CTZ (**5**); iii) 6.8 µM long 2I-BODIPY-CTZ (**6**) + LgBIT-HiBiT and iv) 12.5 µM long BODIPY-CTZ (**5**) + LgBIT-HiBiT

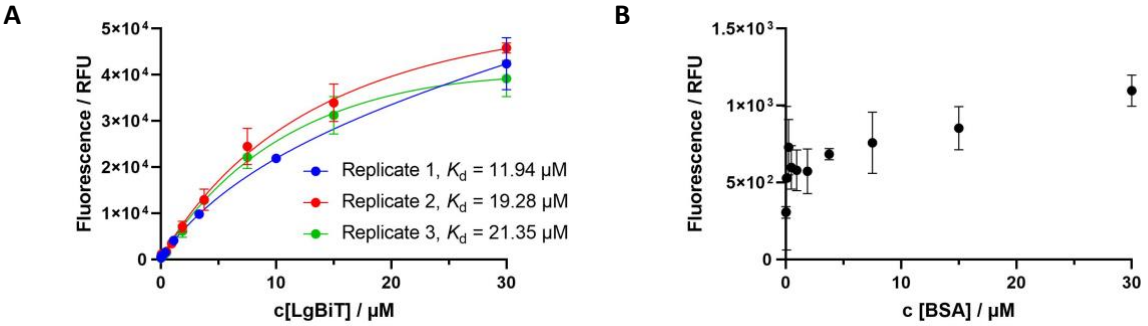

Figure SR13: Fluorescence titration of LgBiT (A) and BSA (B) at constant Si-DMA concentration (25 µM) showing a binding affinity of LgBiT to Si-DMA (K_d = 17.50 ± 5.0 µM). BSA hardly affected the Si-DMA emission.

References

[1] D. B. G. Williams, M. Lawton, *J. Org. Chem.* **2010**, *75*, 8351.
[2] G. R. Fulmer, A. J. M. Miller, N. H. Sherden, H. E. Gottlieb, A. Nudelman, B. M. Stoltz, J. E. Bercaw, K. I. Goldberg, *Organometallics* **2010**, *29*, 2176.
[3] "Horiba Scientific: A Guide to Recording Fluorescence Quantum Yields", can be found under http://www.horiba.com/fileadmin/uploads/Scientific/Documents/Fluorescence/quantumyieldstrad.pdf, **2018**.
[4] R. E. Kellogg, R. G. Bennett, *The Journal of Chemical Physics* **1964**, *41*, 3042.
[5] Z.-C. Yang, M. Wang, A. M. Yong, S. Y. Wong, X.-H. Zhang, H. Tan, A. Y. Chang, X. Li, J. Wang, *Chemical communications (Cambridge, England)* **2011**, *47*, 11615.
[6] G. Wu, F. Zeng, S. Wu, *Anal. Methods* **2013**, *5*, 5589.
[7] J. V. Herráez, R. Belda, *J Solution Chem* **2006**, *35*, 1315.
[8] G. Linden, L. Zhang, F. Pieck, U. Linne, D. Kosenkov, R. Tonner, O. Vázquez, *Angew. Chem. Int. Ed.* **2019**, *58*, 12868.
[9] N. Epelde-Elezcano, V. Martínez-Martínez, E. Peña-Cabrera, C. F. A. Gómez-Durán, I. L. Arbeloa, S. Lacombe, *RSC Adv.* **2016**, *6*, 41991.
[10] J. J. M. Lamberts, D. R. Schumacher, D. C. Neckers, *J. Am. Chem. Soc.* **1984**, *106*, 5879.
[11] G. Linden, O. Vázquez, *Chemistry* **2020**, *26*, 10014.
[12] A. K. Di Gennaro, L. Gurevich, E. Skovsen, M. T. Overgaard, P. Fojan, *Phys. Chem. Chem. Phys.* **2013**, *15*, 8838.
[13] A. Sheehan, T. Mikulchyk, C. S. P. de Castro, S. Karuthedath, W. Althobaiti, M. Dvoracek, Sabad-e-Gul, H. J. Byrne, F. Laquai, I. Naydenova et al., *J. Mater. Chem. C* **2023**, *11*, 15084.
[14] GOLD BIOTECHNOLOGY, "Certificate of Analysis, Coelenterazine 400 a", can be found under https://goldbio.com/documents/1185/C-320-COA_Sample.pdf.
[15] J. Lee, A. S. Wesley in *Bioluminescence in Progress* (Eds.: F. H. Johnson, Y. Haneda), Princeton University Press, **1967**, pp. 35–44.
[16] Y. Ikeda, M. Tanaka, R. Nishihara, Y. Hiruta, D. Citterio, K. Suzuki, K. Niwa, *J. Photochem. Photobiol. A* **2020**, *394*, 112459.
[17] Y. Ohmuro-Matsuyama, H. Ueda, *Anal. Chem.* **2018**, *90*, 3001.
[18] *Computer Aided Chemical Engineering*, Elsevier, **2015**.
[19] R. A. Copeland, *Enzymes*, Wiley, **2000**.
[20] E. P. Coutant, S. Goyard, V. Hervin, G. Gagnot, R. Baatallah, Y. Jacob, T. Rose, Y. L. Janin, *Org. Biomol. Chem.* **2019**, *17*, 3709.
[21] E. Dufour, L. Moni, L. Bonnat, S. Chierici, J. Garcia, *Org. Biomol. Chem.* **2014**, *12*, 4964.
[22] M. N. Chatterjee, E. R. Kay, D. A. Leigh, *J. Am. Chem. Soc.* **2006**, *128*, 4058.
[23] D. J. Yoo, M. M. Greenberg, *J. Org. Chem.* **1995**, *60*, 3358.
[24] M.-L. Yuan, T.-Y. Jiang, L.-P. Du, M.-Y. Li, *Chin. Chem. Lett.* **2016**, *27*, 550.
[25] Z. M. Jászay, T. S. Pham, K. Gönczi, I. Petneházy, L. Tőke, *Synth. Commun.* **2010**, *40*, 1574.
[26] D. Klamann, H. Hagemann, *Organische Stickstoff-Verbindungen mit einer C,N-Doppelbindung*, Georg Thieme Verlag, Stuttgart, **1990**.
[27] A. Shakhmin, M. P. Hall, J. R. Walker, T. Machleidt, B. F. Binkowski, K. V. Wood, T. A. Kirkland, *Chemistry* **2016**, *22*, 10369.
[28] M. Hall, T. Kirkland, T. Machleidt, A. Shakhmin, J. R. Walker, K. V. Wood, W. Zhou, US2018/0119200A1, **2017**.
[29] L. Albert, A. Peñalver, N. Djokovic, L. Werel, M. Hoffarth, D. Ruzic, J. Xu, L.-O. Essen, K. Nikolic, Y. Dou et al., *ChemBioChem* **2019**, *20*, 1417.
[30] D. Bensinger, D. Stubba, A. Cremer, V. Kohl, T. Waßmer, J. Stuckert, V. Engemann, K. Stegmaier, K. Schmitz, B. Schmidt, *J. Med. Chem.* **2019**, *62*, 2428.

[31] S. Kolemen, O. A. Bozdemir, Y. Cakmak, G. Barin, S. Erten-Ela, M. Marszalek, J.-H. Yum, S. M. Zakeeruddin, M. K. Nazeeruddin, M. Grätzel et al., *Chem. Sci.* **2011**, *2*, 949.
[32] M. N. Romanelli, A. Bartolini, C. Bertucci, S. Dei, C. Ghelardini, M. G. Giovannini, F. Gualtieri, G. Pepeu, S. Scapecchi, E. Teodori, *Chirality* **1996**, *8*, 225.
[33] H. Akizawa, M. Imajima, H. Hanaoka, T. Uehara, S. Satake, Y. Arano, *Bioconjug. Chem.* **2013**, *24*, 291.
[34] R. Bollhagen, M. Schmiedberger, K. Barlos, E. Grell, *J. Chem. Soc., Chem. Commun.* **1994**, 2559.
[35] G. Scherer, M. L. Kramer, M. Schutkowski, U. Reimer, G. Fischer, *J. Am. Chem. Soc.* **1998**, *120*, 5568.
[36] R. M. Moshikur, M. R. Chowdhury, R. Wakabayashi, Y. Tahara, M. Moniruzzaman, M. Goto, *Int. J. Pharm.* **2018**, *546*, 31.
[37] E. J. Bae, W. G. Choi, H. S. Pagire, S. H. Pagire, S. Parameswaran, J.-H. Choi, J. Yoon, W.-I. Choi, J. H. Lee, J. S. Song et al., *J. Med. Chem.* **2021**, *64*, 1037.
[38] L. Li, M. d. G. Jaraquemada-Peláez, H.-T. Kuo, H. Merkens, N. Choudhary, K. Gitschtaler, U. Jermilova, N. Colpo, C. Uribe-Munoz, V. Radchenko et al., *Bioconjug. Chem.* **2019**, *30*, 1539.
[39] K. Hager, A. Franz, A. Hirsch, *Chemistry* **2006**, *12*, 2663.
[40] *Org. Synth.* **1929**, *9*, 66.
[41] S. Maity, S. Manna, S. Rana, T. Naveen, A. Mallick, D. Maiti, *J. Am. Chem. Soc.* **2013**, *135*, 3355.
[42] C. Zhang, J. Zhao, S. Wu, Z. Wang, W. Wu, J. Ma, S. Guo, L. Huang, *J. Am. Chem. Soc.* **2013**, *135*, 10566.
[43] J. Ma, X. Cui, F. Wang, X. Wu, J. Zhao, X. Li, *J. Org. Chem.* **2014**, *79*, 10855.
[44] S. Grimme, S. Ehrlich, L. Goerigk, *Journal of computational chemistry* **2011**, *32*, 1456.
[45] M. J. Frisch, G. W. Trucks, H. B. Schlegel, G. E. Scuseria, M. A. Robb, J. R. Cheeseman, G. Scalmani, V. Barone, G. A. Petersson, H. Nakatsuji, X. Li, M. Caricato, A. V. Marenich, J. Bloino, B. G. Janesko, R. Gomperts, B. Mennucci, H. P. Hratchian, J. V. Ortiz, A. F. Izmaylov, J. L. Sonnenberg, D. Williams-Young, F. Ding, F. Lipparini, F. Egidi, J. Goings, B. Peng, A. Petrone, T. Henderson, D. Ranasinghe, V. G. Zakrzewski, J. Gao, N. Rega, G. Zheng, W. Liang, M. Hada, M. Ehara, K. Toyota, R. Fukuda, J. Hasegawa, M. Ishida, T. Nakajima, Y. Honda, O. Kitao, H. Nakai, T. Vreven, K. Throssell, J. A. Montgomery, Jr., J. E. Peralta, F. Ogliaro, M. J. Bearpark, J. J. Heyd, E. N. Brothers, K. N. Kudin, V. N. Staroverov, T. A. Keith, R. Kobayashi, J. Normand, K. Raghavachari, A. P. Rendell, J. C. Burant, S. S. Iyengar, J. Tomasi, M. Cossi, J. M. Millam, M. Klene, C. Adamo, R. Cammi, J. W. Ochterski, R. L. Martin, K. Morokuma, O. Farkas, J. B. Foresman, D. J. Fox, Gaussian 16, Revision B.01, Gaussian, Inc.: Wallingford, CT, 2016.
[46] D. Kosenkov, *Journal of computational chemistry* **2022**, *43*, 1320.
[47] J. T. Ly, K. F. Presley, T. M. Cooper, L. A. Baldwin, M. J. Dalton, T. A. Grusenmeyer, *Phys. Chem. Chem. Phys.* **2021**, *23*, 12033.